

Performance evaluation of an ensemble neural network system of estimating transtibial prosthetic socket pressures during standing, walking and condition perturbation

Philip James Davenport

Submitted in partial fulfilment of the requirements for the award of Doctor of Philosophy

Bournemouth University

Submitted April 2017



Philip Davenport

Performance evaluation of an ensemble neural network system of estimating transtibial prosthetic socket pressures during standing, walking and condition perturbation

Abstract

Providing suitable prosthetic sockets for the restoration of function following lower-limb amputation remains a significant issue in medical device prescription. Poorly designed sockets are associated with discomfort, poor quality function and injury, with quality linked to the capability of the socket to adequately distribute the forces from ambulation. Despite this link, systems of measuring stump-socket interface pressure have not seen use in clinical practice, in part due to limitations in functional performance. A technique using neural networks to relate external socket deformation to the internal pressure distribution was recently developed: this method has several advantages over contemporary systems but had not been evaluated in detail in dynamic situations.

A wireless system estimating transtibial socket pressure distribution was produced. When supplied with simulated socket loads, an estimate produced from a group of networks (an ensemble) demonstrated improved accuracy and reduced variance. Work was undertaken to identify optimal design in terms of input data conditioning and post-estimate correction. This demonstrated that these can provide significant accuracy and reliability improvements.

Measurements were taken from two transtibial amputees during standing, walking, walking on slopes, walking with coronal plane misalignment and walking with an alternative socket liner. An evaluation of the contributions to variance confirmed the applicability of ensembles in this application.

The system proved capable recording significant differences in socket load distribution between different prosthesis configurations. For future investigation, this demonstrates that the technique is sensitive enough to examine the changes in the application of force which are present during daily use, device set-up and common fault conditions.

The results of this study support further development of the practical aspects of the system, future work in producing a realistic load training system and extrapolation of results to other sockets, structures and engineering problems.

Contents

Abstract	1
List of Figures.....	11
List of Tables.....	15
Publications List.....	18
Journal articles.....	18
Conference papers	18
Internal conference presentations.....	19
Preface.....	20
Acknowledgements	21
1. Introduction.....	22
1.1 Background.....	22
1.2 Statement of problem	25
1.3 Aims and Objectives	26
1.4 Document Organisation	27
1.4.1 Literature Review	27
1.4.2 Data Collection System.....	27
1.4.3 Neural Network Parameter Investigation	28
1.4.4 Practical Investigation	28
1.4.5 Evaluation and Conclusions.....	29
1.5 Study Restrictions.....	29
1.6 Summary	30
2. Literature review	32
2.1 Amputation in the United Kingdom	32
2.2 Definitions	35
2.2.1 Biomechanical definitions	35
2.2.2 Limb anatomy.....	37
2.2.3 Gait cycle	39

2.2.4	Amputation	40
2.2.5	Basic prosthesis componentry	41
2.3	Prosthesis prescription	42
2.4	Clinical considerations	44
2.4.1	Issues of importance	44
2.4.2	Comfort	46
2.4.3	Tissue quality.....	50
2.4.4	Energy efficiency	52
2.4.5	Skin conditions	52
2.4.6	Additional pressure management	55
2.4.7	Social considerations.....	55
2.5	Socket design	56
2.6	Socket pressure measurement techniques	59
2.6.1	In-socket discrete sensors.....	59
2.6.2	Through-socket strain sensors.....	60
2.6.3	Force-sensitive resistors	61
2.6.4	Force-sensitive capacitors	62
2.6.5	Optical systems.....	63
2.6.6	Finite element analysis	64
2.6.7	Indirect measures	67
2.7	Socket pressures with perturbation.....	70
2.7.1	Configuration changes	71
2.7.2	Alignment Changes	72
2.7.3	Slope walking	73
2.7.4	Terrain changes.....	75
2.7.5	Mass changes	76
2.7.6	Confounding factors.....	78
2.8	Artificial Neural Network Load Estimation	78

2.9	Critical appraisal	83
2.10	Summary	84
3	Systematic Literature Review of Transtibial Socket Load Changes with Socket Alignment Changes	86
3.1	Introduction.....	86
3.2	Methodology	87
3.3	Results	88
3.4	Discussion	94
3.5	Conclusions.....	96
4	Theoretical background and data preparation	99
4.1	Data collection and training preparation	101
4.1.1	Problem definition	101
4.1.2	Strain gauge measurement.....	102
4.1.3	Temperature correction.....	104
4.1.4	Time average.....	105
4.1.5	Structure loading.....	106
4.1.6	Material behaviour assumptions	108
4.1.7	Linear load superposition	109
4.1.8	Noise injection	110
4.1.9	Pre-processing summary.....	112
4.2	Neural network training	114
4.2.1	Neurons and neural networks	114
4.2.2	Levenberg-Marquardt algorithm	120
4.3	Post processing.....	129
4.3.1	Polynomial correction.....	129
4.3.2	Ensemble estimate.....	130
4.3.3	Post processing summary	131
4.4	Evaluating network performance.....	133

4.5 Hardware and Software Design	133
4.6 Design of Measurement Rig.....	134
4.7 Ethical approval and risk assessment	138
4.8 Selection criteria	140
4.8.1 Unilateral, transtibial amputation	141
4.8.2 Amputation from trauma	141
4.8.3 Amputation >6 months old.....	141
4.8.4 SIGAM Grade D/E/F	141
4.8.5 Cognitive ability to complete tests	141
4.8.6 Skin damage on residuum	142
4.8.7 Significant co-morbidity.....	142
4.9 Collection software	142
4.10 Collection procedure.....	145
4.11 Collection testing	152
4.12 Summary	155
Chapter 5 - Changes in system performance with alterations in training data conditioning and network design	157
5.1 Introduction	157
5.2 Network design parameters	158
5.3 Hidden neuron number	162
5.3.1 Methodology	162
5.3.2 Results	162
5.3.3 Discussion	164
5.4 Noise injection method.....	165
5.4.1 Methodology	165
5.4.2 Results	165
5.4.3 Discussion	168
5.5 Noise injection magnitude	169

5.5.1	Methodology.....	169
5.5.2	Results.....	170
5.5.3	Discussion.....	172
5.6	Critical appraisal of network modification approach.....	173
5.7	Summary	174
Chapter 6 – Evaluating ensembles of neural networks on problem data.....		176
6.1	Introduction.....	176
6.2	Ensemble construction testing.....	177
6.2.1	Methodology.....	178
6.2.2	Results.....	180
6.2.3	Discussion.....	182
6.3	Mixed ensembles	183
6.3.1	Methodology.....	183
6.3.2	Results.....	184
6.3.3	Discussion.....	185
6.4	Controlling constituent network parameters	186
6.4.1	Methodology.....	186
6.4.2	Results.....	187
6.4.3	Discussion.....	191
6.5	Critical appraisal of ensemble approach	191
6.6	Conclusions.....	195
Chapter 7 – Impact of constructing ensembles featuring a polynomial correction factor ..		197
7.1	Introduction.....	197
7.2	Evaluating polynomial function order	198
7.2.1	Methodology.....	198
7.2.2	Results.....	200
7.2.3	Discussion.....	203
7.3	Ensembles with polynomial correction	204

7.3.1	Methodology	205
7.3.2	Results	206
7.3.3	Discussion	209
7.4	Second level polynomial correction.....	210
7.4.1	Methodology	210
7.4.2	Results	211
7.4.3	Discussion	212
7.5	Critical appraisal of polynomial correction	213
7.6	Summary	214
Chapter 8 – Static and dynamic measures of prosthetic socket load.....		216
8.1	Introduction	216
8.2	Static measurements – equal weight bearing	217
8.2.1	Methodology	217
8.2.2	Results	217
8.2.3	Discussion	221
8.2.4	Summary.....	222
8.3	Static measurements with varied applied bodyweight	222
8.3.1	Methodology	222
8.3.2	Results	223
8.3.3	Discussion	227
8.3.4	Summary.....	228
8.4	Dynamic measurements	229
8.4.1	Methodology	229
8.4.2	Results	229
8.4.3	Discussion	237
8.4.4	Summary.....	238
8.5	Variance sources investigation	239
8.5.1	Methodology	239

8.5.2	Results	241
8.5.3	Discussion.....	242
8.5.4	Summary	244
8.6	Critical evaluation of dynamic measurement approach	244
8.7	Conclusions.....	246
Chapter 9 Socket load measurement with perturbation		248
9.1	Alignment perturbation.....	249
9.1.1	Methodology.....	249
9.1.2	Results.....	249
9.1.3	Discussion.....	254
9.1.4	Summary	255
9.2	Slope walking.....	256
9.2.1	Methodology.....	256
9.2.2	Results.....	256
9.2.3	Discussion.....	261
9.2.4	Summary	263
9.3	Liner change	263
9.3.1	Methodology.....	263
9.3.2	Results.....	264
9.3.3	Discussion.....	267
9.3.4	Summary	268
9.4	Combined perturbation.....	268
9.4.1	Methodology.....	268
9.4.2	Results.....	269
9.4.3	Discussion.....	274
9.4.4	Summary	275
9.5	Critical appraisal of system perturbation approach.....	276
9.6	Summary	276

10. Critical Appraisal and Future Work.....	278
10.1 Introduction	278
10.2 Chapter 4 – Testing specification.....	278
10.3 Chapter 5 – Network design	280
10.4 Chapter 6 – Ensemble networks	281
10.5 Chapter 7 – Polynomial functions.....	281
10.6 Chapter 8 – Static and dynamic recording.....	282
10.7 Chapter 9 – Perturbed walking	282
10.8 Summary	284
11. Conclusions	285
11.1 Background, Aims and Objectives.....	285
11.2 Contributions to knowledge	286
11.3 Limitations of Approach.....	287
11.4 Difficulties in Approach.....	288
11.5 Implications.....	288
11.6 Recommendations for future work	289
11.7 Final Considerations.....	290
References	291
Appendix	311
A1 – ISPO World Congress, Lyon France (2015)	313
A2 Medical Physics and Engineering Conference, Manchester UK (2016).....	314
A3 Multidisciplinary Engineering Optimisation Conference, Belgrade Serbia (2016)	315
A4 Systematic Literature Review, Journal of Medical and Biological Engineering (2017).....	316
A5 ISPO Annual Scientific Meeting, Lille France (2016)	317
A6 ISPO World Congress, Cape Town South Africa (2017)	319
A7 ISPO World Congress, Cape Town South Africa (2017)	320
A8 World Congress on Condition Monitoring, London UK (2017).....	321
A9 Study Risk Assessment.....	322

A10 Full Study Protocol	323
A11 Full Study Participant Information Sheet	334
A12 Full Study Participant Consent Form.....	338
A13 Participant Data Collection Form Template.....	339
A14 VLink-LXRS Data Sheet (Lord Microstrain)	341
A15 Mounting Rig Plate 1	343
A16 Mounting Rig Plate 2-4.....	344
A17 LabView ANN MATLAB Code.....	345
A18 Polynomial Fitter MATLAB Code	346
A19 Polynomial Correction MATLAB Code.....	348
A20 Ensemble Generation MATLAB Code.....	349
A21 Ensemble Analysis MATLAB Code	350
A22 Ensemble Summation MATLAB Code	352
A23 Ensemble Evaluation MATLAB Code	353
A24 MATLAB Distribution Generation Code	355
A25 LabView LXRS Collection Code	356
A26 LabView VLink Average Code	359
A27 LabView VLink Conditioning Code	360
A28 LabView File Path Code.....	363
A29 LabView DAQ Conditioning Code.....	364
A30 LabView DAQ Average Code	368
A31 LabView Ensemble Specification Code	369
A32 Abbreviations	371

List of Figures

Figure 1 - Definitions of amputation levels in the lower limb	32
Figure 2 - Anatomical Planes Definition.....	36
Figure 3 - Anatomical directions	36
Figure 4 - Joint motion direction definitions.....	37
Figure 5 - Bilateral knee varus - normal - knee valgus positions	37
Figure 6 - Muscles of the lower limb.....	38
Figure 7 - Vertical component of the ground reaction force, and location of key events	40
Figure 8 – Basic components and position of transtibial prostheses. Coronal plane view ...	41
Figure 9 - Key loading of a PTB socket.	56
Figure 10 - Potential transtibial prosthesis alignment changes.....	87
Figure 11 - Flowchart describing the search strategy employed.....	89
Figure 12 - Load and Measurement example used in this chapter	102
Figure 13 - Close up view of the strain gauges in use 4x4mm.....	103
Figure 14 - The Wheatstone bridge circuit	103
Figure 15 - The 3-Lead quarter bridge configuration.....	104
Figure 16 - A simplified representation of the means of structure loading	107
Figure 17 - Images of the loading rig. Left: the spring element.....	107
Figure 18 - Illustration of the theory of superposition	109
Figure 19 - Constant Noise Injection Model.	111
Figure 20 - Linear Noise Injection Model.....	112
Figure 21 - Flow diagram of the training process.	113
Figure 22 - Representation of a biological neuron	114
Figure 23 - The McCulloch-Pitts Neuron.....	115
Figure 24 - A single neuron with a single input.....	116
Figure 25 - Examples of commonly used artificial neuron transfer functions.....	116
Figure 26 - A single neuron featuring multiple inputs	117
Figure 27 - A single layer of multiple neurons	118
Figure 28 - A two layer network	119
Figure 29 - A pattern recognition problem.....	125
Figure 30 - Polynomial equation fitted to the residual error of an output channel.....	129
Figure 31 - Flow chart for the processing of test case data.....	132
Figure 32 - CAD model of the VLink measurement node.	135

Figure 33 - Left: A close up view of a strain gauge of the type used in this study. Right: View of the gauge for scale	136
Figure 34 - CAD model of an example socket, with the measurement rig fitted with VLink nodes below it	137
Figure 35 - Measurement rig cap, as seen from below.....	138
Figure 36 - Wireless Collection software interface	143
Figure 37 - Network generation software interface.....	145
Figure 38 - Loading positions on the test sockets of the two participants	146
Figure 39 - Example static standing recording.	151
Figure 40 - Example vertical ground reaction force	152
Figure 41 - Repeated loading tests.....	153
Figure 42 - Temperature correction calculated across an example test session	154
Figure 43 - Drift of an example channel voltage	155
Figure 44 - The instrumented test socket, with positions of loading indicated.....	158
Figure 45 - Effect of linear-type noise injection on training cases	159
Figure 46 - Effect of absolute value-type noise injection on training cases.....	160
Figure 47 - Naming convention in use for network configurations	162
Figure 48 - Changes in mean network RMS% error with differences in the number of neurons in the hidden layer	163
Figure 49 - Probability plots of RMS error on test data for groups of networks with different numbers of hidden neurons.....	164
Figure 50 - Changes in mean network RMS error with node number, noise injection and noise injection method.	166
Figure 51 - Variation in network error with changes in hidden neuron number and magnitude of linear noise injection.	171
Figure 52 - Probability plot for constituent network RMS % errors for a particular ensemble, and the distribution for a set of ensembles.....	180
Figure 53 - Range of constituent network estimates for three examples loads across the load range.....	194
Figure 54 - Probability plots for constituent network estimates	194
Figure 55 - Residual network error on an example channel from a single network.....	198
Figure 56 - Example polynomial correction factors of varying order.....	199
Figure 57 - The effect on networks of using polynomial correction factors of various orders, as compared to the matching uncorrected networks.....	201
Figure 58 - Probability plot of corrected networks error on test data.....	202

Figure 59 - The effect on RMS error of including polynomial correction and of correcting networks with the best fit function on training data.....	203
Figure 60 - Alterations in mean constituent network accuracy with alterations in variance of maximum noise injection variance	206
Figure 61 - Alterations in mean group accuracy with alterations in variance of maximum noise injection.....	207
Figure 62 - An example of a 2nd stage correction polynomial function.....	211
Figure 63 - Vertical ground reaction force recorded from the participant standing with the prosthetic limb on a force platform.....	218
Figure 64 - Participant 1 socket load distributions for each test session, from ensemble estimate of 3-4 seconds of even standing	219
Figure 65 - Participant 2 socket load distributions in equal standing, from ensemble estimate of 3-4 seconds of even standing	220
Figure 66 - Sum of socket loads for each participant and test session.....	221
Figure 67 - Measures of changes in applied vertical ground reaction force in each participant and session	223
Figure 68 - Measured sum of total socket load for each participant and session.....	225
Figure 69 - Average socket load distribution measurements for participant 1.....	226
Figure 70 – Measured changes in socket load distribution for participant 2 with changes in applied bodyweight	226
Figure 71 - Vertical force components recorded in each measurement session	231
Figure 72 - Mean and variance graphs for Participant 1, Session 1a.....	232
Figure 73 - Mean and variance graphs for Participant 1, Session 1b.....	233
Figure 74 - Mean and variance graphs for Participant 1, Session 2.....	234
Figure 75 - Mean and variance graphs for Participant 2, Session 1.....	235
Figure 76 - Multi-Layer linear effects model used in this section.....	240
Figure 77 - Inter-network variance for a single trial from participant 1	241
Figure 78 - Results from the output of the multi-layer models of each output channel	242
Figure 79 - Participant wearing the socket in equal standing.....	244
Figure 80 - Static load distribution with change in applied bodyweight. Participant 1, induced varus and valgus.....	249
Figure 81- Static load distribution with change in applied bodyweight. Participant 2, induced varus and valgus.....	250
Figure 82 - Participant 1, mean and variance of flat walking with induced varus.....	250
Figure 83 - Participant 1, mean and variance of flat walking with induced valgus	251

Figure 84 - Participant 2, mean and variance of flat walking with induced varus	252
Figure 85 -Participant 2, mean and variance of flat walking with induced valgus.....	253
Figure 86 - Mean and variance of participant 1 walking uphill, sessions 1a, 1b and 2	257
Figure 87 - Mean and variance of participant 1 walking downhill, sessions 1a, 1b and 2. .	259
Figure 88 - Mean and variance of participant 1 flat walking using the second liner	264
Figure 89 - Mean and variance of participant 1 uphill walking using the second liner.....	265
Figure 90 - Mean and variance of participant 1 downhill walking using the second liner...	266
Figure 91 – Mean and variance of socket loads of participant 1 walking uphill with induced varus	270
Figure 92 - Mean and variance of socket loads of participant 1 walking uphill with induced valgus.....	270
Figure 93 - Mean and variance of socket loads of participant 1 walking downhill with induced varus	272
Figure 94 - Mean and variance of socket loads of participant 1 walking downhill with induced valgus.....	272
Figure 95 - Socket load distributions, participant 2 flat walking.....	283
Figure 96 - Augmented reality application prototyped in this project	284

List of Tables

Table 1 - List of study aims and objectives	26
Table 2 – UK Limb-Loss Level incidence, 2011-2012 (UNIPOD 2013)	33
Table 3 - Amputation reason incidence in the UK in 2010-2011 (UNIPOD 2012)	33
Table 4 - Definitions of key gait cycle events in typical walking	39
Table 5 - SIGAM grade descriptions, Ryall et al, (2003)	42
Table 6 - Pain definitions from the IASP (Loeser and Treede 2008)	46
Table 7 - Socket comfort score single item score	47
Table 8 - Comfort and fit related questions within the TAPES-R tool.....	48
Table 9 - Comfort and fit related questions in the PEQ.....	49
Table 10 - Fundamental principles of stress theory as applied to biological tissue	50
Table 11 - Skin conditions seen in lower-limb amputees	53
Table 12 - Summary of literature of neural network applications to load distribution.	83
Table 13 - PICOS characteristics for inclusion criteria in the systematic review	87
Table 14 - Characteristics of eligible report standards	88
Table 15 - Description of included studies.....	91
Table 16 - Description of ratings of conclusion confidence.....	92
Table 17 - Reported evidence from included studies.	93
Table 18 - Standard deviation as percentage of applied load	108
Table 19 - The characteristics of wise crowds, as described by Surowiecki (2004)	127
Table 20 - Design specification of measurement device	134
Table 21 - Inclusion/Exclusion criteria for participation.	140
Table 22 - Wireless collection software options.....	143
Table 23 - Network generation software options.....	144
Table 24 - Load position definitions for each participant	147
Table 25 - Summary of experimental collection sessions.....	149
Table 26 - Example of test procedure sessions.....	149
Table 27 - Participant details	150
Table 28 - Network training parameters common to all trained networks.....	161
Table 29 - Characteristics of RMS error on test data in groups of networks with different hidden neuron numbers	163
Table 30 - Characteristics of groups of networks of varying noise injection method.	167
Table 31 - Results of significant differences between groups	168
Table 32 - Performance characteristics with variation in noise injection magnitude	170

Table 33 - Group comparisons between 5% maximum injection networks and matching groups of 0% and 10% conditioned networks.....	172
Table 34 - Network parameters that are varied between ensemble designs.....	178
Table 35 - Repeatability evaluation of 10 identically specified ensembles.....	179
Table 36 - Alterations in ensemble performance with changes in training data conditioning and hidden neuron number.	181
Table 37 - Changes to ensemble performance with alterations in hidden neuron number, maximum noise value and noise injection model.....	182
Table 38 - List of tested mixed origin ensembles.....	184
Table 39 - Mixed origin ensemble RMS errors..	185
Table 40 - Example distributions of various network specifications.....	186
Table 41 – RMS % error (SD) of the mean constituent network of each ensemble	188
Table 42 – RMS % error (percentile) of constructed ensembles.....	188
Table 43 - Calculated p values from paired t-test comparisons of each ensemble to the group of constituent networks.....	188
Table 44 - Estimation of significant differences between constructed ensembles following an ANOVA test.....	190
Table 45 - Neural network training parameters used throughout this chapter	200
Table 46 - Effect of polynomial correction on a group of networks using different orders of polynomial function.	201
Table 47 - Statistical calculations comparing polynomial corrected groups of networks with different order correction functions	202
Table 48 - Example of the effect on accuracy on an example output channel.....	203
Table 49 - Description of the specification of ensembles	205
Table 50 - Uncorrected and Corrected network accuracy on test data.....	207
Table 51 - Uncorrected and corrected network accuracy and the accuracy of ensembles created from these networks.....	208
Table 52 - Results of t-tests comparing various networks and ensembles.....	208
Table 53 - Network and ensemble accuracy on test data including 2nd stage polynomial correction	212
Table 54 - Test notation description.	218
Table 55 - Mean vertical force component recorded over 3-4 seconds of quiet standing .	218
Table 56 - Socket load estimates from each test session.....	220
Table 57 - Vertical ground reaction force values	224
Table 58 - Socket load estimates for static standing with adjusted applied bodyweight....	227

Table 59 - Relative load values (mean and SD) for each load position in Participant 1	232
Table 60 - Relative load values (mean and SD) for each load position in Participant 1	233
Table 61 - Relative load values (mean and SD) for each load position in Participant 1	234
Table 62 - Relative load values (mean and SD) for each load position in Participant 2	235
Table 63 - Calculated p values from comparisons of loads between P1S1a and P1S1b.....	236
Table 64 - Calculated p values from comparisons of loads between P1S1a and P1S2.....	236
Table 65 - Calculated p values from comparisons of loads between P1S1a and P2S1.....	237
Table 66 - Contributions to covariance estimate from each model	242
Table 67 - Key values for participant 1 during flat walking with induced varus.....	250
Table 68 - Key values for participant 1 during flat walking with induced valgus.....	251
Table 69 - Key values for participant 2 during flat walking with induced varus.....	252
Table 70 - Key values for participant 2 during flat walking with induced valgus.....	253
Table 71 - Significance calculations comparing participant 1 flat walking to induced varus/valgus alignment changes.....	254
Table 72 - Significance calculations comparing participant 2 flat walking to induced varus/valgus alignment changes.....	254
Table 73 – Load estimates for participant 1 in uphill walking	258
Table 74 - Load estimates during downhill walking in participant 1	260
Table 75 - Significance calculations for participant 1 uphill walking compared to equivalent flat walking.....	261
Table 76 - Significance calculations for participant 1 downhill walking when compared to equivalent flat walking.....	261
Table 77 - Key values of socket load from participant 1 wearing the second liner in flat walking.....	264
Table 78 - Key values of socket load from participant 1 wearing the second liner in uphill walking.....	265
Table 79 - Key values of socket load from participant 1 wearing the second liner in downhill walking.....	266
Table 80 - P Values calculated for new liner test comparisons	267
Table 81 - Socket loads for participant 1 walking uphill with induced varus/valgus.....	271
Table 82 - Socket loads for participant 1 walking downhill with induced varus/valgus.....	273
Table 83 - Significance calculations of difference between uphill walking and induced alignment uphill walking.....	273
Table 84 - Significance calculations of difference between downhill walking and induced alignment downhill walking.....	274

Publications List

Journal articles

Davenport P, Noroozi S, Sewell P, Zahedi S. 'Systematic Review of Studies Examining Transtibial Prosthetic Socket Pressures with Changes in Device Alignment' (2017) Journal of Medical and Biological Engineering 37 (1) p1-17

Conference papers

Davenport P, Noroozi S, Sewell P, Zahedi S. 'A proposed system for automatic categorisation of lower-limb prosthesis alignment using Learning Vector Quantisation and an inverse problem pressure measurement approach' (2015) International Society of Prosthetics and Orthotics World Congress, Lyon France.

Davenport P, Noroozi S, Sewell P, Zahedi S. 'Impact of varying training components for an ensemble neural network system of estimating prosthetic socket pressure distribution' (2016) Medical Physics and Engineering Conference, Manchester UK.

Davenport P, Noroozi S, Sewell P, Zahedi S. 'Applying Ensemble Neural Networks to an Inverse Problem Solution to Prosthetic Socket Pressure Measurement' (2016) Multidisciplinary Engineering Optimisation Conference, Belgrade Serbia.

Sewell P, Noroozi S, Davenport P, Bascou J, Villa C, Zahedi S 'Innovations technologiques dans la réalisation d'emboitures pour prothèses de membre inferieur – une méthode externe d'estimation des interactions entre membre résiduel et prosthèse' (2016), International Society of Prosthetics and Orthotics French Annual Scientific Meeting, Lille France.

Davenport P, Noroozi S, Sewell P, Zahedi S, McCarthy J, McGrath M. 'Sensitivity of an inverse-problem socket pressure measurement system to changes in applied forces from standing' (2017) International Society of Prosthetics and Orthotics World Congress, Cape Town South Africa.

Davenport P, Noroozi S, Sewell P, Zahedi S, McCarthy J, McGrath M. 'An Augmented Reality Method of Visualising Transtibial Socket Pressures and Limb Orientation' (2017) International Society of Prosthetics and Orthotics World Congress, Cape Town South Africa.

Davenport P, Noroozi S, Sewell P, Zahedi S. 'Monitoring the suitability of the fit of a lower-limb prosthetic socket using an artificial neural network in commonly encountered walking conditions' (2017) World Congress on Condition Monitoring, London UK.

[Internal conference presentations](#)

Davenport P 'Clinical Importance of measuring the prosthetic socket interface in transtibial amputees' (2014) BU Design Engineering and Computing Conference.

Davenport P 'Data reduction options for pre-processing prosthetic socket pressure distribution data' (2015) BU SciTech Conference.

Davenport P 'Improving Interpretation of Prosthetic Socket Load Distribution 3D Visualisation and augmented reality software' (2015) BU PGR Conference

Davenport P '3 Minute Presentation – Aided Analysis of Changes in Prosthetic Socket Pressures' (2015) BU 3MP Conference.

Davenport P 'The Wisdom of Crowds – Optimising neural network ensembles for prosthetic socket load estimation' (2016) BU SciTech Conference.

Davenport P 'Optimising noise addition for accuracy and reliability in an artificial neural network estimation of prosthetic socket pressure' (2016) BU PGR Conference.

Preface

This work was funded via an EPSRC Industrial CASE Studentship in partnership between Bournemouth University and Chas A Blatchford and Sons Ltd.

Academic supervision for this project was provided by Professor Siamak Noroozi and Dr Philip Sewell of Bournemouth University and by Professor Saeed Zahedi of Blatchford's Ltd. The work presented in this thesis is a development and extension of earlier work completed by this group and others and is cited as such within this document.

Acknowledgements

Thanks first and foremost go to my study supervisors for their time and effort across the entirety of this project – PhD supervision is always an extensive commitment, and so I would like to express my appreciation to Professor Siamak Noroozi, Dr Philip Sewell and Professor Saeed Zahedi for their assistance, support and advice over the last three years.

My thanks also go to the staff of Chas A Blatchford and Sons Ltd. for the technical support provided to the project, and also for the financial support via the EPSRC CASE industrial studentship that made this research possible. In particular, I would like to recognise the assistance provided by Joe McCarthy and Dr Mike McGrath during the testing phase of this project.

I also wish to thank the amputee volunteers who participated in the experimental phase of this project – people who, without any direct benefit for themselves, offered their time to help obtain the results presented in this thesis.

Postgraduate research is often solitary, but, thanks to the companionship of other students, rarely isolated. Naming everyone who supported this work is impossible, but to highlight just three members of the 5th floor S.o.U.S. - the soon-to-be Drs Aslani, Helvaci and Roberts – I would like to extend my gratitude for their advice, assistance, humour and friendship from day one of my time at Bournemouth University.

Finally, none of this would have been possible without the support of my family: my parents, my brothers and my sister. Having the patience to listen to someone at the other end of the country complain endlessly about some arcane fragment of misbehaving code, the trials of bureaucracy or the manifest injustice of a fair peer review is unlikely to have been fun. So for putting up with this and much more over the years, I'd like to make sure they know they are appreciated. So thank you to each of you.

1. Introduction

1.1 Background

Limb-loss affects thousands of people in the United Kingdom every year (UNIPOD 2013). Reasons for amputation are diverse, but include vascular insufficiency in the peripheral limb, trauma, cancer, elective amputation and congenital absence (Dillingham et al. 2002). Clearly limb-loss remains a permanent deficiency, requiring life-long assistive technology and extensive rehabilitation and clinical support. When ambulation remains a viable goal, a prosthetic limb will be prescribed. Although prosthetic limbs have developed greatly in quality in recent decades, numerous issues remain with the effective supply and use of artificial limbs (Laing et al. 2011).

In particular, the prosthetic socket (the interface between the device and the residual limb) is a common cause for complaint (Klute et al. 2009). The socket is responsible for applying the forces from ambulation to limb tissue. Unfortunately, the tissue in these locations is not intended for supporting loads of this type, meaning that issues including discomfort, pain, skin conditions, excessive sweating are commonly experienced (Butler et al. 2014). The residual limb is also subject to fluctuation in shape and size on both long and short timescales (Sanders and Fatone 2011). The socket must provide adequate distribution of the loads from activities (including applying load to tolerant regions and avoiding load on areas of prominent bone), as well as facilitate effective donning and doffing and providing suitable suspension of the artificial limb.

The effects conspire to make socket design, construction and fitting a predominantly qualitative and artisanal process; dependent to a great extent on the practical skill and expertise of the clinician. In particular, the production of sockets remains difficult to reproduce. There are very few quantitative methods available to support socket design, and none that are in routine clinical use (Al-Fakih et al. 2016).

Of particular clinical interest is monitoring the distribution of pressure loads within the socket environment. Pressure is strongly linked to many key parameters (Lee et al. 2005) including pain and the risk of tissue damage, but conclusive boundaries of what represents safe load are not available and substantial variation seems to exist (Swain and Bader 2002; Linder-Ganz and Gefen 2008; Loerakker et al. 2011). Numerous techniques have been

proposed to provide measurements of socket load, but all suffer from significant drawbacks that prohibit routine use (Sewell et al. 2000).

The earliest designs featured single sensors that were placed between the socket and the limb, but these suffered from inaccuracy from edge effects, and were restricted in the choice of location and resolution (e.g. Appoldt et al. 1968). Later, through-socket transducers provided better measurement performance, but required special test sockets and imposed constraints on functional activity (Sanders and Daly 1993b). Arrays of piezoresistive sensors have become more popular as they provide a greater coverage of the residual limb. However, sensors remain susceptible to error, and the act of placing them within the socket will alter the way the prosthesis is worn (Polliack et al. 2000). Other techniques exist, but remain in development. Estimation from finite element models of the limb/socket system have been attempted, but rely on detailed modelling of the tissue shape, composition and material properties (Dickinson et al. 2017), which is often difficult to obtain and use effectively.

A relatively novel method of estimating socket load distribution has been proposed that uses an inverse problem solution (Noroozi et al. 2005). Rather than measure load directly, the response of the change in the shape of the socket structure to known internal load is recorded, and used to train an artificial neural network as a function estimator to understand the transfer function that comprises the structural behaviour of the system. Then - in the measurement case - the load distribution can be assessed using the external measurements and the trained network only.

Such a system has several advantages over extant systems (Sewell et al. 2010). The system can provide measurement coverage over any portion of the socket interior surface, and a broad coverage of the socket as a whole. There are no aspects of the measurement device that are within the socket/stump interface, keeping the socket environment pristine. The system requires no particular knowledge of the tissue, socket or system material properties, as the system will converge on an appropriate transfer function given enough loading cases and training.

Using artificial neural networks in the estimation of socket load has been investigated by a research group at the University of the West of England and Bournemouth University. The original system used a neural network in combination with a finite-element model (Amali et

al. 2000) – the loading at the socket brim being predicted from a neural network taking the node stresses of the FEA model as input. Although the model demonstrated reasonable accuracy on test cases, the system took a long time to train to the problem.

Subsequent to this attempt, researchers used surface strains as the input to the neural network predictor (Amali et al. 2001). Working with structures of increasing complexity, the changes in strain measurements in response to internal socket loads formed the basis of a system of estimating socket pressures. This work included validation of the assumptions of material behaviour that meant that large numbers of training cases could be generated from relatively few measurements. This represented a significant improvement in the practicality of the system. Other developments at this stage included the introduction of several techniques to improve network training quality, including noise injection on the training input and isolated load cases. Accuracy at this point was estimated at around 88%.

Following this work, the proposed system was extended to feature many more input channels in order to predict load on a greater number of loading positions (Sewell et al. 2005). It was noted that there was a systematic error of underestimation at higher loads and overestimation at lower loads. In order to correct for this, a polynomial equation was fitted to the residual error. Although the positive effect of this was noted, the improvement was not fully quantified, and an evaluation on genuine amputee loads was not made.

At the same time, a sensitivity analysis revealed that several input channels could be removed from the system with only a minor impact on the accuracy of the load prediction (Amali et al. 2008). It was clear that a more effective system could use a smaller number of more diverse inputs, rather than a large number of relatively similar inputs. Systems of this type were quicker to train, and more likely to converge on an appropriate transfer function.

An examination of the ability of the system to collect loads from an amputee participant in a range of conditions was later published (Sewell et al. 2012). Realistic load distributions were obtained from standing, with extreme changes in coronal plane alignment and cyclic changes in load were observed when walking.

More recently, the technique was extended to other engineering problems, including marine plates (Ramazani et al. 2013) and aircraft wing ribs (Amali et al. 2014). This research

included modification of the network architectures and training algorithms, with the potential of improvements in both accuracy of estimates and in the speed of training.

The application of neural networks to socket load distribution has seen significant success, with a practical system of obtaining a load estimate without many of the disadvantages of contemporary systems being produced. Previous research has demonstrated that reasonably accurate estimates can be made, and that measurements can be obtained from static and dynamic situations.

Despite this previous work, many areas of performance evaluation and system ability remain unexamined. Detailed examination of the effect of varying key network design and configuration values has not been undertaken, nor assessment of the variance between trained networks. From a practical perspective, real-world measurements of amputee socket load have been restricted in terms of the number of participants and the range and applicability of the forms of measurement that have been undertaken. These are then the issues that are addressed by this work.

1.2 Statement of problem

The measurement of prosthetic socket load distribution is therefore an area of extensive clinical interest but which has also yet to produce a wholly acceptable means of providing quantitative assessment of a clinical situation. Despite the large numbers of amputees worldwide who require prosthetic sockets, and the drive towards evidence-based practice in healthcare, socket production remains a largely qualitative process in all healthcare settings. Barriers to the use of existing measurement devices include intrusion into the interface, cumbersome acquisition devices and lower quality performance in more complex measurement environments.

A technique that mitigates many of these issues is the use of artificial neural networks to estimate internal load distributions, however detailed examination of the response of the system to variation in design characteristics has not taken place. Furthermore, the residual error remains relatively high compared to other systems, and numerous techniques to improve this have yet to be examined. Finally, the ability of the system to characterise changes in static and dynamic loading patterns has not yet been established, and these represent key abilities in a system with the ultimate purpose of clinical use. Thus the

problem that is addressed in this work is that of characterisation of system performance, exploration of techniques to improve performance and examination of the abilities of the system to complete clinically relevant measurements.

1.3 Aims and Objectives

In order to support the structure of the thesis, several aims and objectives are specified:

Aim	Identify issues of concern for clinicians and literature gaps that exist in the measurement of prosthetic socket pressure
Objectives	Thorough literature review covering lower limb prosthetics, clinical issues relating to amputation and means of clinically assessing residual limb load.
	Systematic review of investigations examining transtibial socket pressure distribution with alignment perturbation
Aim	Establish the impact of varying controllable parameters of training data preparation and system construction on the quality of the system output.
Objectives	Evaluate neural network system accuracy and variance when training data is modified by varying the method and type of noise injection and the number of network hidden neurons is changed.
	Evaluate the impact on system accuracy and variance of combining groups of networks into ensemble solutions, and the effect that the previously examined system modifications has on this implementation.
	Quantify the effect of post-estimate correction for systematic network error, both on an individual network and ensemble system levels.
Aim	Determine if the sensitivity of the neural network estimation system is sufficient to detect changes in socket loading caused by typical walking conditions and commonly experienced system perturbation
Objectives	Construct a measurement system capable of safely and effectively measuring prosthetic socket surface strains of transtibial amputees
	Collect data from static and dynamic loading of these participants on level ground and commonly encountered system perturbation (i.e. altered weight bearing, slopes, socket alignment and liner specification)
	Evaluate for statistically significant changes in load within individuals between typical and perturbed conditions.

Table 1 - List of study aims and objectives

1.4 Document Organisation

In order to address these issues, several blocks of work were undertaken. These can be broadly divided into review, design of a new data collection system, network parameter investigation and practical evaluation of amputee measurement. The approach used is summarised here.

1.4.1 Literature Review

A thorough review of the available literature was carried out in order to better understand the context and importance of socket load measurement. This included investigating the state of amputation and prosthesis supply in the UK and elsewhere, and the process of designing and prescribing socket devices including the various design theories that make up the state-of-the-art of limb management. This was supplemented by a review of the understanding of pain and comfort as these relate to prosthetics, including the use of questionnaires and other tools to qualitatively assess prosthesis quality. Once the importance of pressure measurement was established, the various approaches tried previously and the latest techniques being investigated in this area were critically evaluated. The previous work carried out into neural network techniques of socket load measurement are also examined. Finally, the response of socket load to changes in the measurement environment was investigated. The majority of studies carried out examine flat, comfortable walking only, when it is of clear clinical interest to understand the relationships between load and more complex, more realistic situations. This work forms chapter 2 in this document.

A systematic review of one particular form of system perturbation was carried out into the effects on socket load distribution from altering the socket alignment. This is a process that every lower-limb amputee undergoes, but has seen relatively little attention in the literature. The process of completing this systematic review and the conclusions from it that indicate that results are scarce and research is of limited applicability is the subject of chapter 3.

1.4.2 Data Collection System

Review of the limitations of previous iterations of the neural network approach to socket load distribution informed the design of the equipment used in this research. Tools

developed for the collection, processing and interpreting of surface strains and load estimates are discussed in chapter 4.

1.4.3 Neural Network Parameter Investigation

The previous work completed provided only limited information on the effect of varying key system parameters. These design choices have the potential for improving the accuracy and consistency of network estimates, considerations with high importance for clinicians and researchers. In chapter 5, large numbers of networks are produced with varying training and construction. In particular, the model and magnitude of the noise injection of input data was modified: this represents an accessible means of controlling the width of the transfer function target. In addition to this, the number of hidden neurons was modified – this is a value that has implications for effectiveness and efficiency of training. The ideal number is not known a priori, and by investigating the effect of changing this value an improved system could be produced.

Chapter 6 extended this work by combining the produced networks into ensembles. Review of techniques to improve performance identified that combining networks into groups and producing an average estimate had good potential for improving the accuracy and variance of solutions. Through combining estimates in this way, a significant reduction in error could be made.

Work carried out in previous research had utilised polynomial correction functions to accommodate the residual error from neural network estimates. This work did not evaluate the effect of this correction in detail, nor the potential for more complex corrections. In Chapter 7, the effect of varying polynomial order and the impact of secondary levels of correction are examined. The improvement effect was confirmed, but tuning these parameters did not have a significant effect.

1.4.4 Practical Investigation

In chapter 8, practical testing with two transtibial amputee participants is described. A set of static tests involving standing with varying bodyweight was carried out, including repeated measures within and between collection days. Results for flat walking are also evaluated in this chapter, demonstrating plausible change in load and significant differences between participants. An analysis of the sources of variance was completed,

highlighting the critical contribution from network variance and providing further support for the creation of network ensembles in this application.

The final set of experimental results are described in chapter 9. Following the review of system perturbation completed in chapter 3, the importance of evaluating the ability of a measurement device to recognise the changes in load pattern from these situations was highlighted. In this section, the results of practical testing on slopes, from an alternative liner and with coronal alignment changes were examined. Although statistically significant changes were limited in most comparisons, the system did prove capable of reporting meaningfully different load patterns.

1.4.5 Evaluation and Conclusions

This chapter is followed by a critical evaluation of the approach taken and suggestions for the future direction of research in Chapter 10. This includes potential expansion of testing to other clinical populations and possible avenues of technical investigation. The work is then summarised in the conclusions (Chapter 11).

1.5 Study Restrictions

Several limitations on the scope of the project were put in place early in development. The first restriction was to limit testing to normal stress only. Although it is widely recognised that aspects of loading such as shear stresses and friction are important clinically, in order to provide measurements with sufficient coverage of the socket surface a much larger number of sensing elements are required. This was not easily achievable with the measurement hardware available. It was decided to prioritise the investigation of network configuration, data preparation and ability of the system to characterise loading situations. Measurement of shear loads in combination with normal pressure has been shown to be challenging but possible (Bascou et al. 2015), and could be considered in future implementations of a system of this type.

A further restriction was to limit investigations to transtibial prosthetic sockets. As described previously, the neural network technique has been applied to other engineering problems successfully. Prosthetic socket measurement with this technique has in the past been carried out on transtibial sockets exclusively. Although there is nothing that precludes study of other lower limb prostheses, transtibial amputees represent the largest functional

amputee group with a substantial socket structure, and so may represent the group that can see the greatest benefit from measurement, the most accessible testing population and which has an extensive literature to enable comparisons (both of previous neural network system studies and other research). Again, future work may wish to extend investigations to transfemoral sockets or other structures.

1.6 Summary

The study of prosthetic limb load distribution is one of widely recognised clinical importance, but which has seen only limited consensus form on the practical design of artificial limb sockets. This can be partly attributed to the lack of convenient quantitative measurement tools – the socket is a challenging measurement environment and the diversity of amputees means that the ability to generalise results is restricted.

A recently developed neural network technique of estimating structural load distribution has the potential to mitigate many of the issues present in contemporary socket measurement techniques. It can keep the socket environment pristine, provide broad coverage of the socket surface including areas of higher curvature and can be applied to the actual device being used by the amputee. The system has had the essential performance validated and been improved with the application of data processing techniques. However, several areas offer the opportunity for improvement in terms of the accuracy and reliability of the load estimation. Both of these characteristics are critical for the clinical acceptance of the technique – practitioners rely on load estimates that are consistent and correct. The sensitivity of the system to common changes in loading conditions is also not clear – although such systems have seen limited evaluation in situations including static alignment changes, the ability to record differences in dynamic situations is not yet clear.

A literature review covering issues relevant to the assessment of socket load is completed, including a critical evaluation of research into socket load in cases of system perturbation. In order to evaluate system performance and potential improvement techniques, a revised hardware and software implementation is produced. Several methods of altering data input, network architecture, system construction and post-estimate processing are investigated. Subsequent to this, the methods developed are implemented in an evaluation

of two transtibial amputees in a range of realistic measurement scenarios, and the ability of the system to distinguish these conditions is evaluated.

The next chapter covers the literature review of research in the areas of prosthetics, socket load distribution measurement and the neural network technique of load estimation.

2. Literature review

2.1 Amputation in the United Kingdom

In the UK, numbers of amputees can only be estimated. Records of new amputees from prosthetic centres were collected by the Limbless Association Centre (UNIPOD 2013). In the most recent year published, they identified 5906 new amputees. This figure does not represent the complete number of amputees, only referrals to prosthetics centres – some amputations are revised to higher levels, and some amputees lose multiple limbs.

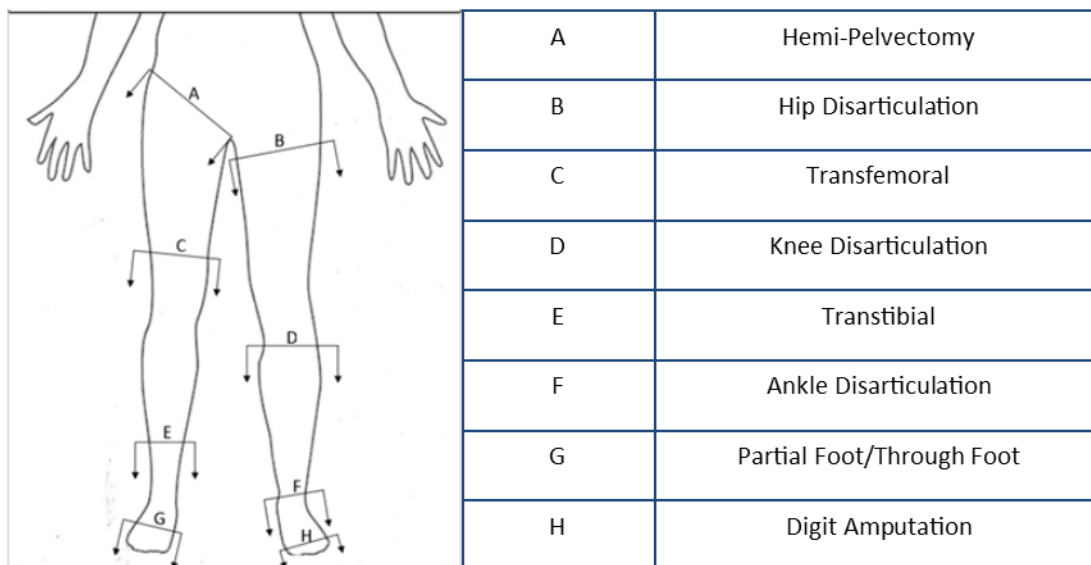


Figure 1 - Definitions of amputation levels in the lower limb

In Figure 1 different amputation levels are shown, and Table 2 indicates the incidence reported in the UK in 2012. The majority of amputations are in the lower limb. Most amputations are because of insufficient blood supply to tissue - once tissue oxygenation has been compromised, tissue begins to die and must be removed. This is often secondary to conditions such as diabetes –peripheral neuropathy means that tissue damage goes untreated. As the highest tissue loads are in the foot, amputation commonly occurs at this level. Other relatively common causes of limb vascular insufficiency include serious infections. Other reasons for amputation are from trauma as a result of vehicle or industrial accidents, and from war injuries. The average age for this reason is younger, and patients tend to have less co-morbidity in addition to the amputation.

Amputation Level	2012 Number	2012%
Toe or finger	116	2.0%
Through Foot	75	1.3%
Ankle Disarticulation	72	1.2%
Transtibial	2994	50.6%
Knee Disarticulation	154	2.6%
Transfemoral	2055	34.8%
Hip Disarticulation or higher	58	1.0%
Upper Limb	383	6.5%
(Congenital No-Amputation)	(29)	0.5%
TOTAL	5906	100%*

Table 2 – UK Limb-Loss Level incidence, 2011-2012 (UNIPOD 2013) *Does not sum exactly due to rounding of percentage totals.

Less common causes are as a result of cancer: to prevent metastasis or when tumour size is extensive. Limbs may also be amputated voluntarily in some conditions where routine loading is difficult. Finally, the limb may be congenitally absent (e.g. constriction by the amniotic band), requiring a prosthetic device.

Primary Reason for Amputation	Number	Percentage
Vascular Insufficiency	3140	52.9%
Trauma	594	9.9%
Infection	507	8.5%
Congenital Absence/Anomaly and Elective	310	5.2%
Cancer	148	2.5%
Neurological Disability	86	1.4%
Other/Not recorded	1203	20.0%

Table 3 - Amputation reason incidence in the UK in 2010-2011 (UNIPOD 2012)

The proportion of these amputation reasons is altering with population demographics. As the population ages a greater number are at risk from issues requiring amputation. Ziegler-Graham (2008) estimated that the US amputee population would double between 2005 and 2050. The often sedentary lifestyle in the developed world is a greater risk for type II diabetes and its complications. Improvements to traumatic injury care and post-surgery rehabilitation mean both an increase in amputees and more referrals to services for return-to-function prosthetics. Similarly in terms of war injuries, improvement in personal

protection and the speed and quality of emergency care has meant that injuries that were once fatal now require prosthetic treatment (Gabriel 2013).

A 2010 published study into lower limb amputation incidence reported that the number of amputees per person with diabetes was relatively consistent – however as the overall incidence of diabetes is increasing, the overall burden on health services did increase (Vamos et al. 2010).

The perioperative mortality rate of amputees remains high: a study of 130 major lower-limb amputations carried out between 1998 and 2009 at a hospital in the English Midlands reported that the 30 day mortality rate was 15.3%, rising to 29.3% for all inpatients (Jordan et al. 2012). Of the patients who survived to rehabilitation assessment: 63% received a prosthesis while 21.5% were regarded as unsuitable for device prescription. The remainder either declined the use of a device, or died prior to prescription. Transtibial amputees typically achieved better outcomes than transfemoral, and exhibited greater functional ability.

Further amputation of either the contralateral or ipsilateral limb is also commonplace. A 2007 study carried out in South Wales (Kanade et al. 2007) identified that amongst individuals with amputation secondary to diabetes mellitus, a further amputation was carried out in almost 50% of cases within two years of the original amputation. In only 22% of cases was this to the opposite limb.

The number of persons using a prosthetic device is difficult to estimate. In addition to unreported abandonment of the device, established amputees may not require more than infrequent care from health providers. The change due to immigration/emigration is also not quantified. An estimate from 1997-1998 (NASDAB 1999) was of ~62,800 UK amputees (~51,960 lower limb).

2.2 Definitions

2.2.1 Biomechanical definitions

For consistency in description throughout this thesis, the following definitions of planes, directions and motions will be adhered to. These are broadly accepted within the biomechanics literature, and are included here for completeness.

The human body is conceptually divided into three mutually orthogonal planes. The plane that bisects the body into *left* and *right* halves is called the sagittal plane, and represents the parallel to typical walking. The coronal plane divides the body into *front* and *back* halves. Finally, the transverse plane is at right angles to both of these, and cuts the body into *top* and *bottom* (Figure 2).

Directions on the body relate to these planes. Anterior describes the front surface, and posterior the back surface along the sagittal plane. Medial refers to the side in the coronal plane closest to the bisecting centreline of the body, and lateral the opposite. Finally, proximal (or superior) refers to the surface closer to the top of the body, and distal (or inferior) the point further from the centre. These are shown diagrammatically in Figure 3.

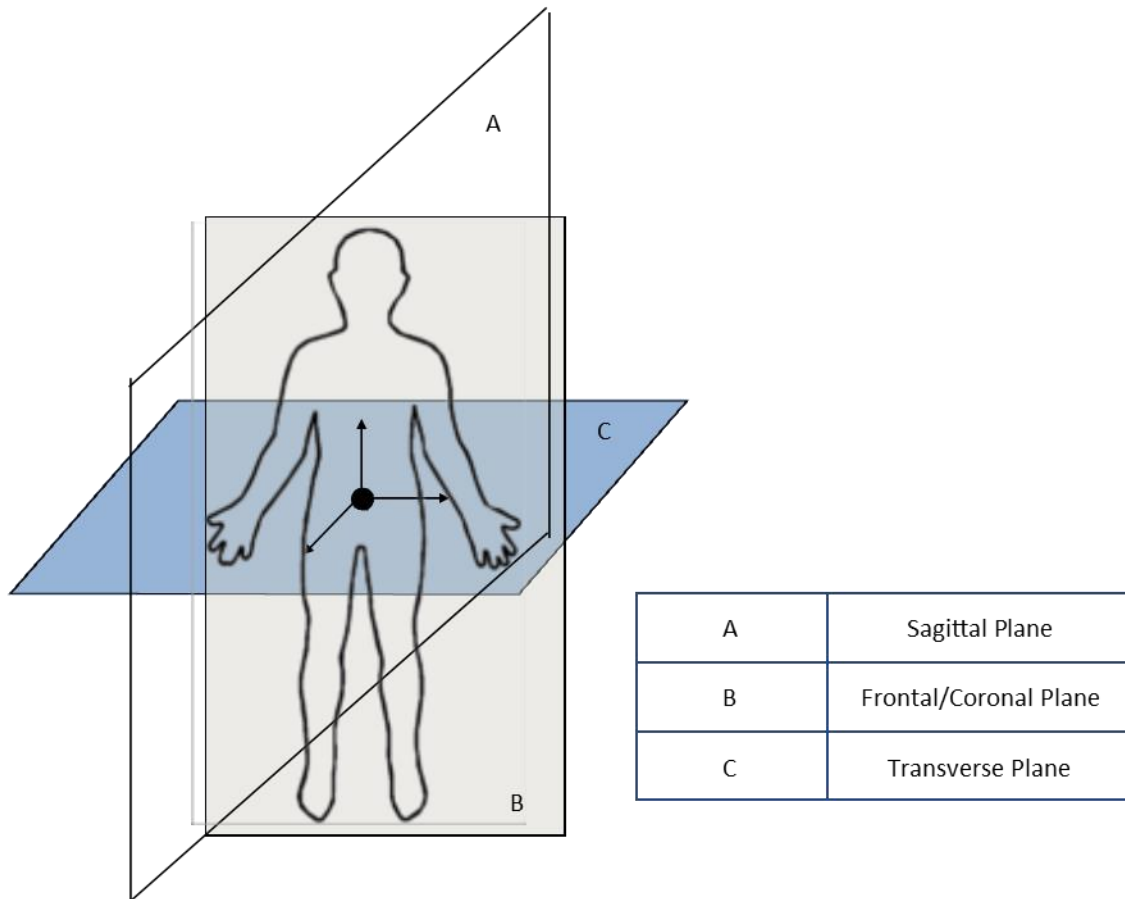


Figure 2 - Anatomical Planes Definition

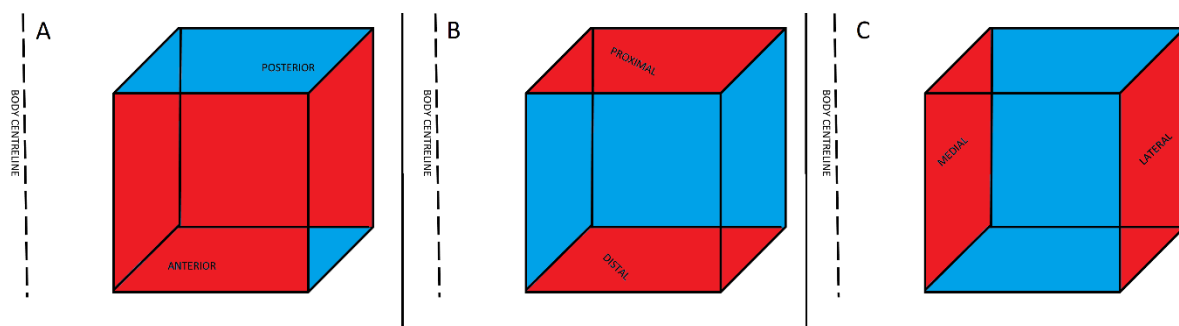


Figure 3 - Anatomical directions, highlighted in red. A = Anterior/Posterior, B = Proximal/Distal, C = Medial/Lateral

Joint motion has a similar set of terminology. Flexion describes the closing of a joint, and extension the opening of a joint. In the lower limb, this is predominantly in the sagittal plane. Sagittal ankle motion is conventionally described as either dorsiflexion (movement of the dorsal surface of the foot towards the shank) or plantarflexion (extension of the joint to point the toes). Adduction (in the coronal plane) describes motion at a joint which acts to move the distal segment towards the centreline of the body, with abduction the opposite.

In the transverse plane, movement is described as rotation: internal rotation moves the distal segment towards the centreline, external rotation away from the centreline. In the coronal and transverse planes, the definitions are mirrored on each limb: the motion they describe is the same (Figure 4).

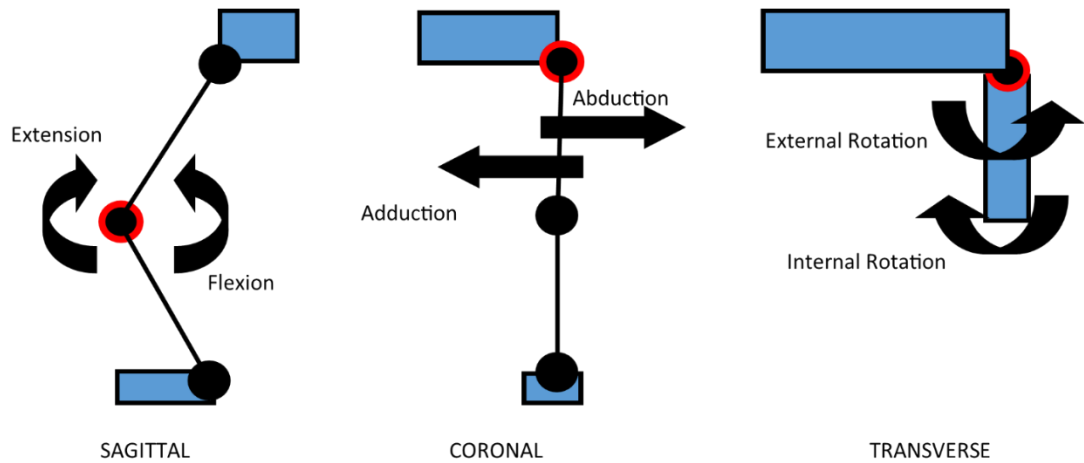


Figure 4 - Joint motion direction definitions, with moving joints highlighted in red

Finally, joint varus and valgus are defined. These have a particular application in describing the knee joint: a varus knee joint is one that is positioned laterally compared to the hip/ankle (bowlegged). Valgus is the opposite, the knee is more medial than expected (knock-kneed). These have utility in describing prosthesis alignment where the foot/ankle is positioned in such a way that the knee joint is pushed inwards or outwards (Figure 5).

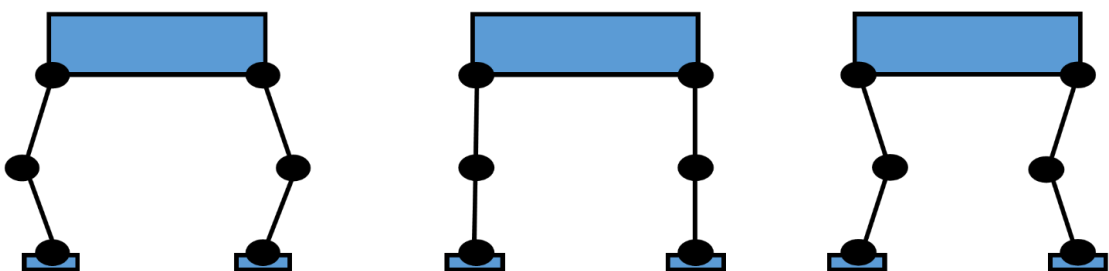
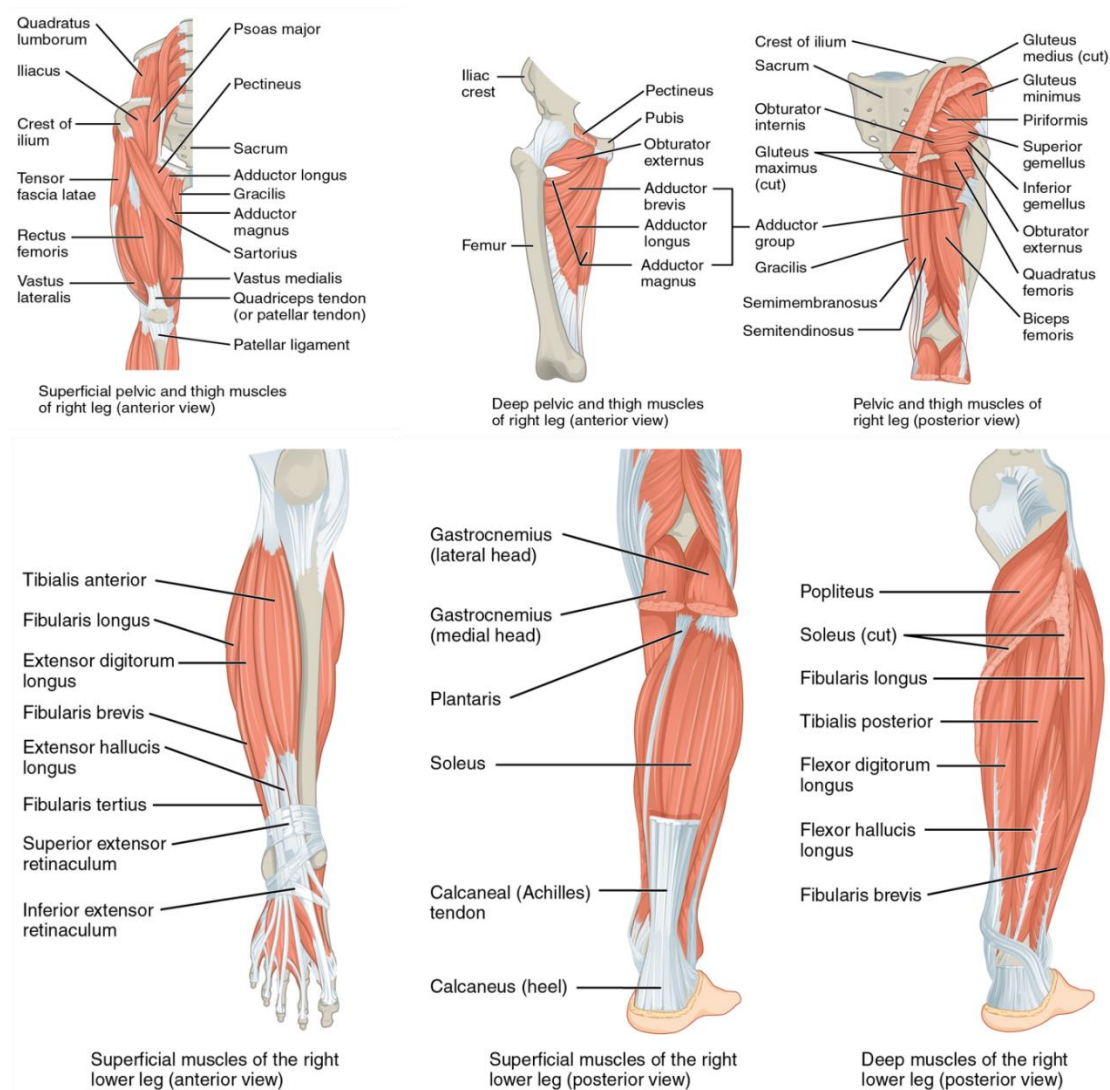


Figure 5 - Bilateral knee varus - normal - knee valgus positions

2.2.2 Limb anatomy

The lower limbs are attached to the torso at the pelvis, a large bony structure that contains the origins of many muscles. Each limb has three major joints (from top- to bottom) the hip, knee and ankle. The hip is a ball joint connecting the long bone in the thigh, the femur, to the pelvis, and which permits movement in each plane. The knee's predominant function is

as a hinge joint connecting the tibia in the shank to the thigh. This moves mostly in the sagittal plane, with limited movement in other planes. The knee also contains the patella, a sesamoid bone on the anterior face of the knee joint that aids in knee extension. It connects to the femur with the quadriceps tendon and to the tibia with the patellar tendon. The ankle joint is involved in foot articulation, predominantly in flexion/extension between the talus and the tibia/fibula in the shank. Associated joints in the foot (the subtalar joint and the inferior tibiofibular joint) and further down between the tarsals and metatarsals and toes are also present.



Images licenced under Creative Commons Attribution 4.0

Openstax Anatomy and Physiology via commons.wikimedia.org

Figure 6 - Muscles of the lower limb

2.2.3 Gait cycle

Unimpaired walking at a comfortable speed has a common pattern and is subdivided into sections for convenience of description and interpretation. A gait cycle can be divided in the proportion ~60:40 into stance and swing: the time spent with the limb on the ground and in the air. Each side is offset such that there is double contact for around 20% of the gait cycle.

Section	Description
Initial Contact	Impact absorption with full leg extension and heel contact
Midstance	Transition of the limb over the ankle, single support
Late Stance	Active plantarflexion for forward propulsion
Early Swing	Dorsiflexion, hip and knee flexion
Late Swing	Limb extension and preparation for heel contact

Table 4 - Definitions of key gait cycle events in typical walking

By plotting the ground reaction force recorded under the foot during a single step (Figure 7), the key features of the step can be observed. The applied bodyweight rapidly increases as the leg moves into single support before dropping to a local minima as the body transitions over the stance foot. The force increases again as the body is propelled forward and the contralateral foot makes contact.

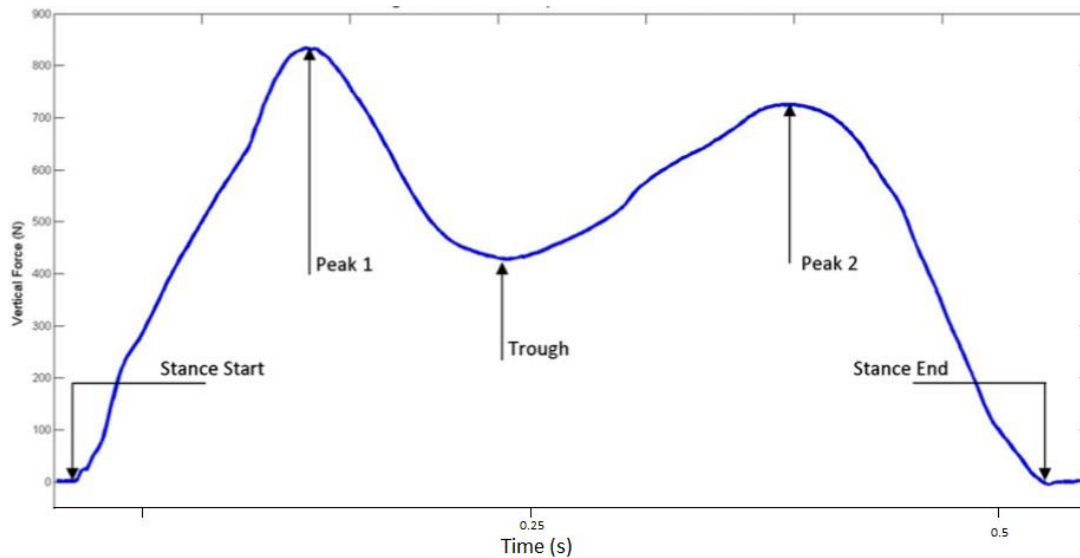


Figure 7 - Vertical component of the ground reaction force, and location of key events in gait stance.

2.2.4 Amputation

A short description of the amputation process is included so that later discussion of the implications of socket design is provided appropriate context. Given the permanent nature of amputation, it is considered in serious cases of dysvascular disease, infection, cancer or significant trauma. Prior to amputation the quality of the blood supply to tissue is considered to identify the appropriate level of amputation – the surgical team attempt to preserve biological joints wherever possible, and preserving the length of the residual limb to make fitting a prosthesis better (in transtibial amputation, the lower third of the limb is not amputated through as tissue coverage is not sufficient to provide distal coverage). Other issues considered at this point include: neurological quality, wound healing potential and associated conditions.

The procedure for transtibial amputation is described here. The tibia is cut 2-3cm shorter than the anterior soft tissue, and the fibula 1cm closer than this. Typically the stump is formed using a posterior flap of muscle and tissue from the gastrocnemius and fixed to the anterior face. The severed nerve endings are packaged into the tissue. The overall aim is to produce a roughly cylindrical stump without notable skin flaps or crevices, while also avoiding significant regions of scarring or adherent tissue.

After some weeks, the amputee is often ready for an initial prosthetic socket fitting to enable weight bearing through the residual limb. This will typically last 3-6 months as fluid

volume of the limb reduces in this time. During the volume reduction, the fit of the socket is maintained using socks of increasing thickness. Once volume has stabilised, a 'permanent' or 'definitive' socket is created for more long term use. Volume changes still occur, so further fittings are required.

2.2.5 Basic prosthesis componentry

Although specific configurations of prosthetic limbs are individual, the required components follow a consistent pattern (Tang et al. 2008). The interface between the limb and the prosthesis is known as the socket, and may be of varying design and material based on the preferences of the patient and the prosthetist. The socket may be held to the limb by aspects of its design, or may require another means of suspension. Historically this was achieved using belts, straps and corsets, but more recent methods include pin/lock devices at the distal end or silicone liners featuring vacuum suspension. The socket/liner system may also contain gel or foam patches to provide additional accommodation to anatomical features.

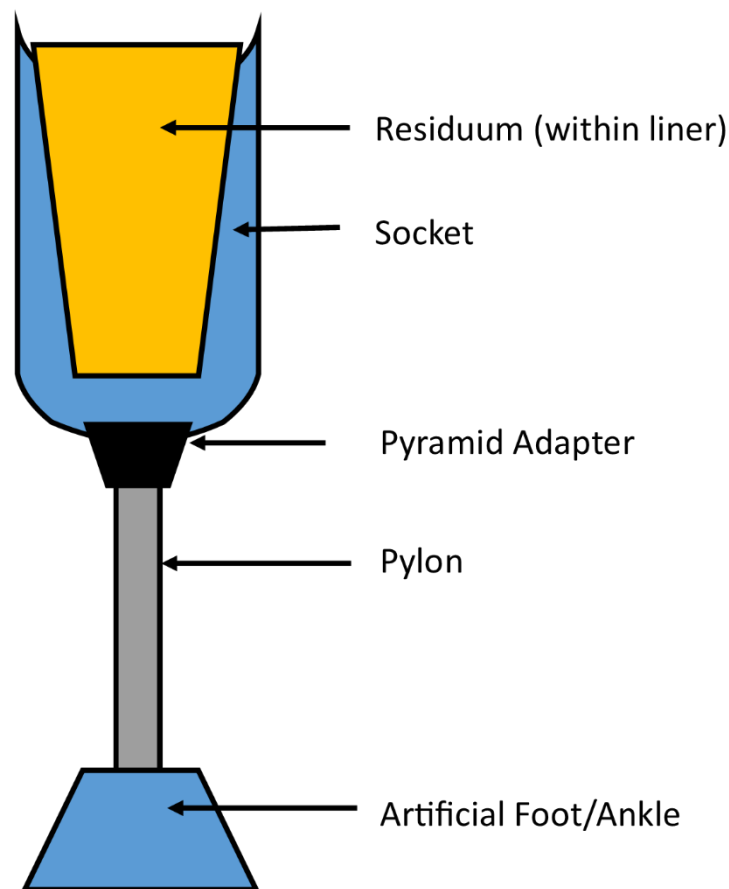


Figure 8 – Basic components and position of transtibial prostheses. Coronal plane view

The socket is fixed to the rest of the artificial limb via a pyramid adapter that enables the alignment of the device to be adjusted. The limb is given an appropriate height using a pylon. An artificial foot completes the functional components – these are of varying complexity, including simple rigid designs, solid-ankle/cushion-heel (SACH) feet, energy spring/return (ESR) feet to dynamically adjustable hydraulic designs. The choice of component is a balance between the requirement for stability and reliability of foot contact to the more natural ankle motion. The whole prosthesis may be given a cosmetic cover of foam or silicone.

2.3 Prosthesis prescription

Prescribing a lower-limb prosthetic requires the prosthetist to make several considerations regarding the ability and requirements of the amputee. A means of grading mobility is to use the SIGAM (Special Interest Group in Amputee Medicine) specification (Ryall et al. 2003). This ranks amputees using a standard questionnaire, and classifies into 6 groups A-F (Table 5).

Grade	Description
A	Limb wearing abandoned or cosmetic only
B	Therapeutic wearer wear prosthesis only for transfers, to assist nursing, walking with the physical aid of another or during therapy
C	Walks on level ground only, <50m with or without the use of walking aids
D	Walks outdoors on level ground only, and in good weather, more than 50m with or without walking aids
E	Walks more than 50m. Independent of walking aids except occasionally for confidence or to improve confidence in adverse terrain or weather
F	Normal or near normal gait

Table 5 - SIGAM grade descriptions, Ryall et al, (2003)

The considerations of amputee ability inform the selection of componentry. Some components are effectively off-the-shelf, and differ in size or material. Others, such as the artificial foot-ankle device can vary in complexity. The choice of component is predicated on the ability of the amputee, both in terms of control and a cost-benefit analysis of the function provided by the device.

The key customised component of the prosthesis is the socket. The traditional process for providing a patella-tendon bearing socket is described here. The prosthetist places the residual limb in slight flexion. This bunches the hamstring muscles at the back of the knee, as these have to be accommodated by the eventual socket. The stump is covered with a fabric sock, and inked to highlight key regions that must be taken into account during the socket construction process. The fabric is coated in plaster and used to make a negative model of the residual limb. When a positive model is made, the indicated regions are transferred onto this shape. This positive model is modified to alter the shape of the socket. Points are eroded to make the socket fit closer to the residual limb –to increase loading at these positions at places thought to be load tolerant. Material is added to produce space for accommodating structures such as the fibular head. Finally, the whole model is eroded such that the finished socket is reduced in size.

The finished plaster model is used to create the check socket –used to confirm the socket design. This socket is temporary and adjustable. After checking that the socket can be appropriately positioned and provides a suitably comfortable experience, it is used to create the definitive socket. Otherwise, the check socket is discarded and the process restarted.

The definitive socket is made from a resilient material, a plastic, thermoset resin or composite. The definitive socket is prescribed during another appointment, where the device is aligned with the remainder of the components, typically using observational gait analysis.

Further details of the design intentions of the prosthetist in the socket manufacturing process are included in Section 2.5.

Another aspect of the prosthesis is the suspension, the mechanism by which the socket and the rest of the prosthesis is held onto the body. The weight of the prosthesis system acts to pull the socket from the body, particularly during the swing phase of gait. Suspension, in conjunction with socket design also acts to prevent excessive translation and rotation of the socket.

Traditional socket suspension used straps and corsets around the thigh to keep the prosthesis in place. As the PTB socket design became more popular from the 1960s

onwards, socket suspension became integrated in the socket design – features such as supracondylar and suprapatellar shaping (Breakey 1973).

Some prostheses use a rubber sleeve around the top of the socket to the residuum. More recently, the hydrostatic principle of socket design meant the introduction of the ICEROSS silicone socket (Cluitmans and Geboers 1994) meant that suction could be used to suspend the prosthesis – the positioning of a one-way valve in the base of the socket meant that as the stump is placed into the socket the air is forced out through the valve and the socket held to the limb. The suspension requires a well-fitting socket to work, but can be enhanced by using liner designs which feature annular bands. The use of roll-on liners which adhere to the tissue thoroughly has also meant that designs which use locking pins which fix to the socket with a ratchet mechanism (Klute et al. 2011).

The prescription of a suspension system requires a thorough assessment of the functional ability of the amputee. For example, the use of roll-on liners requires dexterity and strength on the part of the amputee. Vacuum suspension has generally high quality, but can be noisy as the air escapes (which may be unattractive), and the suspension is less reliable and consistent.

In summary, the provision of a prosthesis requires a great deal of consideration of the potential options for device supply. Each option has a range of positive and negative attributes which have different priorities between amputees. The effects of each design have been examined in numerous publications, but there remains no conclusive body of recommendations which enable prosthetists to supply devices within an evidence based framework (Laing et al. 2011; Resnik and Borgia 2015).

2.4 Clinical considerations

The use of prosthetic limbs is subject to numerous issues that inform the quality and utility of the device, and work has been carried out to determine what issues of importance amputees face in daily living. A brief survey of the work reviewing these issues is presented, with a particular focus on transtibial amputees.

2.4.1 Issues of importance

An study of 109 amputees (59 below knee) used a custom 29-item questionnaire (Nielsen et al. 1989; Nielsen 1991). Respondents identified comfort as the key issue (52%), followed

by function (38%). Cosmesis of the prosthesis and the cost of the device made up the remainder. 57% were in moderate or severe pain for the majority of the time they wore the prosthesis. Despite this, three quarters described moderate-to-high life satisfaction. Amputees felt that they were under-involved with their care, and that they received inadequate information.

A similar methodology was employed by Legro et al. (1999), using validated questionnaires – the Prosthesis Evaluation Questionnaire (PEQ) and the SF-36 standard health questionnaire (n=92). Four themes of interest were found: the fit of the residual limb in the socket, the mechanical function of the prosthesis, cosmesis and the relationship with the clinical team. Fit represented the issue of greatest importance, in both the rating scales and the descriptive answers. Other issues– e.g. residual limb health – are also implicated in prosthesis fit.

Traumatic injury amputees were questioned by Pezzin et al. (2000), using SF-36 scores and a questionnaire. 36% reported constant or occasional residual limb pain that they rated as severe, 24.4% described severe wounds or sores on the residual limb (n=78). The authors associated inpatient rehabilitation duration with improvements in functional outcome. The same team reported on satisfaction with their prosthetic (Dillingham et al. 2001) in the same population – only 43% reported that they were happy with the comfort of their prosthetic (lower than satisfaction with appearance, weight, ease of use and prosthetic services). 24.3% had issues with skin irritation or wounds, 23.1% with perspiration and 16.7% with pain.

A larger review by Pezzin et al. (2004) (935 participants) found higher satisfaction–24.3% were unsatisfied with overall performance, and 24.5% unsatisfied with socket fit. The authors found that several factors that were predictive of device use were not predictive of satisfaction. Participants reported frequent hospital visits for device adjustment – nine times a year on average.

Klute et al. (2009) used a focus-group to examine issues of importance. “All prosthetic users had difficulties or problems at all stages in the processes of selecting, fitting, customising and using their prosthesis”, and the quality of socket fit specifically. Issues remained challenging due to “the difficulty in measuring ... socket fit and socket comfort”.

2.4.2 Comfort

Standard definitions for pain in humans have been proposed by the International Association for the Study of Pain (IASP). The most recent relevant terms are included in Table 6.

Pain	an unpleasant sensory and emotional experience associate with actual or potential tissue damage or described in terms of such damage
Noxious stimulus	an actually or potentially tissue-damaging event
Nociception	the neural process of encoding and processing noxious stimuli
Nociceptive stimulus	an actually or potentially tissue damaging event transduced and encoded by nociceptors
Nociceptive pain	pain arising from activation of nociceptors
Sensitization	increased responsiveness of neurons to their normal input or recruitment of a response to normally subthreshold inputs
Pain tolerance level	the maximum intensity of a stimulus that evokes pain and that a subject is willing to tolerate in a given situation

Table 6 - Pain definitions from the IASP (Loeser and Treede 2008)

The definitions depend on the nociceptive theory of pain – that particular sensory neurons respond to stimulus that risk damage to body elements. Nociceptors are responsible for identification of levels of tissue stress that can be damaging.

The socket comfort score (SCS) was proposed by Hanspal et al. (2003) in order to provide a straightforward method for evaluating residual limb discomfort. The authors identified this as missing from existing outcome measures – absent completely from such measures as the Prosthetic Profile of the Amputee, and as a single element from the Trinity Amputation and Prosthetic Experience Scale (TAPES) which has not been validated as an isolated question. Past studies examining socket comfort specifically relied on using the qualitative descriptions from participants without standardisation of questioning.

Item	Question	Response Range
1	On a 0 to 10 scale, if zero represents the most comfortable socket fit, how would you score the comfort of your socket fit of your artificial limb at the moment?	0-10 (Verbal)

Table 7 - Socket comfort score single item score

The SCS was evaluated on 44 UK patients including a mix of amputee aetiologies and amputation levels. Results demonstrated significant inter-assessor ($p < 0.001$) correlations, both before and after any interventions, demonstrating that the interviewer was not critical for the use of the test. The test also demonstrated good correlation between changes in SCS and ratings of socket fit. For the 29 participants who were issued a modified socket a significant improvement was also reported ($p < 0.001$).

As part of the question, comfort is not defined. This is in common with other methods, where the meaning is left up to the participant to determine. The authors themselves suggest that comfort could be defined as the absence of nociceptive stimulation travelling to the cerebral cortex as the opposite of pain/discomfort. This approach adopted the validated scales used in pain clinics.

The SCS was later evaluated as part of a study into outcome measures in amputation rehabilitation (Hebert et al. 2009). This was the only metric relating to amputee sensory/pain function that could be identified. The simplicity and utility of the method was praised. However the technique was given a score of minimal validity due to the paucity of studies evaluating this method.

The SCS was reviewed again in by Heinemann et al. (2014). No further validation studies had been identified by the time of this review. It was described as a lower-limb patient reported outcome measure, without available normative data.

Another tool, the Trinity Amputation and Prosthesis Experience Scale (TAPES) also contains a question relating to socket fit, as part of a broader evaluation of the quality of life with amputation in a 54 part survey (Gallagher and MacLachlan 2000). Respondents are asked to rate the comfort of their prosthesis on a five point scale (very dissatisfied to very satisfied). In the revised version of the questionnaire - the TAPES-R - the question on comfort is

retained, although the possible answers are reduced to three (Gallagher et al. 2010). Other aspects of the tool measure psychosocial adjustment, restrictions on common activities, satisfaction with aspects of the prosthesis and overall satisfaction.

Item	Question	Response Range
Vii	Fit	Not Satisfied-Satisfied-Very Satisfied
Viii	Comfort	Not Satisfied-Satisfied-Very Satisfied
	Please circle the number (0-10) that best described how satisfied you are with your prosthesis	0 Not at all satisfied-10 Very Satisfied

Table 8 - Comfort and fit related questions within the TAPES-R tool

The prosthesis evaluation questionnaire (PEQ) contains 54 scales that ask users to rate various aspects of their prosthesis function. This includes the fit of the prosthesis, comfort while standing and sitting, and residual limb pain over the previous four weeks. Questions also examine the impact on daily living that poor fit and poor comfort would be expected to have. Questions are answered on a visual analogue scale. Although section 7 of the PEQ describes the issues of importance to amputees, there is not a question that covers comfort or socket fit specifically.

Item	Question	Response Range
1B	Over the past four weeks, rate the fit of your prosthesis	terrible-excellent
1D	Over the past four weeks, rate your comfort while standing <i>when using your prosthesis</i>	terrible-excellent
1E	Over the past four weeks, rate your comfort while sitting <i>when using your prosthesis</i>	terrible-excellent
2H	Over the past four weeks, rate how often you had pain in your residual limb	never-all the time or almost all of the time
2I	If you had any pain in your residual limb over the past four weeks, rate how intense it was on average	extremely intense-extremely mild
2J	Over the past four weeks, how bothersome was the pain in your residual limb	extremely bothersome-not at all
6A	When the fit of my prosthesis is poor, I will get...	nothing done-everything done
6B	When the comfort of my prosthesis is poor, I will get...	nothing done-everything done

Table 9 - Comfort and fit related questions in the PEQ

The guidance documentation for the PEQ included definitions for specific bodily sensations – in particular sensations was explained as ‘pressure’ or as a ‘tickle’ (specifically in reference to phantom limb) and pain as a “more extreme sensation described by terms such as ‘shooting’, ‘searing’, ‘stabbing’ ‘sharp’ or ‘ache’”. Although these descriptions are useful, they may also relate to comfort issues that, while linked to residual limb health, are not causally linked to poor socket fit (for example heterogenic ossification, neuromas or folliculitis). Alternative methods that include subsections that examine socket comfort and fit also exist. However, each of the tools examined contained over fifty separate questions, with many relating to aspects such as psychological acceptance of the amputation, satisfaction with the quality of the prosthetic care in general. These aspects remain valid for evaluation of clinical care, but have only limited relevance to the topic of this thesis, and requiring the participants of this study to complete these lengthy questionnaires represents an undue burden for limited return.

2.4.3 Tissue quality

In 2002 Mueller and Maluf created a 'Physical stress theory' which attempted to summarise the mechanisms for tissue adaptation and damage.

Fundamental Principles of Stress Theory (Mueller and Maluf 2002)	
A	Changes in the relative level of physical stress cause a predictable response in all biological tissues
B	Biological tissues exhibit 5 characteristic responses to physical stress: <ul style="list-style-type: none"> • Death • Injury • Increased Tolerance • Maintenance • Decreased tolerance Specific thresholds define the upper and lower stress levels for each response
C	Physical stress levels lower than the maintenance range result in decreased tolerance to subsequent stresses – atrophy
D	Physical stress levels that are in the maintenance range result in no apparent tissue change
E	Physical stresses that exceed the maintenance range (overload) result in increased tolerance to subsequent stresses – hypertrophy
F	Excessive stress levels cause tissue injury
G	Extreme deviations from maintenance stress that exceed the adaptive capacity of tissue causes tissue death
H	The level of exposure is a composite value of the magnitude, time and direction of stress application
I	Individual stresses combine in complex ways to contribute to the overall stress exposure. Tissues are affected by the recent stress history
J	Excessive physical stress may occur by: <ul style="list-style-type: none"> • A high magnitude stress for a brief period • A low magnitude stress for a long duration • A moderate magnitude applied many times
K	Inflammation occurs immediately following tissue injury, and renders the injured tissue less tolerant of stress than it was prior to injury. Injured and inflamed tissues must be protected from subsequent excessive stress until acute inflammation recedes
L	The stress thresholds required for a given tissue response may vary among individuals depending on the presence or absence of modulating variables. Factors that can affect thresholds include: <ul style="list-style-type: none"> • Movement and alignment • Extrinsic factors • Psychosocial factors • Physiological factors

Table 10 - Fundamental principles of stress theory as applied to biological tissue

Several mechanisms for pressure-related tissue damage have been proposed, with varying evidence for their involvement and interaction. Differences are expected in disparate tissues and locations, in the inhomogeneity of physiology and between deep tissue injury and 'superficial' pressure ulcers.

The simplest mechanism is that the mechanical action of stress physically damage tissue cells directly, causing cellular necrosis (Mak et al. 2010). This damage is more commonly seen after high impact pressures (when it creates contusions), and may be a mechanism in longer-duration but lower-peak stresses. Although the proximate cause of an ulceration site is the death of tissue, it is unclear if direct damage to cells occurs in sufficient quantity to create an ulcer.

Local interruption of blood supply to tissue has long been implicated in pressure injury (Brand 2006). The compression of tissue during loading can collapse the capillaries that deliver oxygen to cells if the external pressure exceeds the blood pressure in the microvasculature. Given that cells cannot survive indefinitely without this circulation, this is a plausible explanation for tissue death. It is also recognised that risk of ulceration is greater in those with an already compromised vascular system (e.g. in diabetes). However, the loads experienced in residual limbs are lower in magnitude and duration than those that tissues can survive, meaning that other mechanisms are also in effect.

A development to this hypothesis is that pressure not only interrupts the supply of oxygen but also inhibits the ability of the lymphatic system to remove metabolic waste from tissue. If this material builds-up significantly, it can also contribute to cell death (Shoham and Gefen 2012).

Finally, ischemic reperfusion has been suggested as a mechanism for tissue damage (Coleman et al. 2014). As applied pressure loads the tissue, the supply of fluid is decreased, and then rapidly increases above normal once supply is restored. This increase also boosts the amount of highly reactive molecules present in the tissue. This oxidative stress generates inflammation and cell necrosis.

Three distinct loading types exist. The first is normal pressure, where tissue is compressed between the loading force and an underlying structure. In the prosthetic case this is between the prosthetic socket and the tibia/fibula. The second form, shear stress, is the

result of loads that are tangential to the tissue surface. The final case is friction, where the material properties of the socket wall and the tissue contribute to a resistance to translational motion of the interface.

2.4.4 Energy efficiency

The energy expenditure of amputee activity is known to be higher than in matched unimpaired controls. An extensive review was published in 1999 (Waters and Mulroy 1999). They reported that the deficiencies in energy efficiency arose from the absence of control of the artificial limb, requiring additional compensatory movement. However, the overall performance was also strongly linked to the presence or absence of additional medical conditions. Thus although there is a relationship between the level of amputation, there is an equally significant dependence on the activity capacity imposed by the primary medical condition. Thus traumatic transtibial amputees may have very capable movement and energy efficient activity.

Additional work has been done to examine the effect of changes in device design - for example the change in efficiency when dynamic elastic feet are used in the place of SACH feet (Gard 2006). Other work suggests that qualities of the residual limb are also implicated in energy efficiency, e.g. stump length (Gailey et al. 1994).

2.4.5 Skin conditions

Numerous skin conditions can be triggered as a result of poorly fitting sockets and prolonged application of pressure to tissues unsuited to loading. Early work was summarised by Levy (1980). He identified commonly encountered conditions (Table 11). The paper suggested that many of these skin conditions could be mitigated through appropriate prosthetic prescription and rehabilitation.

Bacterial/Fungal infections	The environment of the socket is suited for bacterial growth. It is mitigated by appropriate hygiene
Eczematisation	Persistent dermatitis at the distal stump
Epidermoid cysts	Painful cystic formations within tissue
Stump oedema	Created by the altered fluid distribution within the stump, made worse by poorly fitting prosthetics
Contact dermatitis	Caused by persistent contact with allergenic material
Folliculitis	Deeper infection of exposed hair follicles
Ulcers	Pressure-related damage to tissue caused by high magnitude or long duration load. Exacerbated by poor tissue vascularisation

Table 11 - Skin conditions seen in lower-limb amputees

Skin breakdown was reviewed by Sanders et al. (1995). Their conclusion was that adaptation of skin and deeper tissue was essential for the residual limb to become load tolerant, and for successful rehabilitation. They identified several mechanisms of tissue damage, noting that this relationship was affected by a number of factors - moisture, temperature, age, smoking, immobility and vascular supply. The position of tissue relative to the underlying bone was also implicated in the probability of tissue damage. Friction and shear stresses were also identified: the slip of tissue over contact surfaces (for example 'pistoning' within the prosthetic socket) is a factor in pressure injury formation – one study (Bennett et al. 1979) found that the required normal pressure for blood flow occlusion was halved when shear stress was added, meaning that a well-designed, well-fitting socket is important for residual limb health.

The relative frequency of skin conditions has been examined (Lyon et al. 2000). They found dermatologic issues in one third of the amputees they examined – most common were general dermatitis, epidermoid cysts and folliculitis. A larger study (Dudek et al. 2005) found higher incidence: 40.7%. Transtibial amputees were more likely to report skin issues. The most reported issue was ulcers (26.7%) followed by 'irritation' (17.6%) and epidermoid cysts (15%). Their hypothesis was that the combination of relatively thin tissue covering and high activity meant that socket issues were more common within transtibial amputees.

Traumatic amputees were surveyed in the same year (Pezzin et al. 2000). 24.4% reported severe wounds or sores on their residual limb (n=78). A later study attempted to identify protective and provocative determinants of skin disorders (Meulenbelt et al. 2009). The incidence in this study was relatively high at 63%. Protective determinants were older age, male sex and amputation from vascular causes. Provocative determinants were antibacterial soap use, smoking, and very regular stump washing.

A younger population with was reviewed by Koc et al. (2008). Of the 142 amputees included in their study, at least one skin problem was identified in 105 (73.9%). 12.4% of patients had more than one dermatologic problem. The most common cases were of irritant and contact dermatitis, but 12 different conditions were found.

Issues with the quality of the literature of prosthetic limb skin condition were highlighted in literature reviews (Bui et al. 2009; Butler et al. 2014). They comment on the low number of studies and participants and also on the consistency of description and classification of skin conditions.

The temperature of the socket environment has long been cause for complaint. The socket forms an impermeable barrier that retains moisture from sweat. Amputees also tend to sweat in greater amounts than unimpaired walkers due to the lower surface area to volume ratio, which, combined with higher exertion from activity mean that the coupling between core temperature and extremity temperature is tighter. The amputee also has fewer options regarding customisation of coverage for adjusting to external changes in temperature – the socket, sock, liner and suspension are all required for the prosthesis to be used. A review summarised the prevalence of temperature-related discomfort (Ghoseiri and Safari 2014). Their meta-analysis estimated that 53% of amputees experienced heat or perspiration discomfort within their socket.

In Legro et al. (1999) sweating was often cited as an issue with the socket interface, along with rashes, blisters and ingrown hair, all associated with increased temperature. Hagberg and Brånemark (2001) surveyed the consequences of lower limb amputation (in an exclusively non-vascular, transfemoral population). Heat and sweating were the most common issue quality of life (72% of participants), and sore and skin irritation (also related to temperature effects) was cited in 62% of cases.

2.4.6 Additional pressure management

Socket loads are managed in the first instance by the design of the socket and liner system. A historical perspective of the issues involved in the socket-liner system is described in section 1.5. Briefly, the aim of load management is to selectively load regions of the stump whilst also avoiding significant load gradients within the tissue.

Volume management is required due to long and short term changes in residuum volume. The fit of the socket can be maintained by the use of socks – covers of variable thickness that act to increase the volume of the stump in the socket. Management of this is sometimes troublesome (Sanders et al. 2012).

Alternatively, sockets may be fitted with air- or fluid-filled bladders that can be selectively alter the volume of the internal space (Sanders et al. 2013). These systems have the advantage that the socket volume can be customised to fit the current condition of the limb. However, the system also has a complex interaction with the volume of the residuum: reducing the socket space can also cause the volume of the stump to reduce in turn, with adjustments following each other. Sanders study found that 15/19 transtibial participants lost stump volume during the testing session.

2.4.7 Social considerations

A study on issues of importance (Legro et al. 1999) examined several issues of social and situational concern within a group of lower-limb amputees. Although these were typically rated less important than functional issues, concerns such as integration of the prosthesis with preferred clothing, eliminating noise and odour from the prosthesis, acceptance with partner and family members and the ability to provide care to others and that the device is not burdensome on family members.

Klute et al. used a focus group approach to identify limb concerns (Klute et al. 2009). Amputee participants universally expressed difficulties at all stages in the prosthetic supply process, from selecting to using the device. Recommended research priorities included 'smarter' limbs, the requirements for understanding the impact of components, education in amputee issues and adequate support networks for users.

2.5 Socket design

Prosthetic sockets have been produced since antiquity in response to illness and injury, but remained simple in design and insufficient in quality until the second half of the 20th Century (Al-Fakih et al. 2016). A group of clinicians in the USA created and described the patella-tendon bearing (PTB) socket, a revolutionary design which quickly became the clinical standard for below knee amputees (Radcliffe and Foort 1961; Foort 1965).

The philosophy behind the PTB design is that certain areas of the residual limb were more tolerant of load than others – broad, flat areas of thicker tissue could withstand higher greater magnitude and longer duration of load than those with thinner tissue covering, underlying ridges or points of bone or the stump end. A summary of load tolerant regions is shown in Figure 9.

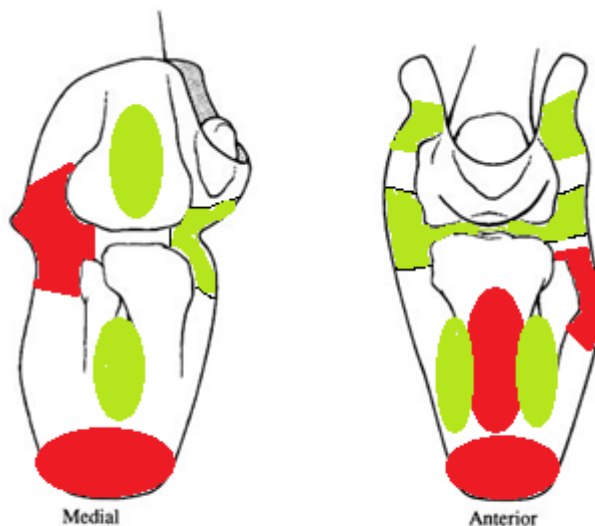


Figure 9 - Key loading of a PTB socket. Green regions were considered load tolerant, red areas where bony protrusions limit acceptable load

The key feature of the PTB socket was the extensive load that was intended to be placed at the patella tendon. In some users this proved problematic – the excess pressure at this location caused pain or injury. Furthermore, the necessity of external suspension meant that pistoning (vertical motion of the limb relative the socket) with the effect that skin abrasions were common.

The next development in socket design was the introduction of total-surface bearing (TSB) sockets (Staats and Lundt 1987). These consist of a hard external socket and a silicone liner that forced the residuum into a conical shape, with distal suspension. A TSB socket with a

silicone liner attempted to provide relatively equal loading across the residual limb – the high friction between the silicone and the socket reducing pistoning of the limb in the socket, and vacuum or a distal locking pin providing suspension (Kristinsson 1993; Hachisuka et al. 1998).

This has a different approach to producing a comfortable application of force: rather than applying considerable load to particular regions, the load was distributed, theoretically reducing the pressure gradients between regions and therefore reducing stresses within the tissue itself. The produced designs were typically less obtrusive than the previous PTB sockets, but came with other disadvantages. The use of a functional silicone liner layer is an additional expense, and is not easy to don or doff in people with limited mobility. Furthermore, the use of close-fitting silicone liners was also associated with perspiration issues and resultant skin irritation (Hachisuka et al. 2001).

Another form of socket design explicitly used the hydrostatic principle of fluid mechanics to provide suitable loading. A variant of the TSB design, the socket shape is defined by applying a consistent, equal load around the residual limb by means of hydraulics or pneumatics (Goh et al. 2004). The expectation is that tissue will 'flow' into a configuration that equalises load distribution, conforming to Pascal's law of fluids. Such sockets also utilised the results of a study by Rogers and Wilson (1975) examining the response of tissue to extended loading – by keeping the pressure below the boundary of dangerous combinations of load and duration, then applying external pressure at a 'safe' level during the casting process. Then, the produced socket theoretically maintains an even pressure distribution during day-to-day loading.

As noted by Silver-Thorn (1996), a further advantage of the hydrostatic technique is that the socket creation does not depend as much on the expertise of the prosthetist – rather than attempt to hand craft bespoke solutions, the socket shape is defined almost wholly by the equal pressure being applied to the limb. This makes hydrostatic sockets not only quicker to produce, but also simpler to reproduce, an aspect of PTB/TSB sockets that is almost impossible to achieve manually.

Computer-Aided-Design/Computer-Aided-Manufacturing (CAD-CAM) systems have also been used in the creation of below-knee prostheses (Saunders et al. 1985, 1989). Here, the shape of the residual limb is modelled, either by contact with a mechanical sensor, or by

some imaging technique. Once the shape of the stump is obtained, the process of rectification, scaling or adjusting is completed digitally – in a sense mimicking the manual adjustments traditionally made on the plaster positive model in PTB socket manufacture.

Once a suitable shape has been produced, the shape of the corresponding socket is defined, and supplied manufacturing system to either produce a positive cast that is draped with socket material, or, more recently, has the socket shape directly formed using additive manufacturing (Hsu et al. 2010). The latter – otherwise known as ‘3D Printing’ has seen only very limited practical use.

Such an approach has distinct advantages in terms of the reliability and repeatability of the socket creation process. The shape, structure and consistency of the residuum is tracked and recorded by the modelling system. Furthermore, the design of the socket can be recreated more easily, and can be finely adjusted if some elements prove unsuitable. Finally, the structure of the socket can be more creatively adjusted – one experimental system uses areas of variable compliance within the socket wall such that the socket can flex in preferential areas in response to load (Rogers et al. 2008). This was achieved by building in grooves into regions of the socket wall, techniques which cannot easily be achieved in traditional manufacturing. However, the utility of CAD-CAM systems is restricted by the accuracy of the shape-sensing portion of the process: the method cannot easily account for the particulars of the interior anatomy of the residuum, and will necessarily produce a model of the limb when it is unloaded. As the tissue flows during standing or walking, the shape of the ideal socket will also change.

Other amputation levels contain other approaches to socket manufacture. One example, developed for transhumeral amputees but recently applied in the lower limb is known as the high-fidelity socket. Rather than attempting to provide a socket that encompasses the residuum fully, the HiFi socket uses alternating longitudinal bands of high pressure and release (Williams and Altobelli 2011). This enables a firm grip of the femur, whilst also allowing tissue to flow into the voids in the socket wall.

A final note is made of the technique of osseointegration, which makes the socket component unnecessary in users who undergo this procedure (Brånemark et al. 2001). Predominantly tested in above-knee amputees (but also in transhumeral, transtibial and digit amputations), an implant is fixed within the long bone. A surgical process places a long

metal stem along the bone axis, and bone is encouraged to infiltrate this device until it is rigidly fixed. The distal end of the stem protrudes through the stump and ends in an abutment to which the prosthesis is attached. The majority of walking forces are transmitted through this linkage, facilitating a more natural connection to the prosthesis rather than through the soft tissue of the residuum. Users testing osseointegrated prostheses report encouraging recovery of function (Hagberg and Brånemark 2009).

The technique is not suitable for all amputees— surgical recovery and creating enough strength at the bone-metal interface is a long and challenging process, taking many months without full mobility. The inclusion of a metal stem also alters the mechanical performance of the bone around it, meaning that over time the distal edge of the femur becomes weaker. An issue is also found at the skin-stem interface – the tissue does not adhere effectively to the stem, meaning that wound drainage and infection remain common causes for complaint.

2.6 Socket pressure measurement techniques

2.6.1 In-socket discrete sensors

An in-socket based sensing system using a semiconductor strain gauge system was reported in a prosthetic application in 1970 (Sonck et al. 1970). The measurement element was a 'Kulite' sensor, a disc of silicon with a strain gauge and Wheatstone bridge directly formed onto the sensing surface, with overall dimensions of 3.2mm diameter and a thickness of less than 1mm. Measurements were obtained with a ribbon of wires that passed from the sensor to the measurement apparatus.

Kulite sensors were used in several studies from the 1970s onwards. Rae and Cockrell gave a detailed report on the transducer specification (1971), describing a greater pressure range and improved temperature sensitivity compared to contemporary designs and comparable performance in terms of repeatability, nonlinearity and hysteresis.

However, both studies reported drawbacks in terms of practical use: although the individual sensors were lightweight, when combined with others into small arrays of elements, the rigidity of the block would create crosstalk errors when loaded. Similarly, the rigidity of individual discs of each sensor would create stress concentrations at the sensor edge when the stiffness of the surrounding tissue was taken into consideration. Choices of

locations of measurement were also limited – the sensing element required a flat mounting surface – with the corresponding problem that wide regions could not be assessed. Studies also reported fragility of the connections. Further issues in terms of practicality were related to measurement limitations of the era – large numbers of simultaneous measurement were not possible, and so walking trials were routinely combined. Difficulty in reliably placing sensors in the same precise locations was described.

2.6.2 Through-socket strain sensors

The major contemporary means of socket pressure measurement also used strain gauges, but in a piston configuration. Here the transducer is mounted through the socket wall, such that the sensing element is a small disc flush with the socket surface. As pressure is applied to the cap surface in the normal direction, the diaphragm deflection is proportional to this force. By mounting a full-bridge foil strain gauge to this diaphragm, the change in voltage can be used to measure the contact pressure. The earliest experimental measurement of socket pressures used designs like this (e.g. Appoldt et al. 1968). Shear stresses were examined using a similar design, placed within the same socket spaces, and developed by the same group.

A significant advantage of the design by Sanders and Daly (1993a) is that by mounting additional gauges on the opposing faces of the supporting beam of the piston, it was possible to simultaneously measure shear stresses. A set of four gauges in one bridge configuration was sufficient to measure shear force in one direction – therefore eight gauges are required for shear measurement in both planes.

The mounting of such a system requires that a hole be drilled through the socket wall, and the instrumentation fixed to the external wall. The choice of position and the number of positions is limited by the size of the sensing element diameter, the requirements of the instrumentation construction and the need to maintain the integrity of the socket shape. These designs are somewhat more bulky than alternative methods and the additional weight and the compromising of the socket structure may lead to alteration of the pressure distribution under investigation.

An advantage of the system is that the quality of the recording is fairly high. Nonlinearity was assessed at 2.11%, hysteresis at 3.01% and crosstalk at 0.73%. Overall RMS error was

evaluated at 4.18% in the normal direction. Shear errors were lower: 0.89% total RMS error. Crosstalk errors are particularly low in this form of design (Williams et al. 1992; Al-Fakih et al. 2016).

Unfortunately, the required instrumentation in this design required a relatively high power to sustain – the large numbers of strain gauges per sensor meant that the energising current required to perform measurements was high. This in turn meant that study participants remained tethered to the measurement rig.

Alternative designs utilising semiconductor strain gauges were also proposed, with many of the same advantages and disadvantages (Williams et al. 1992).

2.6.3 Force-sensitive resistors

More recently, some researchers used discrete force-sensitive resistive (FSR) elements in order to perform pressure measurements. One such system was used by Seelen et al. (2003). This consisted of a strip of relatively large round sensors (diameter 1cm). The significant advantages of such systems are the material properties of the sensors – thin and flexible. This means that the sensors can be placed within the socket at the limb/socket interface without the limitations present in older sensor systems.

The principle of function is that the sensing element contains a conductive liquid which has a high resistance in an unloaded state. When normal pressure is applied, the distance between the faces of the sensor reduces and the overall resistance decreases in such a way that the output of the Wheatstone bridge is also changed.

In addition to the small surface individual sensors, many systems combined many such sensors into large arrays. For the first time, large areas of socket surface were investigated. Although these were not able to assess shear forces, the system had many advantages over discrete sensors. The socket can remain unaltered, so the true prosthesis of the participant can be used in testing instead of a changed, test-specific prosthesis. The flexibility and small thickness of the system mean that with relatively few sensors, the complete stump surface can be assessed at fairly high resolution. However, the systems also suffer from poorer measurement performance than many other designs (Al-Fakih et al. 2016).

A method of estimating the errors in the FSR system was described by Buis and Convery (1997). The sensors were loaded cyclically by a pneumatic pressure application rig, indicating a 2% variation of across the sensor array, with an additional static offset. The literature describes 1% change in output per degree change in temperature. The authors comment on the issues inherent to testing on curved surfaces – changes in the resistive contact volume as the film curves mean that values of pressure are linked to the geometry of the residual limb. A year later four sensor arrays were used to provide complete coverage of the residual limb inside a PTB socket (Convery and Buis 1998).

Two array sensor designs – the Rincoe and the Tekscan ‘FSocket’ sensors – were tested on a model residual limb with an air pressure vessel (Polliack and Landsberger 1998; Polliack et al. 2000). They found less error on flat surfaces than curved surfaces for both sensor types. FSocket sensors were more accurate, but produced greater drift and hysteresis errors. A similar set of bench tests on the Pressure Distribution Sensor System for Sockets was described by Hachisuka et al. (1998). Although differences between sensor devices were small, hysteresis, temperature sensitivity and performance deficit under higher speed loading/unloading were seen. The review of Mak et al. (2001) cited the unknown effect of shear coupling on the accuracy of FSR sensors.

2.6.4 Force-sensitive capacitors

An alternative to force sensitive resistors is to use force sensitive capacitor. The principle of operation is to build parallel conductors separated by an insulating material. As the material is compressed, or the overlapping area of the two conductive plates is increased, the capacitance of the component alters in a way that is measurable. The earliest use of such a system in a prosthetic application was by Meier et al. (1973). More recently, the construction of arrays of capacitive elements was produced by Novel (Munich, Germany). Sensor performance is thought to be of higher quality than equivalent FSR arrays, but with reduced resolution. The performance of such arrays is still thought to be poorer on curved surfaces – the effective distance between the conductive plates reduces without pressure being applied.

Capacitive elements have also been recently used in a 3D printed prosthetic socket sensor (Laszczak et al. 2015). The sensor body is a 20x20mm frame 4mm thick. The overlap of capacitive elements provides the sensing system. The system demonstrated equivalent

performance to other measurement techniques in linearity across the expected measurement range, with the critical advantage that the measurement of shear within the socket was now possible at a low cost. However, the dimensions of the sensing element are high compared to other systems, and the number of simultaneous measurements is limited.

A further complication of capacitive systems is that they require extensive filtering in order to eliminate crosstalk – the close placement of similarly sized charged plates makes the precise measurement of capacitive changes difficult without this corrective action. However at the same time they have lower temperature sensitivity than similar FSR designs.

2.6.5 Optical systems

The most recent development in socket pressure measurement utilises Fibre Bragg Sensors (FBGs) in order to measure deformation of a fibre optic element (Al-Fakih et al. 2013). The inclusion of a region of the fibre with a periodic variation of the refractive index causes a particular region of the spectrum of the applied light source. The particular frequencies reflected changes when the grating region is stressed, and by measuring this shift the applied pressure can be estimated. The use of optical sensing makes the system impervious to electromagnetic interference.

Such a system has distinct advantages – the measurement is accurate and sensitive to pressure, and the nature of the interference effect means that multiple signals can be multiplexed into the same fibre. The fibres themselves can be inserted into the socket environment or built into the liner or socket structure (Galvão et al. 2017). Furthermore, the system can be constructed in such a way that shear forces can be measured by incorporating fibres at different angles within the sensor position (E. Al-Fakih et al. 2012).

The system is not yet commercially available, and the materials themselves are somewhat complex to manufacture. The use of known spectrum light and detection also requires extensive instrumentation that is not yet portable or convenient to use outside of laboratory environments (Al-Fakih et al. 2016a; Al-Fakih et al. 2016b). Finally, the system is susceptible to damage to the optical fibres which may be difficult to detect.

2.6.6 Finite element analysis

Finite element analysis (FEA) as an alternative to experimental measurement of socket interface pressures had become a practical possibility by the late 1980s. FEA modelling relies on the creation of a model of the prosthesis/residuum system from mathematical elements with estimated interactions and material properties: by applying external loads to the system, the distribution of forces at particular points of interest can be estimated. The socket is often modelled as a rigid boundary (in comparison to the more pliant soft tissues), liners modelled as boundary elements as linear springs and so on. By modifying the application of external loads and the precise construction of the system model, many behaviours and conditions can be evaluated.

The earliest work in transtibial amputees was published in 1987 (Childress and Schnur 1987; Steege et al. 1987a; Steege et al. 1987b). 3D models of residual limbs were produced based on CT scans in three participants, and a parametric study of effective stiffness of the tissue and liner components was undertaken. Results were validated against a strain gauge diaphragm transducer; however detailed results were not presented at this stage.

Quesada and Skinner (1991) described a model of a below knee prosthesis capable of assessing normal and shear stresses on the residuum during a simulated heelstrike loading condition. The authors noted that clinically relevant changes in limb loading could be obtained by modifying the construction of the prosthesis materials.

Contemporaneous research (Silver-Thorn et al. 1992; Steege et al. 1992) used a modified model to measure different applications of medial-lateral force, flexion-extension moment and loading modification via prosthesis alignment. This information was used in a proposal for a socket design procedure utilising the results of these studies as part of a CAD-CAM system.

In 1993 (Sanders and Daly 1993b) a model was presented of a single transtibial amputee, with residuum geometry produced by magnetic resonance imaging. The residuum was then modelled with different properties with skin and fat, muscle and the Pelite liner, with results of socket stresses were measured with reference to a strain gauge pressure measurement device. The authors recognised that the model was still simplistic when compared to real prostheses; in particular that tissue was modelled as homogenous and

isotropic. Slip at the interface was also not included. The result was that the model was not accurate in representing the effects of applied loads.

The difficulty of modelling the slip effects at the skin/liner/socket interface was recognised in a study of non-linear transtibial prosthesis modelling published by Zhang et al. (1995). The sensitivity of the model to the value of friction selected was highlighted.

In a 1998 review of early work in FEA (Zhang et al. 1998) highlighted the difficulties experienced in the modelling of these techniques: in particular the large, non-linear deformations experienced by tissue, boundary non-linear properties (including friction/slip effects) and material non-linearity – viscoelasticity, time dependent properties, anisotropy and over-time changes in composition and properties. The difficulties of appropriate loading were also reported; particularly the variability of load magnitude and direction.

In 2000 (Zachariah and Sanders 2000), a suggestion that gap models be replaced by automated contact models was made, thus avoiding the issues of defining an arbitrary correspondence between the hard and soft surfaces, and more effectively describing slip between these interfaces. The authors felt that the results of this study were more reflective of prosthetics experience in this situation.

Friction and slip were implemented in a publication by Zhang and Roberts (2000), and compared against a set of experimental measures. Although the results were deemed good in terms of magnitude and direction of normal and shear stresses, the estimates were on average 11% lower than the experimentally measured values. The model was tested with a 'standing' load only.

The elements of a dynamic model incorporating the automated contact model was described by Jia et al. (2004). The socket was tested using results obtained from an inverse-dynamics model of the residual limb, including both variable external loads and the effects of inertia. It was found that inertial effects were significant during swing phase, up to 20.1% of the average load.

Liner stiffness was investigated by Lin et al. (2004) in a study of a single unilateral transtibial amputee. The authors concluded that sliding of the stump within the socket was a crucial

parameter of FEA model design. A moderate sensitivity to liner stiffness modelling was reported, however the effect was not easily predictable.

By the mid-2000s, FEA models were being used in investigations of other aspects of transtibial socket care. In 2005 Lee et al. (2005) examined regional differences in pain threshold using a variety of indenters and positions across the residuum. Pain threshold was variable across the limb and between participants. The FEA model successfully measured that the peak stresses at the skin were close to the pain threshold of the volunteers in the study. Peery et al. (2006) attempted to model residual limb temperature using FEA, with a good overall correlation to experimental measures.

Papers by Portnoy et al. (2007, 2008, 2009, 2010) investigated the development of real-time FEA models to predict tissue stresses. The boundary conditions were set by measurements taken from force sensors placed in-between the socket and the residual limb, and then supplied to an FEA model based on a simplified limb geometry obtained by X-ray imaging and indenter studies of tissue stiffness. Such an approach ameliorates one of the key difficulties experienced in FEA studies: the time required procuring clinically relevant results from a test session. However the residual limb model was oversimplified compared to contemporary models – work that the authors aimed to rectify with a more detailed study of residual limb anatomy via MRI.

In particular, the 2010 report (Portnoy et al. 2010) developed a handheld instrument that evaluated tissue stresses during a range of activities including stair, slope and uneven terrain. Modelling the effect of the tibia compressing the tissue at the stump end was able to identify meaningful changes in tissue loading during more complex tasks.

The complexity of generating a reasonable computer model of the residual limb was illustrated by Sengeh et al. (2016). Their methodology included (as part of the process of investigation) imaging, patient specific models, in-vivo indentation of tissue and inverse finite element optimisation of the key tissue parameters. Although the force predictions were considered reasonable (~7% difference), the difficulties of producing a useable model were clear.

In summary, the FEA modelling approach is in some ways an attractive method of providing patient specific load estimates. It can be adjusted for stumps and sockets of any dimension,

and can provide results for within tissue loading which is not easily achievable in other ways. However, the complexity of this approach requires detailed measurement of the residuum and socket systems and a considered approach to the application of loading and boundary conditions. The process is further hindered by the large degree of inter-subject variance in terms of limb constitution and the challenges of altered device prescription and practical use. Some issues have not yet been investigated in detail: these include the differences present between imaging and actual use (Papaioannou et al. 2010), and alteration of the stump condition over time. These issues have restricted the routine clinical use of such techniques. A recent systematic review into FEA and lower limb assessment was published in 2017 (Dickinson et al. 2017)

2.6.7 Indirect measures

Several recent papers describe directly measured loading of prosthetic components. There are distinct benefits to such devices over conventional inverse dynamic analysis, and prosthetic studies have unique advantages with this technique. The approach is to use strain gauge pairs to collect values with varying relationships to planar forces and moments. Through careful alignment and calibration, direct assessment of the planar values for force and moment can be made at a point close to the prosthetic interface. Inverse dynamics relies on several assumptions relating to rigidity of components and joint dynamics that can have limited validity in prosthetics users, in addition to the usual limitations of three dimensional gait analysis in amputees (Kent and Franklyn-Miller 2011).

Berme et al. (1975) described an instrumented method for measuring prosthetic forces, moments and shear forces at a point on the prosthesis as being developed in Strathclyde in the late 1960s. Their device is described using two levels of strain gauges to measure M/L (medial-lateral) and A/P (anterior-posterior) moments, and axial load and torque. Their design uses a tube/flange design: bending moment and axial gauges were bonded to the surface at least 15mm from either flange.

Sanders et al. (1997) identified three substantial uses for a six-directional transducer: evaluating and designing components, use in finite element analysis and as a prosthetic fitting tool. Each kind of investigation is benefitted by a thorough assessment of the forces and moments present during different actions. This group developed a prosthetic-specific load cell: this consisted of two rings connected by three beams.

During testing, moment values were found to be more reliable than force values, with axial force being underestimated. The system was initially tested clinically with a single subject. Issues with the design that were identified include the possibility of strain gauge misalignment and hence increased cross-talk. Additional development to cope with more strenuous activity was also suggested.

The thesis by Boone (2005) describes efforts in measuring socket reaction moments. The device described measures axial forces and sagittal and coronal moments. This system is not able to measure transverse moments, and these were neglected as the preliminary results indicated these were ~100 times smaller than the other components. These moments as measured near the base of the socket about an origin that is on the axis of the prosthetic shank, and collinear with the centre of the angular measurement device. Overall error was less than 3% for moments in the sagittal and coronal planes.

A study by Frossard et al. (2003) describes a wireless force and moment sensor used with a transfemoral amputee during activities of daily living. The authors identify the issues with inverse dynamics – namely the limits imposed by a lack of information about the inertial aspects of the residuum and the prosthesis and the compromises in modelling the system using traditional models. The difficulties in measuring conditions other than flat walking were also considered. Furthermore, they concluded that direct kinetic devices are unsuitable for all subjects due to the length of the instrumentation required.

The system was tested on a single transfemoral amputee, measured walking on flat, sloped ground and stairs. The authors reported that there were several applications for this design, specifically in the design and testing of prosthesis components.

Dumas et al. (2009) published a study of inverse dynamic modelling in the measurement of forces and moments with direct measurement. Maximum RMS errors were 56N and 5 Nm, and described as reasonably small. The authors state that the study demonstrated the typical errors seen in 3D measurement of prosthetic components. Differences in the modelled joint geometry may also be responsible for some errors. Improved classification of results was completed by the same team using the same set-up (Frossard and Stevenson 2011). Activity was divided into directional locomotion, localised locomotion, stationary loading and inactivity.

The same transducer was used in a study of transtibial amputees (Neumann et al. 2012). The device was mounted rigidly between the pylon and the socket, and in a test of the resultant force was within two percent of the magnitude as measured by a force platform. The authors concluded that transducer obtained patterns were able to detect differences in components, activities whilst eliminating many of the characteristic deficiencies of gait lab studies. The same team used this system to examine the loading due to transverse plane moments on the residual limb during flat and curved path walking (Neumann et al. 2013b). Curved path walking is difficult to assess using gait laboratories and inverse dynamics due to the problems of placing and hitting measuring equipment.

Socket moment impulse was used as an outcome measure in a study of alignment alterations, defined as the area under the socket reaction moment curve during stance, as measured using a Smart Pyramid in 10 transtibial amputees (Kobayashi et al. 2014a). The authors discussed the use of moment impulse in analysis of alignment: that the goal is not to minimise but to normalise this outcome measure. For example, they measured lower extension moment impulse with a high degree of anterior misalignment than in the nominal position. They suggest that acceptable limits may exist for assessment of adequate alignment.

The authors completed a further study on the effect of alignment changes, this time in ESR prosthetic feet (Kobayashi et al. 2014b). This study also used a Smart Pyramid. Footsteps from each trial were normalised to body mass and averaged for 25 different component configurations. Additional reports (Kobayashi et al. 2014c) measured the effect of random perturbation in both sagittal and coronal planes, using the same device and processing.

Socket reaction moments were used in a study to perform dynamic alignment of transtibial prostheses (Kobayashi et al. 2015) – direct kinetics were measured in a range of angular and translational changes in socket position, and found to be sensitive to these differences. However, the difficulty in interpreting kinetic changes when these were linked to the alteration in gait kinematics was highlighted: as were the issues in supplying an acceptable alignment when a range of these values may exist.

A new load cell, the 'iPecs' was validated in a 2014 study (Koehler et al. 2014). The system was tested on a single transtibial subject, and compared to an inverse-dynamics model.

Mean RMS errors were 3.4% for force measurements and 5.2% for moments at full scale output. The authors concluded system was a comparable alternative to force platform measurement and that direct measurements may produce lower errors at proximal joints than inverse dynamics.

The results have direct relevance to transtibial socket mechanics, and demonstrate systemic changes to within-socket biomechanics from changes in prosthetic component alignment. The results published also indicate the advantages of this measurement over inverse dynamics, in that longer collection sessions, with a wider range of test conditions and more directly relatable results are possible. However, studies by this group failed to present ground reaction force measurements, thus understanding the impact on direct kinetics is difficult to evaluate.

The majority of studies reported socket moments about the geometric centre of the socket. Although these measures seem sensitive to alterations in device configuration, the ability of such techniques to provide understanding of the conditions within the stump socket interface is limited. Pressure values vary between locations on the stump, and so the measurement of these changes in socket loading may be of limited use in quantifying the quality of socket fit as opposed to changes in broader aspects of the device.

2.7 Socket pressures with perturbation

The aim of clinicians' prescribing prosthetic devices is to restore as much appropriate function as possible to the user. This may represent practical ability, or could be limited to providing stability or cosmetic appearance. The set-up of the prosthesis therefore has a notionally optimal configuration that maximises these abilities. The multiple degrees of freedom available to the prosthetist may mean that there are several ways to achieve this. Perturbation of the system refers to the changes in the system that move it away from the optimum.

Perturbation can be deliberately induced into the system. The geometric positioning of the prosthesis components can be altered away from those considered most suitable, creating misalignment in rotation or translation. Alignment is a universal aspect of prosthesis configuration, and so understanding the changes in performance that can be created by

deviation from the optimum can be a useful means of understanding the system as a whole.

Changes in the device configuration can also be induced by altering the components in use. Examples include the use of active or passive joints, alternative liners or suspension or the use of devices such as torsion or shock absorption. Each of these has the potential to alter the manner in which the prosthesis is loaded in ways that differ from the considered optimum.

Perturbation can also be created by the environmental conditions that the system is used in. Contemporary prosthesis set-up is performed on level and uncluttered surfaces. Amputees will commonly encounter surface conditions that are different to this: examples include slopes, cambers, uneven terrain, curbs, steps and more. This can represent perturbation that affects how the device is used in practice, and understanding how the loading of the system changes in response to these factors is important in considering the effectiveness of the design in these circumstances.

2.7.1 Configuration changes

A recent systematic review into prosthetic interventions was published by Highsmith et al. (2016). This identified several key areas of research into transtibial prosthesis prescription; including socket design, foot and ankle technology and post-operative management. Despite this, relatively few studies measure changes in socket load distribution with changes in these configurations.

A study by Beil et al. (2002) measured load in five positions in nine participants, comparing a total surface bearing socket with a vacuum-assisted socket. Significantly lower pressure impulse and peak pressure was identified with the vacuum socket. The authors speculated that this was due to reduced volume loss within the stump.

Beil and Street also examined interface pressure with a change in suspension type (Beil and Street 2004), with an intervention that compared vacuum and pin-lock suspension. In contrast to the earlier work in socket design, suspension did not create significant changes during stance phase, but did alter the loading pattern of suspension vacuum.

Rajutukova et al. (2014) provided a summary of the biomechanical compensation for improperly configured prostheses – in transtibial amputees these include vaulting, foot whip, circumduction, trunk bending, foot slap, knee hyperextension and pistoning. Each of these may represent movement inefficiency, and can be substantially corrected with appropriate set-up.

2.7.2 Alignment Changes

Alignment refers to the process of arranging prosthetic components into suitable geometric positions. It is a required process in the supply of a functional prosthesis, as incorrect positioning will make standing and walking difficult as forces are applied to the residual limb in a suboptimal manner. The nature of modern prosthetic limbs means that there are numerous means of adjusting the configuration of components – these include the rotation and translation of components, and adjustment of the height of the socket relative to the ground. This redundancy means that there may be several methods of producing a functionally equivalent alignment – differences in strategy may produce other effects such as an improved cosmetic result.

Alignment is typically carried out in three stages. Firstly, the bench alignment is completed without the user present to produce a roughly suitable set-up. This takes into account manufacturers recommendations for combinations of equipment. Next, the limb is fitted to the user for a static alignment, where a suitable height is established and a more-or-less stable system produced. Finally in dynamic alignment, the user will be observed walking and the prosthesis fine-tuned to produce competent, comfortable and cosmetically acceptable gait. In higher level amputation, further work to account for the introduction of additional artificial joints must take place.

The biomechanical effects of alignment were examined in a systematic review by Neumann (2009). This review identified that significant changes in lower limb kinematics, kinetics and temporal-spatial parameters could be observed when socket alignment was perturbed away from the optimal position. However, numerous shortcomings in the state of the literature were identified – in particular studies were often limited in methodological value, in the number of participants and in the quality of data reporting. Neumann's review did not draw detailed conclusions on pressure response to alignment change.

A systematic review of the effects of alignment change on the in-socket pressures of transtibial amputees was completed as part of this project and is reported in detail in Chapter 3. A brief narrative summary of key studies is presented here.

The earliest study to examine socket pressures was reported by Pearson et al. (1973). This studied 10 amputees' responses to sagittal and coronal plane translation (and one participant in rotation in these planes), with measurements at 4 positions on the residuum surface. Results demonstrated variation in response to alignment changes, but a broadly consistent and in-plane effects were reported.

By the 1990s work by Sanders and others reported a more complex response. The inter-participant variance was highlighted, along with the effects of inter-session changes. These investigations were made possible with systems that could cover a greater part of the socket surface, although simultaneous measurement of large numbers of sensors was not practical.

Later studies began to use in-socket arrays, and more complex outcome measures. In addition to previously used maximum and average pressures, outcomes such as pressure-time integrals and sub-maximal pressure duration. These often proved to be a more sensitive outcome measure.

Several studies describe a biomechanically plausible effect in that load changes response in-plane to alignment changes (i.e. sagittal plane changes alter the anterior and posterior surface loads). The situation is substantially complicated by the individual differences between participants in terms of the residual limb and the original alignment configuration. These effects are explored further in chapter 3, but the importance of alignment perturbation is well-established as a factor that is within the control of prescribing clinicians, is applied to all functional prosthesis users and can have substantial biomechanical impact.

2.7.3 Slope walking

The first reported study of socket pressures during walking on slopes was published by Dou et al. in 2006. Their single-subject case study reported the changes in socket pressures of a transtibial amputee walking on a flat surface, a non-flat surface, stairs and a slope with a

gradient of 11/135 cm. Measurements used an FSR system collected at 50Hz. The sensors were placed over five positions of interest within the socket: four anteriorly and one posteriorly. Three collections of 5-6 steps were completed on each walking surface.

The results were reported using four measures: mean peak pressure at each position, mean peak pressure >90% of peak, time spent at >90% of peak pressure and the corresponding pressure time integral. In common with many studies, pressure values were highly variable between measurement sites. Pressure characteristics during basic ambulation were typically not predictive of changes due to walking condition.

Results from this study are limited: in particular there is limited detail in the presented results, such as measurement variance. The authors also suffered equipment failure, and shear forces were not recorded.

In 2009 Wolf et al. carried out a larger study in 12 transtibial participants. All were unilateral traumatic amputees, except for one case of cancer. Six participants used an ICEROSS system, with a range of other socket designs also used. The demographics of the cohort were older (age 43-59). Pliance sensors (Novel GmbH) were also used in this study – this time collecting at 60Hz and in 3 positions (patella tendon, anterior-distal and posterior-medial). Tests were carried out on the flat, on stairs and on a 7 degree slope. The authors identified greater changes in slope walking compared to the stair walking condition. Down slope walking induced the greatest changes: anterior-distal pressures became higher than posterior pressures.

Although this study has a higher methodological quality than that of Dou et al., there are still limitations. There was large inhomogeneity of participants in terms of age, ability and socket design. Results were not adequately separated by these factors and may have used inappropriate statistical tests to describe significance.

The final existing study of slope walking and socket pressure was published by Eshraghi et al. (2015). This also recruited 12 participants, this time of mixed aetiology. Mean age was slightly younger (mean (SD) = 46.8 (12.3)). In contrast to the earlier studies, FSocket (Tekscan Ltd) sensor arrays were used, collected at 50Hz, and taken as an average of over six trials. Participants walked on a slope of 7.5 degrees, and measurements were taken in three different suspension types (pin/lock, magnetic lock and Seal-In).

Ascent increased anterior-proximal and posterior-proximal pressures, similar to the study by Dou. Lower pressure at the anterior-distal region was also identified, in opposition to Wolf. Small differences in the effect from liner system changes were observed. Variance was higher in descent than ascent. Pin-Lock and magnetic suspension had typically lower peak pressures than the seal-in system.

Gholizadeh (2016) reported a study of a single transtibial amputee. The participant was fitted with a new TSB socket. The study used four Tekscan sensors, and tested on flat ground, stairs and a slope (angle unspecified). Results were reported for the original PTB socket and the revised TSB socket.

Results were expressed for 12 positions, three on each aspect of the limb. The average peak pressure over five trials in each position for the PTB and TSB socket was reported, but only as a graph of results with limited numerical representation of variance and comparison to flat walking.

2.7.4 Terrain changes

Uneven terrain is also of interest – the majority of studies are of walking in safe, flat ground. However these are not representative of real-world conditions experienced by amputees – with small irregularities in support, adjustments to gait patterns must take place.

Dou et al. studied socket pressure with changes in walking terrain in a single transtibial amputee (Dou et al. 2006). Their apparatus to simulate non-flat road was constructed from convex shapes. Three measurement trials were made, and pressure examined on five locations with a 'Pliance' sensor system. Compared to natural gait, pressure increased at the patella tendon and the popliteal depression, but decreased at the remaining three locations. Pressures during typical walking were not regarded as highly predictive of pressures in perturbed states.

A study of 18 transtibial amputees (Curtze et al. 2011) used the extrapolated centre of mass technique proposed by Hof (2007) to assess gait on an irregular surface. They found that the stability was not affected by surface, and not significantly different to the unaffected

limb. Walking speed and step length both decreased, but other measures seemed to be unchanged. In contrast to unimpaired walkers, amputees did not widen their step width.

Loose stone surfaces were tested in a pair of papers by Gates et al. (2012, 2013). In the first study 13 young transtibial amputees walked along a pit filled with smooth rocks. Amputees adapted by taking shorter and wider steps, with higher variability. Toe clearance was up to four times higher on the rock surface. Lowering of the body centre of mass was also evident. Margins of stability were evaluated in the second paper. As on the uneven terrain, average margin of stability was unchanged in transtibial walkers, although variability increased. The study was limited by the choice of population— young amputees are considered better able to adapt.

Perturbation of transtibial gait using a CAREN gait analysis environment was examined by Beltran et al. (2014). Gait was modified using pseudo-random medio-lateral translations of the walking platform. Nine transtibial amputees were tested, with the conclusion that the margin of stability was equivalent between the amputees and the controls during normal walking and with perturbation of the visual field – however during physical perturbation, amputees demonstrated poorer lateral stability.

It appears that terrain changes may be capable of providing greater distinguishing power between capable amputees. Younger, more active people with comparatively distal amputation levels can retain high quality movement ability, and hence more challenging tasks than flat walking may be necessary to provide a meaningful measure of action capacity.

2.7.5 Mass changes

Altering the position of the centre of mass of the limb has effects on the inertial behaviour of the artificial limb – in modelling the motion of the prosthesis as a pendulum, the alteration of mass has the effect of altering the cadence of walking of the user. In more complex (i.e. multi-segment) models, the predicted impact of changing this parameter is less clear, however it was felt that unaccustomed shifts from the typical value could cause alterations to the selected gait pattern employed by amputees. A systematic review of studies investigating this phenomenon was published by Selles et al. (1999), which identified four studies reporting results on transtibial amputees between 1966 and 1998.

Gailey et al. (1994) performed an analysis on energy cost measurements which included an evaluation of the effect of the mass of the prescribed prosthesis of 39 participants. No significant differences in oxygen consumption were found, even controlling for the effect of stump length, age, walking speed and baseline energy expenditure. Similarly, self-selected walking speed did not alter significantly between the 'heavy' prosthesis and 'light' prosthesis groups.

In a subsequent study by Gailey and colleagues (Gailey et al. 1997), energy expenditure measures were used to assess 10 transtibial amputees when treadmill walking when the prosthesis was modified by adding 454g and 907g of mass (evenly distributed around the shank segment on the amputated side). No significant changes in energy expenditure were experienced during steady-state motion.

A case study of a single transtibial amputee was published by Hillery et al. (1997). In this work, the prosthesis was fitted with 530g and 1460g added to the distal foot – a change with greater implication for inertial changes than in earlier work. Although statistical differences were not assessed, the alterations in added mass created changes in the kinematic and kinetic properties of the participants movement. In particular, stride length increased.

Walking speed and metabolic cost of walking were measured by Lehmann et al. (1998) for alterations in position of the centre of mass of the prosthesis (proximal or distal) and overall mass (42%-70% of normal limb mass) in 15 transtibial participants. Locating the centre of mass of the system distally increased energy cost. In contrast, changes in mass had no significant impact on either walking speed or energy cost, even with changes of up to 1.5kg between the light and heavy configurations.

Selles et al. (2004) measured kinematic and kinetic changes in gait strategy in 10 participants. They identified that a kinematic-invariance strategy was used, where these were similar in different mass and inertial configurations, with greater changes in joint moment (and hence muscle activity and energy cost).

A study by Smith and Martin (2013) investigated altering prosthesis mass as a means of improving gait symmetry in transtibial amputees – proximal masses did not improve

kinematic measures or reduce gait cost as earlier models had predicted. Their recommendation was that this should not be considered as a method of improving these parameters, but that proximally placed mass did not induce significant changes in these measures.

In summary, the review of literature in this area suggests that the positioning of additional prosthetic mass has a greater impact of user's gait than the value of mass itself. Transtibial amputees appear able to adequately compensate for extra weight as long as this does not greatly alter the inertial properties of the limb away from their customary prosthesis.

2.7.6 Confounding factors

A major cause of difficulty in understanding the effect of prosthesis changes is that the volume of the residual limb is subject to changes over time. The long-term fluctuation of this was examined by Fernie and Holliday (1982) in a study of 49 amputees using a water immersion technique. This identified that the most significant changes in stump volume occurred in the early stages post-operatively. The atrophy of tissue in the stump was counteracted by a tendency to gain weight overall after amputation. Fluctuation was also observed to a lesser extent in mature amputees. However, inter-participant variance was high.

Short-term variation in limb volume also exists. A study of socket loads in transtibial amputees (Sanders et al. 2005) monitored 8 transtibial amputees for changes in limb volume between morning and afternoon and then at 5 week intervals. Although load value changes on the level of within-day changes did not reach significance in this study, the loads did adjust over longer time scales.

The importance of volume change is that it directly affects the quality of fit of the socket. It affects the timing of the supply of the initial prosthesis, the use of fit management techniques and the requirement for socket replacement. A systematic review of volume measurement was published in 2011 (Sanders and Fatone 2011).

2.8 Artificial Neural Network Load Estimation

The concept of measuring socket load with neural networks came from work in the late 1990s to generate a tool for producing comfortably fitting sockets using a case-based

approach (Vinney et al. 2000). The requirement of this system to incorporate the range of parameters that relate to the quality of fit led to research into a FEA model of the socket, and the training of an neural network using the results from the model to produce a generalised transfer function between the output and input (Amali et al. 2001).

This solution used a three layer backpropagation neural network utilising the delta-bar-delta learning rule. An FEA model of a transtibial socket using 281 nodes was loaded in 10 positions around the socket brim. The stress at each node was used as the input to the neural network – the output being the forces at the socket brim.

The system was validated against randomly applied loads at the same locations. Accuracy against problem cases was reported as around 10%. Issues with the technique were in the number of training cases required to train the network (a common neural network issue) and training time. The suggestion of using photoelasticity (shown to correlate with FEA results on components (Andrews et al. 2001), and socket surface strain (Sewell et al. 2000) was made. The neural network advantages were recognised: in particular the estimation of loads from new conditions is very fast.

Work to combine the photoelastic effect with ANN techniques continued (Noroozi et al. 2004; Sewell et al. 2005). Photoelasticity is a phenomenon in which the stress in a transparent material can be observed: by applying polarised light and viewing the test material under a matching filter, the concentration of reflection fringes can be associated with particular strains. During tests of pure bending on a small test piece, ANN estimates and experimental measurements were close, although notably poorer at the lower end of the applied load range. Error on random load patterns was 4-8%.

Concurrently, work was being conducted to use surface strains on a socket model as the inputs to the neural network (Sewell et al. 2005). Tests were conducted on aluminium tubes, plastic cones and on realistic sockets. Innovation in the training data preparation included the use of linearity and superposition of loads and the use of noise injection on the training inputs. The number of hidden layers was set to the number of output values. Loading was achieved via a steel C-section instrumented with a strain gauge. Poor performance on low load cases was identified, with error magnitude variable.

The second iteration of the design during this project utilised rosette rather than individual strain gauges. 15 strain inputs were used to characterise 4 load positions. At this point the error of the network across the measurement range was evaluated, and the concept for a polynomial correction factor developed in order to improve performance at the extremes of the measurement range. Furthermore, the introduction of 'isolated' load cases in the training process in order to facilitate estimates on this form of load pattern was also investigated. At this point the spring-loaded arm was introduced (section 4.1.5).

The accuracy of the system on a realistic socket was around 12%. The system was tested during standing, walking and some modification of the socket configuration, although this was limited by the size and bulk of the collection hardware.

Results from this system using the photoelastic effect were published in 2005 (Sewell et al. 2005), as were extensions of the solution to other structures of interest such as aircraft components (Noroozi et al. 2005, 2006). The system was implemented with 15 strain gauge rosettes (i.e. 45 distinct inputs) and 16 socket regions in a transtibial amputee (Amali et al. 2006).

Error on test data was 8.8%. This did not use a polynomial correction factor, and errors were greater at low and high load positions. Loading from axial force whilst it was being worn was reported: here high loads were measured at points around the patella tendon and gastrocnemius origin, as expected in a PTB socket.

Amali et al. (2008) described a sensitivity study to assess the potential for simplifying the network inputs. Removing eight rosettes from the input pattern could reduce network training time by 30% while only increasing error by 1.3% (from 7.5% to 8.8%). Quantitative data were compared to qualitative reports from the participant and a photoelasticity study. The authors concluded that successful convergence onto an appropriate transfer function could not be guaranteed with high numbers of input values when these did not adequately distinguish between applied loads.

A fuller discussion of the polynomial correction factor was published in 2010 (Sewell et al. 2010). The methodology fitted 5th order polynomial equations to the residual error patterns. The values of corrected network values were visually very close to the target

values when supplied with generated superposition data, but were not explicitly reported numerically, and were not evaluated on physically measured data.

Sewell et al. (2012), studied the response of networks in some standing and walking. The authors were able to detect a change in pressure values when bodyweight was increased over the prosthetic side, and changes were also evident when translation of the foot relative to the socket was introduced. Dynamic measurements from walking were made, but only examined to demonstrate cyclic changes in applied pressure. Error of the network in use was estimated at 10% on test data.

The methodology was most recently applied to submerged marine plates (Ramazani et al. 2013) and aircraft wing ribs (Amali et al. 2014). In the former, an alternative technique was trialled: rather than a single network estimating 13 outputs using the input data, the input strains were supplied to 13 networks, each with one output corresponding to a single load output. In this approach it was possible to customise networks to different load positions, and improve overall performance by targeting aspects of the solution that demonstrated poorer performance. It was possible to reduce error by including an additional layer of hidden neurons in 2 networks. However the solution may be susceptible to errors on noisy data as the estimations of load are linked by structural behaviour.

The latter paper examining aeronautical structures used the more conventional structure of a single network, but used the Levenberg-Marquardt training algorithm in a 15-10-2 configuration. This work examined the effect of varying the number of hidden nodes within the network, identifying that this could significantly affect the quality of the load estimates. The best performing networks demonstrated an error of 8%, in common with previous work.

A Paris based group has also begun to investigate the ANN technique for measuring socket pressure (Bascou et al. 2015). Their approach has been to measure normal and shear forces simultaneously. To achieve this, socket loading during is conducted using an INSTRON machine, with the effect of both normal and shear load in the positions of interest, then subtracting the effect of pure normal loading. The large number of outputs necessitates many input strains and a large number of hidden neurons to enable convergence. Accuracy was reported as broadly similar to previous designs, but notably poorer on shear

measurements. A joint conference presentation was completed by this author in 2016 (Sewell et al. 2016).

A summary of prior work is shown in Table 12.

Paper	Input	Output	Nodes	Learning Algorithm	Estimated Problem Error
Amali et al., 2001	FEA Stresses	Socket Stresses	281-10-10	Delta bar delta	<10%
Noroozi et al., 2004	FEA Stresses	Beam Stresses	4-3-1 4-3-2	Delta bar delta	<4% <8%
Amali et al., 2006	Rosette Strain Voltages	Socket Stresses	45-16-16	Delta bar delta	9%
Amali et al., 2008	Rosette Strain Voltages	Socket Stresses	21-16-16	Delta	7.5%
Sewell et al., 2010	Rosette Strain Voltages	Socket Stresses	45-16-16	NR	12% <12% with correction
Sewell et al., 2012	Rosette Strain Voltages	Socket Stresses	30-16-16	NR	8.7%
Ramazani et al., 2013	Single Gauge Strain Voltages	Plate Stresses	16-50-13 16-20-1 16-20-20-1	NR	<7%
Amali et al., 2014	Single Gauge Strain Voltages	Aircraft Rib Stresses	15-10-2	Levenberg Marquardt	5%
Bascou et al., 2015	Rosette Strain Voltages	Socket Stresses (Normal and Shear)	36-NR-30	NR	<14.5% Normal <58% Horizontal Shear <75% Vertical Shear

Table 12 - Summary of literature of neural network applications to load distribution. NR means that this was not explicitly reported. FEA stands for Finite Element Analysis

2.9 Critical appraisal

The difficulty of producing definitive conclusions on the considerations relevant to prosthetic literature has been reported across the literature (Neumann 2009; Highsmith et

al. 2016). Lower-limb amputees represent a significant clinical population, and one that contains a number of stubborn challenges. Amputees form an extremely variable group, and behaviour of the stump and socket is predicated on the particular situation and configuration of the residual limb. Thus, combining results across study participants and over studies is complex.

Further to this, the methodological quality of many prosthetic studies is poor – the difficulty of producing highly valid studies restricts the usefulness of results. The nature of an amputation acts to preclude the use of many methodologies, with the effect that the majority of studies are observational in nature. Examples include the difficulty in blinding either participants or researchers to intervention, issues in removing confounding effects of volume changes or system set-ups and the ethical issues involved in deliberately supplying equipment that is not optimally configured.

2.10 Summary

Around 6000 new amputees are referred to UK prosthetic centres every year. The majority of these amputations are transtibial, with most amputations the result of vascular insufficiency. A range of device options exist, but functional prosthetic limbs require an interface between the artificial and residual limbs. This is the most common cause of prosthesis dissatisfaction: poorly fitting sockets are associated with numerous poor outcomes. Socket design remains a predominantly artisanal process: sockets are handcrafted to effectively respond to the individual demands of each residual limb. The principles of socket loading are only partially understood, and several designs of socket exist.

Socket quality is related to the distribution of pressure across the socket-limb interface. The load distribution has been challenging to measure effectively, and despite clinical interest has yet to be introduced into routine clinical practice. A review of existing socket measures has demonstrated significant barriers to routine use, including instrumentation error, interference with the interface and the requirement for detailed understanding of the geometry and material properties of the residual limb and prosthesis.

Socket pressure is also affected by several factors which can act to alter the application of load to the residual limb. These include mechanical factors, such as device alignment,

equipment configuration or socket design, may include environmental factors, such as terrain, slope or stair walking and may result from biological effects, such as variation in stump volume. These act to complicate the measurement of socket load, and can represent valuable context to explain changes or differences in measurement of residual limb condition.

In the next chapter, an explanation of a novel means of socket load measurement is provided. This has the potential to overcome many of the issues described above, and aid in the clinical prescription of prosthetic devices. A description of the method used to monitor socket deformation is given, and how this is converted into measurement of socket load reported. This is followed by a review of previous work using this form of system in load monitoring applications.

3 Systematic Literature Review of Transtibial Socket Load Changes with Socket Alignment Changes

3.1 Introduction

In the previous chapter, the state of the literature concerning amputee rehabilitation, with particular focus on the supply and quality of prosthetic sockets was surveyed. This identified that although the socket was of critical importance to the successful rehabilitation and compensation following amputation, it was a common cause for complaint amongst active amputees. Poorly fitting sockets are implicated in discomfort, pain, pressure injury and restrictions on use. Successful sockets can use a variety of designs to accommodate load, either by selectively applying force to particular regions or by attempting to equalise loading across the residuum. The load distribution is also known to vary according to changes in the use environment. Local changes in pressure can therefore have clinical implications.

These condition changes can come from various sources. Socket design changes, prosthesis equipment modification, walking terrain (slopes, stairs or other surfaces) and other situational changes have all been shown to alter pressure distributions. Of particular interest is prosthetic alignment. This refers to the geometric position of the prosthetic limb relative to the residual limb. The suitable alignment of components is something that is performed at every lower-limb prosthesis prescription. An optimal positioning in terms of rotation and translation of the socket provides a stable, cosmetically acceptable prosthesis with suitable load distribution. Perturbation of alignment away from optimal has consequences for load distribution.

A systematic review of the changes in socket load with alignment modification was carried out, and is reported in this chapter. A rigorous search strategy was used, and all articles conforming to the criteria were assessed using the guidelines for a state-of-the-science review published by the American Academy of Orthotists and Prosthetists (AAOP). The internal and external validity of each study was assessed, and the conclusions rated in terms of confidence. The common threats to validity were reviewed. This study was later published (Davenport et al. 2017). The results from this study are used in the design and reporting of practical assessment of transtibial socket loads presented in this work.

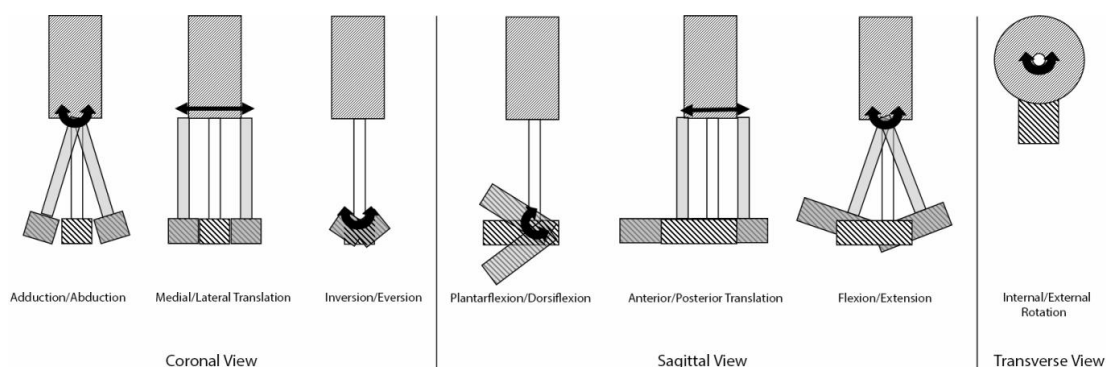


Figure 10 - Potential transtibial prosthesis alignment changes. Not shown are changes in pylon length.

The biomechanical effects on load in transtibial amputees anticipated with alignment changes were examined several reports, e.g. (Neumann 2009; Laing et al. 2011). It should be noted that when angular alignment changes are introduced, there is a compounding effect of the artificial limb reducing in effective length, which will create additional effects on the movement patterns employed by the user.

3.2 Methodology

The review was completed using the American Academy of Orthotists and Prosthetists guidelines for a state of the science review (Hafner 2008). These were written with regard for the probable design and quality of studies in the field – i.e. case-controlled and without a randomised-controlled design. Eligibility criteria (Table 13 and Table 14) were designed using the PICOS framework (Participant-Intervention-Comparison-Outcome-Study type).

Section	Criteria
Participants	<ul style="list-style-type: none"> • Unilateral transtibial amputees • Any prescription of functional prosthesis (excluding osseointegration)
Intervention	<ul style="list-style-type: none"> • Any (single or combination) of translation or rotation of prosthetic components that altered the geometric position of the artificial foot relative to the residual limb
Comparison	<ul style="list-style-type: none"> • Between altered alignment states and 'normal' or neutral' conditions
Outcome	<ul style="list-style-type: none"> • Quantitative measurement of socket-residuum pressure (normal stress) • Any mechanism for achieving this measurement
Study Type	<ul style="list-style-type: none"> • Any primary research, including case series or case studies

Table 13 - PICOS characteristics for inclusion criteria in the systematic review

Section	Criteria
Language	<ul style="list-style-type: none"> • Studies published in English
Publication Type	<ul style="list-style-type: none"> • Peer reviewed journal articles of primary research (i.e. excluding literature reviews, letters to the editor, commentaries etc.)
Publication Date	<ul style="list-style-type: none"> • Database inception - April 2016

Table 14 - Characteristics of eligible report standards

Four major databases were searched - Web of Science, CINAHL, ScienceDirect and RECAL legacy. This provided coverage of all the likely sources of prosthetics studies described by the AAOP guidelines.

3.3 Results

The process of study selection and inclusion is shown in Figure 11.

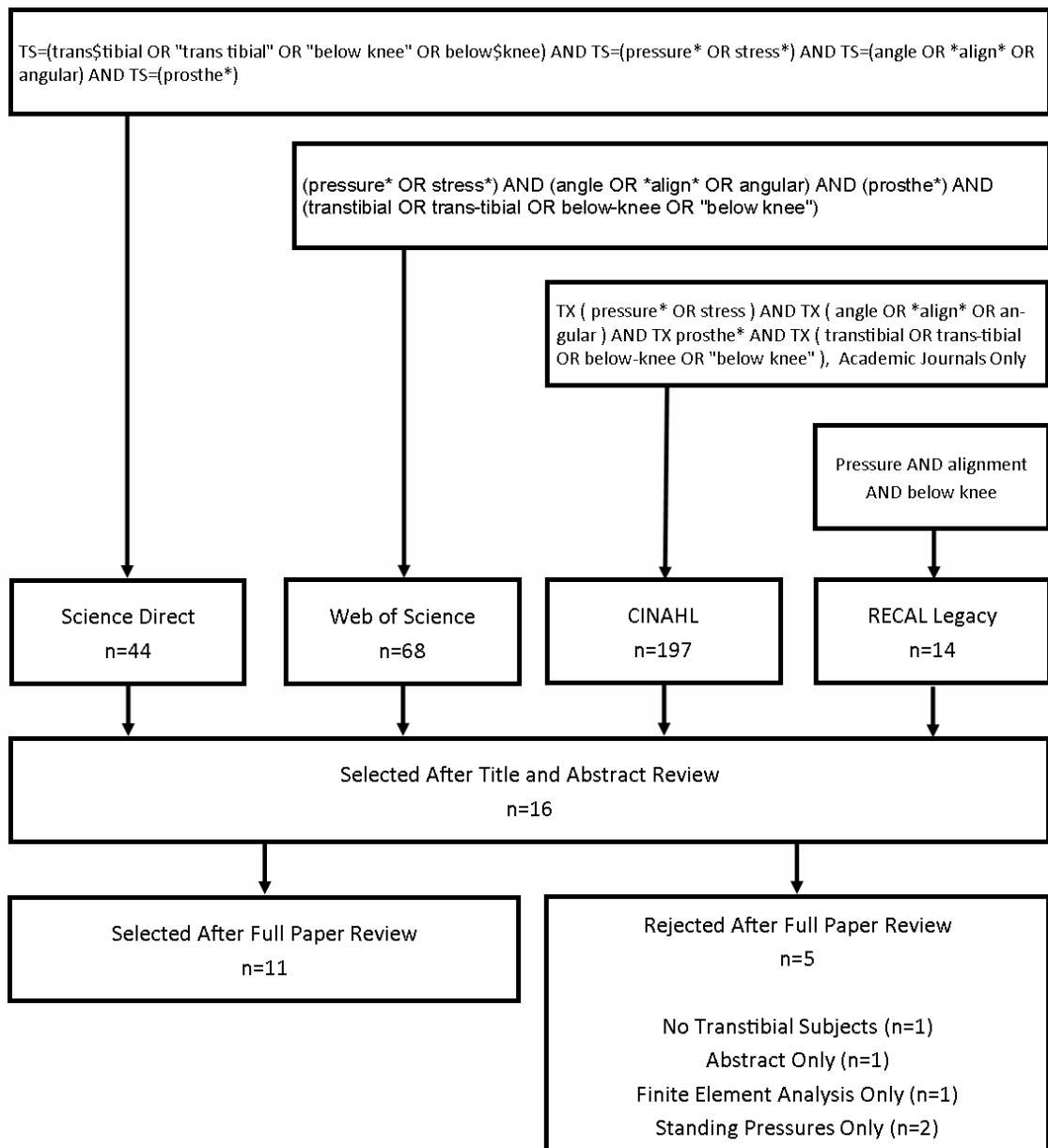


Figure 11 - Flowchart describing the search strategy employed.

The studies included in the review were examined for details on the design, conduct and results. A summary of this is included in Table 15. To provide an evaluation of study quality, set of assessment criteria supplied by the AAOP were and used to assess studies internal and external validity: these examined the quality of the design and presentation of results. The scores from this assessment were used to rate each study, and provide an estimate of the confidence that could be held in each study's conclusions (Table 16).

Lead Author	Participants	Gender	Measurement Sites	Collection Frequency	Intervention
(Pearson et al. 1973)	10 ^a	10M	Patellar tendon, distal anterior tibia, lateral/medial tibia	NR	A/P -10/-5/0/5/10 mm M/L -10/-5/0/5/10 mm F/E -10/-5/0/5/10° Ab/Ad -10/-5/0/5/10°
(Winarski and Pearson 1987)	2	NR	Patellar tendon, gastrocnemius	200Hz	F/E -10/-6/-3/0/3/6/10°
(Sanders et al. 1993)	3	3M	Antero-medial proximal, antero-lateral distal, antero-medial distal lateral, postero-proximal, postero-distal	125Hz	Ankle DF/PF 6/0/-9°
(Sanders et al. 1998)	2	2M	Antero-lateral distal, antero-lateral medial, antero-lateral-mid, antero-medial-mid, antero-lateral proximal, antero-medial proximal, lateral-distal, lateral-proximal distal, lateral-mid, lateral proximal, posterior distal, posterior-mid, popliteal fossa	175Hz	Subject specific AP, ML translation Ab/Ad rotation Ankle DF/PF
(Zhang, Turner-Smith, et al. 1998)	1 ^b	NR	Lateral condyle, medial condyle, patellar tendon, lateral tibia, medial tibia, antero-distal, popliteal depression, medial gastrocnemius, lateral gastrocnemius	200Hz	F/E -8/0/8°
(Sanders and Daly 1999)	3	3M	As in Sanders et al. 1993	125Hz	Subject specific Ankle DF/PF

(Seelen et al. 2003)	17	11M 6F	Array measurement on anterior, medial and lateral aspects	50Hz	5mm heel and forefoot wedging
(Kang et al. 2006)	10	NR	Array measurement	NR	F/E 10/5/0°
(Jia et al. 2008)	1	1M	Array measurement	50Hz	F/E -6/0/6°
(Neumann et al. 2013a)	2	1M 1F	Array measurement, regions selected on patellar tendon, popliteal depression, distal tibia and gastrocnemius	200Hz	A/P -5/0/5 mm
(Courtney et al. 2016)	1	1M	Array Measurement	NR	A/P -10/0/10 mm M/L -10/0/10 mm F/E – 3/0°

Table 15 - Description of included studies. ^a Only one participant completed angular alignment changes. ^b Although five participants were recruited, only one completed alignment changes. NR= Not reported. A/P is anterior posterior, M/L is medial/lateral, F/E is flexion/extension, Ab/Ad is abduction/adduction, DF/PF is ankle dorsiflexion/plantarflexion.

Definition of confidence levels in conclusions	
Rating	Description
High	High confidence can be placed in the findings of this investigation. The article is methodologically strong, or has methodological issues that are unlikely to impact the confidence with which the outcome statement can be made. Tests of statistical significance have been undertaken.
Moderate	Moderate confidence can be placed in the findings from this investigation. There are some methodological issues that detract from our confidence in the findings.
Low	Low confidence can be placed in the findings from this investigation. There are significant methodological issues which compromise the confidence with which outcome statements can be made.

Table 16 - Description of ratings of conclusion confidence

Of the 11 studies included in the review, 7 were rated as having low internal/external validity, and 4 as having moderate internal/external validity. No studies were classified as providing high quality evidence. A summary of the evidence supplied by studies (and the associated confidence in these conclusions) is shown in Table 17.

Evidence summary with associated confidence		
Confidence	Lead Author	Key Conclusions
High	N/A	None
Moderate	Sanders (1998)	<ul style="list-style-type: none"> The majority of measured sites demonstrate significant pressure changes with alignment modification, with an emphasis on the posterior surface. Compensations to one alignment change are not necessarily symmetrical in response to opposite alignment alterations.
	Sanders (1999)	<ul style="list-style-type: none"> Misalignment effects are similar in magnitude to within and between session variances in experienced participants.
	Seelen	<ul style="list-style-type: none"> Plantarflexion increases subpatellar pressure and decreases tibial end pressure. Dorsiflexion decreases subpatellar pressure and increases tibial end pressure
	Kang	<ul style="list-style-type: none"> A/P realignment alters pressure distribution in a systematic and consistent manner, including significant changes at the subpatella and tibial end regions
Low	Pearson	<ul style="list-style-type: none"> Greater sensitivity to angular changes than translation changes
	Sanders (1993)	<ul style="list-style-type: none"> Wave form shape changes were not consistent across sites or across subjects
	Jia	<ul style="list-style-type: none"> Duration of sub-maximal pressure alters significantly, as does the time-pressure integral (to a greater extent than peak pressure alone).
	Neumann	<ul style="list-style-type: none"> Fitted linear regression models are potentially unique for individuals and also for socket designs and alignments.
	Courtney	<ul style="list-style-type: none"> Individual responses are evident to alignment changes and associated socket design.

Table 17 - Reported evidence from included studies.

The articles identified exhibited a range of threats to their internal and external validity. In terms of internal threats, the range of scores was from 9 (Sanders et al. 1993) to 18 (Courtney et al. 2016) out of a possible 30.

3.4 Discussion

The majority of studies included no blinding to intervention. Four studies blinded participants to alignment changes. Only one study (Zhang et al. 1998) reported double-blinding. It has been suggested that fully effective blinding of participants is unlikely in prosthesis configuration studies; however there is evidence to suggest that transtibial amputees have only a limited ability to detect changes in device alignment (Boone et al. 2012). Investigators were blinded in four studies: alignment was altered by a separate team member. The suitability of each alignment intervention was not well described by researchers or participants. Only Neumann (2013a) used a method to rate the acceptability at each stage.

All studies recruited using samples of convenience. This meant that although inclusion criteria were well reported, exclusion criteria were poorly described. The quality of test socket fit was not described in the majority of studies.

Further to this, adaption to each intervention was also likely inadequate in all studies. Although the literature does not provide a firm recommendation for suitable acclimatisation time to alignment changes, a review of socket design changes found that allowed accustomisation times were around three months (Yeung et al. 2013), although alignment changes are considered less significant than a socket design change. Most studies did not describe the adaptation time: the two that did (Jia et al. 2008; Sanders et al. 1998), restricted adaptation time to five minutes or less. Two studies described acclimatisation time, one (Sanders et al. 1998) deliberately minimised adjustment time, reportedly to maximise the measurement changes.

Attrition of participants during studies was low. The exception was Neumann, who recruited four participants but reported results for two: this was due to equipment failure. Only two studies ((Sanders et al. 1998; Sanders and Daly 1999)) involved measurements in multiple sessions, in the former, two participants each in two sessions, and in the latter three participants, one each of whom took part in two, three and four sessions.

The use of sensor arrays has created a new issue in study reliability. As the arrays cover areas greater than the positions of interest on the interface, subsections of the array are used to

report pressures: the choice of the size and position of these windows is to some extent a subjective process. Several studies (Kang et al. 2006 and Courtney et al. 2016) used arrays, but did not report their methods for isolating subsections. Neumann presented the precise size and location of the subregions of sensels included in their analysis.

Several studies did not include sufficient detail on the calibration methods employed and were marked as containing threats to validity. In-socket pressure measurement is a challenging process, and sensors are known to suffer from numerous limitations to performance (Pirouzi et al. 2014). For this reason it is important that authors report on the method and results of calibration of the sensors in use, or clearly reference work which does so.

Statistical significance was only evaluated in a few studies and a universal lack of justification for the use of parametric tests. As the assumption in the use of these tests is that the results are consistent with a normal distribution, it is important for this to be confirmed. The failure to report the results of such tests may mean that non-parametric equivalent tests would have been more appropriate.

Several publications did not report results with sufficient detail. Some collected data but then failed to include it (e.g. Pearson 1973). For some, thorough presentation of data was only completed for some aspects of the intervention (e.g. Neumann et al. 2013a; Winarski and Pearson 1987).

Similarly, some statistical tests employed were also misused within included studies, e.g. using multiple t-tests without correction when an ANOVA test (Barton and Peat 2014) may be more appropriate. Doing so reduces the chances of a type I error.

Extensive conclusions on the impact of alignment changes on prosthetic socket pressure are difficult to draw due to the significant inhomogeneity of techniques and interventions reported. Nevertheless, there appears to be moderate evidence for a systematic and repeatable change in pressures on the anterior and posterior surface in response to sagittal rotational alignment alterations within individuals. Lower quality evidence supports the idea that although changing alignment does cause meaningful shifts in pressure patterns across the

socket, these changes are particular to individuals and to socket designs. Moderate-rated evidence from Sanders and Daly (1999) indicates that the changes from alignment can be similar in magnitude to the variance assessed between measurement sessions. Socket pressure measurement is known to be subject to numerous confounding factors (e.g. stump volume change), and this may be one reason for the dearth of stronger evidence statements.

Several studies commented on the greater sensitivity to angular changes than pure translation. It seems likely that this is because rotational changes will also act to alter the effective limb length of the prosthesis, which is hard to compensate for (particularly given short acclimatisation time). No studies performed an additional correction for changes in prosthesis length.

Moderate evidence supports the biomechanical assumptions of early theoretical work in the field. In particular; increases in subpatellar pressure/decreases in distal posterior pressure in response to plantarflexion of the ankle and to socket extension and the opposite in response to ankle dorsiflexion/socket flexion, consistent with consideration of the socket as a pseudo-joint (Tang et al. 2015).

Although the majority of studies reported values of peak pressure change only, one study concluded that greater differences were evident in other measures of loading response, such as pressure time integral. It is possible that there is greater distinguishing power contained within the measurements of interface pressure than is suggested by the basic values reported by the majority of studies. Unfortunately, the limited nature of the reports of these data precludes detailed analysis.

3.5 Conclusions

A systematic literature review was completed on the topic of transtibial socket load changes with alterations in device alignment. 11 peer-reviewed journal articles were identified which met the inclusion/exclusion criteria, and these were evaluated in detail using assessment criteria developed by the American Academy of Orthotists and Prosthetists. This graded the conclusions drawn by each study and assembled into a set of evidence statements with varying degrees of confidence.

Included studies varied widely in terms of the intervention, the measurement methods used, data processing and the outcome measures reported. Gaps were identified in many aspects of alignment change, with only very limited data available in many configurations. Study quality was never rated higher than moderate in either internal/external validity, and was rated as low in the majority of cases.

Several aspects of studies were particularly poorly represented: the quality of socket fit, the quantification of the initial alignment state and the clinical suitability of the alignment interventions were commonly underreported. The nature of the study design also acted as a limit to the utility of results: all articles were classed as before-after studies, and the quality of data presentation and statistical evaluation was also often poor.

Despite this, some conclusions could be drawn with moderate confidence. In particular, there appear to be reliable changes in socket load in response to sagittal plane rotation on the anterior and posterior surfaces. However, several studies highlighted the significant individual component of the alignment-load response. Load changes were not necessarily symmetrical about neutral alignment, and changes could be masked by differences of similar magnitude due to changes between measurement sessions.

Some limitations in the approach taken are present. By limiting inclusion of articles to the English language, some work may be missed. As the sole reviewer, the study was susceptible to subjectivity in opinion on study quality and technical approach (although this was reduced by the use of the AAOP review process).

The results of this study were used to inform the approach taken in work completed in this project. In particular, although the experimental methodology was similar to this previous work, attempts were also made to assess the changes between and within-sessions. Alignment change interventions were kept to those of reasonable clinical significance and statistical evaluation of results was carefully considered. The results of this work is presented in Chapters 8 and 9.

In the next chapter, the design and development of the hardware and software used throughout this work is described. In addition, the process of ethical approval and risk management is also reported. This is followed by an evaluation of the accuracy and reliability of the produced system, and of the impact of configuration changes to the measurement system.

4 Theoretical background and data preparation

In the previous chapters, the state-of-the-art in research into the difficulties lower-limb amputees face was reviewed. In particular, the importance of understanding the pressure distribution at the limb-socket interface was examined. It was also established that current methods for evaluating this relationship suffered from a range of issues which restricted their application in clinical practice.

In this chapter, the theoretical framework for a different form of socket pressure measurement is established. The technique of using an artificial neural network to investigate socket load has been explored and shown to be a promising approach to this measurement problem, both in terms of feasible measurements and for advantages in the recording process. However, the variation in the estimate from the production of training networks has not been examined in detail, nor the potential for improvements from particular configurations.

The basis of the technique is that rather than attempt to measure within-socket loads directly, the relationship between internal loads and the change in shape of the socket structure is estimated via a neural network. A simplified problem with a low number of measurements and loads is defined, and the process of conditioning the recording to provide sufficient training cases is described. This is followed by an explanation of the means of constructing and training a neural network to model the transfer function. Means of improving the output of the network estimate are discussed.

This is followed by a summary of the practical development of hardware and software tools to collect practical socket load measurements. A review of the risk assessment carried out and the process of ethical approval for the planned studies are also presented.

The techniques described in this chapter are investigated experimentally in later chapters. In particular, the impact of data conditioning and network architecture is examined in Chapter 5. In chapter 6, the construction of groups of networks into ensembles is evaluated, followed by Chapter 7, which explores the effect of modelling residual network error with a correction factor. Subsequent chapters apply these results to measurements within amputee volunteers,

results which will act to clarify the ability of the system to monitor dynamic loads and respond to changes in applied load.

A wide range of computational techniques exist that could be implemented to estimate load distributions. Here, a short summary of the problem is given to justify the use of feedforward-backpropagation neural networks in this study.

The application in question can take advantage of supervised learning. In contrast to some problems, where the outcome in terms of associations of data may be completely unknown from the source material, in this case there is a clear *a priori* relationship that can be exploited. By using a method of collecting training data (where the relationship between strain voltage change input and the load output in particular positions is implicit in the structure of data supplied to the system) and combining measured loads into combinations of load distributions (using the assumptions of linear material behaviour and superposition of loads, Section 4.1.6), a more efficient learning process can be utilised (Schöllhorn 2004).

The problem is also one of the estimation of a set of transfer functions relating structural loading with the deformation of the material being loaded. The problem of socket loading is somewhat resistant to analytical solutions (for example finite element analysis) due to the complexity and individual geometry of the socket and the particular nature of the residual limb (Sewell et al. 2000). In this application, it is sufficient for there to be some assumed relationship between the input and output: an artificial intelligence technique can establish a solution, given enough information to characterise the situation. Neural networks of this type have been applied to many other situations that are difficult to describe using conventional analysis: examples include dynamic vibration problems (Noroozi et al. 2016), and the structural issues described in section 2.8. Feedforward-backpropagation neural networks can be considered a mature technique (Yu and Wilamowski 2011), albeit one with a limited history of application in this precise problem. As the problem can be considered a form of transfer function estimation, many forms of artificial intelligence techniques more suited for classification, clustering or data reduction can be neglected (i.e. Kohonen maps (Barton et al. 2006), support vector machines (Kamruzzaman and Begg 2006) and other types (Pandey and Mishra 2009)).

The problem in this application can be modelled as a series of discrete situations that can be examined individually. This can be an average of loading taken over a period of time (for example, during a few seconds of stable standing, where the structural deformation can be assumed to remain relatively consistent) or may represent the load experienced at a single point in time. The results in the latter case are not critically dependant on the loading situation immediately preceding the instant in question. For this reason, a simpler model from a feedforward-backpropagation network is sufficient, and more complex models featuring time-dependent characteristics are not required (as described in e.g. Garhwal 2013). This eliminates the need to consider recurrent network structures or similar designs.

In summary, the choice of feedforward-backpropagation neural networks for an application of the type covered by this work is a function of the problem under examination. As the situation is one where a set of transfer functions must be estimated, where input patterns can be treated in isolation and where supervised learning can be used, neural networks of this type are a suitable choice. In addition, the essential applicability, if not the detailed behaviour, has previously been established. The work presented here is therefore in the context of developing the understanding of a working technique, the evaluation of solution quality and methods to improve this, and in extending understanding to novel measurement situations.

4.1 Data collection and training preparation

The methods described in this chapter have been developed as part of a research project that has proposed the use of neural networks to solve structural loading problems. A review of previous work using the technique was reported in Chapter 2.

4.1.1 Problem definition

In order to demonstrate the neural network system, a simplified situation is specified: one using four external strain measurement voltages to predict the values of three loads imposed on a structure (Figure 12). Signals are conditioned in the same manner as in the socket application, but the reduced scale of the problem condenses the description.

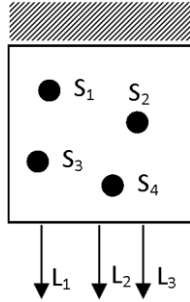


Figure 12 - Load and Measurement example used in this chapter. S_{1-4} represents deformation measurement positions. L_{1-3} is load applied to the structure in 3 different positions

The target 'seed' file is shown in equation (1).

$$\begin{bmatrix} S_{01} & S_{02} & S_{03} & S_{04} \\ S_{11} & S_{12} & S_{13} & S_{14} \\ S_{21} & S_{22} & S_{23} & S_{24} \\ S_{31} & S_{32} & S_{33} & S_{34} \end{bmatrix} \begin{bmatrix} L_0 \\ L_1 \\ L_2 \\ L_3 \end{bmatrix} \quad (1)$$

The seed file consists of a set of practically obtained measurements used in the generation of large numbers of training cases. It contains two components – values representing the effect on the measurement gauges from the loading states (S_{01} to S_{34}), and values representing the loads being applied (L_0 - L_3). In this example, the measurement section is 4 x 4 (for 3 load states plus one unloaded state by four measurement positions), and the load values section 4 x 1 in size.

4.1.2 Strain gauge measurement

In this work foil resistive strain gauges were used. The choice of strain gauges is explored in more detail in Section 6.2, but in brief, these devices are cheap, well-understood and responsive to changes in socket load (Amali et al. 2006). The measurement element of these gauges consists of a pattern of conductive material with a long path through the measurement region (Figure 12). When the gauge is in tension the cross-sectional area of the conductor decreases. When current is passed through the conductor the effective resistance alters in a consistent manner. Under compression, the cross-sectional area increases, creating the opposite effect (*Practical Strain Gauge Measurement* 1999).

Strain on the measurement gauge alters the resistance of the gauge according to equation (2). The GF term stands for gauge factor.

$$\text{Strain} = \frac{\Delta R_G / R_G}{GF} \quad (2)$$

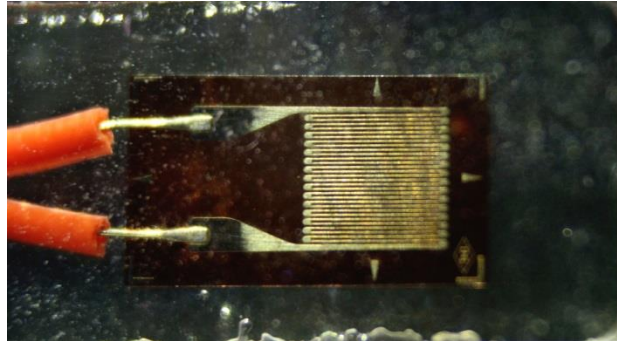


Figure 13 - Close up view of the strain gauges in use in this project. The resistive grid is 4x4mm. The entire gauge is enclosed in a flexible coating

Measurements from the strain gauges are first conditioned by placing the measurement gauge into a Wheatstone bridge (Figure 14). As single measurement gauges were being used, quarter-bridge completion circuitry was used. Bridge circuits are used as an alternative to detecting the very small change in gauge resistance – by placing the gauge into the configuration shown in Figure 14 with three other resistors of matching resistance. When the circuit is energised with V_{in} , the change in V_{out} is given by equation (3).

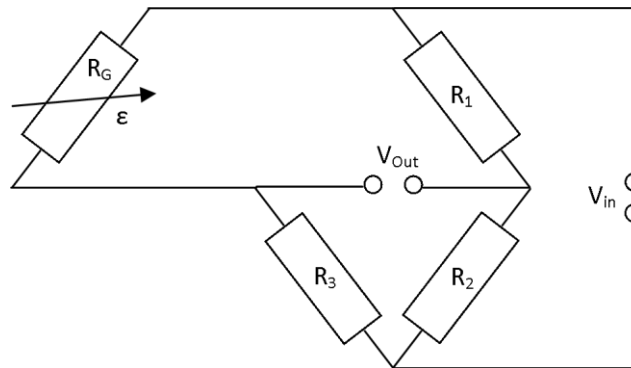


Figure 14 - The Wheatstone bridge circuit. V_{in} is the energising voltage, V_{out} the reading taken. R_{1-3} are balancing resistors, with R_G the strain gauge resistor

$$V_{out} = V_{in} \left[\frac{R_3}{R_3 + R_G} - \frac{R_2}{R_1 + R_2} \right] \quad (3)$$

The system used in this implementation used a three lead configuration. As lead resistances R_{L1} and R_{L3} are the same, the effects of variance in the lead wire resistance are significantly reduced. The bridge completion is modified to that shown in Figure 15.

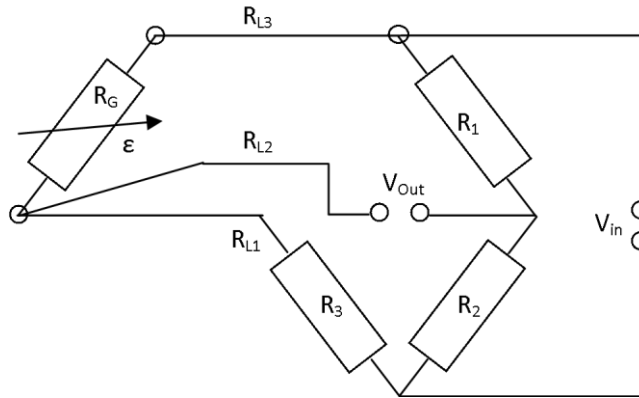


Figure 15 - The 3-Lead quarter bridge configuration used in this thesis. R_{L1-3} are the resistances in the cabling as the gauge is somewhat remote to the bridge circuit. The values of R_{L1} and R_{L3} must be similar, R_{L2} is less critical.

The output of the bridge completion circuitry is then a set of output voltages which vary with the application of strain. The hardware used in this study was capable of 16 bit resolution (i.e. 65,535 distinct readings). The overall measurement range was ± 2.5 mV. The measurement voltages were centred as changes could be in either direction. This range and resolution provided an adequate balance between capturing the complete changes in voltage from use with the socket during walking and the sensitivity to detect small differences.

Quarter-bridge completion has the advantage of not requiring the accurate positioning of an additional measurement gauge for balancing the circuit, a requirement that is not practical within this application. However, this comes at a cost of reduced sensitivity, somewhat higher noise and no temperature compensation (Hoffmann 1986).

4.1.3 Temperature correction

The strain measurements are supplemented by a temperature correction gauge. This achieved with an additional gauge that was unloaded throughout measurements. By comparing the change in reading from this unloaded gauge over time, a correction factor can be calculated an

applied to the other channels. The compensation gauge was mounted on an unloaded element of the same material to closely replicate the temperature changes occurring.

As the temperature gauge is susceptible to small scale fluctuation, the initial two seconds of recording were taken as the baseline reading. Subsequently, values were adjusted according to a two-second moving average. The effect of this is shown in equation (4) and (5). F represents the sampling frequency.

$$\text{Temperature Channel } T = \begin{bmatrix} VT_1 \\ VT_2 \\ VT_3 \\ \vdots \\ VT_n \end{bmatrix} \quad (4)$$

$$\text{Temperature Baseline } T_0 = \frac{\sum_{n=0}^{2F} VT_n}{2 * F} \quad (5)$$

The temperature correction applied at frame 'i' can then be assessed using (6):

$$T_{ci} = \left(\frac{\sum_{i-2F}^i VT_i}{2 * F} \right) - T_0, \text{ For } i > 2 * F, \text{ Else } T_{ci} = 0 \quad (6)$$

The modification to the recorded gauge voltages is therefore (for time frame i, equation (7)):

$$[S_{1i} \ S_{2i} \ S_{3i} \ S_{4i}] = [V_{1i} - T_{ci} \ V_{2i} - T_{ci} \ V_{3i} - T_{ci} \ V_{4i} - T_{ci}] \quad (7)$$

Therefore, for the first two seconds of any recording, the strain gauges are uncorrected, and in all subsequent frames, the output of each gauge is modified according to the change in the dummy gauge averaged over the previous two seconds.

4.1.4 Time average

Following temperature correction, the recorded voltage readings may be averaged over some time period in order to remove the high frequency fluctuations in the measurement signal. A summary of this for a single row of the seed file is shown below (for R the duration of the average, F the sampling frequency and S₀ representing the unloaded measurement, (8)):

$$[S_{11} \quad S_{12} \quad S_{13} \quad S_{14}] = \left[\frac{\sum S_1}{R*F} - S_{01} \quad \frac{\sum S_2}{R*F} - S_{02} \quad \frac{\sum S_3}{R*F} - S_{03} \quad \frac{\sum S_4}{R*F} - S_{04} \right] \quad (8)$$

This process is repeated for each of the loaded states. Thus a file can be produced that contains the mean effect change in the strain values for each load condition that accounts for the effects of long term temperature drift, high frequency noise and the original measurement values.

4.1.5 Structure loading

A representation of the loading rig used to train sockets is shown in Figure 16. The vertical beam is fitted with a spring that applies a consistent force on the structure, applied via a circular plate fitted with a ball-joint to ensure a force is normally applied (Figure 17). The function of this loading rig was first described in a project report published in 2005 (Sewell et al. 2005). This completed numerous validation evaluations to confirm the reliability and linearity of the system. It was a replacement for simpler loading devices which applied load at several points simultaneously.

The work presented in that project provided an estimate of the consistency of the applied load to be within 1.2%. The rig was not substantially altered in this work – the measurement gauge that recorded the deformation of the beam arm was modified to a single quarter-bridge completion gauge in order to function with the wireless measurement nodes in use. The vertical height and the rotation at the base (which facilitate loading any point on the socket wall) were fitted with measurement scales in order to help keep loading reliable between test cases.

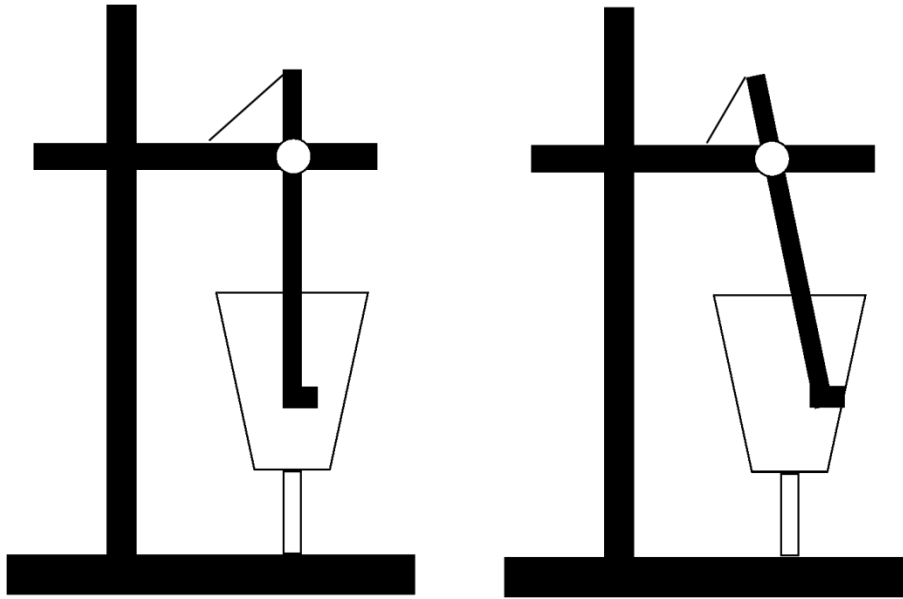


Figure 16 - A simplified representation of the means of structure loading. As the beam is brought into contact with the structure wall, the long beam bends slightly, a deflection that is picked up by the strain gauge mounted on this element

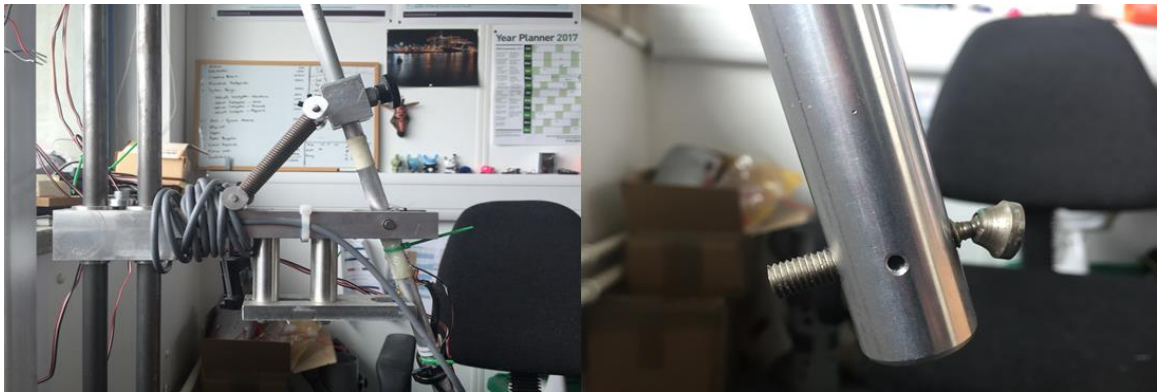


Figure 17 - Images of the loading rig. Left: the spring element, and the mounted instrument gauge. Right: the contact element with a ball-joint to ensure normal force application.

The beam used to apply the force to the structure was instrumented with a strain gauge. This gauge was conditioned in the same way as the other measurement gauges. The relative change in this gauge is normalised to the strain recorded at maximum load, equation (9). In practice the force measurements were very close in magnitude.

$$\begin{bmatrix} L_0 \\ L_1 \\ L_2 \\ L_3 \end{bmatrix} = \begin{bmatrix} 0 \\ \frac{L_1 - L_0}{L_{max}} \\ \frac{L_2 - L_0}{L_{max}} \\ \frac{L_3 - L_0}{L_{max}} \end{bmatrix} \quad (9)$$

The loading system was the same as used in previous studies of this form of measurement (see section 2.4). The only difference was that the height of the loading frame and the rotating socket mount were fitted with measurement scales to more accurately repeat loading events.

Once this process is complete, the seed file is ready to be used in the construction of the training data. The loading rig was capable of providing consistent and reliable loading to the socket: an example of a variance expressed as the standard deviation of readings as a percentage of the applied load is shown in Table 18.

Test Load	Percentage Variance
1	0.61%
2	0.92%
3	0.59%
4	0.52%
5	0.41%
6	0.83%
7	0.71%
8	0.51%

Table 18 - Standard deviation as percentage of applied load for eight loading measurements

4.1.6 Material behaviour assumptions

Two assumptions about the behaviour of the measurement system are made in order to provide sufficient training cases to enable the transfer function relating loads to strains to be modelled. The first of these is the structure behaves linearly with respect to load.

An example of this is given below (Equation (10)). The effect of a load equivalent to half L_1 ($0.5L_1$) is shown. It is equivalent to the half of the change in voltage recorded for the full load L_1 .

$$[0.5L_1] = [0.5 * (S_{11} - S_{01}) \quad 0.5 * (S_{12} - S_{02}) \quad 0.5 * (S_{13} - S_{03}) \quad 0.5 * (S_{14} - S_{04})] \quad (10)$$

Similar modifications to the relative change in strain with the application of load can be made to any magnitude of load in any of the selected loading positions.

4.1.7 Linear load superposition

The second assumption made is that superposition of loading remains valid. This is shown diagrammatically in Figure 18.

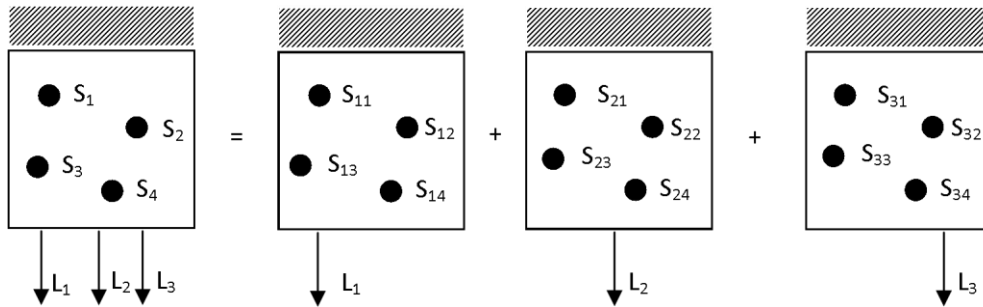


Figure 18 - Illustration of the theory of superposition. The effect of multiple loads on the measurement gauges is equivalent to the sum of the effects of those loads applied separately

In order to produce training cases that represent to combinations of multiple loads, the sum of the effects of singly-applied loads is produced. An example desired load, L_x is shown in equation (11) and (12):

$$L_x = [0.75L_1 \quad 0.5L_2 \quad 0.25L_3] \quad (11)$$

$$\begin{bmatrix} S_{1x} \\ S_{2x} \\ S_{3x} \\ S_{4x} \end{bmatrix} = \begin{bmatrix} 0.75 * (S_{11} - S_{10}) + 0.5 * (S_{21} - S_{20}) + 0.25 * (S_{31} - S_{30}) \\ 0.75 * (S_{12} - S_{10}) + 0.5 * (S_{22} - S_{20}) + 0.25 * (S_{32} - S_{30}) \\ 0.75 * (S_{13} - S_{10}) + 0.5 * (S_{23} - S_{20}) + 0.25 * (S_{33} - S_{30}) \\ 0.75 * (S_{14} - S_{10}) + 0.5 * (S_{24} - S_{20}) + 0.25 * (S_{34} - S_{30}) \end{bmatrix} \quad (12)$$

By building a file of random combinations of loads and calculating the effect that this has on the measurement values, sufficient training cases can be generated to represent the transfer function.

Also constructed at this stage are so-called ‘isolated’ loads. These are training cases where load distribution is set to zero in all but one position. This improves network training in cases where one load is dominant (Sewell et al. 2012).

4.1.8 Noise injection

The training data can be further modified in order to improve the generalisation of the neural network to new cases which do not conform to the exact pattern modelled by the assumption of a perfectly linear response. A detailed investigation into modifying noise injection is presented in chapter 5: a technique used in previous work (Amali et al. 2006) is shown below in (13):

$$\begin{bmatrix} mS_{1x} \\ mS_{2x} \\ mS_{3x} \\ mS_{4x} \end{bmatrix} = \begin{bmatrix} S_{1x} \pm 1\mu\epsilon \\ S_{2x} \pm 1\mu\epsilon \\ S_{3x} \pm 1\mu\epsilon \\ S_{4x} \pm 1\mu\epsilon \end{bmatrix} \quad (13)$$

In this example, input values are modified in a random direction by $1 \mu\epsilon$ to form mS_{nx} , the modified input value. This is applied to the input file.

Alternatives to this are also possible, e.g. altering the magnitude of the applied change to be related to the maximum measured on that channel (equation (14)) where ‘A’ is a predefined factor.

$$\begin{bmatrix} mS_{1x} \\ mS_{2x} \\ mS_{3x} \\ mS_{4x} \end{bmatrix} = \begin{bmatrix} S_{1x} \pm Rand() * A * (S_{Max1} - S_{01}) \\ S_{2x} \pm Rand() * A * (S_{Max2} - S_{02}) \\ S_{3x} \pm Rand() * A * (S_{Max3} - S_{03}) \\ S_{4x} \pm Rand() * A * (S_{Max4} - S_{04}) \end{bmatrix} \quad (14)$$

This creates the pattern seen in Figure 19, where the width of the band of values is related to the factor chosen and the range of values observed during training. In this thesis this is referred to as the constant noise model. The method of selecting a single value of microstrain was not applied – as values were not converted into strain values and instead would vary with the

range of measurement selected, the noise model described in equation (14) was used in its place.

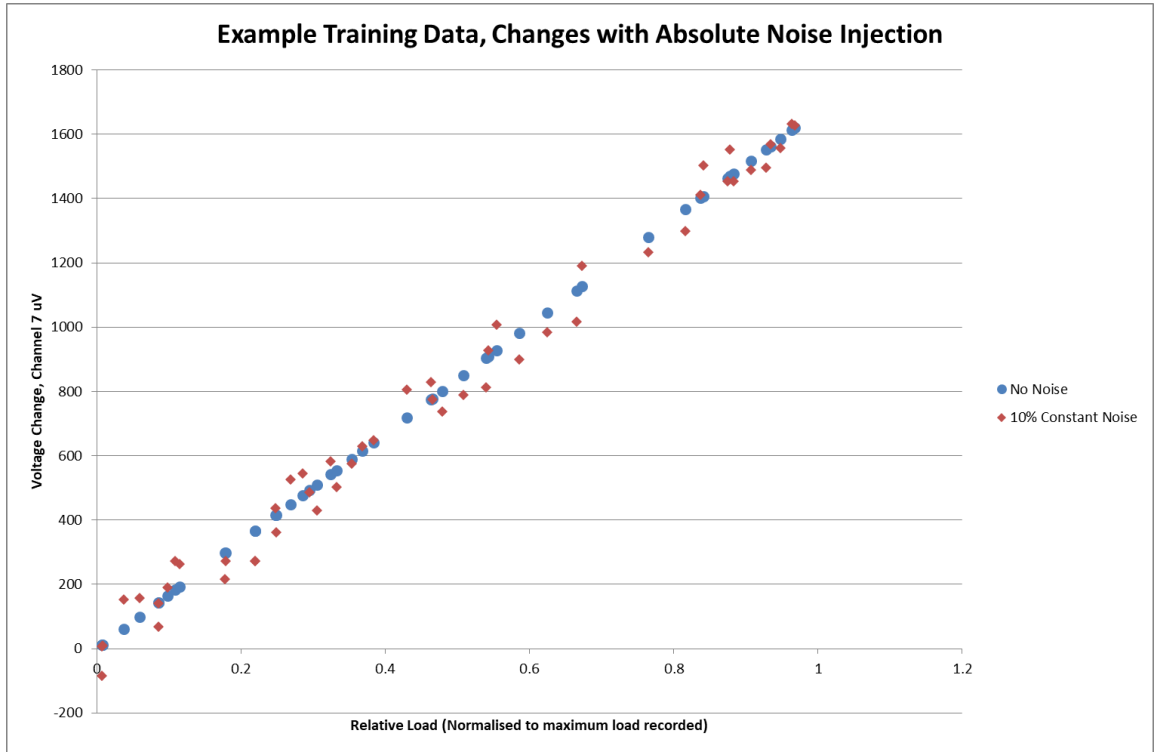


Figure 19 - Constant Noise Injection Model. The 'isolated' loads for a single input channel and single load position are shown for both altered and unadjusted input values. Here $A=0.1$ or 10% constant noise injection.

Another model (here referred to as the 'linear' model, equation (15)) was created to vary the noise injection in a manner that varied with the measured load:

$$\begin{bmatrix} mS_{1x} \\ mS_{2x} \\ mS_{3x} \\ mS_{4x} \end{bmatrix} = \begin{bmatrix} S_{1x} \pm Rand() * B * S_{1x} \\ S_{2x} \pm Rand() * B * S_{2x} \\ S_{3x} \pm Rand() * B * S_{3x} \\ S_{4x} \pm Rand() * B * S_{4x} \end{bmatrix} \quad (15)$$

This model creates the load distribution shown in Figure 20 - a cone shape where higher magnitude loads are allowed to deviate from the ideal linear response to a greater level than lower loads on the same output channel, controlled by the 'B' term.

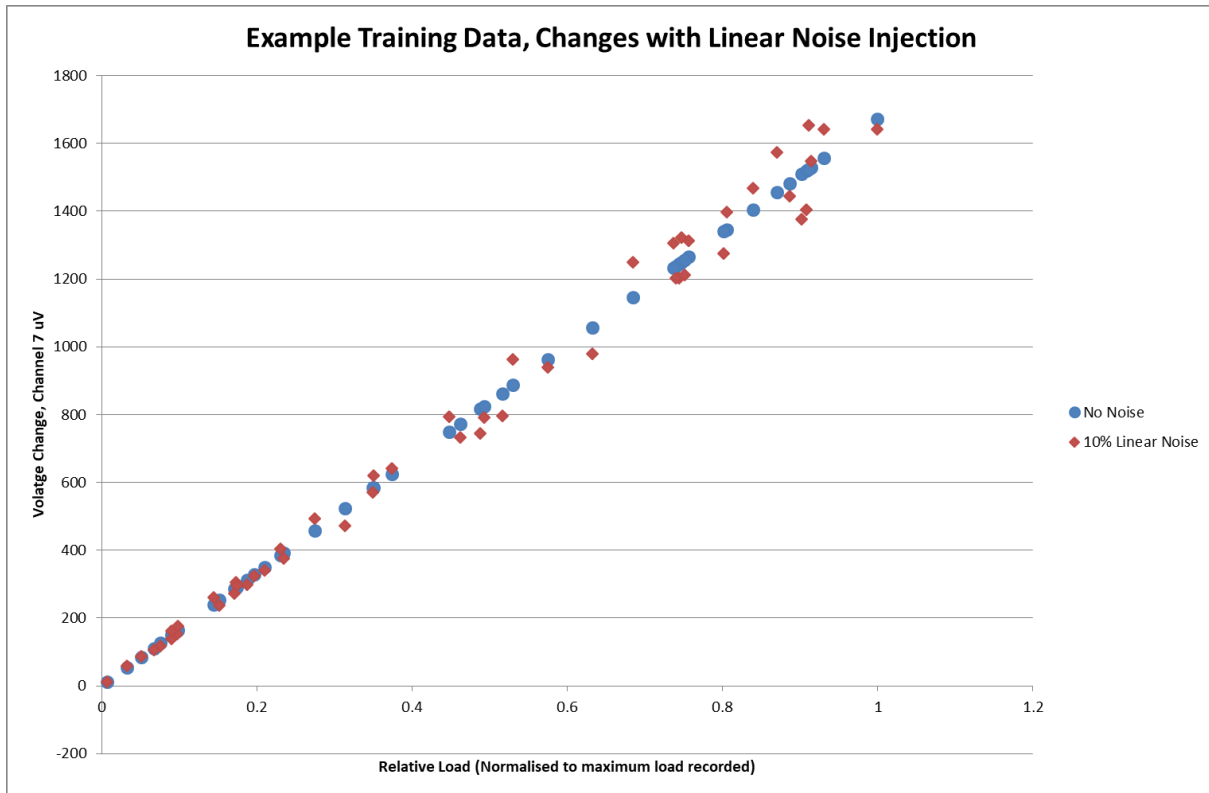


Figure 20 - Linear Noise Injection Model. The 'isolated' loads for a single input channel and single load position are shown for both altered and unadjusted input values. Here $B=0.1$ or 10% linear noise injection.

4.1.9 Pre-processing summary

The completed block diagram for the training process is shown in Figure 21, demonstrating the key functions (white blocks), the optional functions (grey blocks) and outputs (red outlined blocks).

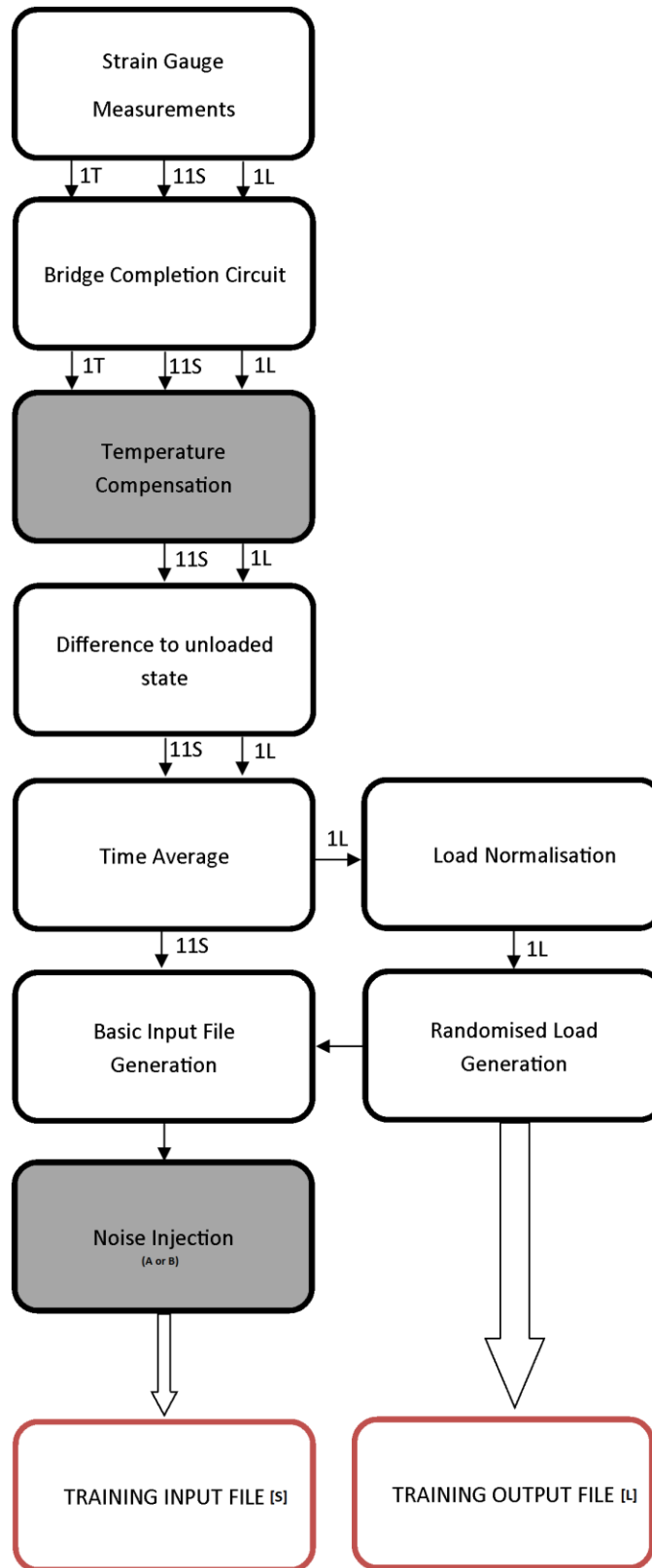


Figure 21 - Flow diagram of the training process. S refers to measurement gauge output, T the output of the temperature compensation gauge and L the output of the loading gauge

4.2 Neural network training

With the two files required for network training (one of the deformation measurements and another with corresponding loads), the network training process can begin. This section includes a description of artificial neurons, and the training method used.

4.2.1 Neurons and neural networks

The brain is a computational device to mediate interactions with the body's environment, receiving information from receptors and producing responses through effectors. This is achieved with networks of cells known as neurons. A human brain is estimated to contain as many as 10 billion neurons, each with thousands of connections to others. The brain is cited as the most complex material in the universe (Huang and Luo 2015).

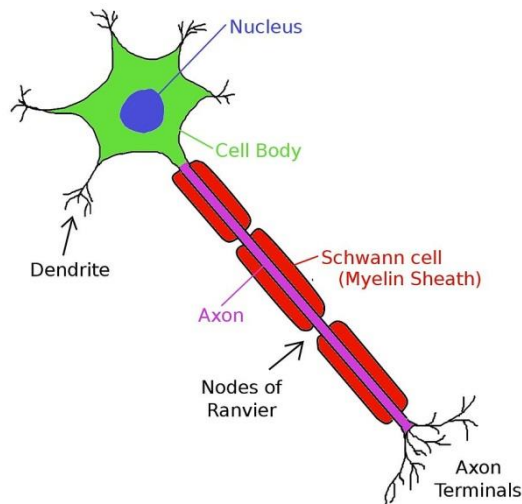


Figure 22 - Representation of a biological neuron - "Neuron1". Licensed under CC BY-SA 3.0 via Wikimedia Commons

A representation of a neuron is shown in Figure 22. It is capable of producing electrical pulses known as action potentials. The cell body is responsible for determining this activation. The neuron receives input through the dendrites, which detect the activations of other neurons. If the signals pass a certain threshold, the neuron activates. Axons transmit the neuron's action, and activation can be communicated between neurons via the axon terminals.

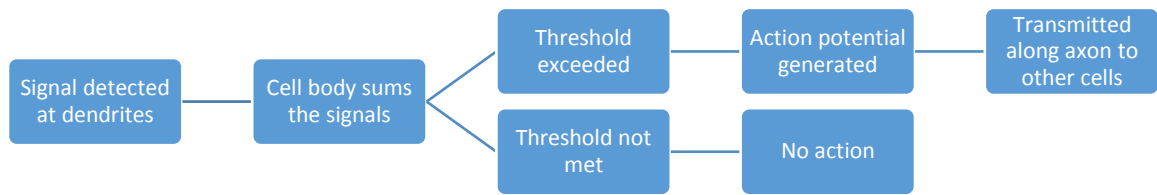


Figure 23 - The McCulloch-Pitts Neuron (McCulloch and Pitts 1943)

A model of biological neurons known as the McCulloch-Pitts neuron (Figure 23) was the basis for the development of artificial neural networks. A set of inputs are read and summed by a processing unit with some pre-defined activation function. The output from this function is then passed onto other units. Simple examples of transfer functions that are used include the sigmoid function or the threshold function (Hagan et al. 1996).

The training process is the task of adjusting the weight and bias values throughout the network to most accurately represent the unknown relationship between the input and output values. In these applications, the training phase is carried out by initially randomising the weight and bias values.

The simplest artificial neuron has a single input and output, a summing stage and a transfer function (Figure 24). The input term p is scaled to between 0 and 1, and then scaled by factor w , the weight, and shifted by the bias term b . This result is fed into the transfer function f to produce the output a (equation (16) and (17)).

$$x = wp + b \quad (16)$$

$$a = f(x) \quad (17)$$

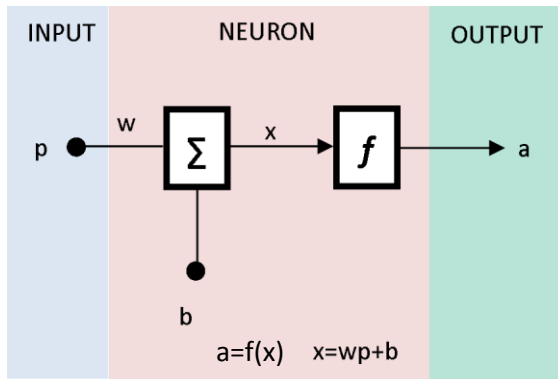


Figure 24 - A single neuron with a single input.

Various transfer functions may be specified (Figure 25). These, in combination with the weight and bias values used determine the output from the neuron, making it possible to specify many kinds of performance.

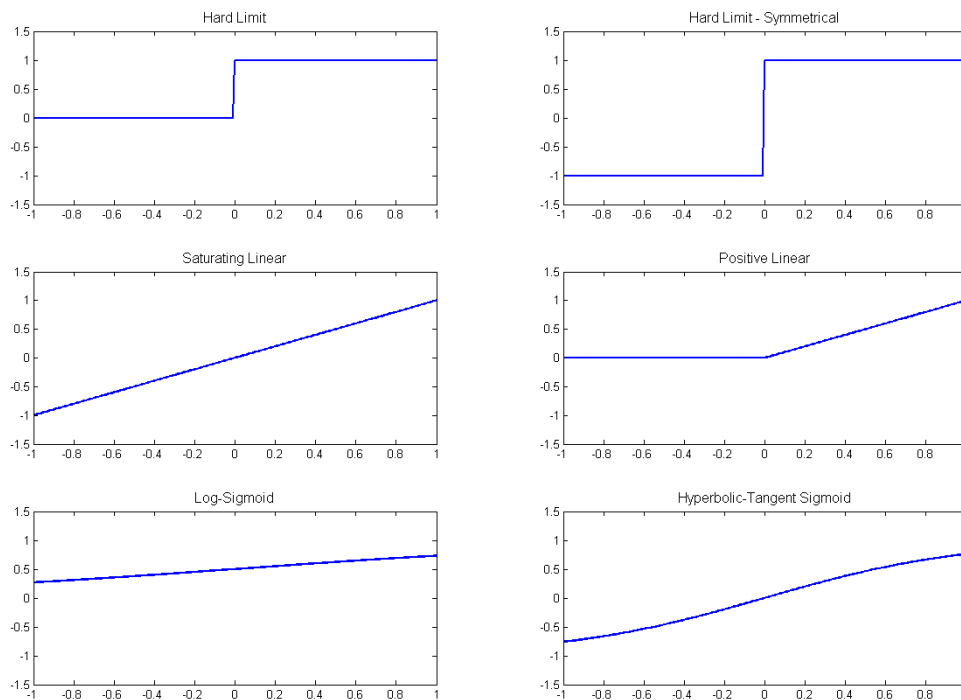


Figure 25 - Examples of commonly used artificial neuron transfer functions, created using MATLAB functions evaluated between -1 and 1

The next development in these systems is to produce a multiple input neuron. Rather than a single input p , these are a vector, \mathbf{p} , each with a corresponding weight w to form the vector \mathbf{w} . The neuron sums the effect of these inputs and retains a single bias value and transfer function, making the output of the neuron as shown in equations (18) and (19) and Figure 26.

$$x = (w_1p_1 + w_2p_2 + \dots + w_np_n) + b = (\mathbf{w}\mathbf{p} + b) \quad (18)$$

$$a = f(x) \quad (19)$$

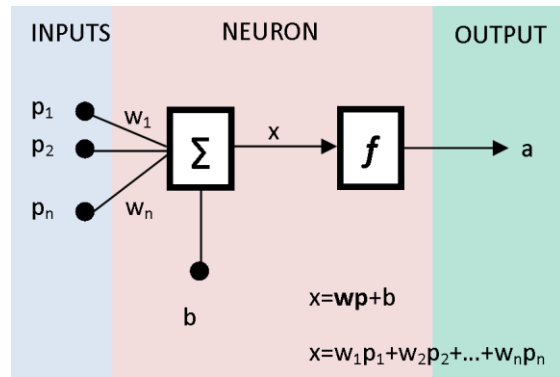


Figure 26 - A single neuron featuring multiple inputs

It is possible to obtain multiple outputs by producing a layer of neurons, each with its own weight vector, bias value and transfer function. The neurons share inputs, but can produce different outputs when given the same data. An example of this implementation is shown in Figure 27, and the equation governing its behaviour in equations (20) and (21). In this case, the weight vector w is converted into the weight matrix \mathbf{W} , and the output to the output vector \mathbf{a} .

$$\mathbf{x} = (\mathbf{W}\mathbf{p} + \mathbf{b}) \quad (20)$$

$$\mathbf{a} = f(\mathbf{x}) \quad (21)$$

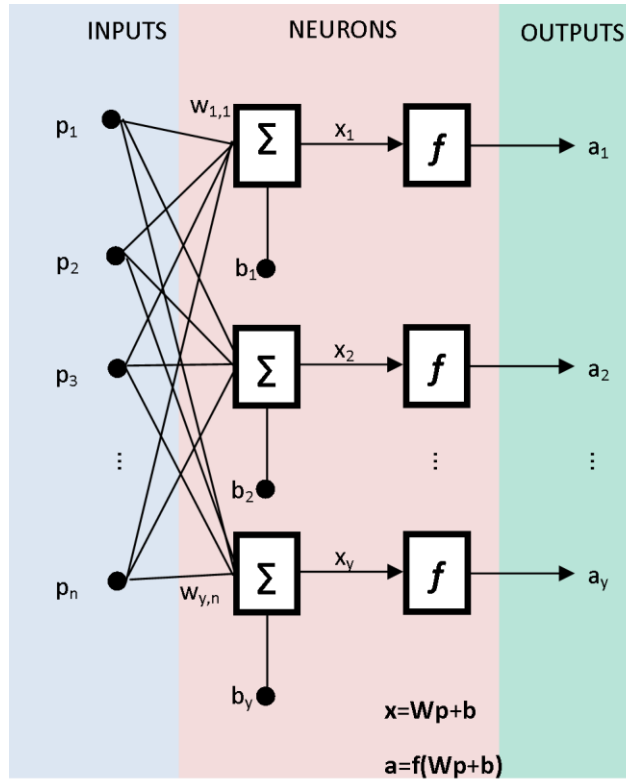


Figure 27 - A single layer of multiple networks, where each neuron receives all the input values

The final stage of this implementation is to create multiple layers of neurons, where the outputs of one set of neurons are used as the inputs of a second set of neurons. By combining the effects of different weights, biases and transfer functions, it is conceptually possible to replicate complex, non-linear transfer functions. A diagram of a multi-layer network is shown in Figure 28. The output array of the network is defined in equations (22), (23) and (24). The superscript in this instance refers to each layer of neurons – i.e. f^1 refers to the first column of functions.

$$\mathbf{x}^1 = \mathbf{f}^1(\mathbf{W}^1\mathbf{p} + \mathbf{b}^1) \quad (22)$$

$$\mathbf{x}^2 = \mathbf{f}^2(\mathbf{W}^2\mathbf{x}^1 + \mathbf{b}^2) \quad (23)$$

$$\mathbf{a} = \mathbf{f}^2(\mathbf{W}^2\mathbf{f}^1(\mathbf{W}^1\mathbf{p} + \mathbf{b}^1) + \mathbf{b}^2) \quad (24)$$

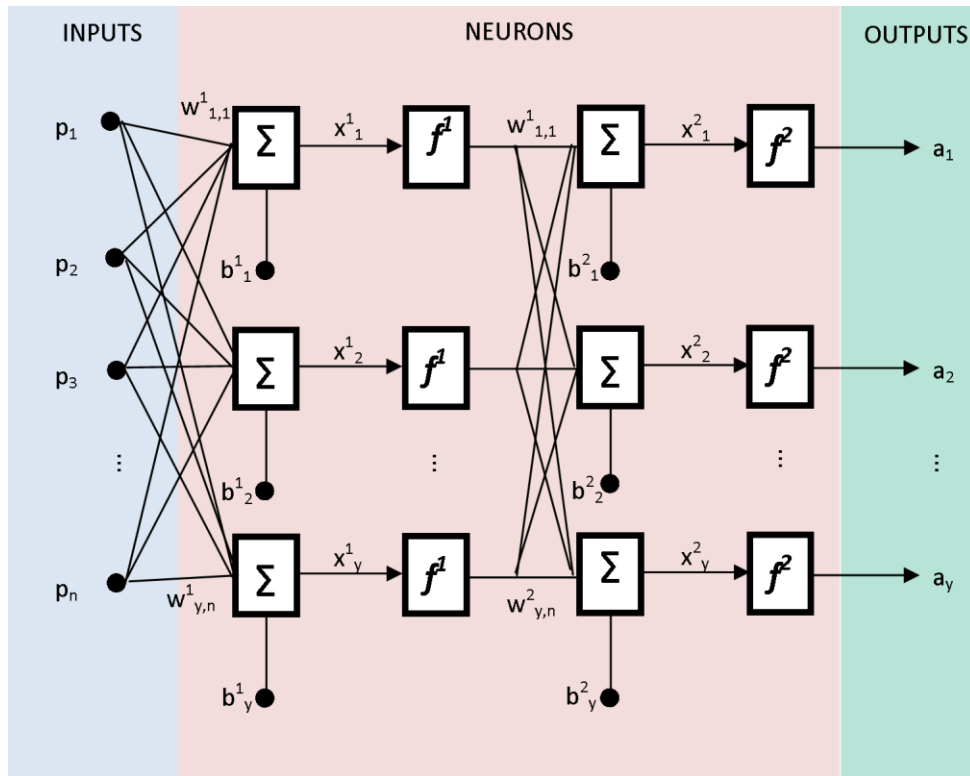


Figure 28 - A two layer network, where the first 'hidden' layer receives the complete input vector, and a second 'output' layers takes as its input the results from the first layer of neurons to produce the output vector a

The number of neurons in layers of the network need not be the same; however the input and the output layer neurons are specified by the problem. In the four strain-three load case in section 2.1, the size of vector \mathbf{p} is 4, and the size of the output vector \mathbf{a} is 3. Networks in this thesis use two layers of artificial neurons to provide an output. The first, 'hidden' layer uses a positive-linear transfer function, and the second 'output' layer uses a tangent-sigmoid function. The terminology of hidden neurons refers to the fact that the number of neurons in the hidden layer cannot be identified from the number of inputs or outputs, and forms part of the 'black box' of the network solution. This combination of transfer functions is able to identify a solution to this problem with the additional restriction of results being positive values only.

Networks of this type can be trained to represent functions using backpropagation. Examples of the desired relationship are presented to the (randomised) weight and bias values. The output is compared to the target. The weight and bias values are then adjusted to alter the performance of the network. Through iteration, improvements in the function estimation are

retained and performance improves until an accuracy goal is reached. One method of iteration is known as the Levenberg-Marquardt training algorithm.

4.2.2 Levenberg-Marquardt algorithm

The Levenberg-Marquardt algorithm is widely used in neural network training (e.g. Schollhorn (2004)). It can reliably minimise the mean square error of a function, and this is the performance index used in neural networks. The algorithm can mimic different training algorithms – the steepest descent and the Gauss-Newton algorithms providing the stability of the steepest descent technique with the speed of the Gauss-Newton method, and, for relatively small problems, represents a good balance of speed and reliability. Historically, the major drawback of this technique was the large number of values calculated and stored in each training epoch.

Here, a simplified derivation of the algorithm is presented, adapted from Yu and Wilamowski (2011). The definitions and indices in this section are as follows:

- p , the index of training input patterns, from 1 to P
- m , the index of training output targets, from 1 to M
- l and j the indices of neuron weights, from 1 to N the number of weights
- k , the number of training iterations
- e , the error reported for each input pattern

The sum of square errors E is shown in equation (25):

$$E(\mathbf{x}, \mathbf{w}) = \frac{1}{2} \sum_{p=1}^P \sum_{m=1}^M e_{p,m}^2 \quad (25)$$

For \mathbf{x} the input vector, \mathbf{w} the weight vector and $\mathbf{e}_{p,m}$ the training error at output m from pattern p (equation (26))

$$\mathbf{e}_{p,m} = \mathbf{d}_{p,m} - \mathbf{o}_{p,m} \quad (26)$$

where \mathbf{d} is the target output vector and \mathbf{o} the network output.

The steepest descent algorithm

The steepest descent algorithm uses the derivative of the total error function (27):

$$\mathbf{g} = \frac{\partial E(\mathbf{x}, \mathbf{w})}{\partial \mathbf{w}} = \left[\frac{\partial E}{\partial w_1} \quad \frac{\partial E}{\partial w_2} \quad \dots \quad \frac{\partial E}{\partial w_N} \right]^T \quad (27)$$

with the update rule relating to the weight vector being as shown in equation (28):

$$\mathbf{w}_{k+1} = \mathbf{w}_k - \alpha \mathbf{g}_k \quad (28)$$

α is the step size, (or learning constant). The slow convergence arises from the small changes in the gradient when the network is close to the solution, meaning that the changes between each weight update are also very small.

Newton's method

Newton's method relies on the calculation of the Hessian matrix, a second order derivation of the total error function, (29).

$$H = \begin{bmatrix} \frac{\partial^2 E}{\partial w_1^2} & \frac{d^2 E}{\partial w_1 \partial w_2} & \dots & \frac{d^2 E}{\partial w_1 \partial w_N} \\ \frac{d^2 E}{\partial w_2 \partial w_1} & \frac{\partial^2 E}{\partial w_2^2} & \dots & \frac{d^2 E}{\partial w_2 \partial w_N} \\ \dots & \dots & \dots & \dots \\ \frac{d^2 E}{\partial w_N \partial w_1} & \frac{d^2 E}{\partial w_N \partial w_2} & \dots & \frac{\partial^2 E}{\partial w_N^2} \end{bmatrix} \quad (29)$$

The gradient vector \mathbf{g} can be expressed as:

$$-\mathbf{g} = \mathbf{H} \Delta \mathbf{w} \quad (30)$$

such that:

$$\Delta \mathbf{w} = -\mathbf{H}^{-1} \mathbf{g} \quad (31)$$

and the weight update rule is:

$$\mathbf{w}_{k+1} = \mathbf{w}_k - \mathbf{H}_k^{-1} \mathbf{g}_k \quad (32)$$

Gauss-Newton algorithm

One issue with the Newton's method is the calculation of the Hessian matrix H . In the Gauss-Newton method, the Jacobean matrix is calculated instead:

$$J = \begin{bmatrix} \frac{\partial e_{1,1}}{\partial w_1} & \frac{\partial e_{1,1}}{\partial w_2} & \dots & \frac{\partial e_{1,1}}{\partial w_N} \\ \frac{\partial e_{1,2}}{\partial w_1} & \frac{\partial e_{1,2}}{\partial w_2} & \dots & \frac{\partial e_{1,2}}{\partial w_N} \\ \dots & \dots & \dots & \dots \\ \frac{\partial e_{1,M}}{\partial w_1} & \frac{\partial e_{1,M}}{\partial w_2} & \dots & \frac{\partial e_{1,M}}{\partial w_N} \\ \dots & \dots & \dots & \dots \\ \frac{\partial e_{P,1}}{\partial w_1} & \frac{\partial e_{P,1}}{\partial w_2} & \dots & \frac{\partial e_{P,1}}{\partial w_N} \\ \frac{\partial e_{P,2}}{\partial w_1} & \frac{\partial e_{P,2}}{\partial w_2} & \dots & \frac{\partial e_{P,2}}{\partial w_N} \\ \dots & \dots & \dots & \dots \\ \frac{\partial e_{P,M}}{\partial w_1} & \frac{\partial e_{P,M}}{\partial w_2} & \dots & \frac{\partial e_{P,M}}{\partial w_N} \end{bmatrix} \quad (33)$$

The gradient function in terms of the Jacobean matrix can be expressed as:

$$\mathbf{g} = \mathbf{J}\mathbf{e} \quad (34)$$

for the error vector \mathbf{e} :

$$\mathbf{e} = \begin{bmatrix} e_{1,1} \\ e_{1,2} \\ \vdots \\ e_{1,M} \\ e_{P,1} \\ e_{P,1} \\ \vdots \\ e_{P,M} \end{bmatrix} \quad (35)$$

The Hessian matrix can be approximated by the Jacobean matrix according to the following relation:

$$\mathbf{H} \approx \mathbf{J}^T \mathbf{J} \quad (36)$$

The weight update rule for the Gauss-Newton algorithm can be expressed as:

$$\mathbf{w}_{k+1} = \mathbf{w}_k - (\mathbf{J}_k^T \mathbf{J}_k)^{-1} \mathbf{J}_k \mathbf{e}_k \quad (37)$$

Levenberg-Marquardt algorithm

The advantage in the Gauss-Newton method and the calculation of the Jacobean matrix is that it means that the 2nd derivatives in the Hessian matrix are not necessary. Unfortunately, the algorithm suffers from the same issues in oscillation about the solution in situations with a complex error topologies – this is the case if the matrix $\mathbf{J}^T \mathbf{J}$ is not invertible. To achieve this, the Hessian matrix approximation is modified further using a combination coefficient (μ , ($\mu > 0$)) and the identity matrix. As the main diagonal of \mathbf{H} will feature only positive values, it will always be invertible.

$$\mathbf{H} \approx \mathbf{J}^T \mathbf{J} + \mu \mathbf{I} \quad (38)$$

Therefore the update rule in equation (37) is modified to:

$$\mathbf{w}_{k+1} = \mathbf{w}_k - (\mathbf{J}_k^T \mathbf{J}_k + \mu \mathbf{I})^{-1} \mathbf{J}_k \mathbf{e}_k \quad (39)$$

When the combination coefficient μ is small, the weight adjustment rule is similar to the Gauss-Newton algorithm and the algorithm trains quickly. When μ is large, then the weight update happens slowly, but with high stability. If, following the error evaluation, the error is smaller than the previous value then the value of μ is divided by a positive factor greater than 1, the ϕ factor. \mathbf{w}_k is set to the value of \mathbf{w}_{k+1} and the training process repeats. If the error was greater, then μ is set to $\mu * \phi$, the value of \mathbf{w}_k is retained and equation (39) is re-evaluated. The process may stop when E_k falls below a set threshold.

The end result is a learning algorithm that converges quickly and with stability, and is regarded as one of the most efficient methods for training multilayer perceptron networks of the type

used in this work. There are some issues which limit the applicability of this function – the approximation of the Hessian matrix has to be calculated at each weight update, which for large networks is computationally expensive. Another is that the Jacobean matrix has to be stored at each iteration, and this has the size $P \times M \times N$ (patterns*outputs*weights), and this may be memory intensive on large networks. For networks of the size and type of this application, the Levenberg-Marquardt algorithm is well suited.

Training can be stopped when the error goal (the difference between training and target values) reaches some pre-set value, or when the number of validation checks (defined as the number of successive training iterations where the validation performance fails to decrease), or several other parameters.

Such a configuration of training data and neural network architecture is sufficient for the production of a solution to the load measurement problem.

It is possible to modify aspects of the network architecture to improve the overall performance of a network. In particular, the choice of hidden neurons used within the implementation has to be made based on trial-and-error rather than a clear guideline on what choice is most effective. Choosing too few hidden neurons risks the network failing to converge onto an appropriate solution. Conversely, selecting architecture with too many neurons makes the training time and the size of the produced network larger, with the concomitant hazard of over-specifying the transfer function.

During training, it is necessary to stop the training process at some point and restrict further adjustment of the weights and biases within the network construction. However, the point at which to stop is also not consistently defined, and is likely to have problem-specific properties. Figure 29 shows an example of the issues in network under- and over-training in a classification problem.

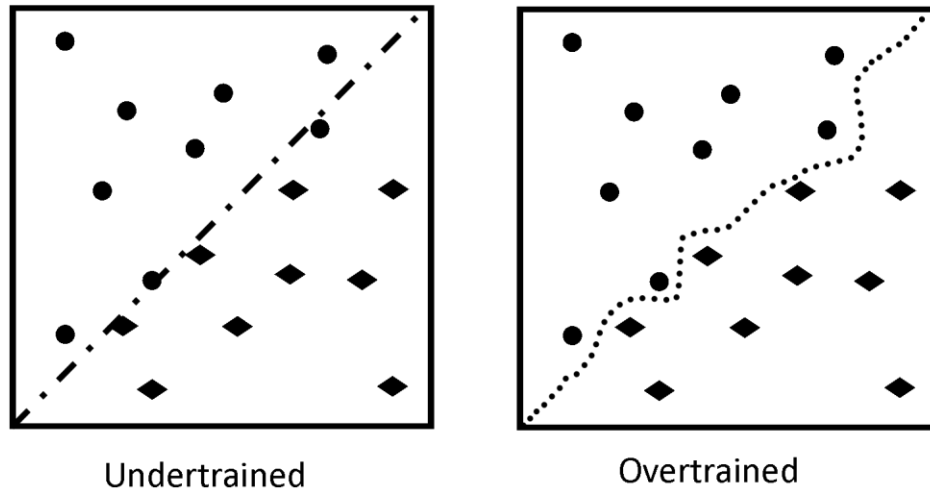


Figure 29 - A pattern recognition problem where circles represent a different sample to diamonds. On the left, the network is undertrained, and misclassifies borderline cases. On the right, overtraining means that significant regions are on the wrong side of the decision border, leading to poor performance on real data

The generation of a transfer function in socket measurement is more complex due to additional solution dimensions. For this reason, the implementation of the neural network code within the MATLAB environment contains several methods of stopping the training process.

The training file is randomly divided into three segments. 60% are used in training, 20% to validate the performance and as a guide to when to stop training and 20% of cases are reserved as an independent test of network performance.

Firstly, the number of training epochs is used to limit training time. An epoch is the application of the whole training file to the training procedure – multiple epochs represent repeated application of the same data. The number of epochs required is related to the size of the training file. The epoch stopping point was set to 100 throughout the work resented here, and using this criterion as the training end point was typically representative of the network failing to converge on an appropriate solution.

Performance goal is a measure of the error between the network estimate and the target values. Once a predetermined target of accuracy on a set of training cases is reached (as defined by the MSE), then training is stopped as the accuracy goal has been reached.

The gradient parameter refers to the rate of change of the weights and bias. If the gradient reaches a pre-set minimum, then the rate of change of the internal neuron values (and hence the difference in the network estimate) is negligible. In this work, the gradient threshold to stop training was set to 1×10^{-7} , and was rarely used as the training end reason.

A damping factor is used to control the training algorithm. The initial value is increased or decreased depending on the changes in performance of the network solution. A maximum value this term is set as a training end point to signify convergence on a solution.

The validation check parameter causes the training procedure to stop if the validation case performance increases more than the specified number of times since the last improvement in performance. This was set to 6 throughout the network training process.

If the training procedure is prolonged beyond the point of stabilisation of performance, then overall quality of the network solution risks lower quality on new data. The network accuracy on the training, test and validation cases can be displayed by the MATLAB training program: ideally the accuracy of the test and validation cases has remained stable and accurate for several training epochs as this demonstrates good convergence on a transfer function.

Several issues are present with this kind of implementation which uses a small number of physical measurements in order to produce a large number of training cases. One is that the relationship between applied load and expected deformation measurement is too close: the network is unable to generalise the solution to cases when values differ from the idealised relationship. Measurements from strain gauges are susceptible to interference, and although this can be managed to an extent, they will never perfectly match the model proposed by the training cases. A technique known as noise injection is used to model this variance in the training data.

The final technique discussed to enhance estimation performance is to collate the estimates from multiple networks. Even with optimised parameters, residual error will remain. Hansen and Salamon (1990) recognised that identifying an appropriate solution (in terms of the internal weight values, but also more generally in terms of hidden neurons etc.) was a solution

with many local minima. The selection of these values and the point at which training is stopped is different between runs of the training process. A solution is contingent on the initial randomisation of weight and bias values, the selected training cases and the order in which cases are supplied to the training algorithm. The approximation that the network produces is based on a particular subset of the possible input, with the effect that while networks will contain some residual error when supplied with new test cases, the magnitude and direction of these errors is, to an extent, random.

The variance between network solutions will cause a distribution of estimates around the target. By taking an average across the estimates of multiple networks (an *ensemble*), a result potentially closer to the true value can be made. This observation has been made in other fields: Galton (1907) reported that the mean of all estimates of a ‘Guess the weight of a cow’ competition at a county fair was closer than the estimate from any of the ‘experts’ present. The aspects of a wise crowd that may be capable of performing feats such as this were identified by Surowiecki (Table 19).

Characteristic	Description
Diversity	Different estimators provide different value estimates
Independence	Estimators do not depend on each other to provide a value
Decentralisation	Estimators are able to specialise in differing ways
Aggregation	A means of combining estimates into a single output

Table 19 - The characteristics of wise crowds, as described by Surowiecki (2004)

The characteristics of wise crowds correspond well to the properties of neural networks. Networks are diverse in that they produce different estimates as a result of the variance in the training process. Estimates between networks are considerably independent, as one network is not informed by the estimates produced by others. Decentralisation is ensured by the network training algorithm being able to settle onto different local minima. Aggregation is facilitated by the use of a mean of all estimates.

Ensembles of networks have been widely used in many artificial intelligence applications in medicine and other fields, with particular focus in the literature on classification problems. Baxt (1992) trained networks to distinguish myocardial infarction patients, with networks trained to focus on either the sensitivity or specificity (minimising the rate of false-negatives or false positives). By combining the estimates from networks of each type, simultaneous optimisation of each parameter could be achieved.

Altering the constitution of the ensemble is often required to produce an effective ensemble (Krogh and Vedelsby 1994). They also presented a method for calculating the ambiguity of network ensembles. Altering network architecture has also been investigated as a means of producing diversity, e.g. (Rosen 1996). The aim in that study was to decorrelate the estimates between networks and increase the probability that the mean of the ensemble was closest to the target.

Neural network ensembles have only rarely been applied in limb prosthetics outside the issue of intelligent joint control. The only example located within the literature concerning the socket problem was a study by Jimenez (1997). This study used scans of stumps being assessed for the position of bony prominences –identifying positions of greatest curvature on the surface and which were presumed to correspond to the bony landmarks. The performance of the network ensemble used to locate these positions was compared to a prosthetist. The ensemble network demonstrated equivalent performance to the expert. They later published a study describing dynamic weighting of networks within ensembles, based on each network's estimated certainty of producing an accurate classification (Jimenez 1998), an example of a more sophisticated technique for creating the ensemble average.

Performance enhancements have been proposed for ensemble performance, including 'bagging', 'boosting' and 'stacking'. Bagging (e.g. Breiman, 1996) refers to 'bootstrap aggregation', a statistical technique for resampling a training set to produce multiple training files. Boosting (e.g. Schwenk and Bengio 2000) uses different samples of the training set, with networks trained later in the process given a higher proportion of poorly characterised cases. Stacking refers to the use of multiple layers of networks which use the distribution of individual

network estimates on novel cases to train a further network to identify the best means of compiling the ensemble estimate (Wolpert 1992).

4.3 Post processing

Following the successful training of a neural network (Section 2.2), post-processing of the training data can be carried out to improve estimate quality. The functional principle of these are described here – the effects on simulated load data are described in detail in Chapter 5. The first technique, a polynomial correction, is used to condition the neural network output to account for bias within each output channel. The second, constructing an ensemble of network estimates, is to correct for variance at the inter-network level.

4.3.1 Polynomial correction

Fitting polynomial functions to residual error is described in Chapter 7. This section describes the application of these functions to output data only. Polynomial coefficients are obtained by plotting the network error on a set of loads against each target. An example of this is shown in Figure 30. This is performed by applying the training data to the network.

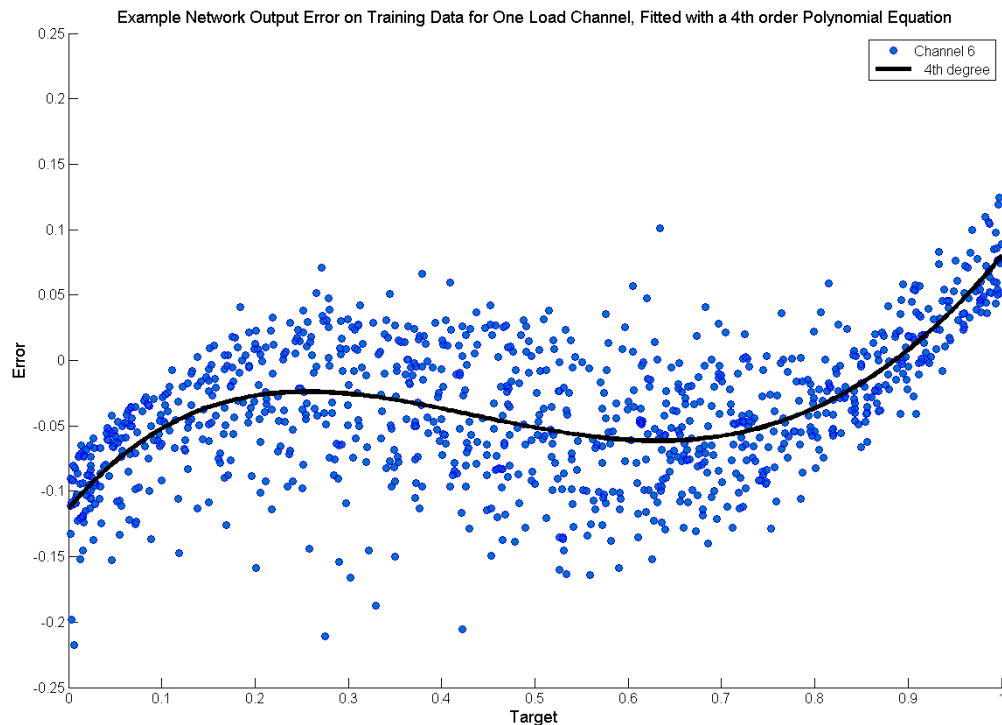


Figure 30 - Polynomial equation fitted to the residual error of an output channel

The output from the polynomial function represents an inherent bias in the network output. This typically takes the form of an overestimation of loads low in the output range, and underestimation at the top of the measurement range. Example functions - (40) - are shown below for the 3 load system described in section 2.1:

$$\begin{bmatrix} f_1 \\ f_2 \\ f_3 \end{bmatrix} = \begin{bmatrix} a_1x^3 + b_1x^2 + c_1x + d_1 \\ a_2x^3 + b_2x^2 + c_2x + d_2 \\ a_3x^3 + b_3x^2 + c_3x + d_3 \end{bmatrix} \quad (40)$$

For a set of network outputs O_1 - O_3 , the corrected load estimates N_1 - N_3 are in equation (41):

$$\begin{bmatrix} N_1 \\ N_2 \\ N_3 \end{bmatrix} = \begin{bmatrix} O_1 + f_1(O_1) \\ O_2 + f_2(O_2) \\ O_3 + f_3(O_3) \end{bmatrix} \quad (41)$$

The correction can be applied to each distribution estimate produced from the network.

4.3.2 Ensemble estimate

In addition to the error present on an individual output channel level, different networks will have a range of estimates when supplied with identical problem data. A detailed examination of this technique is presented in Chapter 6, but the method of combining estimates is described here.

The principle of an ensemble estimate is that a group of network estimates for a particular target load will be distributed around the true value. By taking an average of each estimate, a result close to the target can be identified with a substantial boost to accuracy and reliability.

In equation (42), a table of estimates (N_1 to N_3) from a group of 100 networks are shown. Following this, the ensemble estimates (Ens_1 to Ens_3) are shown (43).

$$\begin{bmatrix} N_{(1)1} & N_{(1)2} & N_{(1)3} \\ N_{(2)1} & N_{(2)2} & N_{(2)3} \\ \vdots & \vdots & \vdots \\ N_{(100)1} & N_{(100)2} & N_{(100)3} \end{bmatrix} \quad (42)$$

$$\begin{bmatrix} Ens_1 \\ Ens_2 \\ Ens_3 \end{bmatrix} = \begin{bmatrix} \sum_{i=1}^{100} N_{(i)1} \\ \sum_{i=1}^{100} N_{(i)2} \\ \sum_{i=1}^{100} N_{(i)3} \end{bmatrix} \quad (43)$$

4.3.3 Post processing summary

Figure 31 shows the process for obtaining load estimates from the system. It is similar to the collection of data for training. The modified gauge readings are submitted to the trained network, and load estimates made. These can then be modified by polynomial functions or network ensembles.

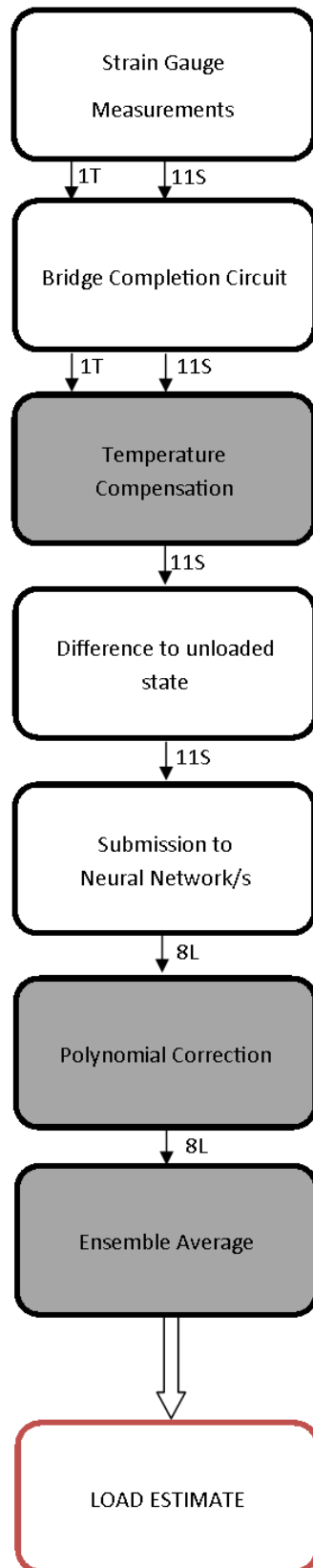


Figure 31 - Flow chart for the processing of test case data. Grey blocks represent optional features. S refers to the output from measurement gauges, T that of temperature compensation measurement

4.4 Evaluating network performance

The training performance of a network is commonly reported as the mean square error (MSE), shown in equation (44). E represents the output of a network from a single set of inputs with the target L .

$$MSE = \frac{1}{n} \sum_{i=1}^n (E_i - L_i)^2 \quad (44)$$

In order to provide a measure that was robust to changes in the magnitude of applied load, the normalised root-mean-square error (equation 45), as used in prior applications (e.g. Sewell et al. 2012) was used here.

$$NRMSE = \frac{\sum \sqrt{(E_i - L_i)^2}}{\sum L} * 100 \quad (45)$$

4.5 Hardware and Software Design

In previous sections of this chapter, the application of neural networks of varying construction, specification and training to simulated load distributions has been made, with the effect of producing significant improvement in accuracy and reliability of the load estimate. However, for a system of this type to be proven as clinically usable, a system for providing measurements in a range of static and dynamic situations must be made. This chapter is concerned with the procedures for generating measurements in these situations.

The design of a measurement rig for obtaining measurements in these situations is specified and described in section 4.6, along with the selection of strain gauges and other components. The process of gaining ethical approval for the intended measurements and the risk assessment of these activities is reported in section 4.7, with a description of the inclusion/exclusion criteria in section 4.8.

A description of the software implementation used throughout the collection process is covered in section 4.9. Finally, the procedure for collecting measurement data in each configuration of interest is covered in sections 4.10 and 4.11.

The design and use of the measurement system described in these sections inform the results described in Chapters 8 and 9, where these inform the utility of a system of this type in clinical and research situations.

4.6 Design of Measurement Rig

During the design process for construction of a measurement rig capable of making the recordings desired for this project, Table 20 was used as guidance:

Requirement	Justification
Collection of at least 12 strain measurement channels, plus temperature compensation and a load measurement	Sufficient collection for a 10 load position system and to collect additional required measurements to complete the network training process
On-board conditioning via bridge completion circuitry	Reduces the requirement for local addition of bridge completion
Wireless transmission of readings, with a range of >20m	Facilitate laboratory scale recording
Means of attaching measurement devices to the participant that is secure, safe and which has minimal impact on the quality of measurement or on the free movement of the participant	Requirements following risk assessment for desired testing
Capable of interfacing with available software (LabView, MATLAB)	These are the software languages that are available without significant additional learning required and which are suited to the tasks
Cost effective	Funding for the project is not unlimited
Additional input channels available	Potential for expansion to additional measurement channels

Table 20 - Design specification of measurement device

After a review of available systems, the VLink module from Lord Microstrain was chosen (Figure 32). A set of three nodes would provide enough coverage for a 12 gauge system, and an additional node was sourced in order to provide capacity for training load collection.

Each node has a weight of ~125 grams. The hardware featured adjustable power radio transmission, with requirements for communication over the desired range and sample rate being met. The projected battery life in this configuration was suggested to be around 8 hours. When the nodes were ordered, they were specified to contain 350 Ω quarter bridge completion.

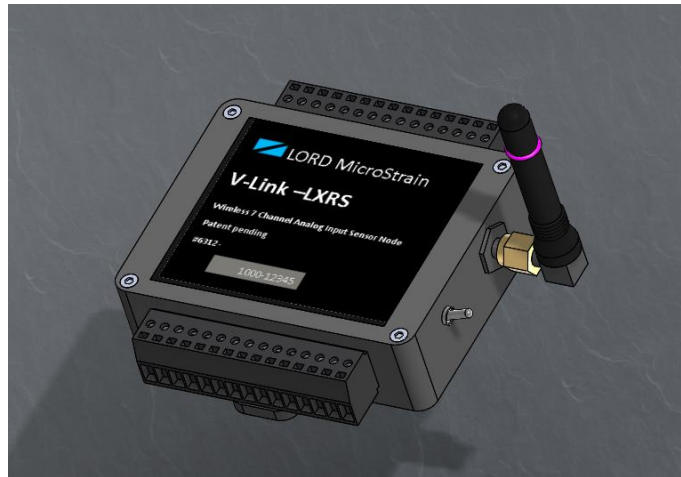


Figure 32 - CAD model of the VLink measurement node.

The measurement gauges chosen were the WFLA-3-350-11-1L model, supplied by the Tokyo Sokki Kenkyujo Co. Ltd. Gauge resistance was specified as 350 \pm 1.5 Ω , with a gauge factor of 2.10 \pm 1%. The resistive grid was 3mm long. The gauges were bonded to specimens using a thin layer of cyanoacrylate.

This value of completion was chosen to match the measurement gauges selected for this study. The work of Amali et al. (2006) found that the differences between rosette components were often not sufficient to produce meaningful changes in measurement that could be used to distinguish between load states. Meaningful differences between strain measurements are required in order for the network to converge on a high quality solution. For this reason, a wider distribution of single gauges with greater range in orientation and position was chosen.

Measurement gauge resistance was also increased, from 120Ω to 350Ω . This acts to reduce the effects of heat generation from the excitation current (From $P=V^2/R$), as well as reducing the sensitivity to variation in the lead resistance. The disadvantage of this choice is the small reduction in sensitivity (mitigated using the measurement range in the collection hardware) and the risk of additional error from degradation of the resistance grid (reduced by the selection of a gauge that is supplied encased in a flexible resin).

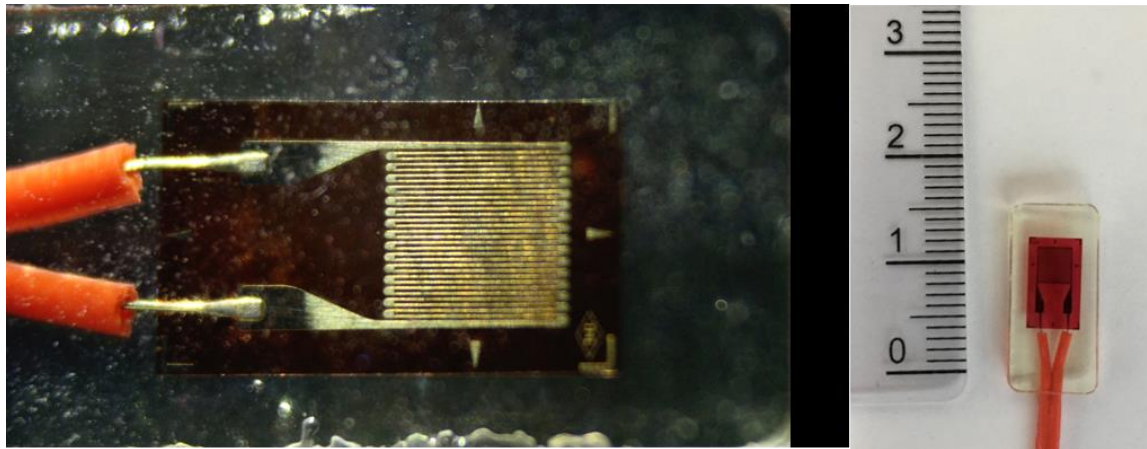


Figure 33 - Left: A close up view of a strain gauge of the type used in this study. Right: View of the gauge for scale, also showing the plastic coating around the gauge element

In order to mount the nodes to the prosthesis, a rig was designed that would provide a firm attachment to the artificial limb. The requirements for this device included making the wearing of the device relatively unobtrusive, to be quick to don/doff and which would minimise the effects on the standing and walking actions of the participant.

Several designs were considered, including mounting the nodes onto a belt or backpack, fixing a plate between the prosthesis and pylon and other potential configurations. The final design is shown in Figure 34 - a set of hinged plates fitted below and around the socket.

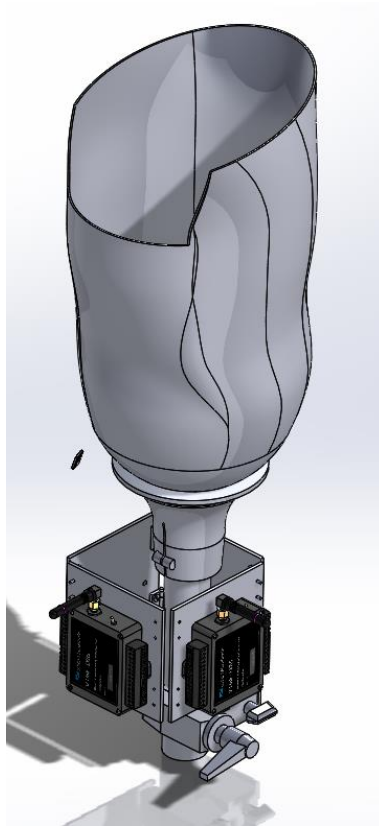


Figure 34 - CAD model of an example socket, with the measurement rig fitted with VLink nodes below it

The rig was mounted to the prosthesis pylon using a commercial camera clamp (Manfrotto). The measurement plates could be bolted to the structure with mounting points on the clamp. The clamp was rated to 15kg. It was adjustable to fit cylindrical or square cross section members of between 13-45mm in diameter.

The advantages of this design are that the additional mass is close-to and symmetric about the long axis of the prosthesis. The positioning minimises the length of the cabling between the measurement gauges and the bridge completion circuit. The rigid connection between the nodes and the prosthesis also reduces noise from movement at the wiring interface. The mounting plates were manufactured at the Bournemouth University mechanical workshop from 1.5mm thick aluminium. The design of these is shown in appendix A15/A16.

The mounting plates were hinged together in a manner which meant that they could be added and removed quickly. Retaining caps which kept the plates in a stable position were manufactured using a 3D printer (Figure 41).

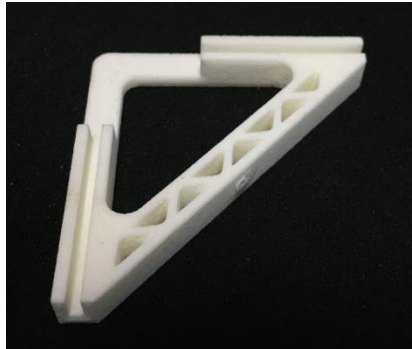


Figure 35 - Measurement rig cap, as seen from below: the channels are at right angles to each other, and these hold the measurement plates at a fixed angle. Each short arm of the triangle is 50mm

The finished rig had a mass of around 1.5 Kg. The principle drawback to the design is that the mass of the system is added to the suspended weight of the prosthesis. Limited evidence suggests that this level of additional weight can be well-tolerated by transtibial amputees, with only limited effects on gait biomechanics (Section 2.7.5).

This study used sockets constructed from Northplex (Northsea Plastics) as the test specimens. Check sockets are produced as part of the supply of a new socket, and (as the name suggests) are used to evaluate the quality of the socket design. In this study, a recent cast of the residual limb of each participant was used to create a check socket, which was then fitted with gauges for network training. Check sockets are less resilient than final sockets, but as they would be worn for only 1-2 hours during testing, this was acceptable.

4.7 Ethical approval and risk assessment

Ethical approval for the conduct of the study was granted in several stages. The initial work, covering the development of the testing hardware and software was assessed as low risk, and required only locally approved risk assessment and ethical approval. This was because there was only a low likelihood of harm to the operator during testing. There were very low risks

associated with the use of electrical devices (always following the intended use) and a minor risk of entrapment when applying forces.

A greater risk assessment was required for the human participation studies carried out later in the project. Bournemouth University Research Ethics committee approval was sought initially for the pilot study, and again resubmitted with only minor alterations for the second phase of testing with additional participants. The summary of the revised full study approval is included in appendix A10-A13. As participants were not recruited through NHS facilities, NHS research ethics approval was not required as part of this work.

The highest risk activity associated with study participation was that of trips and falls whilst wearing the measurement rig. Requiring participants to don a new prosthesis with additional mass from the measurement devices and a potentially altered device alignment may have been difficult for participants to accommodate successfully: increasing the risk of falling. Falling comes with the chance of potentially serious injury.

This risk was mitigated in several respects by the study design. Firstly, the inclusion criteria of traumatic, unilateral transtibial amputees would make the likely participants would have good walking ability and significant capacity for accommodating walking perturbation. The exclusion of participants with a SIGAM grade of below D (Ryall et al. 2003) would have a similar effect, and would ensure that participants had sufficient ability and endurance to complete the required tests (Chapter 2).

The design of the measurement device also mitigated these risks. Although the system was mounted below the socket (adding to the suspended weight of the prosthesis) the additional mass was placed approximately symmetrically around the pylon, reducing unexpected inertial effects. Using a wireless system of data transmission also represents a significant reduction in the risk of tripping on the cabling.

The choice to attempt perturbation from normal gait also represents a risk to the study participant. Studies suggest that amputees have region of alignment configurations which prove acceptable in terms of stability, comfort and maximally functional gait. Moving away

from the clinician’s device prescription risks producing a system where the configuration is not fit for use. As with the use of walking tasks, the risk of this activity was controlled in part by the choice of participant group, but also in the experimental design.

The misalignment of the prosthesis was induced in only small amounts, similar to those reported in recent studies and to those routinely experienced by amputees during their typical socket fitting process. The procedure is usually well tolerated by amputees. Further mitigation was introduced by allowing the participant time to adjust their walking pattern to accommodate the revised device alignment and of course permitting the participant to refuse to complete a test in a configuration they feel they cannot safely use.

To control this risk of using a novel socket, the sockets in use in this study were constructed by experienced prosthetists using recent casts of the residuum. In addition, the required duration of testing where the socket is worn was short, c.2 hours, with the participant able to request breaks as required. Walking tests were also of short duration, and completed at a comfortable pace.

4.8 Selection criteria

As part of the process of gaining ethical approval for the study, the inclusion and exclusion supplied in Table 21 were specified.

Inclusion	Unilateral, transtibial amputation
	Amputation from trauma
	Amputation >6 months ago
	SIGAM grade D/E/F
	Cognitive ability to complete tests
Exclusion	Significant skin damage/pressure injury on residuum
	Significant co-morbidity

Table 21 - Inclusion/Exclusion criteria for participation.

4.8.1 Unilateral, transtibial amputation

This criterion means that the work within this study can be associated with the previous studies in the area, working with structures of similar dimensions, material and loading conditions.

Restriction to transtibial amputees also means that recruited participants are relatively consistent in abilities, and that devices can be configured with good consistency. Transtibial amputees also represent a more substantial part of the literature, aiding in the comparison of results to other systems.

4.8.2 Amputation from trauma

Traumatic amputees are typically younger, healthier, more active, and better able to accommodate the rigors of testing. By recruiting from this population, the testing can be made more variable without substantially increasing the risk of participation.

4.8.3 Amputation >6 months old

Residual limbs are subject to change following amputation, and do not settle to a consistent volume until many months following the amputation. In addition to decreased tolerance of tissues to applied stress, the change in stump volume means that sockets do not remain suitable for long periods of time. By restricting recruitment to established amputees, the ability to accommodate sub-optimal prosthesis configurations and the stability of the residuum is increased.

4.8.4 SIGAM Grade D/E/F

As the required tasks include walking in conditions other than level ground, with a range of device alignments and with additional mass on the limb, the required walking ability of participants is relatively high.

4.8.5 Cognitive ability to complete tests

The ability to perform the required actions successfully and to provide adequate informed consent meant that this requirement was included.

4.8.6 Skin damage on residuum

The existence of current skin conditions or pressure injury was cause for exclusion from the study. As wearing a new socket, particularly in atypical alignment states, can be reasonably expected to cause local increases in tissue load, then avoiding further injury to the participant is essential. Aggravating pressure injury may cause the participant to alter their gait pattern to avoid loading.

4.8.7 Significant co-morbidity

The presence of significant co-morbidity increases the risk of injury as a result of taking part in the study. To avoid this, any potential participants with major additional medical conditions were excluded from taking part in the study.

4.9 Collection software

The process of obtaining measurements broadly followed the flowchart shown in Chapter 2 (Figure 31), with separate software for the collection, processing and storage of data.

The collection stage (included in appendix A25) used a LabView virtual instrument, including aspects of the Lord Microstrain VLink SDK. This allowed the configuration of the hardware, plus display of the streamed measurements and the specification of the metadata. The values obtained from each node are then saved into a text file with the title defined by the time and date of the measurement. Possible configurations are shown in Table 22, and a screenshot of the software in Figure 36.

Data Recording Options	
Record to new file or append to new file	
Start/Stop recording session	
Stream data to file	
Log event	
Select Bridge input channels in use	
Select additional single ended input channels	
Session trial increment	
Basestation COM port in use	
Node Sample Rate	
Node ID in use	

Table 22 - Wireless collection software options

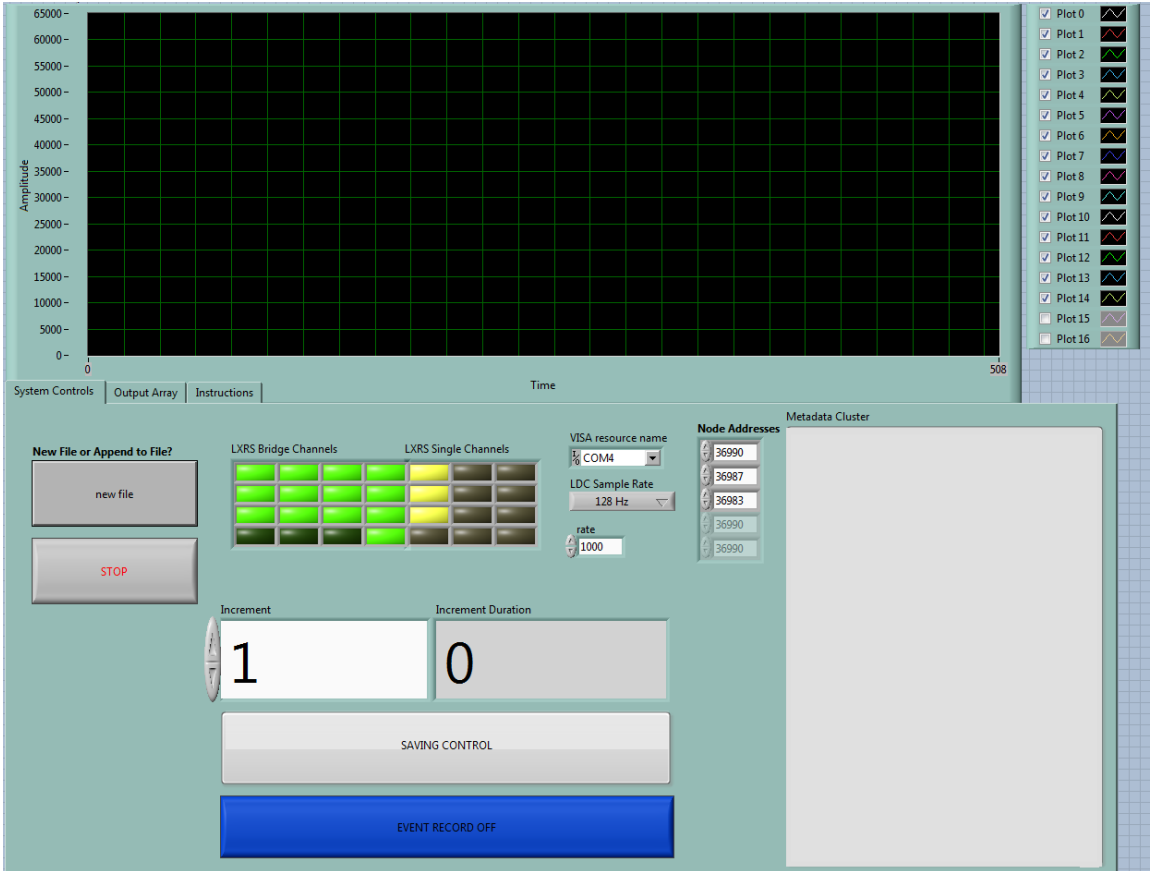


Figure 36 - Wireless Collection software interface

In order to process the information, the collected text file is supplied to a second LabView VI. If this is a training collection (i.e., of measured strains corresponding isolated loads), then this can be used to train a neural network, using the configuration options shown in Table 23.

Otherwise, the file is processed: with reference to a baseline or unloaded state or with temperature compensation. If desired, the processed measurements can be submitted to an existing neural network or network ensemble.

Ensemble Training Options
Input file
Number of measurement channels
Convert from voltage difference to strain difference
Input file includes an unloaded (neutral) section
Location of temperature compensation channel
Sample frequency in selected file
Temperature compensation time offset to use
Number of networks to train
Mean number of hidden neurons
Deviation of hidden neuron number from mean
Mean maximum noise injection value
Deviation of maximum noise injection from mean
Name of saved networks
Maximum training epochs
Training error goal
Number of training file superposition cases
Calculate polynomial correction factors

Table 23 - Network generation software options

The neural network production code was constructed in MATLAB, and a user interface provided in LABVIEW (Figure 37, appendix A17). This implementation uses the training parameters that were identified as best performing in the previous chapters – a Levenberg-Marquardt training algorithm used to train 100 networks of 16 neurons (standard deviation of 1) and a mean of zero noise (standard deviation of 2). Polynomial corrections were implemented on each

networks output channel, selecting the best performing function between 3rd and 9th order based on resubmission of the training data.

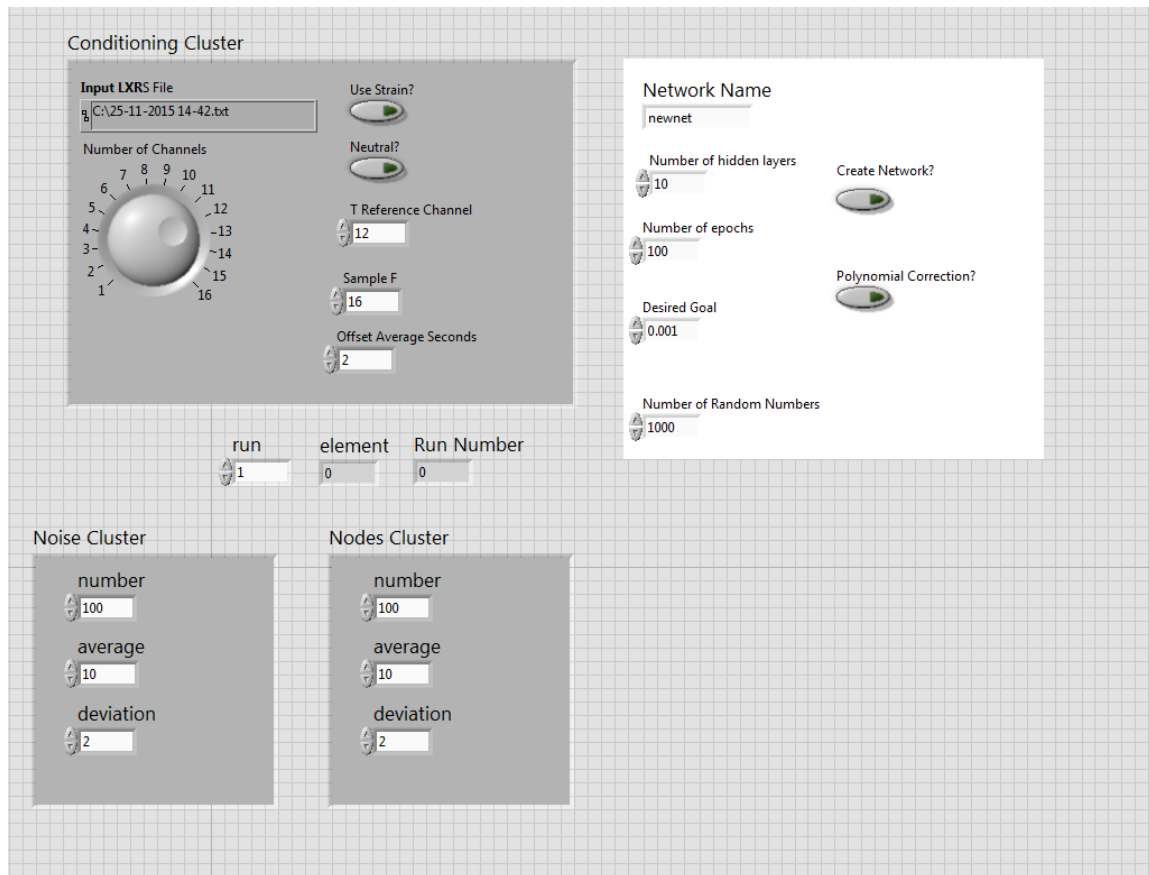


Figure 37 - Network generation software interface

For further processing, examination and presentation, the output of the neural network is stored within MATLAB structures.

4.10 Collection procedure

Practical testing was completed using the gait measurement facility at the Blatchford site in Basingstoke. This area included a clear walkway with an AMTI force platform in the centre. The testing area also contained a constant grade slope.

The sockets constructed for the study participants were each instrumented with 11 strain gauges on the external surface of the socket in a range of orientations and in positions that

broadly covered the device. An additional temperature compensation gauge was mounted to an unloaded section of the device collection rig. Eight load positions were trained per socket (Figure 38). The definitions of each load channel are displayed in Table 24. These positions were chosen in order to provide broad coverage of the socket surface and so as the maximum anticipated changes from slope and alignment changes could be observed.

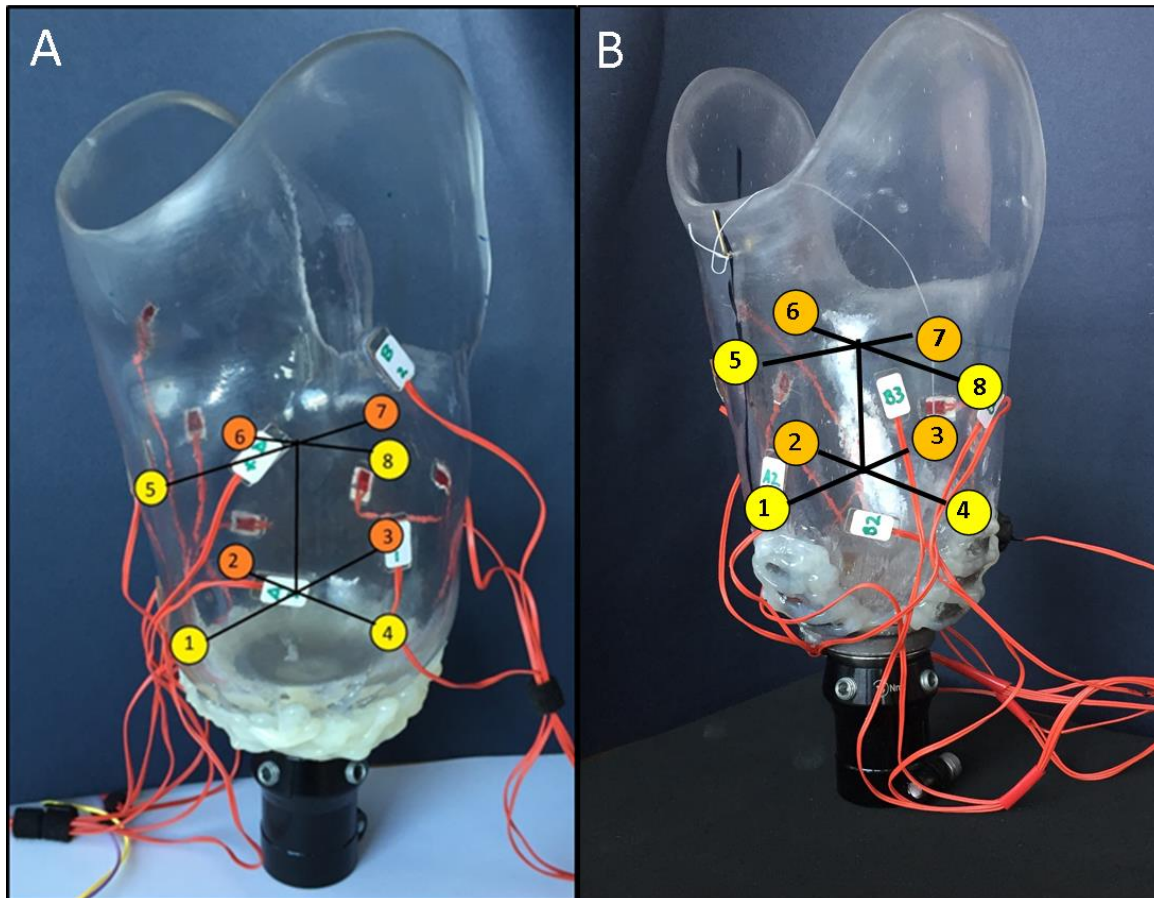


Figure 38 - Loading positions on the test sockets of the two participants. Load positions in yellow are on the nearside and anterior surface, orange on the far and posterior sides. Picture A is the socket of participant 1 (Left sided) and B of participant 2 (Right sided)

Load Channel	Participant 1	Participant 2
1	Distal-Anterior	Distal-Anterior
2	Distal-Medial	Distal-Lateral
3	Distal-Posterior	Distal-Posterior
4	Distal-Lateral	Distal-Medial
5	Proximal-Anterior	Proximal-Anterior
6	Proximal-Medial	Proximal-Lateral
7	Proximal-Posterior	Proximal-Posterior
8	Proximal-Lateral	Proximal-Medial

Table 24 - Load position definitions for each participant. Participant 1 was a left-sided amputee, and Participant 2 right-sided.

The measurement nodes were configured to collect at 16Hz (with the exception of Participant 1-Session 2 (P1S2), where this was increased to 64Hz). Training data from isolated loads on the socket was used to produce load cases to train networks. Training files of 1000 superposition cases were supplemented with 50 isolated loads per position. Training cases were modified using the linear noise injection model. Ensembles of 100 networks were produced – with a distribution of hidden neuron numbers of mean value of 16 with a standard deviation of 1. Mean maximum noise injection was set to 1% of the total, with a standard deviation of 2. Justification for these choices are explored in Chapters 5-7.

Each participant donned their test socket, set to an alignment considered acceptable to both participant and the prosthetist supervising the collection. The participant was allowed to wear the socket for ~10 minutes to become accustomed to the device.

Baseline recording was made with the participant seated and the amputated side offloaded. The participant was then asked to stand with the prosthetic limb on the force platform, and weight roughly equally distributed between the prosthetic and intact sides. A recording of the socket deformation strains was made for approximately five seconds of quiet standing. The participant was asked to place extra weight through the prosthesis side (to around 75% of bodyweight) for another five seconds of measurement, then light standing (~25% of

bodyweight). The actual proportion of bodyweight was validated against the recording from the force platform.

Walking tests were completed with the participant walking at a comfortable, self-selected speed. Trials were kept when the prosthetic side made clear contact with the force platform without the contralateral limb making contact. At least three walking trials were collected.

After flat walking, the participant was asked to walk up and down a 5° slope. This was completed with the volunteer walking at comfortable speed. The force platform was not available in this configuration. Following the completion of the battery of walking tests, the alignment of the socket in the coronal plane was adjusted. This was performed by altering the position of the pyramid adapter on the base of the socket. In bench testing this was approximately 5° of difference from the original alignment.

The participant was free to take breaks at any point, and to refuse to complete any task. A gap of around 20 minutes separated each alignment configuration. The complete battery of tests in each set of conditions took approximately 15 minutes (for static, flat walking and slope walking tests). The total attendance was 90-120 minutes.

Three measurement sessions were completed. The tests completed are summarised in Table 25.

Session	Participant	Date	Configurations tested	Static	Flat	Slopes
1 (Pilot)	P1	04/10/16	Neutral Alignment	Y	Y	Y
			Neutral Alignment,	Y	Y	Y
			Repeated			
2	P1	28/11/16	Neutral Alignment	Y	Y	Y
			Induced Valgus	Y	Y	Y
			Induced Varus	Y	Y	Y
			Neutral Alignment – Alternative liner	Y	Y	Y
3	P2	01/03/17	Neutral Alignment	Y	Y	N*
			Induced Valgus	Y	Y	N*
			Induced Varus	Y	Y	N*

Table 25 - Summary of experimental collection sessions. * Although the participant successfully completed slope tasks in all states, telemetry failure meant that results are not available in these configurations

Session Section	Task	Force Plate Recording
1	Seated, socket unloaded	No
2	Equal Weight Bearing	Yes
3	Heavy Weight Bearing	Yes
4	Light Weight Bearing	Yes
5	Flat Walk	Yes
5	Flat Walk	Yes
6	Flat Walk	Yes
7	Flat Walk	Yes
8	Up Slope	No
9	Down Slope	No
10	Up Slope	No
11	Down Slope	No

Table 26 - Example of test procedure sessions

Two participants were recruited as part of this study. The amputation and customary prosthetic characteristics are reported in Table 27. Both participants were capable and active transtibial amputees.

Characteristic	Participant 1	Participant 2
Gender	Male	Male
Age	54	41
SIGAM Grade	F	F
Amputation Level	Transtibial	Transtibial
Amputation Side	Left	Right
Time since amputation	24 Years	5 Years
Amputation reason	Trauma	Trauma
Stump Description	Short, bony	Well defined, bony, short
Socket Design	Total surface bearing	Total surface bearing
Suspension	Vacuum with 'Silcare' liner	Vacuum with silicone liner
Foot/Ankle Design	Echelon Vac	Echelon Vac

Table 27 - Participant details

During testing, each run was recorded on a collection sheet (Appendix A13). During the processing phase, the strain values were referenced to the unloaded state in each recording configurations. Processing then followed the flowchart shown in (Figure 31).

One issue encountered was that occasional frames of data would not be recorded by the software. Each collection node supplemented the strain measurements with a record of the frame count. By identifying gaps in this record, the missing frames were filled with linear interpolation. The maximum length of such a gap fill was equivalent to two frames of data.

During standing tests, outputs were taken as the average across the duration of the recording (Figure 39). During movement tests, the identification of the walking data corresponding to force plate recordings was made with a marker that was set within the collection software.

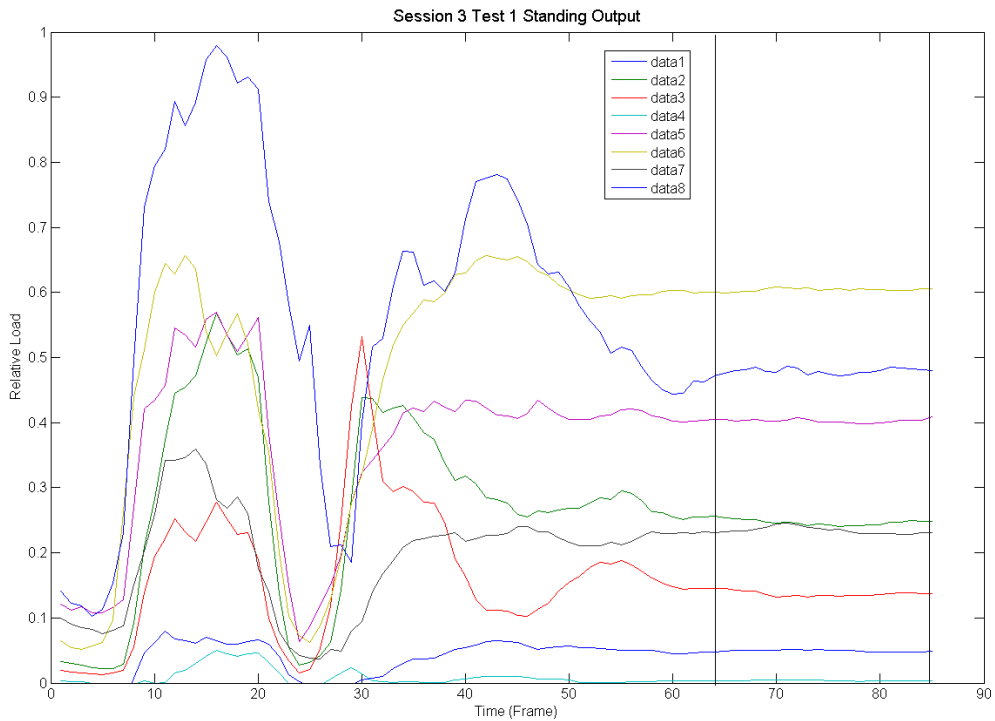


Figure 39 - Example static standing recording, showing a step onto the platform and then steady standing. Once forces reach steady state, loads are taken as the average between the vertical black lines. Loads are measured relative the maximum generated in the training process.

The force plate recording consisted of three time series. The point at which the vertical force component registered above the baseline was identified as the start point of the stance phase. The end point was set when the Fz (vertical) component returned to the baseline. The timing of the first and second peaks and the central trough was taken as the percentage of stance relative to these time points. These could then be used to identify the corresponding values on the network output channels (Figure 40).

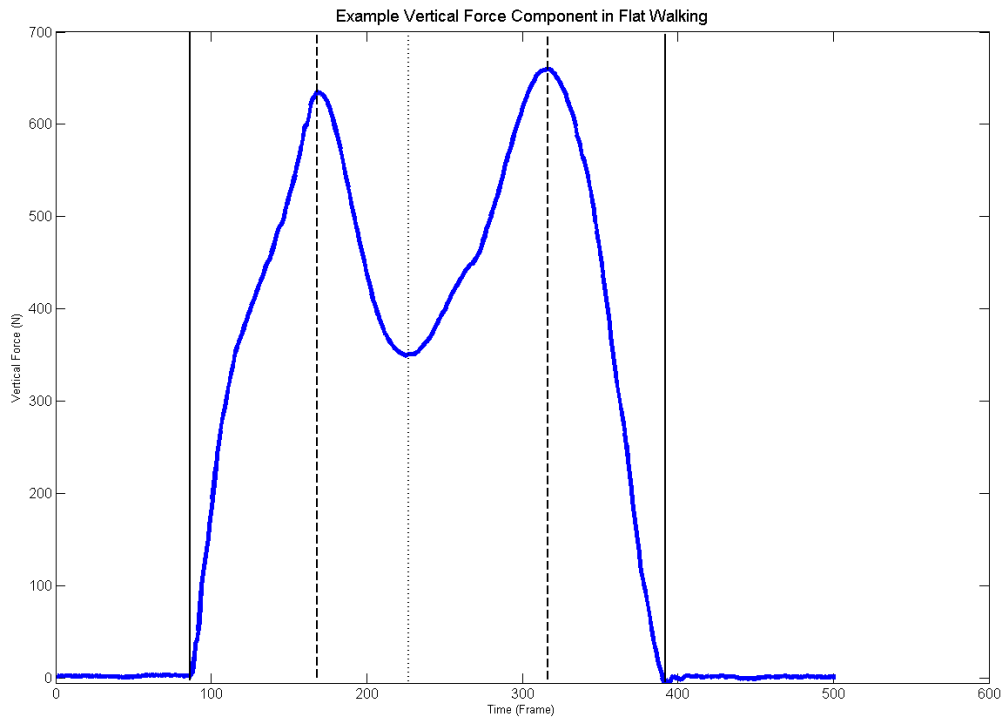


Figure 40 - Example vertical ground reaction force. Solid lines indicate the beginning and end of stance. Dashed lines show the position of the 1st and 2nd peak in force. The dotted line shows the time of the central minima.

During slope walking, the force plate was unavailable, meaning that this procedure could not be used. Instead, the software marker was used to indicate steady state walking (i.e. steps subsequent to gait initiation and prior to gait termination). The stance phases were identified from the transition from baseline readings from the input channel with the highest measurement response.

In Chapter 8, the results from static and dynamic testing in neutral alignment and flat walking conditions are evaluated, including the inter-session and inter-participant changes in estimated socket load distribution. In Chapter 9, the perturbation to the system via changes in device alignment and terrain is assessed.

4.11 Collection testing

In order to validate the performance of the measurement system, several tests were performed on a socket surrogate. A curved section of Northplex plastic was instrumented with

strain gauges of the type used across the study, and loaded with a set of weights in multiple positions on the rim of the test piece. In Figure 41, the effects of three sets of separately collected identical load patterns are shown. Results for the channel are shown were similar for other instrumentation channels.

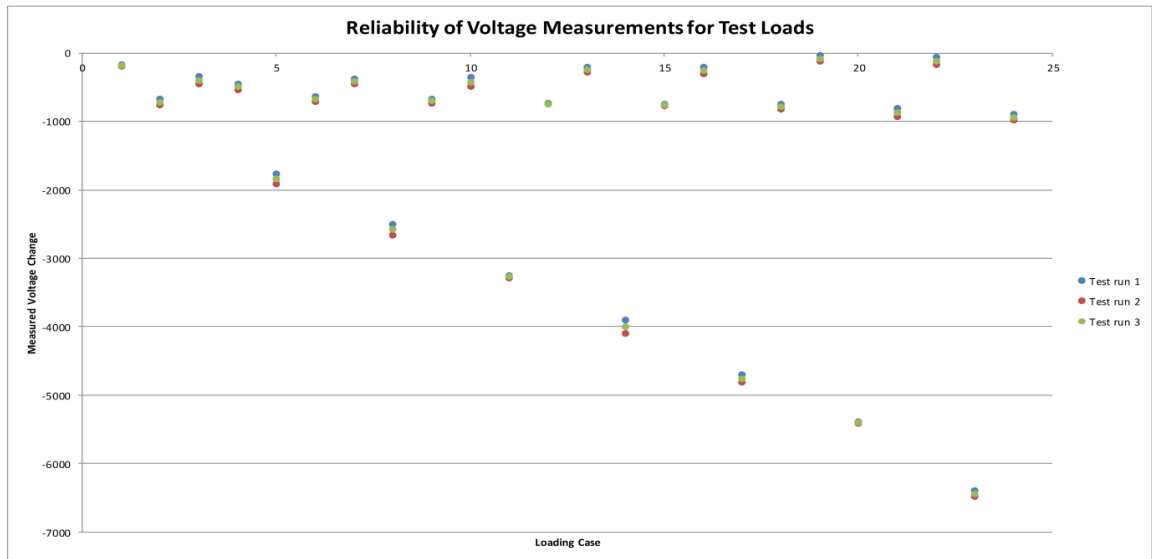


Figure 41 - Repeated loading tests. These are the measured relative voltage difference in a single measurement channel. Loads were applied in three positions with eight distinct magnitudes

Results indicate that the system was able to respond reliably to loading: the average was assessed as a maximum of 4.4% of the total.

The effect of temperature compensation is shown in Figure 42, for an example test session of a participant wearing the device during a set of activities. The plotted trace represents the applied change expressed as a percentage of the original measurement. This was calculated as a two-second moving average.

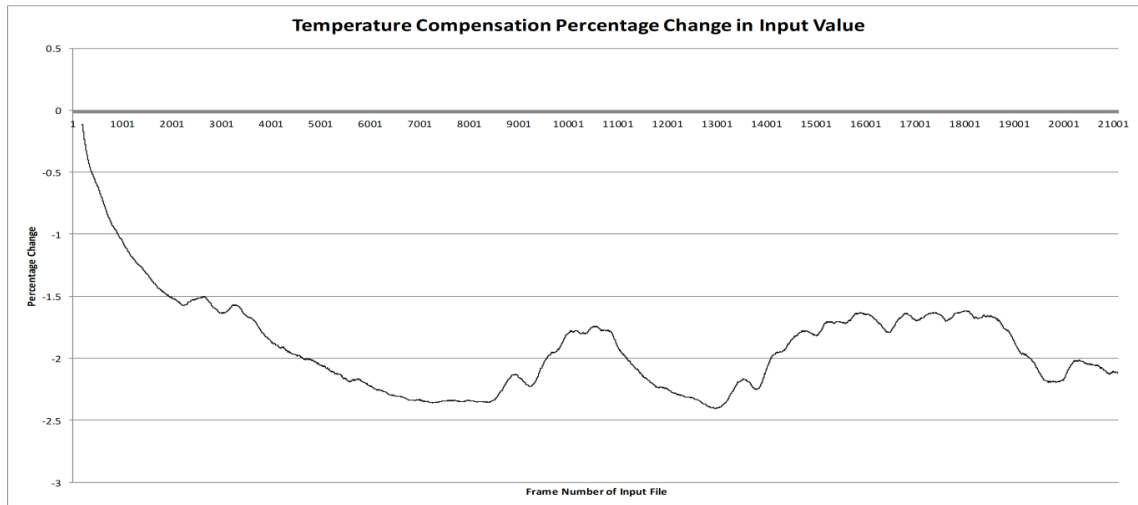


Figure 42 - Temperature correction calculated across an example test session, expressed as a percentage of the output voltage on the temperature compensation gauge

The maximum percentage change applied was <2.5% of the total.

Drift effects were evaluated by applying a constant prolonged load (c.60 seconds) and monitoring the effects on measured readings, with loads removed and reapplied three times. The effects on a single example load channel are plotted in Figure 43. The standard deviation between the mean of each load state was recorded as 1.25%.

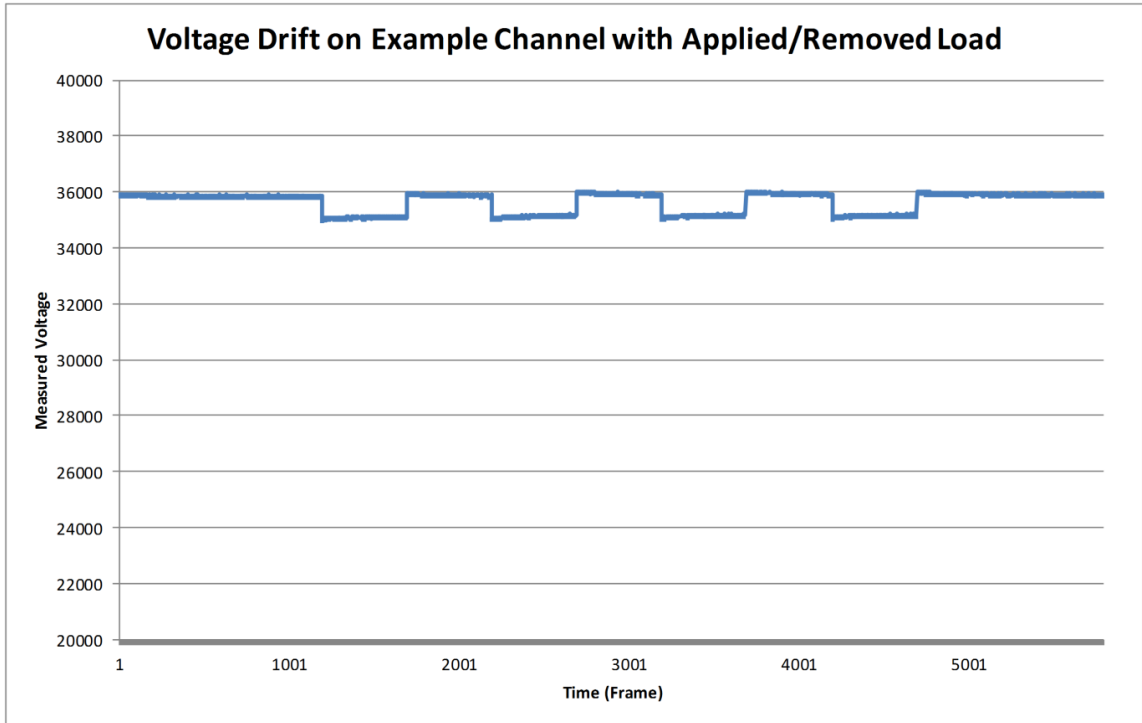


Figure 43 - Drift of an example channel voltage when a load is applied and removed from the test specimen. Y axis is reduced to show the change in output level effectively.

Noise was evaluated using the same test file. The variance during each section of constant applied load was estimated as the standard deviation about the mean value expressed as a percentage – the mean within load variation was 0.5%.

The combined effect of the results presented in this section suggests that the measurement error of a particular value (without temperature correction) is around 6.15%.

4.12 Summary

In this chapter, the techniques for obtaining and conditioning data in order to train a neural network to model the transfer function between loading and the structural deformation was made. Measurements on shape change are collected via foil strain gauges. Using linear superposition, loads are combined to provide varying cases of load distribution, and varied to improve generalisation to the solution.

The architecture and function of artificial neurons was described, along with an effective method of training a neural network to converge on an appropriate solution (using Feedforward Backpropagation and the Levenberg-Marquardt training algorithm respectively). Methods of halting training and evaluating the network performance were also reported.

Potential techniques for improving the estimates from neural networks were discussed: in particular the combination of multiple networks into ensembles, and in the modelling of inherent network error via polynomial functions.

The techniques discussed have implications for the accuracy, reliability and generalisation of solutions when used within a medical engineering application. The effects of controlling these parameters are discussed in the next 3 chapters.

The process of developing the requisite hardware and software for use during experimental testing was presented. The processes followed a rigorous risk assessment, and when relevant the appropriate ethical approval system. An examination of the results obtained from two transtibial amputees during typical walking and with a system perturbed from the optimal set-up is presented in later chapters.

Chapter 5 - Changes in system performance with alterations in training data conditioning and network design

5.1 Introduction

In Chapter 4, the design of neural networks and the supply of conditioned data to train them in an application to characterise loading on a prosthetic socket was discussed. Although the basis of the neural network solution of measuring socket load has been reported in the past, these publications have not performed detailed investigation of the inter-network variation when changes in neural network design and input data conditioning are made.

The optimal specification of these parameters is not known *a priori* in any specific application of neural networks. Although previous iterations of this application were able to successfully characterise the transfer function relating internal loads to external surface strains, whether accuracy could be improved by altering the system configuration was not answered. Other work in similar applications (e.g. Amali et al. 2014) has reported on changes to aspects such as hidden neuron number, and Ramazani et al. (2013) on alternative network designs. No reports examined the repeatability of network training.

To examine these effects, multiple networks were created in groups with alterations to the number of neurons in the hidden layer, the method of adding noise to the training data and the magnitude of this noise injection. The performance of networks with these configurations is evaluated with a separately produced test file. Differences between groups are statistically assessed.

The results presented in this chapter represents the first detailed assessment of network solution reliability in an inverse-socket load distribution measurement, and forms the foundation for the later work in this thesis which examines the impact of selected post-processing techniques.

5.2 Network design parameters

As described in Chapter 4, the training file for the neural network was generated using linear superposition from a seed file of a set of loads applied to an acrylic plastic transtibial socket. Loads were applied using an instrumented spring-mounted arm in eight positions around the internal surface of the socket wall (Figure 44). The external surface of the socket was instrumented with 11 single direction strain gauges fixed with cyanoacrylate in distributed positions and orientation. Temperature compensation used a two-second moving average. All strain gauges were placed in quarter-bridge configurations.

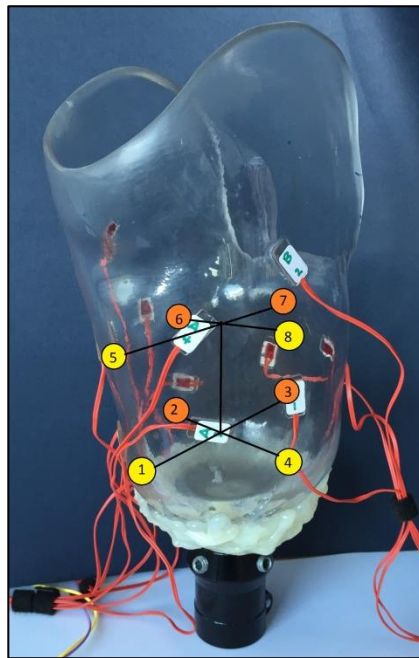


Figure 44 - The instrumented test socket, with positions of loading indicated. Yellow circles are on the anterior and lateral surfaces; orange circles on the medial and posterior faces

Loads were applied for approximately 5 seconds and collected at 16Hz. The load was applied to the socket wall via the system described in section 2.1. Loads were referenced to the measurement from an unloaded state, and normalised to the maximum applied load and used to create the seed file following the process described in Chapter 4.

The seed file was used in the production of the file of superposition loads. In all cases in this chapter, this consisted of 1000 cases of superposition loads, and supplemented by 400 'isolated' loads of random magnitude loads in single positions.

Modification of the training file was carried out in some network specifications. Two methods of noise injection on the training file were pursued: that of a constant noise injection and a linear or percentage noise method. Constant noise injection modified each value of the training case by a random value up to a set percentage of the maximum value in that channel. Linear noise varied each value in the training file by a random value up to a set percentage of that value. The effects of a maximum of 5% noise injection from both methods are shown in Figure 45 and Figure 46. In this chapter, the magnitude of noise injection was varied in this study between 0 and 10%.

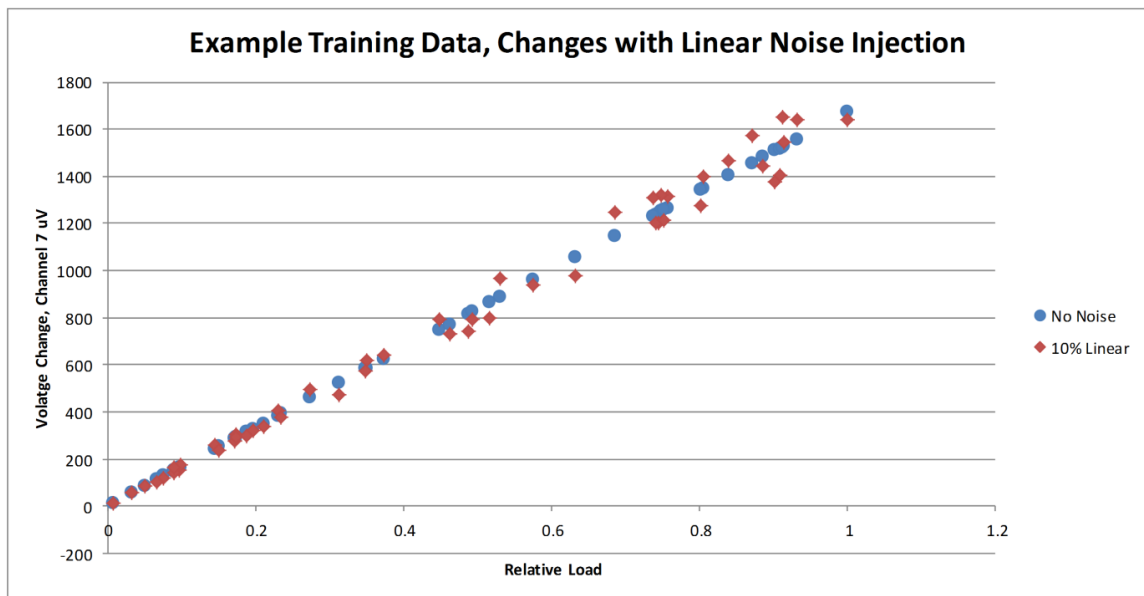


Figure 45 - Effect of linear-type noise injection on training cases. For clarity, these are isolated loads applied in load position 1 on the 7th measurement gauge only

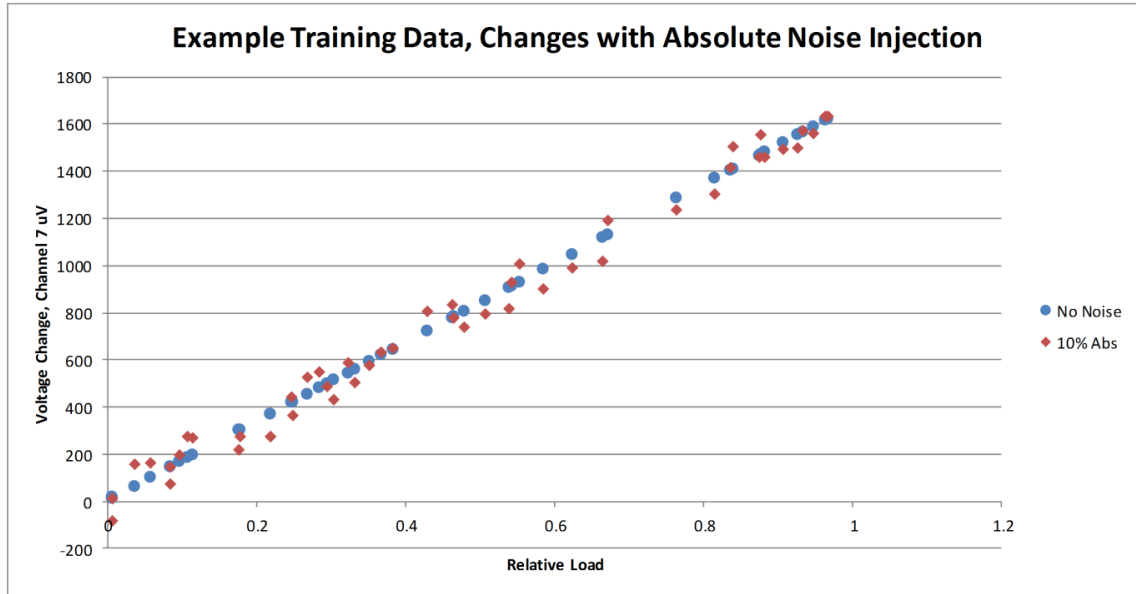


Figure 46 - Effect of absolute value-type noise injection on training cases. For clarity, these are isolated loads applied in load position 1 on the 7th measurement gauge only

Training cases were modified with a temperature compensation factor obtained from the change in reading from a matching unloaded gauge. A two second moving average was applied, and the difference between this reading and that from the first two seconds of the measurement was applied to all subsequent strain measurements.

Training cases were supplied networks with the training parameters are summarised in Table 28.

Parameter	Value
Network Design	Feedforward Backpropagation
Learning Algorithm	Levenberg-Marquardt
Inputs	11 (Strain Voltages)
Outputs	8 (Relative Loads)
Transfer Functions	Poslin-Tansig
Superposition Cases	1000
'Isolated' Cases	400
Maximum Epochs	100
Training Goal	0.01
Maximum Validation Checks	6

Table 28 - Network training parameters common to all trained networks in this chapter

The performance of networks was assessed using a separately recorded file of superposition (i.e. simulated) loads. On another occasion, the same socket was loaded in the same manner as during the creation of the training file, and processed to produce another seed file. This was used to create a test file of 1000 superposition cases and 400 isolated loads, which were then supplied to each trained network. The differences between the target values and the estimates produced by the network were rectified and expressed as a percentage of the total applied load to produce the RMS % error, a score of the accuracy of the network on unseen data.

A study power calculation was performed using the mean and variance from a pilot test group (RMS% error = 10, SD = 1.5 an anticipated RMS% error difference between groups of 0.67%). For $\alpha=0.05$ and a power of 0.8, the minimum required sample per group was calculated to be 79. This was increased to 100 per group.

An explanation of the shorthand description of network specification is shown in Figure 47.

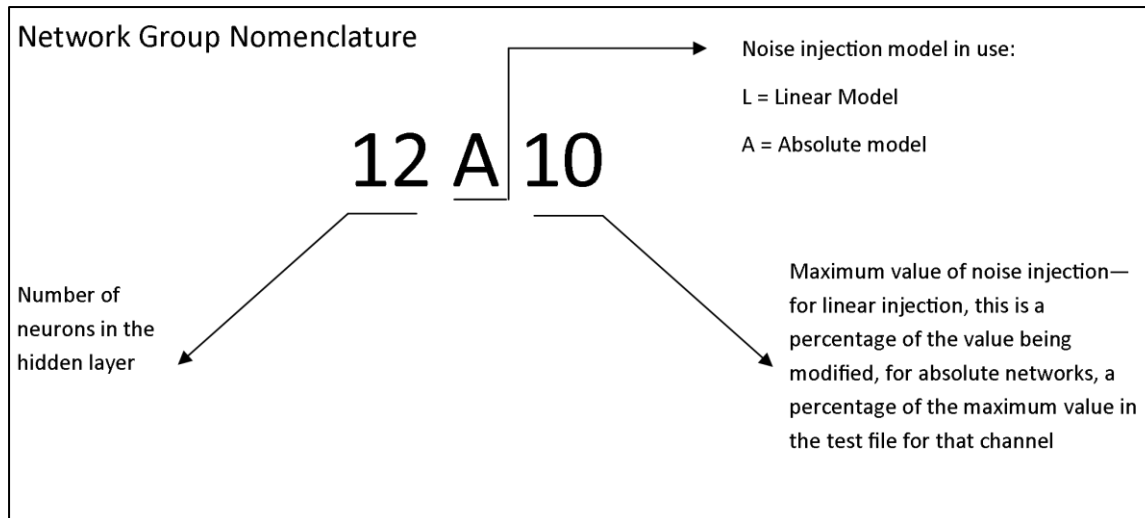


Figure 47 - Naming convention in use for shorthand descriptions of network configurations

5.3 Hidden neuron number

The aim in this section is to examine the changes in network accuracy that arise when the number of neurons in the hidden layer is varied. The optimal value is typically problem-specific, and so a quantitative assessment of the effect of changing this parameter is necessary. The objectives are to evaluate the changes in RMS error % when neuron numbers are altered.

5.3.1 Methodology

In order to investigate the effect of altering the hidden layer size, the number of hidden neurons was set to 12, 16, 20 and 24. The typical approach in this task is to begin with a number of hidden neurons equal to the number of inputs plus outputs (i.e. 19). This experiment therefore examines around this initial figure. At this stage, noise injection was not used. 100 networks were trained in each configuration.

5.3.2 Results

Distributions of network accuracy are shown in Figure 48, and the mean, standard deviation and extremes of accuracy are shown in Table 29.

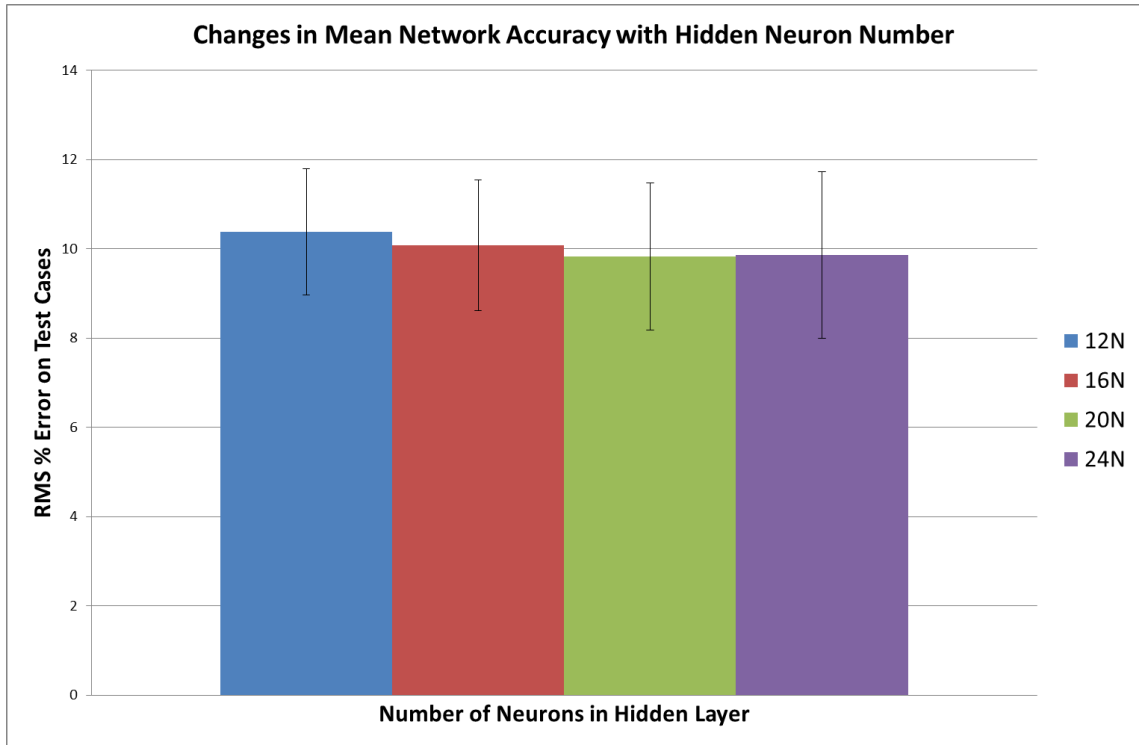


Figure 48 - Changes in mean network RMS% error with differences in the number of neurons in the hidden layer. No noise injection is used in these networks. Error bars indicate ± 1 SD.

Hidden Neurons	Min Error	Mean Error	Max Error	SD	K-S Test of Normality
12	7.96	10.38	12.71	1.41	0.046
16	7.58	10.08	12.54	1.47	0.044
20	7.80	9.82	11.92	1.65	0.091
24	8.10	9.86	11.65	1.86	0.048

Table 29 - Characteristics of RMS error on test data in groups of networks with different hidden neuron numbers. K-S refers to the Kolmogorov-Smirnoff test

Figure 49 is a probability plot of the RMS % errors for each group of neurons to investigate the pattern of distributions. The pattern of normal distributions was confirmed using the Kolmogorov-Smirnoff test (Barton and Peat 2014).

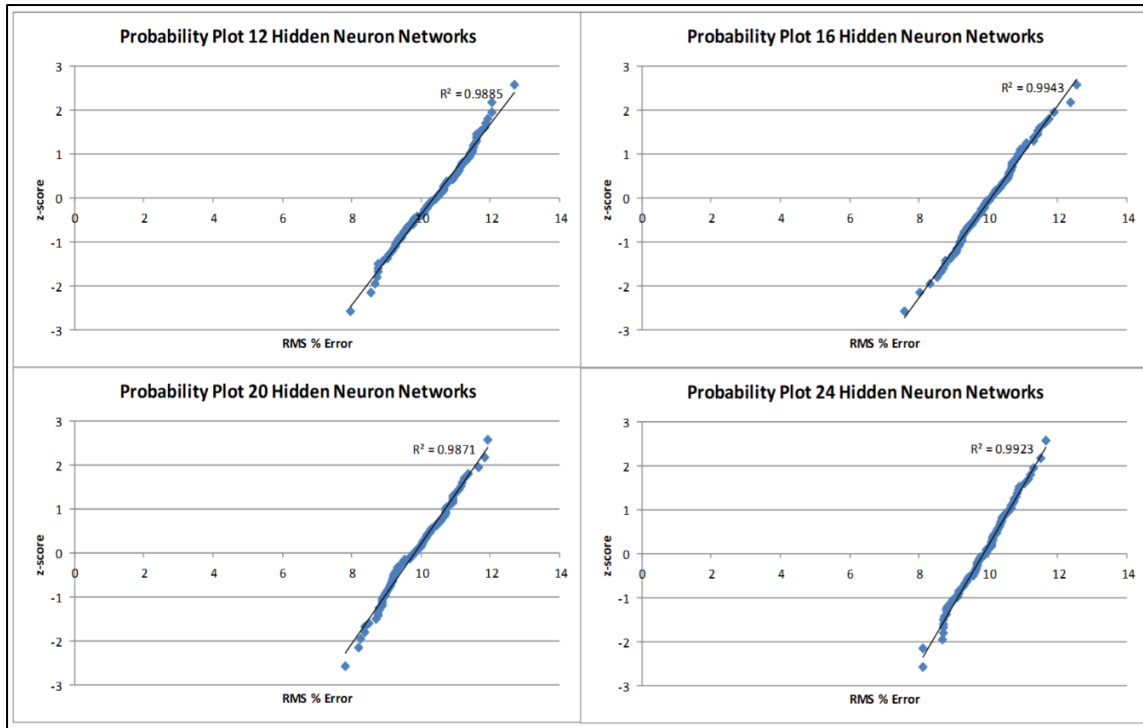


Figure 49 - Probability plots of RMS error on test data for groups of networks with different numbers of hidden neurons, demonstrating the justification of assuming a normal distribution of RMS error

The absence of significant changes in accuracy between was confirmed with an ANOVA test.

5.3.3 Discussion

High quality networks (i.e. those with the lowest RMS% error or most accurate) were broadly comparable in performance to those produced in previous work (Chapter 2). Mean accuracy was slightly lower than the reported values for the previous iteration: however prior network variance is unknown. However noise injection was not implemented at this stage, which would be anticipated to improve generalisation performance.

The lack of significant changes in accuracy with changes in hidden neuron number was somewhat unexpected. Previous work in similar applications found that the network performance did alter with changes in this parameter (Chapter 2) and other examples of neural network solutions found that tuning this parameter is necessary to optimise the quality of the final estimate (Gholipour and Arjmand 2016).

Although there was not a trend for the mean network quality to change significantly, a small increase in standard deviation of network performance can be seen. This was in conjunction with a reduction in accuracy range. It seems that lower hidden neuron number networks have a better chance of producing a high quality network, but also an increased risk of a poorly performing network.

5.4 Noise injection method

In Chapter 4 two different methods for conditioning the training data were described. The constant noise method alters up to a certain percentage of the maximum value recorded on that channel. This forms a constant width band of values for network training. The linear noise model instead creates a cone shape of values, meaning that high values of input are permitted a greater variation than smaller values (as shown in Figure 45 and Figure 46). This choice represents different models of how measurement error is likely to manifest in the training data. The aim of this section is to evaluate if altering these values has a meaningful effect on the quality of individual networks.

5.4.1 Methodology

A maximum alteration of 10% was applied using both the linear and constant noise injection methods. To first ensure that the code used to produce these modifications was not causing any other unintended changes in the network construction, the effect of each system was first evaluated for each value of hidden neuron number previously tested. Groups were evaluated using paired t-tests between each pair of networks with a Bonferroni correction applied. No significant differences were observed.

5.4.2 Results

Figure 50 shows the mean and standard deviation of networks of differing noise injection methods for different combinations of hidden neuron number and between zero noise injection and the maximum of 10%. The mean, minimum, maximum and standard deviation of each group of network configurations is shown in Table 30.

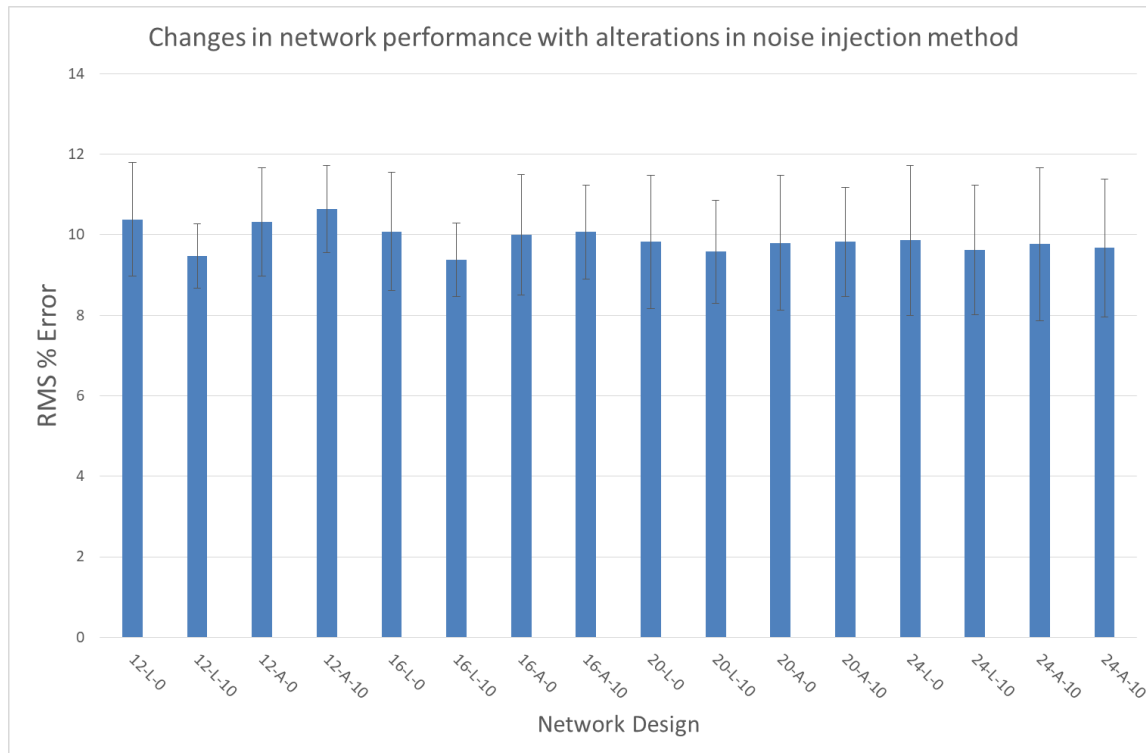


Figure 50 - Changes in mean network RMS error with node number, noise injection and noise injection method. Blue circles indicate 0 noise, linear model. Red circles indicate 10% noise, linear model. Blue diamonds are 0% noise, absolute model and red diamonds 10% noise, absolute model. Error bars are ± 1 SD.

Hidden layer Neurons	Noise Injection Method	Maximum noise percentage	Minimum RMS % Error	Mean RMS % Error	Maximum RMS % Error	Standard Deviation
12	Linear	0	7.96	10.38	12.71	1.41
		10	7.66	9.47	11.90	0.80
	Absolute	0	8.45	10.31	12.09	1.35
		10	7.70	10.63	13.58	1.08
16	Linear	0	7.58	10.07	12.54	1.47
		10	6.82	9.38	10.95	0.92
	Absolute	0	7.13	9.99	12.39	1.49
		10	8.26	10.08	12.93	1.16
20	Linear	0	7.80	9.82	11.92	1.65
		10	7.85	9.58	11.22	1.28
	Absolute	0	8.03	9.80	12.99	1.67
		10	7.91	9.82	12.27	1.36
24	Linear	0	8.10	9.86	11.65	1.86
		10	8.02	9.63	12.73	1.61
	Absolute	0	7.95	9.77	11.75	1.90
		10	7.68	9.67	13.52	1.72

Table 30 - Characteristics of groups of networks of varying noise injection method.

An ANOVA was used to evaluate the statistical differences between these groups, with a post-hoc Tukey test to identify differences between groups. The results from this analysis are shown in Table 31. Only those comparisons of interest (i.e. between the presence or absence of noise injection, between the noise injection method and changes between the numbers of hidden neurons) and when these changes were assessed as significant following correction of the p-value boundary are shown.

Group 1	Group 2	Direction	p Value
12 L 0	12 L 10	Group 2 < Group 1	<0.001
16 L 0	16 L 10	Group 2 < Group 1	<0.001
12 L 10	12 A 10	Group 2 > Group 1	<0.001
16 L 10	16 A 10	Group 2 > Group 1	<0.001
12 A 10	20 A 10	Group 2 < Group 1	<0.001
12 A 10	24 A 10	Group 2 < Group 1	<0.001

Table 31 - Results of significant differences between groups following ANOVA test and post-hoc Tukey tests. Only significant differences are shown.

5.4.3 Discussion

A limited number of significant differences between the network configurations were observed in this set of tests. In evaluating the effect of noise injection, a maximum of 10% noise injection when using the linear model created a significant improvement over the no-noise equivalent group only when networks of 12 or 16 hidden neurons were used. Significant differences were not found with noise injection using the absolute model for any number of hidden neurons, or at higher numbers of hidden neurons for the linear noise model.

Significant differences between each of the noise injection methods used were found in two cases: with 12 hidden neurons and 16 hidden neurons. In both cases, the linear noise conditioning performed better than the absolute noise method (10.31% to 9.47% in the 12 neuron case and 10.07% to 9.34% in the 16 neuron case)

No significant changes were evident between groups trained with the linear noise model when the number of hidden neurons was altered, suggesting that hidden node number is not a critical factor when this method is used.

Significant changes were found when the absolute noise method was used: the use of additional hidden neurons created a significant improvement in the mean performance of the trained networks. However this only reached significance when the 12 neuron group was compared to the 20 and 24 hidden neuron groups when this form of noise injection was used.

The use of noise injection tended to decrease the variance between networks within each group when compared to the zero noise case. In addition to producing a modest benefit in mean network performance, the solution consistency improved. Networks with noise injection and the same hidden neuron number also tended to show a lower RMS error than their zero-noise counterpart. The exceptions to this pattern were the lower hidden neuron groups when the absolute noise injection model was used: here the error increased with the use of noise injection (although the variance did reduce).

The reason for this is linked to the different quality of the training file at low load values. Lower hidden neuron networks seem less able to converge on a suitable transfer function when there is this degree of divergence from the 'perfect' solution at these values. By improving the processing ability of the network by increasing the number of hidden neurons, the transfer function could be appropriately modelled in these cases.

To see if these observations were consistent with changes in the magnitude of noise injection, new groups of networks with an intermediate maximum noise injection values were produced and evaluated.

5.5 Noise injection magnitude

The aim of this section is to identify if the gains in mean network accuracy generated by introducing a noise injection technique could be obtained using smaller values of deliberate error introduction. This would also establish if the patterns identified in section 5.4 were consistent. A smaller value of noise injection may allow a closer representation of the theoretical relationship to be established, enabling more precision. A too-low value may not adequately account for the noise inherent in the measurement.

5.5.1 Methodology

Groups of 100 networks were created using linear noise injection (the results in section 3.4 having indicated that no significant changes were evident in absolute noise networks) and with hidden layer sizes of 12, 16, 20 and 24. Noise magnitude was also tested at 5%. The hypothesis was that the smaller level of noise injection will still create a significant improvement in RMS percentage error on the test file.

5.5.2 Results

The performance of each network group is shown in Table 32 and Figure 51.

Group	Minimum RMS % Error	Mean RMS % Error	Maximum RMS % Error	Standard Deviation
12-L-0	7.96	10.37	12.71	1.41
12-L-5	7.88	9.75	11.61	0.91
12-L-10	7.67	9.47	11.90	0.80
16-L-0	7.58	10.08	12.54	1.47
16-L-5	8.16	9.73	11.73	1.08
16-L-10	6.82	9.38	10.95	0.92
20-L-0	7.80	9.82	11.92	1.65
20-L-5	7.95	9.66	11.48	1.31
20-L-10	7.85	9.58	11.22	1.28
24-L-0	8.10	9.86	11.65	1.86
24-L-5	7.62	9.62	11.06	1.65
24-L-10	8.02	9.62	12.73	1.61

Table 32 - Network performance characteristics with variation in noise injection magnitude

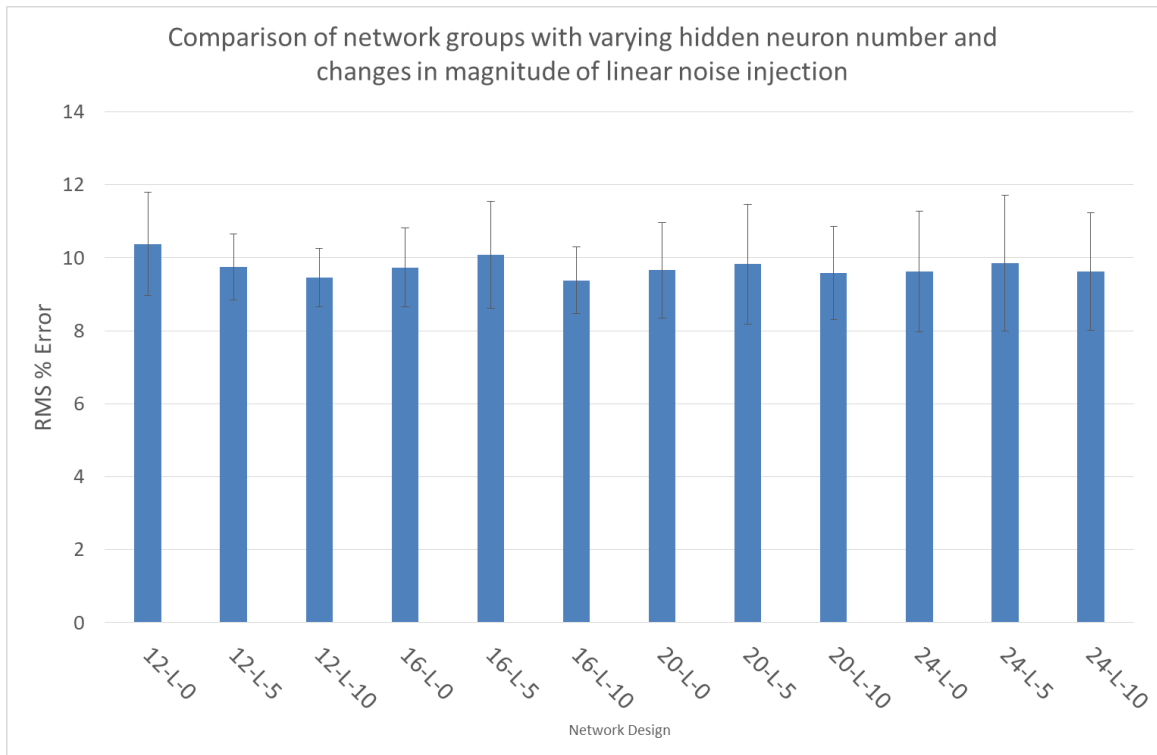


Figure 51 - Variation in network error with changes in hidden neuron number and magnitude of linear noise injection. Three groups are shown per hidden layer size with 0, 5 and 10% maximum noise injection.

Differences in RMS % error between networks of 0% and 5% are compared with unpaired t-tests, as are differences between 5% and 10% values of maximum noise injection. Differences between networks of varying hidden node number and 5% noise injection were compared with a one-way ANOVA (Table 33). Due to the number of comparisons, a Bonferroni correction was applied to revise the significance boundary $p < 0.05$ to $p < 0.0025$.

Test Group	Comparison Group	P value
12-L-5	12-L-0	0.0002*
	12-L-10	0.0262
16-L-5	16-L-0	0.0650
	16-L-10	0.0684
20-L-5	20-L-0	0.4485
	20-L-10	0.6627
24-L-5	24-L-0	0.3356
	24-L-10	0.8624

Table 33 - Group comparisons between 5% maximum injection networks and matching groups of 0% and 10% conditioned networks

The ANOVA calculation identified a between-groups significance value of 0.569: no significant differences.

5.5.3 Discussion

Intermediate values of noise injection fell between those of no-noise and the 10% maximum noise conditions. A maximum noise injection of 5% was only able to produce a significant improvement in the performance of networks in the case of 12 hidden neurons. This was expected for the 20 and 24 neuron test groups as no significant improvement was found at higher noise injection, but demonstrated that 5% injection was not sufficient in 16 hidden neuron networks to produce significant improvement.

A smaller noise injection component had a similar effect to that of larger maximum noise values. The range between the best-performing and worst performing networks reduced within 5% groups as compared to their unaltered counterparts. The standard deviation of networks was also lower, confirming the effect of an improvement in solution consistency when applied to this test data.

5.6 Critical appraisal of network modification approach

The aim of this chapter was to investigate the impact of varying controllable parameters in the network specification that were thought to have an effect on the accuracy and generalisation ability of the network solution.

Only two models of noise injection were considered in this chapter: a linear model and a constant width noise model. These are far from the only possible models for providing this data conditioning for the improvement of generalisation performance. Of particular interest for dynamic measures of socket strains may be to accommodate hysteresis effects in the training process. To achieve this, an inverse of the linear method could be employed, with greater divergence from the ideal superposition relationship at lower loads than at higher loads. Alternatively, some hybrid model containing greater variance at extremes of load may be useful.

Some parameters associated with network training were not investigated in this study. In particular, changes to the overall network architecture, training algorithm or training end points were not examined. These values were found to reliably produce networks of acceptable quality (compared to previous implementations). Some aspects of this were linked to practicality – the Levenberg-Marquardt algorithm used in this study is thought to converge on a solution significantly faster than previously used training algorithms (Hagan and Menhaj 1994). When such a large number of networks are being created, this efficiency is more critical.

Despite the changes introduced to the network training data, the magnitude of differences between the groups of network mean performance was small. The maximum difference in mean network performance was equivalent to a 12.10% improvement over the original error. However, the results also demonstrated the large range of accuracy in network solutions: the best performing network trained has an RMS error of 6.82%: the worst performing network an error of 13.66%. Although the outcome and mean performance of any group of specifications remained similar, the variance within groups – the differences created from the training process - remained high.

The generalisation of the conclusion of this work are also not fully understood. The results are likely to be somewhat specific to the problem as defined in this section, in terms of the structure, the number of loading positions and measurement gauges. However, as an evaluation of an approach to resolving issues of generalisation of network solutions, this work remains useful in understanding the effects of altering readily available parameters.

5.7 Summary

Chapter 2 highlighted the limited work that had been previously carried out to examine the reliability of neural networks that solve inverse-problem load distribution. Optimisation options include the number of hidden neurons used and the means of creating generalisation (both the noise injection model and the maximum magnitude of the adjustment). The lack of statistical evidence of the impact of system design represented a major gap in understanding of this technique.

In this chapter, the effects of varying the training data conditioning and neuron architecture were evaluated. This found that when inter-network variance was taken into account that varying the hidden neuron number without noise injection did not significantly alter overall accuracy. When noise injection was implemented, the linear noise model was able to generate significant reductions in error on a test file in low-neuron configurations. Increasing noise injection magnitude showed improvement in error; however intermediate values were not sufficient to induce significant changes in accuracy (in all but one case).

Overall, results were comparable to previous versions of the system, and the mean network performance in all configurations was capable of adequately modelling the system response when supplied with testing loads. However, the results suggest that the improvements that are possible from manipulation of these parameters are limited: the inter-network variance masks any enhancement on an individual network basis.

Network performance has a normal distribution. This provides supporting evidence that an ensemble average is feasible. The effect of creating these ensemble estimates using identically specified and varying specification ensembles is examined in Chapter 6, followed by an investigation into post-processing techniques in Chapter 7.

The contribution to knowledge presented in this chapter is that varying these components of the network solution in isolation has only a limited impact on mean network accuracy, a conclusion that is founded on the results which demonstrate the scale of inter-network variance. This estimate of variance in the technique provides important context to the clinical use of the device: it suggests that unaltered networks may demonstrate insufficient reliability in estimate accuracy to provide highly-valid results.

Chapter 6 – Evaluating the performance of ensembles of neural networks on problem data

6.1 Introduction

Chapter 5 demonstrated that there remains a need for a reduction in error and inter-network variance in the socket load solution – as identified in chapter 2, ensemble networks may provide a means of achieving this. One positive aspect of the ensemble technique is that it is relatively simple to implement. Another factor is that the method is conceptually more straightforward than many competing techniques. Drawbacks of this design are the increase in computational cost, the requirements for storage and recall of multiple networks and that identical networks would produce identical results: diversity is required for the ensemble to be valuable. Fortunately, the assumptions inherent to the socket measurement system mitigate this issue, as the generation of novel training cases is easily achievable.

Ensembles had not been applied to the socket measurement problem previously: until the latest implementation the time required for network training was prohibitive. With the Levenberg-Marquardt algorithm and the implementation of the code in the MATLAB Neural Network Toolbox, the training time was greatly reduced.

The optimal construction of an ensemble was not known for this problem. It is not clear that the relationships established in Chapter 5 for the production of single networks would be maintained when these networks were used as the constituents for a network ensemble. The first stage of this chapter will examine the effect of constructing ensembles from the same groups of networks examined in Chapter 5. Research into ensembles of neural networks has suggested that creating ensembles from networks of different designs has the potential for even greater benefits. The second section investigates the use of ensembles created from networks of varying design.

These tests provide evidence for the feasibility of introducing a network ensemble solution to this socket measurement problem. In addition to the change that the ensemble makes in terms of solution accuracy and reliability, the means of producing an improved result from

management of the ensemble design has the effect of providing users with confidence in the consistency of presented results.

Results from these investigations were presented at two conferences (Appendices A3/A4)

6.2 Ensemble construction testing

To investigate the effect of creating ensembles from identically specified networks, the estimates from the groups of networks evaluated in Chapter 5 were combined into ensemble averages. All networks used the same essential architecture, the same learning method and the same training end conditions. Each network trained on the same seed file, but with different superposition and isolated load cases. The solution of the ensemble was then calculated as the average of all constituent network estimates.

Parameters that were varied included the number of hidden neurons and the means and magnitude of noise addition. The null hypothesis used was that network ensemble solution percentage error did not differ from the performance of the mean network used to construct the ensemble.

These parameters were chosen in order to evaluate different key features of the network specification. Varying the hidden neuron number is a means of altering the processing power of the system. As the complexity of the underlying relationship is, *a priori*, unknown, the solution may be improved by increasing this value at the cost of marginally poorer efficiency. Altering the noise injection magnitude is a method of varying the generalisation ability of the system: a wider noise injection band is hypothesised to provide a more robust solution although with the drawback that the estimates may be less precise. Similarly, altering the noise injection model is thought to have the effect that different aspects of the transfer function are subject to greater variance from the linear relationship assumed in the process of generating training cases.

These are not the only potential parameters that could be adjusted in a study such as this, but these provide some examination of both the data processing and network production procedures. The reliability of the ensemble construction as a post-processing method is evaluated here, and additional techniques in Chapter 7.

6.2.1 Methods

To reiterate, the means of creating the ensemble average is a simple mean of each network output across the group of networks that make up the ensemble. Equations (42) and (43) from Chapter 4 were expanded to cover the eight socket load outputs.

Common network features described in Chapter 5 were retained, and Table 34 the varied aspects within each ensemble.

Parameter	Values			
Hidden Neurons	12	16	20	24
Maximum Noise Addition	0	5	10	
Noise Addition Method	Percentage		Absolute	

Table 34 - Network parameters that are varied between ensemble designs

To measure the variance of creating ensembles, a set of 10 identically specified ensembles of 100 networks were created using the parameters in Table 35, and evaluated using a problem data set. This consisted of 1400 simulated load cases, generated in the same way as the training set, but produced from a seed file of measurements collected on a different occasion. The percentage RMS error between each network and ensemble estimate and the target was calculated (Table 35). Rather than calculate inter-ensemble variance for every design of ensemble subsequently, this value was used as an estimate for comparison between groups.

Group	Noise Method	Hidden Neurons	Max Noise %	Mean Constituent RMS % Error	Ensemble RMS % Error
1	Absolute	16	5	10.18	7.43
2	Absolute	16	5	10.19	7.24
3	Absolute	16	5	10.15	7.54
4	Absolute	16	5	10.10	7.79
5	Absolute	16	5	10.19	7.39
6	Absolute	16	5	10.24	7.40
7	Absolute	16	5	10.02	7.36
8	Absolute	16	5	10.26	7.66
9	Absolute	16	5	10.23	7.44
10	Absolute	16	5	10.21	7.38
Average (Standard Deviation)				10.18 (0.07)	7.46 (0.16)

Table 35 - Repeatability evaluation of 10 identically specified ensembles

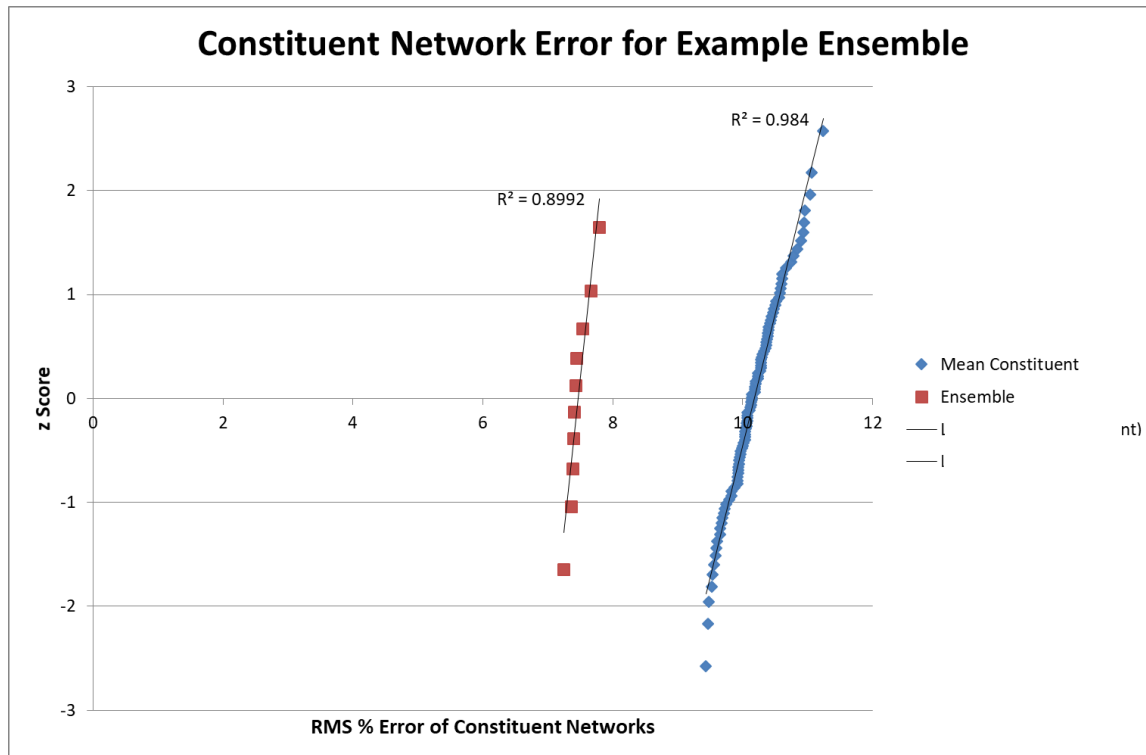


Figure 52 - Probability plot for constituent network RMS % errors for a particular ensemble, and the distribution for a set of ensembles. Also shown are linear trend lines.

Probability plots for both constituent network errors and the distribution of ensemble network errors confirmed that the distributions of both corresponded well to a normal distribution facilitating parametric statistical tests (Figure 56). This was established via the R^2 values of 0.984 and 0.8992, which show a high quality linear fit in both cases and hence a normal distribution.

6.2.2 Results

First, the hidden neurons of the constituent networks were varied between 12 and 20. Results were not significantly different (in the absence of noise injection), but demonstrated improvement over the corresponding mean performing constituent networks (Rows for 0% noise in Table 36).

The next aspect under consideration is the effect of differing magnitudes of noise injection to the training data. The maximum value of alteration of any particular data point was set to 0%

(i.e. no noise injection), 5% of the original value or 10% of the original value (linear model). The results from ensembles created from constituent networks of these specifications are shown in Table 36.

Max Noise		Hidden Neurons			
		12	16	20	24
0	RMS % Error	7.46	7.78	7.63	7.83
	Difference	-2.91	-2.29	-2.19	-2.03
5	RMS % Error	8.15	8.29	8.16	8.22
	Difference	-1.60	-1.44	-1.50	-1.40
10	RMS % Error	8.23	7.95	8.31	8.31
	Difference	-1.24	-1.43	-1.27	-1.32

Table 36 - Alterations in ensemble performance with changes in training data conditioning and hidden neuron number. Max noise refers to the maximum value of adjustment of any training input value. Difference refers to Ensemble Error- Corresponding Mean Constituent Network Error

The final alteration for the design for ensembles of identically specified networks was the difference between the linear and absolute noise injection models (as examined for individual networks in Chapter 5). Input values were modified by a value up to a specified percentage of the maximum applied value. In this work, the percentage was set to 0% (i.e. no noise injection), 5% or 10%. Results are shown in Table 37.

Noise Method	Max Noise	Hidden Neurons				
		12	16	20	24	
Linear	0	RMS % Error	7.46	7.78	7.63	7.83
		Difference	-2.91*	-2.29*	-2.19*	-2.03*
Absolute		RMS % Error	7.30	7.48	7.77	7.69
		Difference	-3.01*	-2.52*	-2.02*	-2.07*
Linear	5	RMS % Error	8.15	8.29	8.16	8.22
		Difference	-1.60*	-1.44*	-1.50*	-1.40
Absolute		RMS % Error	7.36	7.50	7.67	7.71
		Difference	-3.31*	-2.68*	-2.349*	-2.04*
Linear	10	RMS % Error	8.23	7.95	8.31	8.31
		Difference	-1.24*	-1.43*	-1.27	-1.32
Absolute		RMS % Error	7.34	7.38	7.58	7.70
		Difference	-3.29*	-2.68*	-2.24*	-1.97*

Table 37 - Changes to ensemble performance with alterations in hidden neuron number, maximum noise value and noise injection model. Differences marked * indicate a significant difference between the ensemble and the constituent distribution. Each ensemble had a lower error than each mean constituent.

For this set of experiments, the threshold of significance was revised to $p < 0.0021$ due to the number of comparisons. The constituent networks were compared to the corresponding ensembles using unpaired, two-tailed t-tests.

6.2.3 Discussion

In all cases, generating an ensemble of networks improved the accuracy of the produced load distribution estimate when compared to the mean performing constituent network within each ensemble (the 'Difference' rows of Table 37).

Ensembles tended to perform better in lower noise, lower hidden neuron number configurations. Furthermore, the difference between the ensemble average and the mean constituent also decreased when these higher value designs were tested. It can be concluded then that the magnitude of the improvement from an ensemble average was greater for low noise, low neuron networks. Marginal benefits in terms of training and processing time are also expected from networks consisting of fewer processing units.

Varying the number of hidden neurons (when this number remained constant across the ensemble) did not significantly alter the performance of ensembles of networks in this application. This is somewhat in contrast to the anticipated effect that varying this parameter would materially impact the overall accuracy of the ensemble.

Although increasing the maximum magnitude of noise injection did not have a positive effect on the accuracy of networks (error tended to increase with the increase in noise), the linear noise method also tended to have a worse performance than the constant noise model. As the constant method has an overall wider band of variance from the optimal value, this suggests an opposite pattern to the maximum injection magnitude. Potentially, the increased noise at the lower end of the load distribution band provides a better result in this case.

6.3 Mixed ensembles

In addition to constructing ensembles from identically specified networks, ensembles formed by mixing the sources of constituent networks of each of the kinds examined in section 5.2 were investigated. 44 different ensembles were created: each still consisted of 100 networks, but these were taken from larger populations of mixed groups of designs. The purpose of this test was to examine if mixed ensemble designs might provide even greater performance benefits through increasing the diversity of the ensemble solution.

6.3.1 Methods

Ensembles were produced from samples of networks containing many different design architectures and training file conditioning. The full list of tested combinations is shown in Table 38.

Nodes/Noise Method/Noise Magnitude			
12/L/0-10	12/A/0-10	12-24/L/0	12/B/0-10
16/L/0-10	16/A/0-10	12-24/L/5	16/B/0-10
20/L/0-10	20/A/0-10	12-24/L/10	20/B/0-10
24/L/0-10	24/A/0-10	12-24/A/0	24/B/0-10
12-24/L/0-10	12-24/A/0-10	12-24/A/5	12-24/B/0-10
16-20/L/0-10	16-20/A/0-10	12-24/A/10	16-20/B/0-10
12/B/0	16/B/0	20/B/0	24/B/0
12/B/5	16/B/5	20/B/5	24/B/5
12/B/10	16/B/10	20/B/10	24/B/10
12-24/B/0	12-24/B/5	12-24/B/10	
16-20/B/0	16-20/B/5	16-20/B/10	

Table 38 - List of tested mixed origin ensembles. The table is divided into conceptually similar groups. Single node numbers mean all ensemble constituents have the same hidden neuron number. 12-24 means ensemble contains networks of 12/16/20/24 networks. A means absolute (constant) noise, L the linear noise model and B both noise models. The final term refers to the maximum magnitude of noise injection on the training file

Ensembles were created by building a larger database of the original constituent network sources from which a random sample of 100 networks was taken. The ensembles were assessed using the same technique in section 5.2.

6.3.2 Results

For clarity, only the 10 best performing mixed ensembles are shown in Table 39, along with a description of their design. They are statistically compared to the mean ensemble from section 4.2 using paired t-tests with a Bonferroni correction (revised to $p < 0.005$). The value of inter-ensemble variance calculated in Table 35 is used here.

Ensemble	Ensemble RMS % Error	Constituent RMS % Error	P Value
12-24/A/5	7.29	10.29	<0.0001*
12/A/0-10	7.31	10.52	<0.0001*
16/B/0-10	7.32	9.81	<0.0001*
12/B/0	7.32	10.14	<0.0001*
12-24/A/0	7.41	9.91	<0.0001*
16/B/10	7.45	9.60	0.0002*
12/B/10	7.47	10.18	0.0004*
12-24/B/0-10	7.54	9.80	0.0031*
12-24/A/0-10	7.54	10.10	0.0032*
12-24/B/0-10	7.60	9.78	0.0204

Table 39 - Mixed origin ensemble RMS errors. * indicates a statistically significant difference to the mean performing ensemble from section 4.2.

When ranks of mean constituent network accuracy and ensemble network error were compared with a Spearman's Rank, the calculated correlation was $\rho=-0.303$, hence there was a poor correlation between ensemble performance and mean constituent network performance.

6.3.3 Discussion

The construction of mixed groups of ensembles has some utility in the improvement of accuracy on test data. Results were significantly better than the average ensemble of networks of identical design. Although the best performing mixed ensemble showed improved accuracy over the best performing ensemble, this difference was small and not significant when the inter-ensemble variance was included.

The mean performance of constituent networks did not seem to be correlated to the overall performance of the ensemble. This is not therefore a reliable predictor of the eventual ability of the ensemble to produce a high quality load estimate.

There did not seem to be any particular feature of the ensemble construction that was associated with improved performance, with the exception of typically lower numbers of hidden neurons (in common with identically specified ensembles). To investigate the effect of

mixed ensembles further, a more sophisticated technique of controlling the variance of network training conditioning would be required.

6.4 Controlling constituent network parameters

In Chapter 2, it was suggested that in addition to the inherent variance in network solutions produced by training case generation and presentation, that varying the design and specification of constituent networks of an ensemble could also produce accuracy improvements. This section describes an attempt to create and evaluate systematic variance in the conditioning of data used to train the networks making up the ensemble.

6.4.1 Methods

In order to produce an improved generalisation performance of an individual network, noise injection on the training dataset has previously been conducted. However, an ensemble requires diversity of network design in order to provide sufficient coverage of the solution space in order to provide a useful aggregation of estimations. The magnitude of diversity has not been examined in this application previously.

To investigate this effect in a systemic manner, a tool was produced (code in appendix A20) to create various normal distributions of whole numbers of maximum noise injection percentage around a specified mean value and with a specified standard deviation. Validation of this is shown in Table 40.

Target (Mean, (SD))	Test Distribution Mean	Test Distribution Standard Deviation
5 (0)	5	0
5 (1)	4.93	1.01
5 (2)	5.09	1.92
5 (5)	5.08	5.81
5 (10)	5.16	10.11

Table 40 - Example distributions of various network specifications

This distribution of network specifications was then used to control the construction of datasets for network training, with each containing a particular architecture, and with the ensemble as a whole having a consistent and measurable distribution of training noise injection parameters.

In these tests, the instrumented socket described in Chapter 4 was used. Network parameters (with the exception of noise injection) were identical to those used in Chapter 5 with the same training end procedure.

Network performance was evaluated using a separately created set of superposition loads generated from a distinct set of measurements. In contrast to earlier work, this consisted of superposition cases only, rather than a mix of superposition and isolated loads. Although this is arguably a more realistic means of assessment, results are not directly comparable to previous work. Error in this study is likely to be around 2% lower than in section 6.2 – this was estimated by supplying an ensemble with a loading file of the type described earlier.

As described above, the noise injection average maximum magnitude was varied in this study in five values – centred on 0%, 5%, 10% 15% and 20%. The standard deviation of the distribution around this was set to 0 (i.e. identical maximum noise injection), 1, 2, 5 and 10. Due to the nature of noise injection, it is applied either side of the original value. 100 networks were trained for each ensemble, for a total of 2500.

6.4.2 Results

Results of RMS error for constituent networks are shown in Table 41, along with the standard deviation of each ensemble distribution. Results for each ensemble estimate, along with the percentile that the ensemble estimate would occupy in the group of constituent networks are included in Table 42. The percentile value is an evaluation of the relative effectiveness of using the ensemble. A low percentile value indicates that very few networks could be expected to outperform the ensemble. A higher percentile value means that the ensemble error is closer to the performance of an averagely performing single network. For statistical comparisons between ensembles and constituents, a Bonferroni correction was included to compensate for

the number of tests ($p < 0.002$, Table 43). The standard deviation of ensemble solutions was set to 0.16 using the estimate in section 6.2.

Mean (%)	Variation (%)									
	0		1		2		5		10	
0	5.45	(0.91)	5.32	(0.98)	5.17	(0.81)	5.09	(0.67)	5.13	(0.60)
5	5.04	(0.61)	5.10	(0.58)	5.02	(0.58)	5.22	(0.70)	5.00	(0.58)
10	5.05	(0.53)	5.11	(0.66)	4.94	(0.67)	5.06	(0.54)	4.94	(0.51)
15	4.93	(0.44)	4.87	(0.46)	4.78	(0.44)	4.95	(0.53)	4.87	(0.59)
20	4.71	(0.40)	4.81	(0.36)	4.76	(0.37)	4.72	(0.46)	4.75	(0.60)

Table 41 – RMS % error (SD) of the mean constituent network of each created ensemble

Mean (%)	Variation (%)									
	0		1		2		5		10	
0	3.91	(5.9)	3.86	(4.7)	3.95	(3.8)	4.12	(2.8)	4.32	(6.5)
5	4.21	(7.1)	4.33	(6.7)	4.47	(15.0)	4.30	(5.1)	4.26	(9.0)
10	4.36	(6.0)	4.47	(12.1)	4.26	(7.3)	4.42	(11.0)	4.21	(5.9)
15	4.41	(10.2)	4.37	(12.7)	4.27	(9.5)	4.42	(18.0)	4.14	(6.3)
20	4.28	(15.2)	4.38	(10.6)	4.31	(6.1)	4.23	(11.5)	4.19	(15.2)

Table 42 – RMS % error (percentile) of constructed ensembles. The second value indicates the percentile this ensemble would form within the group of constituents. In the absence of extensive repeatability measurement of ensembles, this figure represents the relative effectiveness of using an ensemble over an averagely performing network.

Mean	Variation				
	0	1	2	5	10
0	<0.0001*	<0.0001*	<0.0001*	<0.0001*	<0.0001*
5	<0.0001*	<0.0001*	0.0036	0.0001*	<0.0001*
10	<0.0001*	0.0029	0.0019*	0.0003*	<0.0001*
15	0.0002*	0.0009*	0.0004*	0.0026	0.0002*
20	0.0011*	0.0004*	0.0002*	0.0012*	0.0036

Table 43 - Calculated p values from paired t-test comparisons of each ensemble to the group of constituent networks. * indicates significance following correction

An ANOVA test was used to assess for any significant differences between different ensemble constructions: a post-hoc Tukey test was employed to identify the significant comparisons. The significance boundary was set to $p < 0.0000833$ due to the large number of comparisons made.

Group 1 (Mean %/Variation %)	Comparison (Mean %/Variation %)
(0/0)	(0/10)
(0/0)	(5/1)
(0/0)	(5/2)
(0/0)	(10/0)
(0/0)	(10/1)
(0/0)	(10/5)
(0/0)	(15/0)
(0/0)	(15/1)
(0/0)	(15/5)
(0/0)	(20/1)
(0/0)	(20/2)
(0/1)	(0/10)
(0/1)	(5/1)
(0/1)	(5/2)
(0/1)	(5/5)
(0/1)	(5/10)
(0/1)	(10/0)
(0/1)	(10/1)
(0/1)	(10/2)
(0/1)	(10/5)
(0/1)	(15/0)
(0/1)	(15/1)
(0/1)	(15/2)
(0/1)	(15/5)
(0/1)	(20/0)
(0/1)	(20/1)
(0/1)	(20/2)
(0/2)	(5/2)
(0/2)	(10/0)
(0/2)	(10/1)
(0/2)	(10/5)
(0/2)	(15/0)
(0/2)	(15/1)
(0/2)	(15/5)
(0/2)	(20/1)

Table 44 - Estimation of significant differences between constructed ensembles following an ANOVA test. Only significant differences following a multiple comparison correction are shown

In Table 44, significant differences between ensembles estimates were identified in several comparisons – in particular the very low noise configurations performed significantly better

than many of the higher noise set-ups. In all cases, the left configuration had lower error than those on the right. The greatest number of significant improvements was demonstrated by the ensemble with the lowest overall error: that with a standard deviation of 1 about a mean noise addition of 0%. None of the very low noise configurations were significantly better than each other.

6.4.3 Discussion

The use of variable specification training data in the production of neural networks has a significant impact on the accuracy of the ensemble. In addition to significant improvements over the mean constituent networks, ensembles with low noise and low variation demonstrated significantly better accuracy over those with higher mean maximum noise and larger variation.

This is thought to be because although networks that are trained with a high degree of noise contain excellent generalisation performance, and, on average, perform well on test data, they are also less able to precisely represent the underlying transfer function.

By removing the 'isolated' loads from the testing file, overall RMS error decreased, both for ensembles and for mean constituent networks. This would confirm the notion that this form of applied load is particularly poorly represented by both networks and ensembles without specific measures to counteract this.

By combining results into an ensemble, the requirements for generalisation on an individual network are reduced as the generalisation ability is adequately represented by the inter-network variation on the approximation of the transfer function. Noise injection reduces in utility as there seems to be sufficient variance in performance to produce an accurate estimate.

6.5 Critical appraisal of ensemble approach

As described in Chapter 4, numerous techniques for enhancing the performance of neural network ensembles exist within the literature (for example bagging, boosting and stacking). This thesis has focused on only one of these in detail: a form of bootstrap aggregation performed by forming new network training sets from the initial seed file, and constructing the

ensemble from the entirety of this group of trained networks. This technique was able to produce meaningful improvements both in accuracy and reliability of the final pressure measurement solution: however the potential for further development remains.

Including all networks of a particular configuration regardless of performance may be problematic. Performance tested using the training set is not a guarantee of success on real-world data. The particular nature of this problem, when large training sets are simulated from a small number of physical measurements means that the risk of producing a system that shows poor generalisation performance is somewhat higher. Although this can be mitigated to an extent by burying the poorly performing network under adequate networks, it remains unclear how well the ensemble's performance translates into genuine improvement on novel data.

An associated issue is that the ability of networks to accurately and reliably estimate loads when these are at the extremes of the measurement range is already known to be of lower quality. Ensembles that use a mean of all network estimates will be biased if these are not symmetrical about the target. This can be clearly observed in Figure 53: the pattern of estimates is systematically incorrect at extremes of the load range.

For these reasons, one of the recommendations for a future research direction is to investigate stacking as an approach to improve performance. The correction at this stage is somewhat more complex than the original bias, and so a neural network solution that is able to model the distribution of error across the ensemble is attractive. This would seem to have greater potential than techniques such as boosting as the performance of all networks is remarkably similar despite the larger scale differences observed at the level of individual loads. This suggests that whilst each network demonstrates reasonable performance as a whole, this masks the potential for occasional lapses in ability on particular load cases. Therefore techniques which attempt to control the learning process of subsequent networks may be less successful: the issue is not that networks fail to converge on solutions or that the overall performance is typically inadequate. Rather, the distribution of network solutions around targets is the source of some of the residual error, and this would be targeted by these techniques.

The results in section 6.2 appeared to show that varying the hidden neuron number had only a limited impact on overall ensemble accuracy. This is in some contrast to the results from individual networks in this work and from previous studies of similar applications (Amali et al. 2014). The work presented in section 6.3 suggests that this parameter was less critical than the noise injection value – possibly because the number of hidden neurons studies were all able to sufficiently characterise the transfer function with only minor differences in the average performance of networks.

One limitation of the work as presented is that the process of network generation included all networks that successfully completed training according to the pre-set parameters of performance. This process occasionally produced networks with unusually poor performance on the testing set. This is an issue for the clinical use of the tool as the error is not consistent across the load range, and hence professional users of the device would have greater difficulty in understanding and practically using such a system (Hafner and Sanders 2014).

Research exists which suggests that including all network estimates within the final suggested value may be undesirable (Zhou et al. 2002). Another method of aggregating the network estimates may prove to be superior.

Central to these discussions is the fact that the distribution of estimates from neural networks applied to this problem may not necessarily be symmetrically and normally distributed about the true value. The current implementation of an ensemble average has been relatively straightforward, and to see greater benefits, more sophisticated techniques may be required.

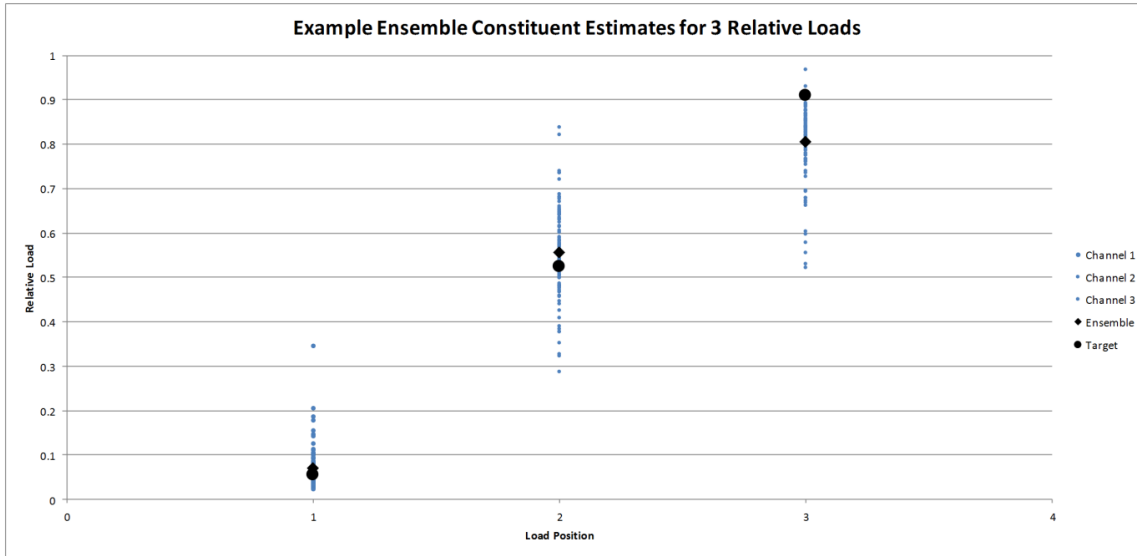


Figure 53 - Range of constituent network estimates for three examples loads across the load range. High loads are underestimated by the ensemble average, low loads overestimated. Loads in the midrange are typically best represented.

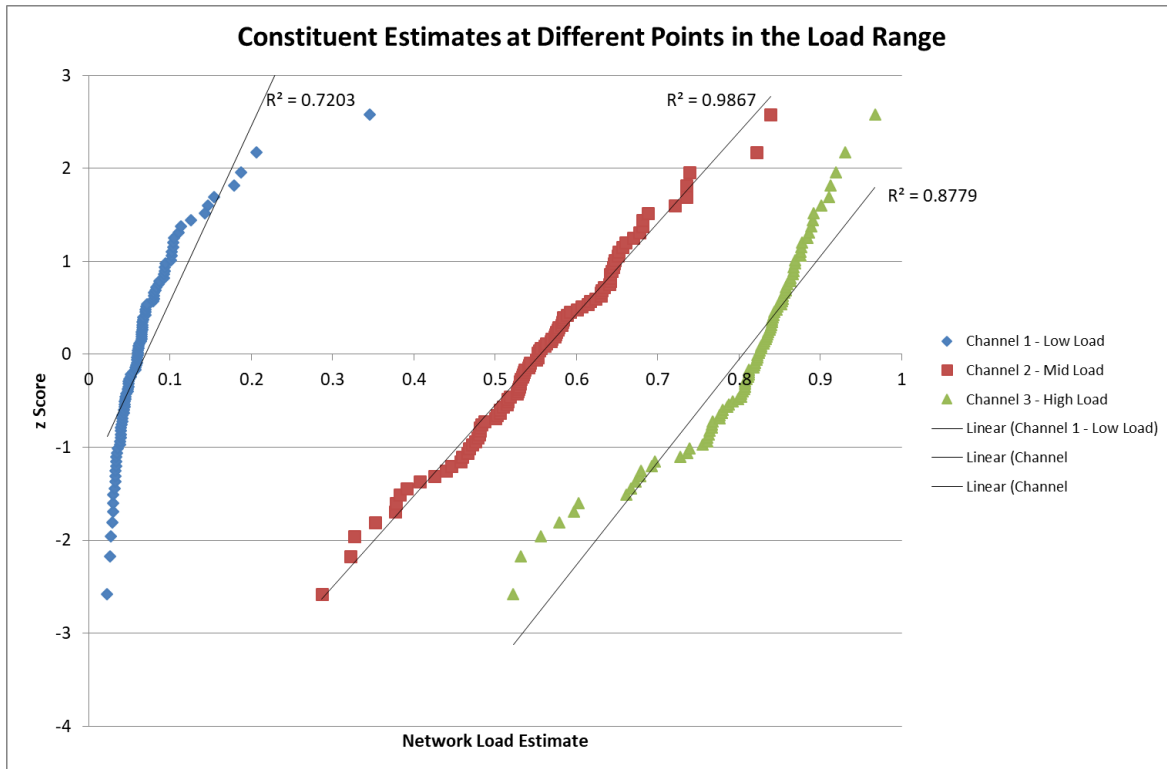


Figure 54 - Probability plots for constituent network estimates of an example low, medium and high relative loads, where each point is a single networks estimate of the load.

Figure 54 illustrates the deviation from the expected normal distribution for loads at different positions across the load spectrum. This particular example is from a selected load case where the first three loads are low, midrange and high respectively. The linear equations are typically well fitted in the mid-range with a high R^2 value, and poorer quality at the extremes.

6.6 Conclusions

Creating ensembles of neural networks is demonstrated to be a valuable technique even in the absence of optimisation of ensemble design. When tested on separate problem data, ensembles were up to 30% more accurate than the mean performing network within them. Furthermore, the chances of successfully training a better performing network were low – typically below 5%. It is therefore concluded that ensembles represent a suitable technique for improving both accuracy and reliability of estimates of load distribution on prosthetic sockets.

By varying the design parameters of training data conditioning applied to networks within ensembles, significant changes in network accuracy could be achieved. However, the patterns that exist in attempting to improve single network performance do not always correspond to improvements in ensemble accuracy: in particular lower noise and lower hidden neuron number ensembles performed better than those with higher values.

Ensembles of mixed specifications had the potential to perform better than those with identically specified networks. This was investigated with software to systematically control the variation of training data modification. This led to further improvement in system accuracy and reliability, with networks of relatively low noise injection performing best of all.

Some issues continue to exist with this implementation; in particular estimation error is not balanced symmetrically at all points in the load distribution, and this will contribute to error in the overall quality of the ensemble estimate. This is examined in Chapter 7.

In summary, ensembles provided a significant improvement in the accuracy and reliability of the neural network solution to measuring socket pressure. When presented with test data, ensembles provided solutions with reduced error and with lower variance than their corresponding constituents. In practice, this means that future implementations of this system

can be used with greater confidence that the output values are being accurately and reliably reported. Varying the constitution of the ensemble design can also yield improvements in this area, although within-network bias in the network solution remains.

Chapter 7 – Impact of constructing ensembles featuring a polynomial correction factor

7.1 Introduction

In Chapter 4, the design of the current and previous iterations of the inverse-problem socket measurement technique was described. One aspect that had been previously developed was the post-network estimate use of a correction factor to account for a systemic issue in the neural network solution of poor performance at measurement extremes. By fitting a polynomial function to the residual error, then when novel estimates are made, the estimate can be evaluated by the polynomial function to find a value for the direction and magnitude of residual error.

The principle of this correction has been demonstrated, but detail on functions fitting, the magnitude of improvement and the reliability of these functions were not reported. In Chapter 5, network configurations and the effect of data conditioning was explored on single networks. In Chapter 6, these networks were combined into ensembles, where the variance of networks around the target was used to produce a more accurate result. Although this produced a substantial improvement, poor performance at certain points was maintained due to the asymmetric distribution estimate error.

This chapter investigates the specification of polynomial functions for improving network performance and the impact of creating ensembles of networks which feature this correction method. The effect of including a second layer of correction to account for the remaining residual error is evaluated.

By improving the response of networks and ensembles at these points in the measurement range, consistency of the solution for clinical cases can be improved.

7.2 Evaluating polynomial function order

An example of the residual error for a single network's estimate of socket load across the measurement range for one output position is shown in Figure 55. This figure was produced by supplying the trained network with the superposition training cases, and evaluating the difference between the network estimate and the target in an example channel. This example case is representative of other measurement channels, but the specifics of the error distribution pattern will vary in magnitude and shape between different load channels and network solutions, meaning that correction functions must be calculated anew for each network channel.

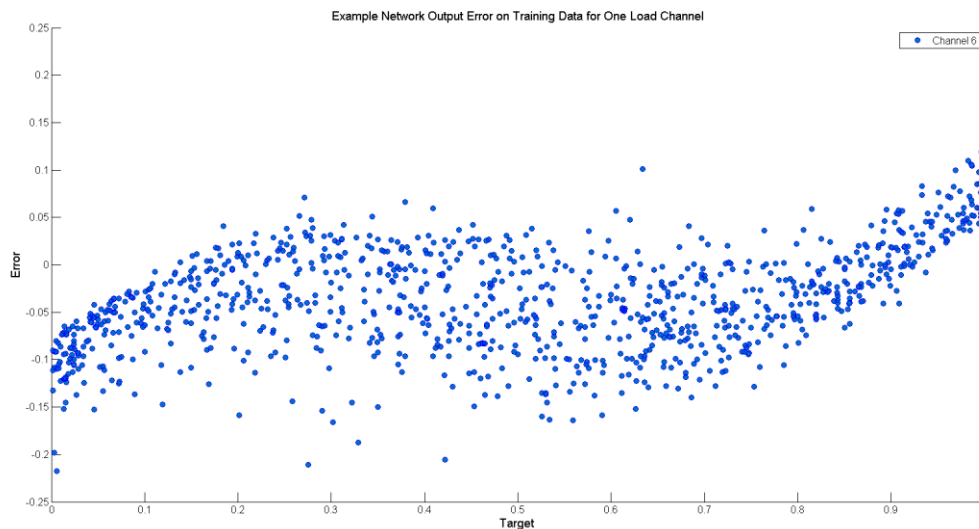


Figure 55 - Residual network error on an example channel from a single network. In this figure, a perfect network solution would lie on the x-axis: a consistent minimal error across all possible load outputs.

In this subsection, the effect of varying the correction function calculation on the RMS % error of a network solution is calculated. This is intended to provide a quantitative estimate of the improvement in accuracy of the load estimate that is produced by the system, and what effect changes in the design of the correction can induce.

7.2.1 Methodology

As described in Chapter 2, the form of error seen in Figure 55 is common to each output channel and has been observed in each instance of the socket measurement via neural network system (Sewell et al. 2010, 2012).

Multiple functions can be fitted to this data, with more or less success. In this work, the order of the polynomial function was evaluated between 3 and 9. Examples of these curves are shown in Figure 56. Polynomial fits are created using the *'polyfit'* function in MATLAB, and evaluated with the *'polyval'* function.

Polynomial functions of order 1 and 2 are neglected in this analysis. A simple visual inspection of the error distribution shows that a linear or parabolic curve will not suitably model the required function.

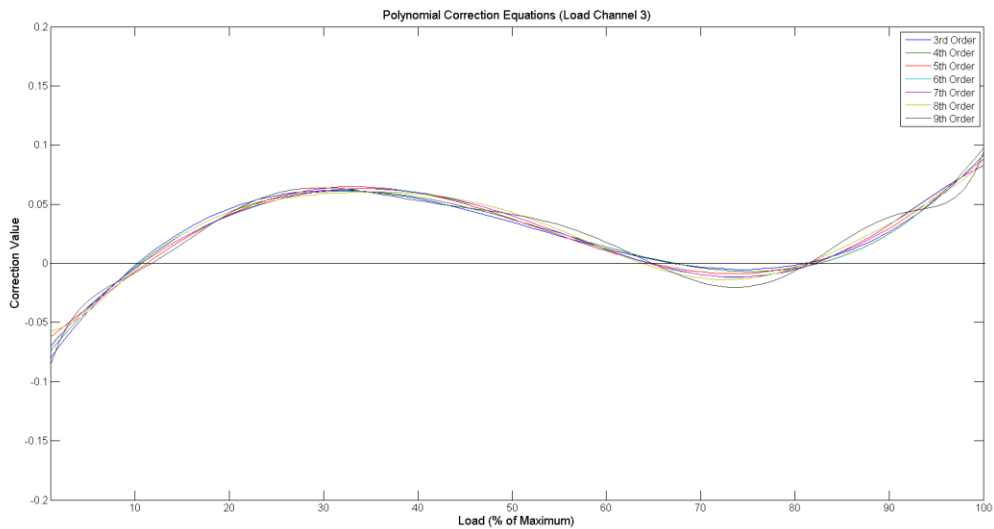


Figure 56 - Example polynomial correction factors of varying order as fitted to the example channel shown in figure 47.

The impact of the polynomial function was evaluated by supplying the function with the training data, applying the factor to the network estimates and re-evaluating the overall RMS % error. Thus, the improvement of each specification of network correction could be quantified, and the best performing correction factor selected for use in future applications of data and used to modify subsequent output.

To evaluate the performance on a group of diverse networks, a group of 100 networks with the parameters specified in Table 45 were trained, the outputs used to create a range of

polynomial correction factors, and the best performing of these on the training data used to condition the response of the networks when they were subjected to a test set of superposition data generated from a distinct seed file.

Parameter	Value
Architecture	Feedforward-Backpropagation
Learning Algorithm	Levenberg-Marquardt
Neurons	11-16-8
Transfer Function	Poslin-Tansig
Networks Trained per group	100
Training noise injection technique	Linear
Training noise injection pattern	Average magnitude 1, standard deviation 2
Superposition Training Cases	1000
'Isolated' Training Cases	400
Training target	0.01
Maximum epochs	100
Maximum validation checks	6
Polynomial correction orders	3 rd -9 th
Test Superposition Cases	1000

Table 45 - Neural network training parameters used throughout this chapter

7.2.2 Results

Figure 57 shows the performance of the group of networks on the test cases, expressed as the RMS% error. Results are also tabulated with the original error, the error following correction and the distribution of these (Table 46).

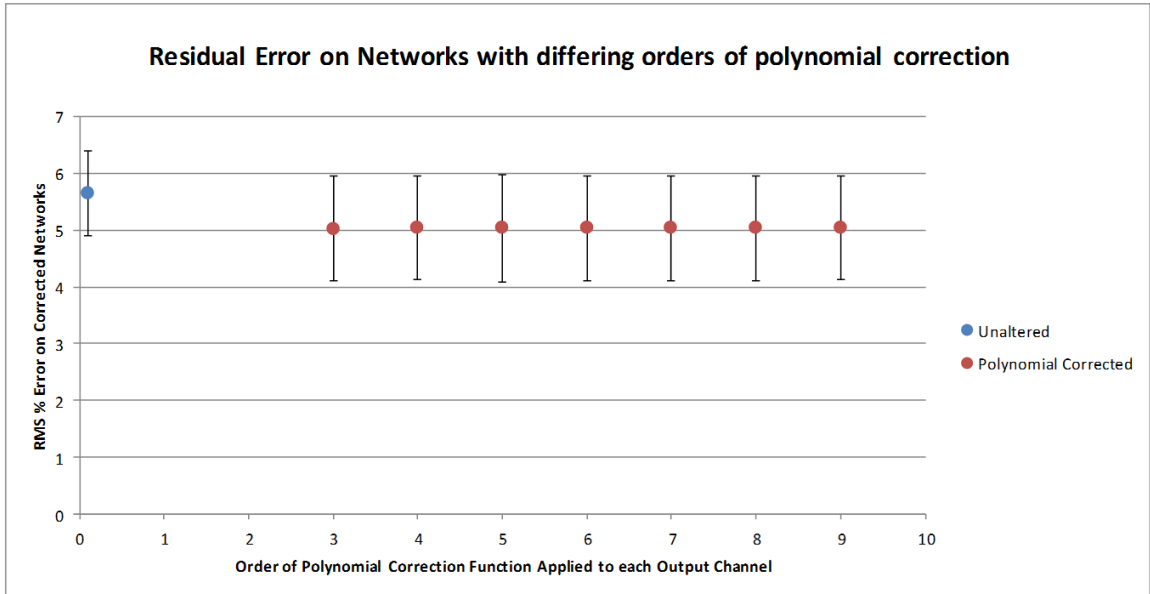


Figure 57 - The effect on networks of using polynomial correction factors of various orders, as compared to the matching uncorrected networks

Correction Method	RMS% Error	Standard Deviation
Uncorrected	5.638	0.743
3 rd	5.029	0.916
4 th	5.032	0.910
5 th	5.034	0.940
6 th	5.028	0.913
7 th	5.029	0.917
8 th	5.034	0.917
9 th	5.031	0.908
'Best Performing'	5.031	0.908

Table 46 - Effect of polynomial correction on a group of networks using different orders of polynomial function. Also shown is the effect of using the best performing polynomial as assessed on the training file.

Normality was confirmed using a Kolmogorov-Smirnoff test ($p < 0.130$), with the probability plot of overall RMS percentage error on corrected networks shown in Figure 58. A paired t-test compared corrected with uncorrected networks, identifying that a significant improvement was made in all cases of polynomial correction order (Table 47). A final test was made between the best performing group of networks using a single order of polynomial correction function and

software that enabled the network evaluation process to select the best performing correction factor: as no significant difference was found, this configuration was used in subsequent analyses (Figure 59).

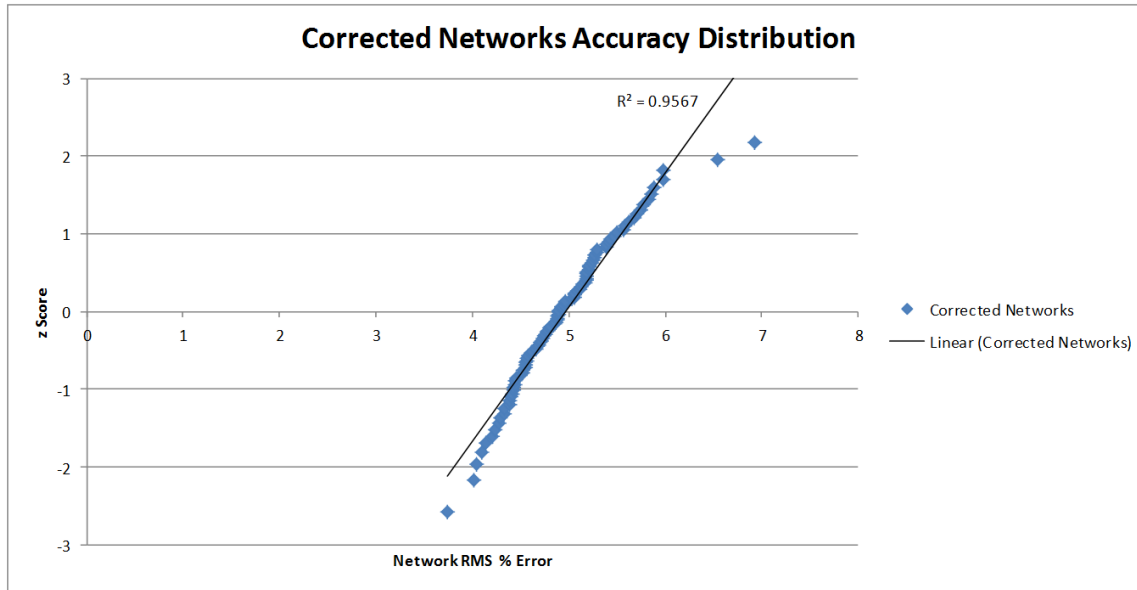


Figure 58 - Probability plot of corrected networks error on test data, demonstrating a normal distribution

Comparison	Maximum Order Polynomial Correction	P value, Paired t-test comparison
Uncorrected	3 rd	P<0.001
Uncorrected	4 th	P<0.001
Uncorrected	5 th	P<0.001
Uncorrected	6 th	P<0.001
Uncorrected	7 th	P<0.001
Uncorrected	8 th	P<0.001
Uncorrected	9 th	P<0.001
Uncorrected	Best Performing	P<0.001
6 th Order	Best Performing	0.979

Table 47 - Statistical calculations comparing polynomial corrected groups of networks with different order correction functions. Also shown is the comparison between the best performing single order network and those assessed as best performing on training data.

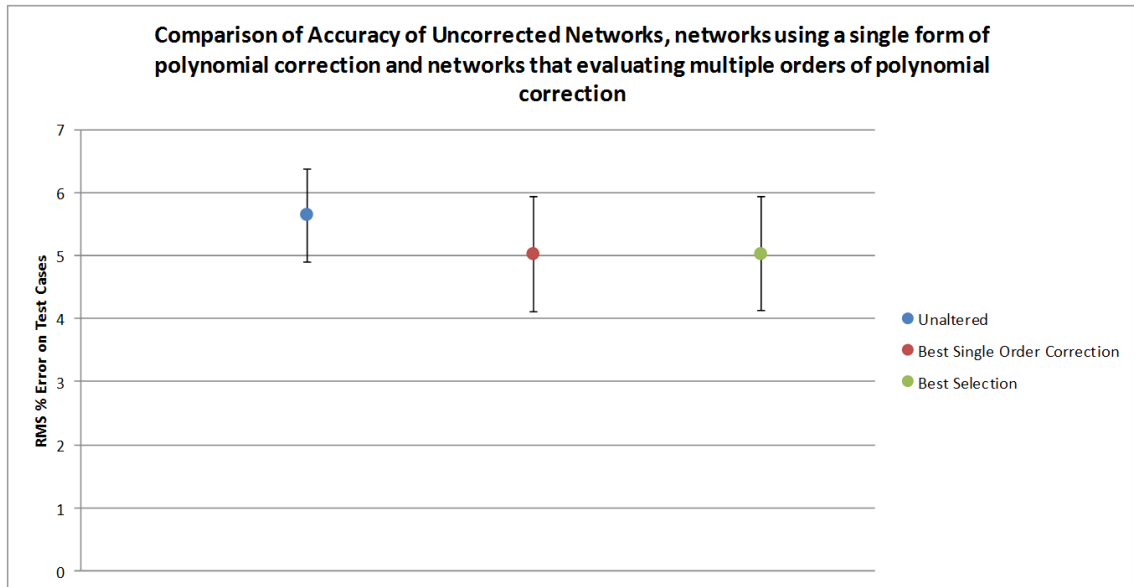


Figure 59 - The effect on RMS error of including polynomial correction and of correcting networks with the best fit function on training data

Finally, the pattern of errors and their distribution was investigated: the average difference from a corrected and uncorrected example channel is shown in Table 48.

Type	Average Difference	Standard Deviation
Uncorrected	5.50%	0.30
Corrected	1.19%	0.14

Table 48 - Example of the effect on accuracy on an example output channel

7.2.3 Discussion

Polynomial correction factors had a significant positive effect on the accuracy of trained networks. By evaluating an at-least 3rd order polynomial equation obtained by resubmitting the training data to the completed network on new data, a reduction in error equivalent to 10% of the residual error could be achieved. Although overall accuracy improved, this was at the cost of a slight increase in the inter-network variance.

Varying the order of polynomial function used to characterise the network residual error did not yield any change in overall performance. Higher order functions have a greater capability to

match the complexity of the network error: however it appears that these are adequately modelled with a 3rd order function. Further improvement in the performance of the mean network in each group was minimal, and insignificant when the inter-network variance was taken into account. It remains unclear how well this conclusion withstands alterations to the training file in use: therefore a system which can evaluate the performance of multiple functions and selected the best performing was implemented.

The typical error was more symmetrically distributed around the target value. This suggests that incorporating the polynomial correction factor into the construction of ensembles of networks would produce a further improvement which would act to mitigate the intrinsic bias of results away from the target value.

One aspect of concern is the performance on outliers in the estimate pattern. It can be observed that in regions of the load range where a typically good network performance is assumed (i.e. midrange) there are occasionally high errors predicted. These are then exacerbated by the polynomial equation, as these fall outside the typical error distribution and are not well accounted for by the correction factor. Therefore, although in general performance is improved, this masks occasional unreliability. This can be substantially corrected for using an ensemble of sufficient size: alternative networks are unlikely to experience errors in precisely the same position, and the combination of estimates will reduce the leverage of this data point.

As a result of this, the next step in this section is the investigation of the effect of constructing ensembles from networks which include a polynomial correction factor.

7.3 Ensembles with polynomial correction

In section 7.2, an analysis of the impact of a polynomial correction factor to correct for systematic error in the load estimates of a neural network was completed. The results suggest that in addition to an improvement in the average accuracy, the produced distribution of estimates may also be more suitable for aggregation within an ensemble across the load distribution range.

In this section, the effects of creating ensembles from networks containing post-estimate conditioning using polynomial functions representing residual network error are examined. The aim is to identify whether this is a suitable technique for improving the accuracy and reliability of the socket load measurement device. This can confirm if these techniques maintain the utility demonstrated in section 7.2 when the networks estimates are combined into ensembles.

Following the work in Chapter 6, the differences in networks constructed with varying levels of noise injection on the training cases when these are combined with the polynomial correction and into an ensemble are tested.

7.3.1 Methodology

The same process for creating trained networks used in section 7.2 was replicated in this study. Networks were trained using a normal distribution of 100 values of maximum noise injection with an average value of zero and a distribution set by the standard deviation values in Table 49. The linear noise injection method was used. Polynomial equations were created by resupplying the training data to the network once training was complete and plotting the difference between the target and estimate against the target distribution to get an estimate of the pattern of residual errors. The best performing polynomial function on each load estimate channel and each network was used to alter the output when producing subsequent estimates.

Title	Description
A0D0	Average injection 0% of maximum, standard deviation of 0%
A0D1	Average injection 0% of maximum, standard deviation of 1%
A0D2	Average injection 0% of maximum, standard deviation of 2%
A0D5	Average injection 0% of maximum, standard deviation of 5%
A0D10	Average injection 0% of maximum, standard deviation of 10%

Table 49 - Description of the specification of ensembles

Networks were assessed using a separately collected seed file that was used to create 1000 superposition load cases. The overall RMS error expressed as a percentage of the total applied load was used to compare the performance of networks.

Networks were combined into ensembles by performing a simple average of each load estimate produced by the group of networks in each ensemble. Results for constituent networks, constituent networks featuring polynomial correction and ensembles of these were produced.

7.3.2 Results

The mean and standard deviation of the constituent networks with and without polynomial correction are shown in Figure 60 and Table 50. Networks featuring correction were compared to those without using paired t-tests. Each comparison was regarded as significant, following a Bonferroni correction to the p value boundary to 0.01. An evaluation of 10 identically specified networks featuring polynomial correction found that inter-ensemble variance in RMS % error was estimated at 0.126 (as compared to the uncorrected ensemble standard deviation in RMS % error of 0.160). A probability plot confirmed the use of parametric statistics.

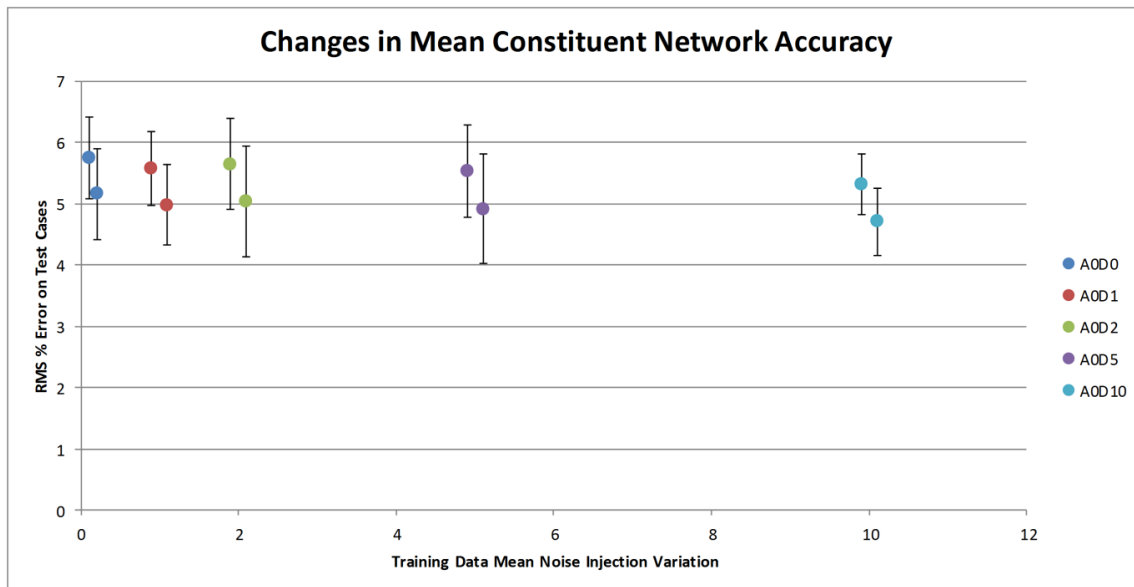


Figure 60 - Alterations in mean constituent network accuracy with alterations in variance of maximum noise injection variance. The first point in each coloured pair is the uncorrected group, the second the matching corrected group

Group	Uncorrected (RMS % Error)		Corrected (RMS % Error)		Statistical Evaluation
	Mean	SD	Mean	SD	
A0D0	5.740	0.664	5.156	0.740	p<0.0001
A0D1	5.568	0.599	4.975	0.656	p<0.0001
A0D2	5.638	0.743	5.031	0.908	p<0.0001
A0D5	5.531	0.749	4.915	0.888	p<0.0001
A0D10	5.313	0.491	4.701	0.550	p<0.0001

Table 50 - Uncorrected and Corrected network accuracy on test data

The comparisons between corrected/uncorrected ensembles and their constituents are shown in Figure 61, and tabulated in Table 51. Results were evaluated statistically using unpaired t-tests (after normal distributions of values had been confirmed), shown in Table 51. The significance boundary was revised to 0.0033.

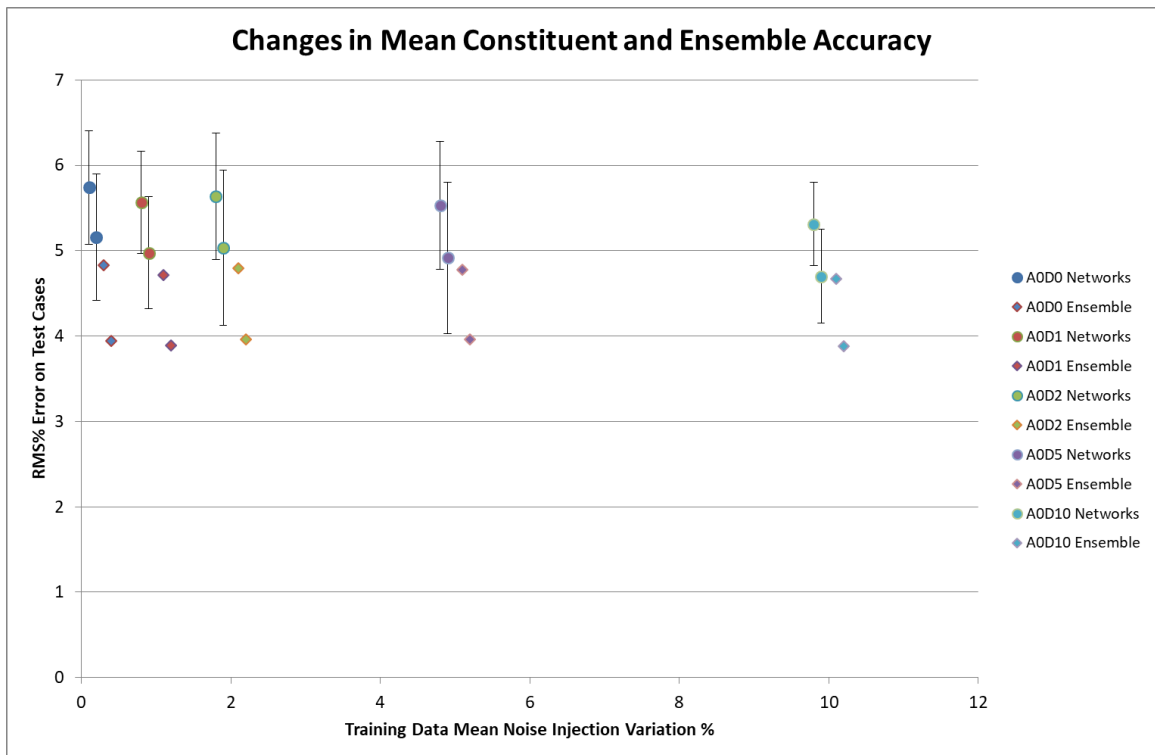


Figure 61 - Alterations in mean group accuracy with alterations in variance of maximum noise injection. The first circle in each pair represents the uncorrected network group, the second circle the corrected network group. The first diamond is the performance of the ensemble constructed from the uncorrected group, the second diamond the ensemble from the corrected group.

Group	Uncorrected Networks		Corrected Networks		Uncorrected Ensemble		Corrected Ensemble	
	(RMS % Error)		(RMS % Error)		(RMS % Error)		(RMS % Error)	
	Mean	SD	Mean	SD	Value	SD (Est)	Value	SD (Est)
A0D0	5.740	0.664	5.156	0.740	4.827	0.160	3.946	0.126
A0D1	5.568	0.599	4.975	0.656	4.711	0.160	3.894	0.126
A0D2	5.638	0.743	5.031	0.908	4.795	0.160	3.959	0.126
A0D5	5.531	0.749	4.915	0.888	4.773	0.160	3.958	0.126
A0D10	5.313	0.491	4.701	0.550	4.674	0.160	3.877	0.126

Table 51 - Uncorrected and corrected network accuracy and the accuracy of ensembles created from these networks

Comparison Group 1	Comparison Group 2	Significance Value
A0D0 Uncorrected Networks	A0D0 Uncorrected Ensemble	p<0.0001
A0D1 Uncorrected Networks	A0D0 Uncorrected Ensemble	P<0.0001
A0D2 Uncorrected Networks	A0D0 Uncorrected Ensemble	P=0.0005
A0D5 Uncorrected Networks	A0D0 Uncorrected Ensemble	P=0.0019
A0D10 Uncorrected Networks	A0D10 Uncorrected Ensemble	P<0.0001
A0D0 Corrected Networks	A0D0 Corrected Ensemble	P<0.0001
A0D1 Corrected Networks	A0D1 Corrected Ensemble	P<0.0001
A0D2 Corrected Networks	A0D2 Corrected Ensemble	P=0.0003
A0D5 Corrected Networks	A0D5 Corrected Ensemble	P=0.0010
A0D10 Corrected Networks	A0D10 Corrected Ensemble	P<0.0001
A0D0 Uncorrected Ensemble	A0D0 Corrected Ensemble	P<0.0001
A0D1 Uncorrected Ensemble	A0D1 Corrected Ensemble	P<0.0001
A0D2 Uncorrected Ensemble	A0D2 Corrected Ensemble	P<0.0001
A0D5 Uncorrected Ensemble	A0D5 Corrected Ensemble	P<0.0001
A0D10 Uncorrected Ensemble	A0D10 Corrected Ensemble	P<0.0001

Table 52 - Results of t-tests comparing various specifications of networks and ensembles

In all cases, groups of corrected networks performed significantly better on unseen data than on their matched uncorrected networks. The work described in Chapter 6 was confirmed in this study in as much that ensembles of uncorrected networks were significantly more accurate

than the mean performance of their constituent networks. Furthermore, when correction was introduced, this relationship was maintained, with corrected ensembles significantly better than their corrected constituent networks. Finally, corrected ensembles were significantly better than their uncorrected counterparts for all network conditioning configurations tested.

To check for significant changes in accuracy between designs of ensemble, an ANOVA test was carried out comparing the different noise injection variance ensemble specifications (i.e. the ensembles specified in Table 49). The result of this test was a $p=0.194$ for uncorrected ensembles. When corrected ensembles were tested in the same way, $p=0.463$. Therefore altering the magnitude of noise injection did not create a significant change in accuracy on this test data.

7.3.3 Discussion

The construction of ensembles from networks including a polynomial correction factor is supported by these results. In addition to the expected result that polynomial correction produced an improvement on an individual network basis, these improvements persisted when networks were combined into ensembles.

The effect of combining uncorrected networks into uncorrected ensembles produced, on average, a 14% reduction in residual error. When corrected networks were used to form corrected ensembles, this improvement increased to an average of 21%. The average combined effect of including both forms of correction was 29%. Although the magnitude of the combined improvement rose with the introduction of noise injection, changes in the scale of this improvement did not reach significance.

The reason for the residual error indicated may be that the specification of the correction factor is partially incorrect. The perfect correction factor would be chosen by the 'true' value of the load: this is inaccurately placed by the inherent pattern of error in each neural network output channel, meaning that the correction specified by the fitted polynomial function is also inadequate. As in reality the system can only use estimated loads as the basis for an evaluation of the appropriate correction factor, an additional error will remain.

For example – one case of load distribution may specify a high load on one particular output channel. This value is typically underestimated by the trained network (for example the right hand side of Figure 55), and shifted left towards the lower end of the load range. The correction factor is specified by this value – and so is misapplied by not including a sufficiently high correction as would be required by the fitted residual error function. Therefore, although the ensemble can correct for outlying errors effectively, there remains a residual error broadly common to each network solution that is not accounted for.

One possibility of reducing this error is to perform a second level of polynomial correction once the ensemble has been created. This has the advantage of values submitted to the polynomial correction function being closer to the target values and being distributed more effectively around the target. Therefore at the extremes of the measurement range, performance may improve further. An investigation into this approach is described in section 7.4.

7.4 Second level polynomial correction

In order to attempt to remove remaining residual error present in the group of neural network estimates, a second stage of polynomial correction applied to the ensemble estimate is investigated. In section 7.3, improvement in ensemble accuracy when constituent networks utilised a polynomial correction function on each networks output channels was confirmed, however a remaining residual error was present.

In this section, modelling the remaining error at the ensemble stage by supplying the ensemble with the network training data and fitting a second level of polynomial correction is trialled. The effect this has on superposition test data is evaluated. This will demonstrate if a valuable reduction in residual error can be produced, potentially creating a more accurate representation of the load distribution.

7.4.1 Methodology

The ensembles of networks created for section 7.3 were resupplied with the superposition training cases used to train the original constituent networks. After the ensemble average (produced from networks using the primary polynomial correction) had been generated, it was compared to the target data, and the residual error plotted against the target loads was used

to produce new polynomial equations to further alter the estimates. The best-performing polynomial functions were preserved.

To evaluate performance, the test data created from a distinct seed file (as used in throughout this chapter) was supplied to the network and compared to the target data. Performance across the test file was calculated as the percentage RMS difference between estimates and targets.

An example of a 2nd level ensemble polynomial function is shown in Figure 62.

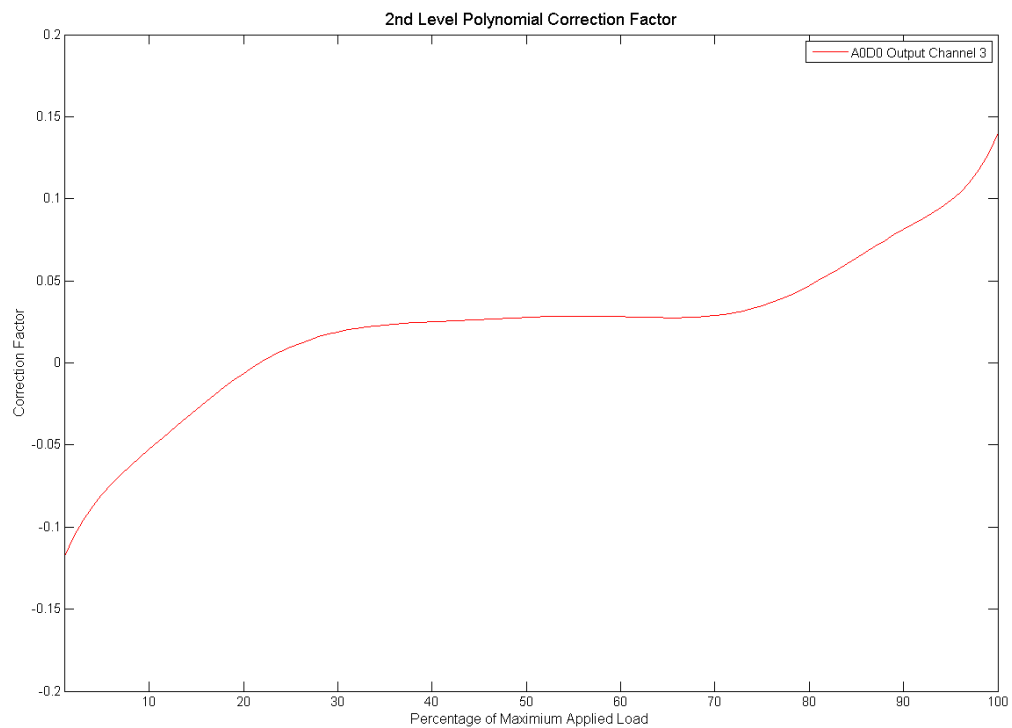


Figure 62 - An example of a 2nd stage correction polynomial function. This is taken from the 3rd output channel, and the A0D0 ensemble.

7.4.2 Results

The performance of each stage of network correction is shown in Table 53, with values representing test case accuracy and range of the constituent networks, ensembles and those featuring correction. These ensembles correspond to those with changes in noise injection investigated in section 7.3.

Group	Mean Constituent (RMS % Error)	Mean Constituent Corrected (RMS % Error)	Ensemble Constituent corrected (RMS % Error)	Ensemble (2 nd Stage Correction) (RMS % Error)
A0D0	5.74	5.16	4.83	25.95
A0D1	5.57	4.98	4.71	24.40
A0D2	5.64	5.03	4.80	24.60
A0D5	5.53	4.92	4.77	27.62
A0D10	5.31	4.70	4.67	27.03

Table 53 - Network and ensemble accuracy on test data including 2nd stage polynomial correction

Use of the second stage correction produced poorer quality load estimate in all cases.

7.4.3 Discussion

Although it had been hoped that including a second level of correction aimed at correcting for residual error at the level of the ensemble estimate would improve accuracy on test data, this did not prove to be the case. Ensembles of this design were significantly poorer in estimate quality when assessed with the test file.

As expected, the 2nd stage correction applied a greater correction at the extremes of the measurement range (where residual error persists) and flat and equivalent to a low relative change in the midrange. However, this was not able to meaningfully improve values on the test case.

The performance of the 2nd level corrected ensemble was marginally better than the ensemble without this feature on values close to the target: however, as before with the single stage correction on constituent networks, the performance on values with a higher residual error were substantially poorer. As before, the error at the extremes of the measurement range was substantially further than the target values.

The reason for this poor performance is potentially due to the differences between the relationships established in the training data differing from the network error observed in the test data. Therefore, although the single layer correction corrects well for broad inaccuracy in the solution, a second layer is too specific to the training data.

An alternative interpretation is that the 2nd layer correction provides much poorer performance on outliers in the test data. The majority of patterns are treated adequately by the correction factor, but many lie further from the curve and are not correctly altered. A second factor exaggerates this effect, reducing overall accuracy further as the impact on typical cases is generally small.

Due to the lack of improvement, the 2nd stage correction technique was not pursued further.

7.5 Critical Appraisal

The choice to use polynomial equations was based on the experience of using these in previous applications, and a visual examination of the residual errors on channels from pilot networks. The results presented in this chapter demonstrate that these equations have very little difference in performance, with only very small changes in the modelled equation evident with the use of higher order functions. Polynomial functions have the advantage of being straightforward to understand and apply to the problem data, which may be a positive factor in a tool to be used in clinical situations. However it remains that other function types may provide superior performance if these are better able to correct for errors in test data rather than repeated analysis of the training data.

This forms the largest drawback in the use of this technique – that the network error on training data differs from the response to test data. The approach used in this chapter mimics what is likely to be possible in practical use of the system – as there are unlikely to be repeated measures with known target values; the generalised system performance has to be estimated from the training data only. As a well-converged network will naturally be capable of providing accurate results on the data used to train it, the system lacks the capability of successfully accommodating substantially novel data: an issue that is common to all artificial intelligence applications.

As in previous chapters, the combination of results into ensembles provided a further boost to error reduction. Ensembles of networks featuring polynomial correction performed substantially better than uncorrected ensembles.

As mentioned in section 7.3.3, the value of the polynomial correction factor is in truth evaluated at the wrong position reducing effectiveness. However, the use of a second stage correction at the level of the ensemble estimate provided an emphatically poorer load estimate. This may be due in part to the effect of poor performance on outlying estimates which do not conform well to the modelled error distribution. As shown in Figure 55, the width of the error band in the midrange is fairly broad. The correction to the estimate is therefore small at these points, but is applied to all values, regardless of appropriateness. A more sophisticated model may incorporate limited application of the correction factor to only certain points of the load range. This would mitigate the unnecessary alteration of values at portions of the estimate distribution. However it would not be successful in improving performance on outliers.

One technique to improve this may be to use stacking – the implementation of a second neural network which can provide a more complex, potentially non-linear combination of the constituent networks into an overall estimate (Wolpert 1992).

7.6 Summary

In the conclusion to Chapter 6, the use of ensembles of networks was indicated by the analysis of network performance on simulated load distribution from distinct seed data. However, an analysis of the patterns of residual error in individual networks and across ensembles demonstrated that systematic error arises from the estimation of loads via neural networks.

Work prior to this thesis identified that modelling residual error on each output channel was a feasible method of overcoming this error; however the implementation of this had not been studied in detail. The effect of varying the order of the polynomial functions used to model error was examined. Although higher order functions produced greater improvements in error correction than lower order values, this did not reach significance when applied to test data.

When ensembles were constructed from networks featuring this correction method, the results improved further. In addition to the expected result of ensembles performing better than their mean constituent, corrected ensembles performed better than ensembles without this factor. Altering ensemble construction did not appear to generate meaningful improvement.

Finally, the process of utilising a second stage polynomial correction at the level of the ensemble estimate was examined. This did not improve results: this was thought to be due to the poorer representation of the error function on test data and the amplification of errors on outlier data.

The results in this chapter demonstrate the utility of the polynomial correction factor within this application, and the improvement possible when applied as part of a network ensemble. This provides further evidence for the improved accuracy, consistency and confidence in results that can be placed in the implementation described in this thesis.

In following chapters, the lessons learned from the design of networks and network ensembles on test data are examined on experimental measures of prosthetic socket loads from amputee participants. Chapters 8 and 9 the application of these networks to static, dynamic and perturbed loading.

Chapter 8 – Static and dynamic measures of prosthetic socket load

8.1 Introduction

Chapters 5-7 described attempts to evaluate and improve the accuracy and variation in the training and use of neural network socket load estimation – by controlling the conditioning of the training data, by combining network estimates into ensembles and by altering the post-processing of estimates. The tuning of these parameters generated significant improvements in the performance of the system when tested with simulated socket loads. In chapter 4, the development of a testing methodology for evaluating performance on loads from amputee volunteers was discussed. At the beginning of Chapter 5, mean solution accuracy was around 10.4%: by the conclusion of Chapter 7, accuracy of 5.8% was possible.

In this chapter, the estimates of load distribution during standing, varied application of bodyweight and during walking at comfortable speeds are reported. Here, these are carried out using a prosthesis configuration considered optimal by the participants and an experienced prosthetist: this will be modified as part of chapter 8. The biomechanical plausibility of the load estimates is considered, as well as the effect on results from the use of ensembles and polynomial correction.

As measurements were taken with two amputee participants across up to three sessions each, this facilitates measurements of inter-session variance and the relative contributions to this from different networks, walking trials and measurement sessions. This in turn provides justification for the use of ensembles of networks within this application.

The results from this work inform the practical use of the neural network system – in addition to the discussion of the use in perturbed measurement states described in Chapter 9, the experiences from these measurement sessions informs the critical evaluation that follows that chapter.

The work presented in this chapter represents the first instance of a neural network socket load system being applied to more than one participant, and to a participant across more than

one measurement session. It also includes the first measurements to report in detail dynamic measures of walking with a system of this type.

8.2 Static measurements – equal weight bearing

The purpose of this set of tests was to evaluate the capability of the developed system to reliably quantify the total force being applied through the socket interface. This was achieved using a test where each participant stood with roughly equal body weight being borne by the amputated and intact limbs.

8.2.1 Methodology

Participants were asked to stand with their prosthetic limb on the force platform in the centre of the measurement space, with weight roughly equally borne between the amputated and intact sides. Recordings were made of quiet standing for 3-4 seconds, and values taken from the force plate averaged over this time. Socket strains were recorded, submitted to networks trained to those structures, and the ensemble average of 100 trained networks used to create a similar over-time average of steady state load distribution.

In all socket load measurements conducted in this chapter, the results are reported as relative loads. In order to scale the input data effectively, the range of change in strain voltage should be assessed. The training load was multiplied in order to match this anticipated range (with the same scaling factor applied to all load positions). Thus during practical measurements, the loads calculated by the neural network are expressed relative to the maximum that is experienced in the socket.

The purpose of this section is to investigate the inter-session consistency of load estimates, and the differences between participant loads.

8.2.2 Results

The notation described in Table 54 is used to refer to different measurement sessions.

Participant 1 took part in three measurement tests split across two dates and participant 2 in one session.

Participant	Session	Test	Notation
1	1	a	P1S1a
1	1	b	P1S1b
1	2	(a)	P1S2
2	1	(a)	P2S1

Table 54 - Test notation description.

The ground reaction force (N) for equal standing as measured by the force platform are shown in Figure 63 and Table 55.

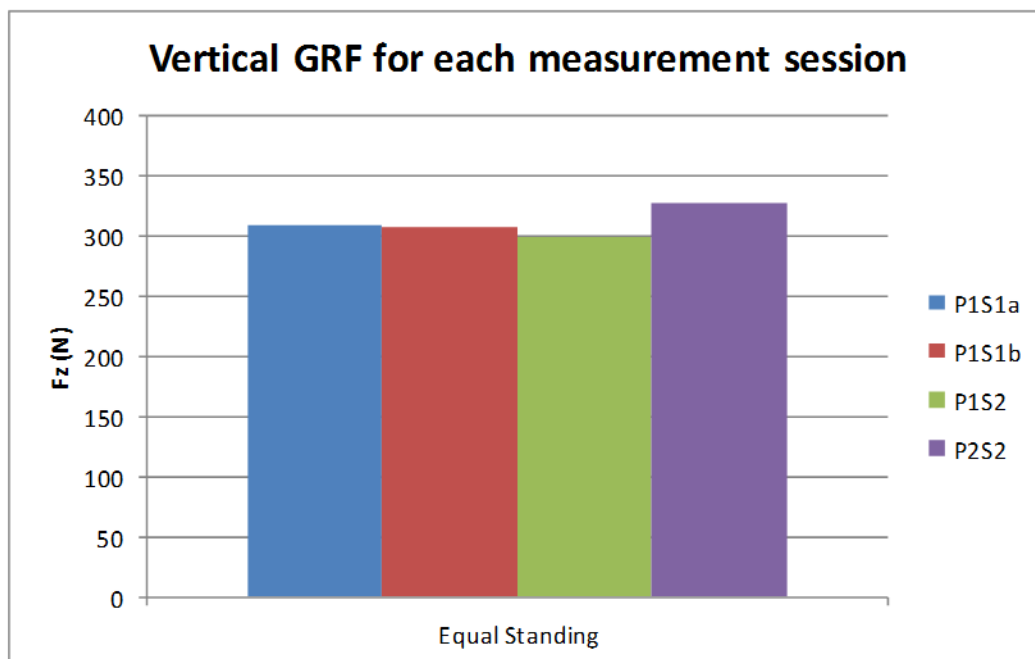


Figure 63 - Vertical ground reaction force recorded from the participant standing with the prosthetic limb on a force platform, following instruction to stand with weight evenly distributed

Session	Mean Fz recorded	% Bodyweight
P1S1a	310	48.6
P1S1b	308	48.3
P1S2	299	46.9
P2S1	328	49.7

Table 55 - Mean vertical force component recorded over 3-4 seconds of quiet standing. Also shown is proportion of bodyweight this represents for each participant

The values of socket load as measured by the socket loading system are shown in Figure 64 and Figure 65, and tabulated in Table 56.

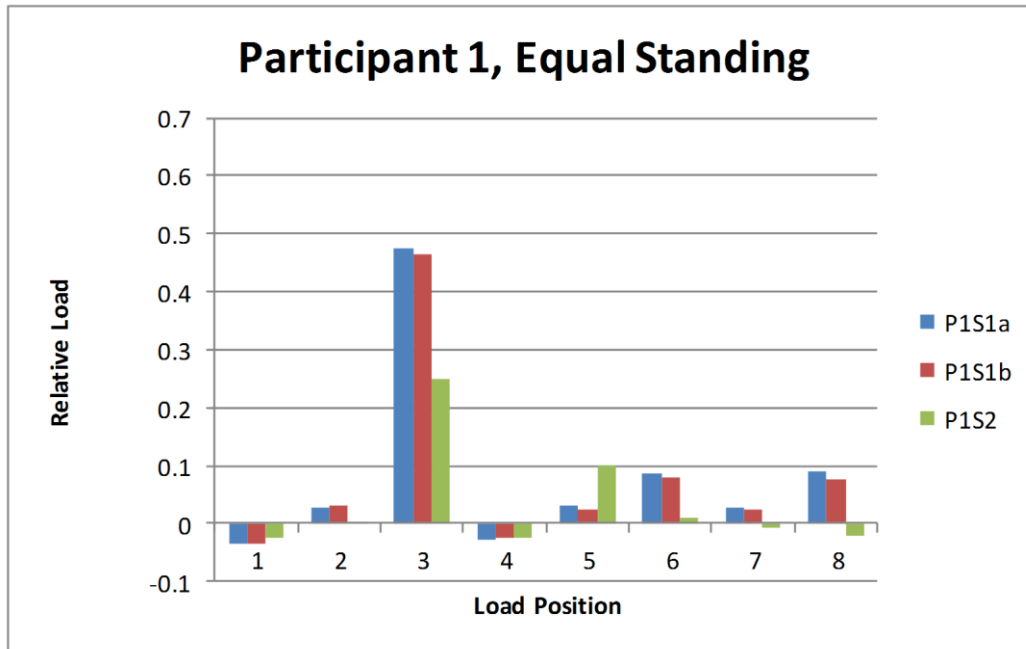


Figure 64 - Participant 1 socket load distributions for each test session, from ensemble estimate of 3-4 seconds of even standing

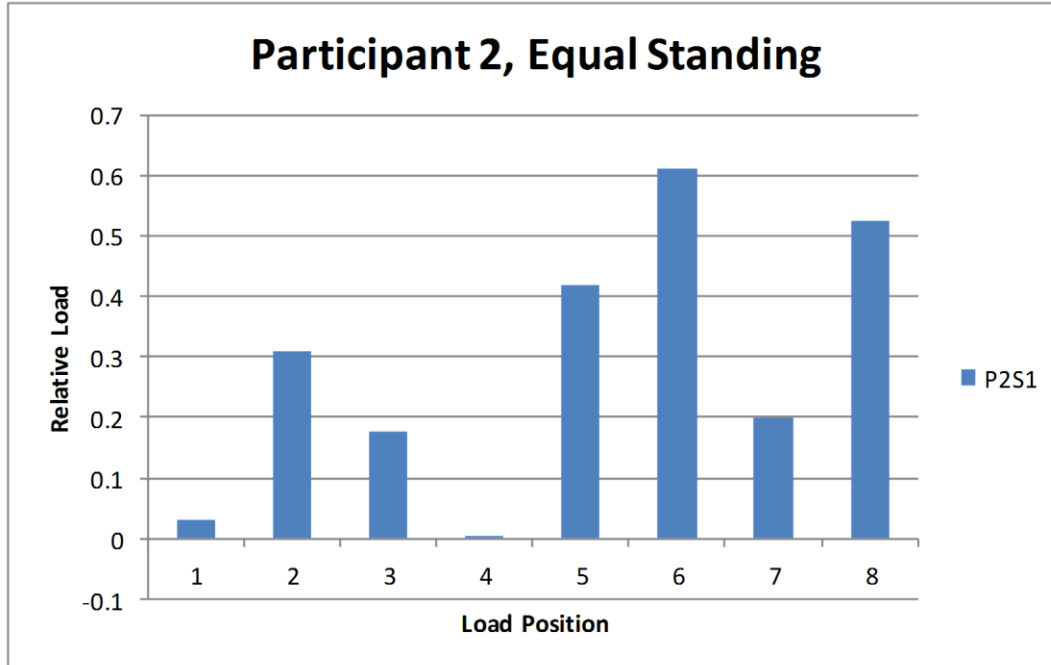


Figure 65 - Participant 2 socket load distributions in equal standing, from ensemble estimate of 3-4 seconds of quiet standing

Session	L1	L2	L3	L4	L5	L6	L7	L8	Sum
P1S1a	-0.034	0.028	0.475	-0.028	0.031	-0.086	0.026	0.091	0.675
P1S1b	-0.035	0.029	0.462	-0.023	0.025	0.077	0.023	0.076	0.636
P1S2	-0.026	0.001	0.249	-0.023	0.100	0.010	-0.009	-0.022	0.279
P2S1	0.029	0.309	0.177	0.002	0.420	0.612	0.200	0.523	2.275

Table 56 - Socket load estimates from each test session

Finally, Figure 66 shows the changes in total measured socket load during equal standing in each measurement session. This is simply the sum of the load in each socket position (also shown as the final column in Table 56).

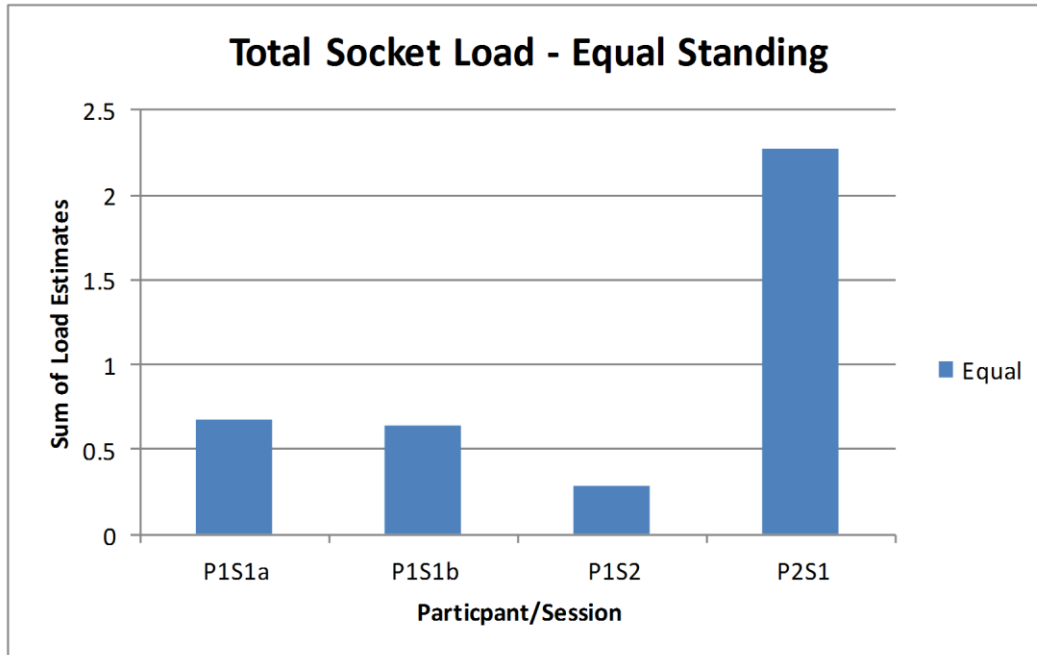


Figure 66 - Sum of socket loads for each participant and test session

8.2.3 Discussion

Both participants were able to stand steadily with even weight distribution for this test. Participant 1 recorded very similar readings within the same measurement session. Inter-session changes were greater. Potentially, this could be due to small weight changes between measurement appointments, or volume changes in that time in the residual limb.

The two participants showed differing pressure patterns. Participant 1 showed a clear peak of load at position 3 (posterior-distal), with other, smaller loads at positions 5-8 (the proximal ring). Participant 2 had a different pattern: The greatest loads during equal standing were placed proximally and medially/laterally, although loading was also present in the anterior and posterior proximal regions and the distal lateral and posterior regions.

Inter-session loads were more substantially different. The sum of loads reported across all socket positions in participant 1 reduced substantially, and to a greater extent than the relatively small reduction in the force applied through the amputated side. The data appears to suggest a change in loading pattern consistent with a shift from posterior to anterior load – the greatest change is in reduction of the distal-posterior load, coupled with an increase in the proximal-anterior load. Broadly similar results have been reported elsewhere in the literature

(e.g. Sanders et al. 1997 Sanders et al. 2000). Reasons for this change cannot be identified with certainty: however candidates include changes in stump volume, change to the device alignment or a change in foot placement during the standing task.

Load was measured as very low to absent in some locations: previous work has also found this. In Sewell et al. (2012), 6 of 16 load locations did not register pressure. In contrast to that work, some estimates were negative; this was a result of the polynomial correction factor, which in some cases was sufficient to adjust the ensemble estimates to negative values. A more realistic measure may be to set any negative estimates to zero rather than allow this.

8.2.4 Summary

The testing reported in this section leads to several interesting conclusions. The system appeared capable of measuring socket loads consistently, even between donning/doffing the socket within one measurement session and between sessions several weeks apart. Secondly, loading patterns are different between users – as would be expected between different sockets and residual limbs. The system produced changes in the sum of load that reflected the magnitude of applied load (albeit exaggerated state for participant 1's inter-session measurements).

The results from this section are developed in section 7.3 which examines the effect of altering the magnitude of applied socket load by altering the percentage of body weight that the user places through their prosthetic side. Sensitivity to these changes informs the interpretation of results from subsequent static and dynamic measures.

8.3 Static measurements with varied applied bodyweight

8.3.1 Methodology

In addition to asking participants to stand with bodyweight evenly distributed, they were also asked to place both less and more weight through the prosthetic side. As before, the contribution to bodyweight support through the prosthetic side was assessed using the force

platform, and the values of socket load distribution evaluated as a time-average of 3-4 seconds of standing.

The tests were completed with the socket in neutral alignment, and loads estimated using the same ensemble of 100 networks with polynomial correction used in section 7.2. The purpose of this test was to determine if the socket load system was capable of measuring changes in the magnitude of applied load reliably – that altered load would measurably affect to sum of loads reported by the system.

8.3.2 Results

The values of applied bodyweight reported for each participant and session are shown below in Figure 67 and Table 57, including the results as a proportion of participant bodyweight.

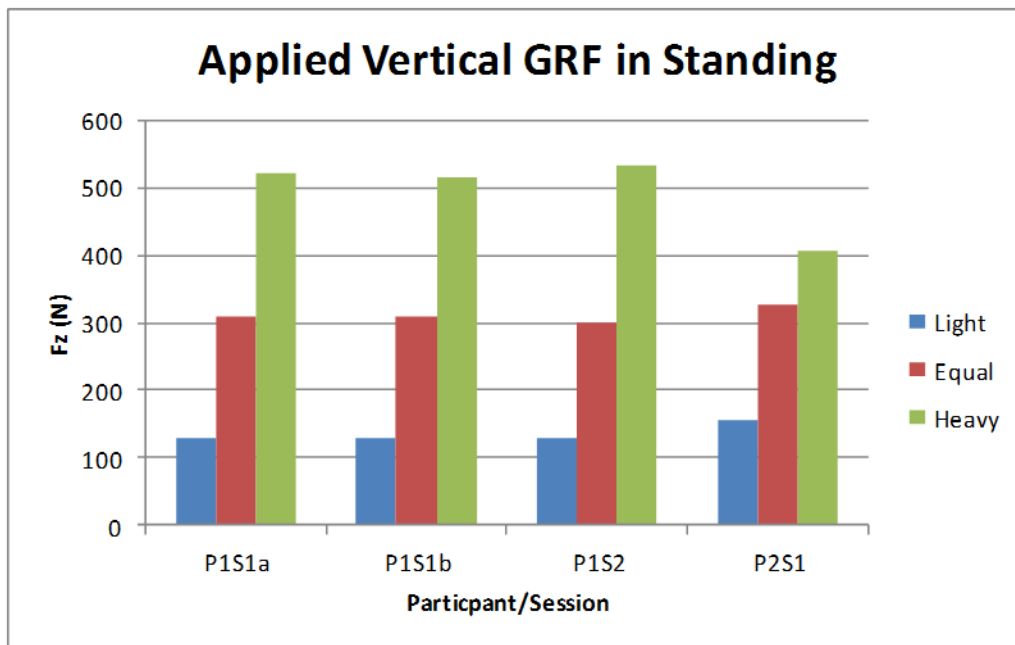


Figure 67 - Measures of changes in applied vertical ground reaction force in each participant and session

Session	Condition	Fz (N)	% Bodyweight
P1S1a	Light	130	20.4
P1S1b	Light	129	20.2
P1S2	Light	129	20.2
P2S1	Light	156	23.6
P1S1a	Equal	310	48.6
P1S1b	Equal	308	48.3
P1S2	Equal	299	46.9
P2S1	Equal	328	49.7
P1S1a	Heavy	520	81.5
P1S1b	Heavy	515	80.7
P1S2	Heavy	533	83.6
P2S1	Heavy	406	61.5

Table 57 - Vertical ground reaction force values

The values of total measured socket load are shown in Figure 68 - as in section 8.2, this was the sum of the average load in each measured position. Figure 69, Figure 70 and Table 58 show the results on a per load position basis. For space, results are expressed here as the average of participant 1's sessions and for participant 2's recordings.

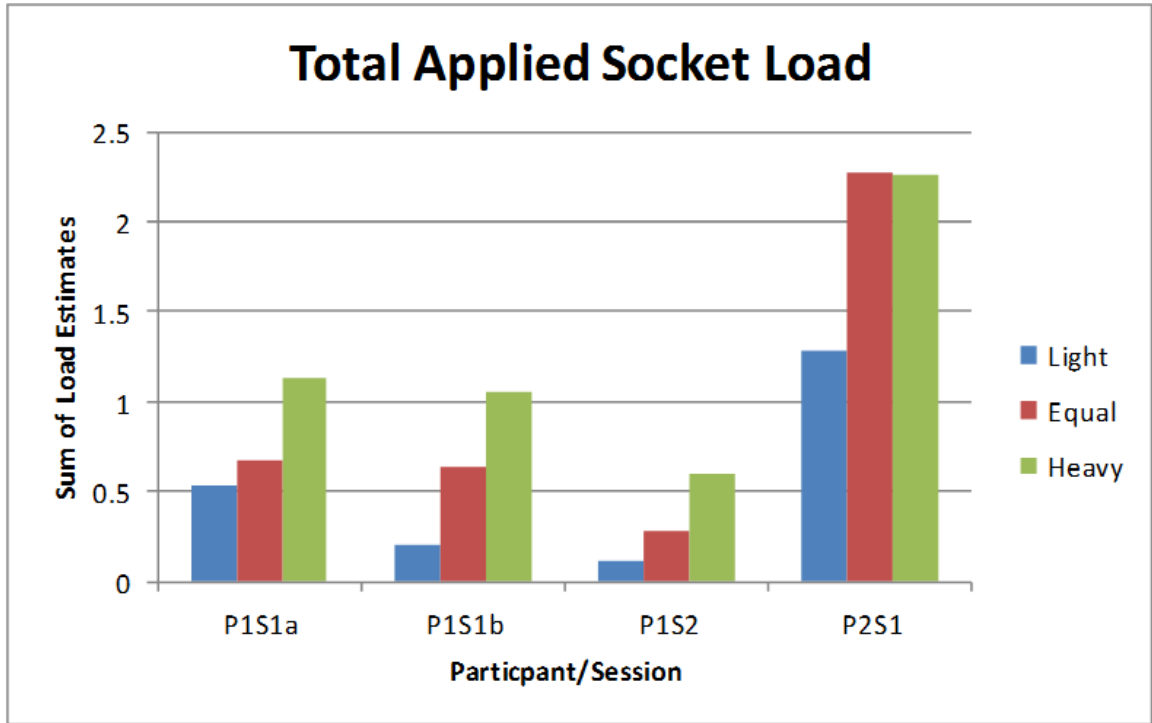


Figure 68 - Measured sum of total socket load for each participant and session, showing changes due to proportion of applied bodyweight

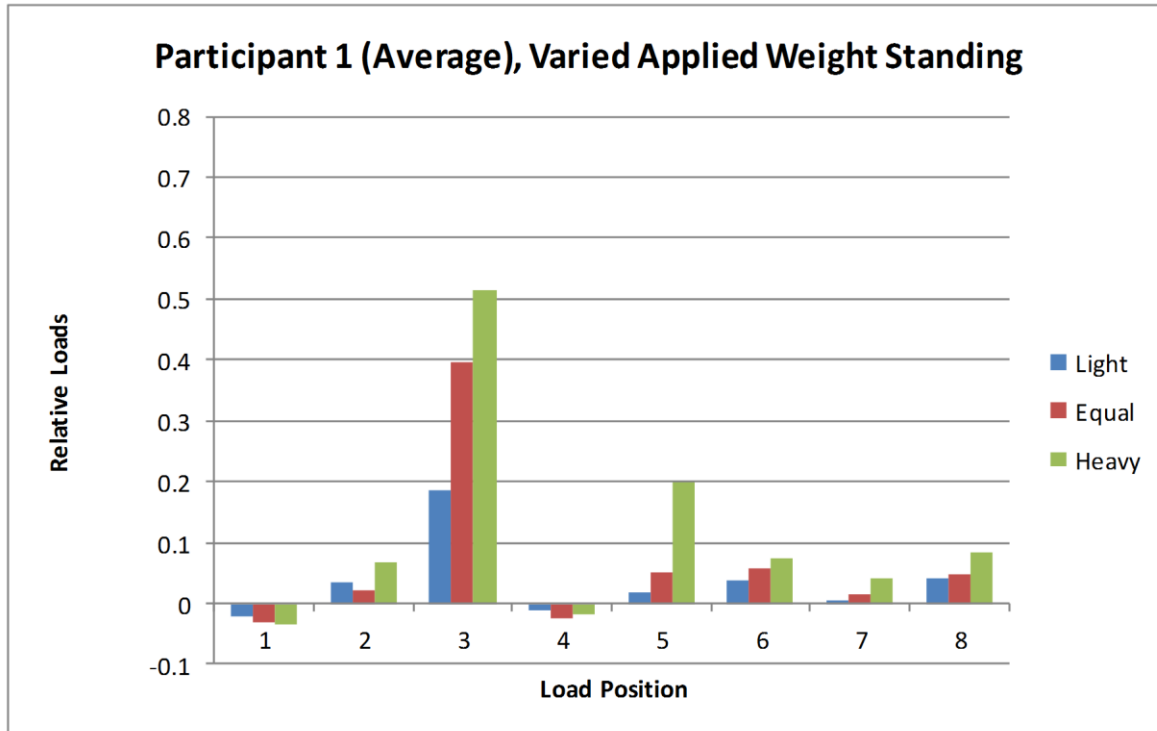


Figure 69 - Average socket load distribution measurements for participant 1, taken as an average across three sessions

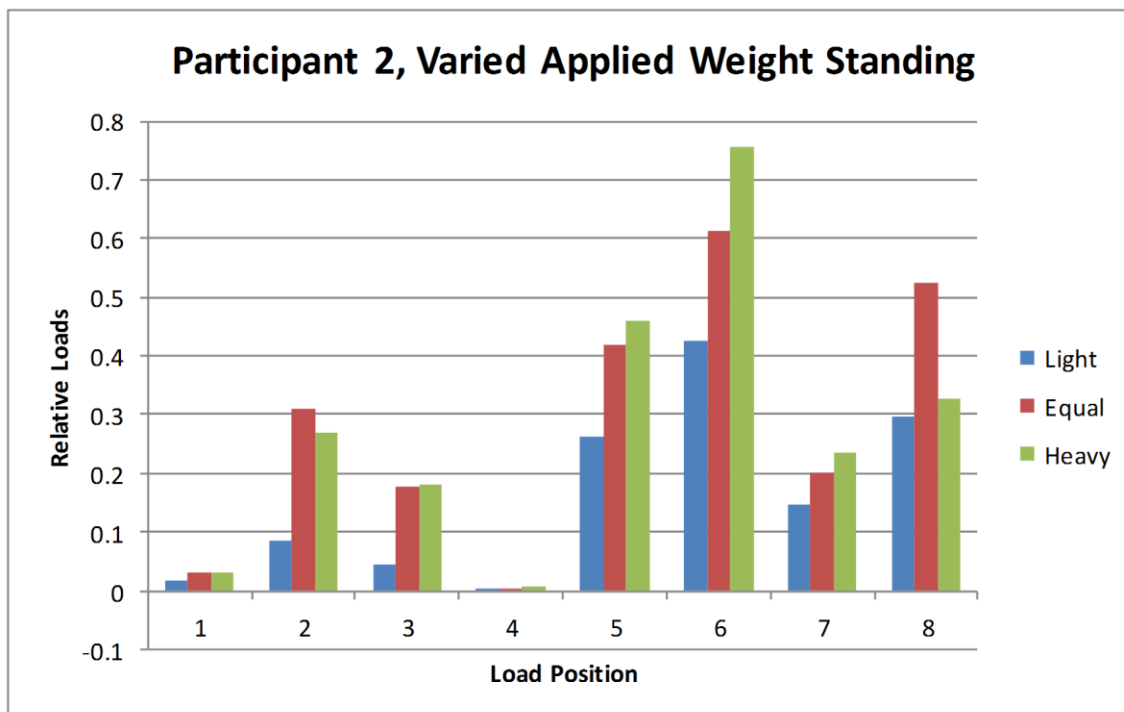


Figure 70 - Measured changes in socket load distribution for participant 2 with changes in applied bodyweight

Session	L1	L2	L3	L4	L5	L6	L7	L8	Sum
P1-L	-0.019	0.033	0.184	-0.012	0.016	0.036	0.006	0.041	0.287
P1-E	-0.032	0.019	0.396	-0.025	0.052	0.058	0.013	0.048	0.530
P1-H	-0.035	0.067	0.514	-0.017	0.199	0.075	0.041	0.083	0.928
P2-L	0.017	0.086	0.044	0.003	0.262	0.427	0.146	0.296	1.284
P2-E	0.029	0.309	0.178	0.002	0.420	0.612	0.200	0.523	2.275
P2-H	0.032	0.269	0.179	0.005	0.458	0.755	0.234	0.325	2.265

Table 58 - Socket load estimates for static standing with adjusted applied bodyweight. L=Light standing, E=Equal standing, H=Heavy standing.

8.3.3 Discussion

Participants were able to selectively load their prosthetic limb on request. Participant 1 was able to do this with high consistency, to within 3% of bodyweight between measurement sessions. Participant 2 elected to apply a lower additional proportion of bodyweight (to ~61% of total, rather than ~81% for participant 1). A particular change was not specified by the test protocol or by the researchers during the session.

The results in Figure 68 show that the system is (to some extent) able to recognise changes in the total applied load. This was reliably achieved in the case of participant 1, where there is a clear progression from low loads to higher loads (largely corroborated by the per-load readings in Figure 69). The precise magnitude of changes was less successful: the size of the difference between low-equal-high states did not reflect the changes in applied load as measured by the force plate. For example, in participant 1, session 1a the low load represented a reduction in applied bodyweight of 28%, whereas the socket measured a reduction of just 23% from the equal standing condition.

Several reasons for this difference are suggested. One is that this is a recurrence of the phenomena described in Chapter 6 for which the polynomial correction factor is supposed to correct – that the network has a tendency to overestimate low loads, contributing to a bias where the reduction in applied load is not well reported by the network. This is not considered a complete explanation, as the pattern was not repeated in other test configurations within the

same subject (e.g. P1S1b). Another potential reason is that the socket is being loaded in positions other than those recorded by the system. Although coverage of the socket surface is broad it is not complete, so if alteration of the load strategy employed by the participant included loading into additional regions this could account for 'missing' proportional changes. Finally, the residual error not eliminated by the use of ensembles, correction factors and the other techniques described in this thesis may also create a proportion of this effect.

Although participant 2 did increase the proportion of bodyweight applied through the prosthesis (as measured by the force platform), this was not recorded by the sum of load values from the neural network system. An examination of the per-position loads in Figure 70 suggests that loading on position 8 (proximal-medial) may be responsible: loading was substantially higher here in the equal weight condition than for either the low or high load states. The expected load changes were observed in all other positions (with the exception of 2 [Distal-Lateral], where the effect was present but smaller than at position 8). The impact of this change may be emphasised by the relatively small difference between the equal and heavy conditions.

8.3.4 Summary

The neural network system appears to be capable of measuring changes in applied static loads to the prosthetic socket when worn by amputee volunteers. Total load and individual load positions responded to alterations of globally applied load in the expected manner (in the majority of cases).

However, the magnitude of changes in loading was less well recorded within sessions. The change from equally applied bodyweight to both lesser- and greater- applied load did not precisely match the changes recorded from the external force platform. The reasons for this are not clear at this stage, and may represent the residual network error distribution or the application of significant loads outside the measurement region.

Following the successful conclusion of static tests, the participants were asked to complete walking trials at self-selected pace in the movement laboratory.

8.4 Dynamic measurements

The design and development of a study protocol for the collection and processing of dynamic socket load data was reported in Chapter 4. The specific details of this methodology are described in this section. The aim of this set of tests was to examine the capability of the system to monitor the changes in socket load distribution that are known to occur during walking situations.

8.4.1 Methodology

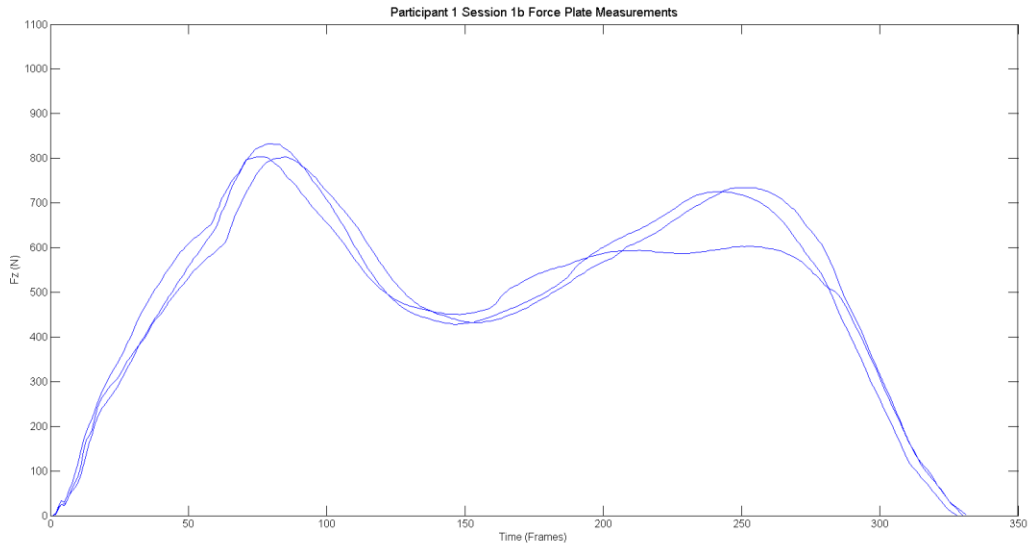
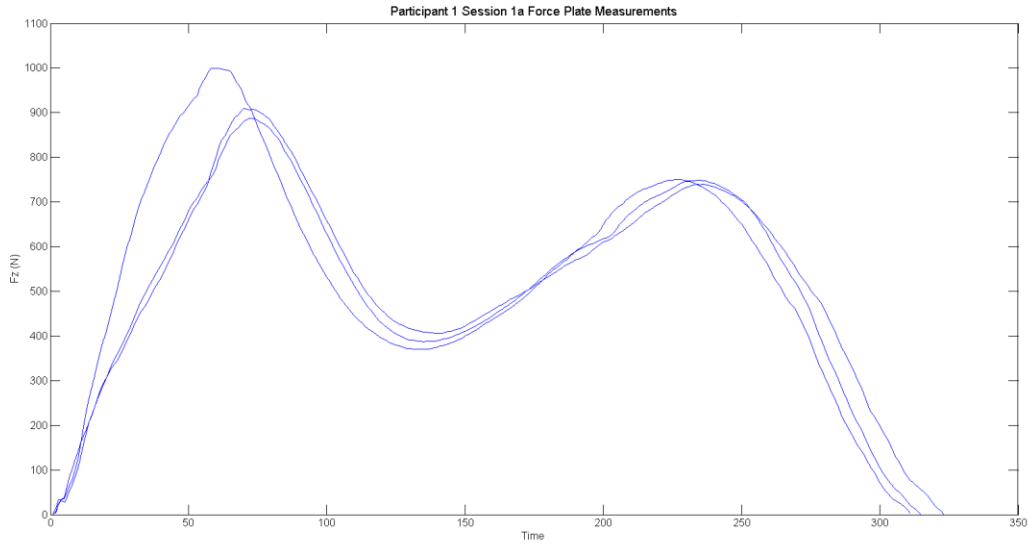
The purpose of this section was to investigate if the neural network system could reliably measure the periodic changes in load that would be expected to be present in walking situations. To achieve this, the participants were asked to walk through the measurement space at a comfortable speed, such that their prosthetic limb came into contact with the force plate in the centre of the room. The times of key points within the gait cycle (initial contact, first peak, central trough, second peak and toe off) were used to isolate values within the load-time output. Three walking trials were recorded in each case.

Results were combined into over-trial averages for each load position in each session for every participant. The variance present in both the Fz and the load distribution patterns when assessed via the ensemble of networks produced for each socket is described.

8.4.2 Results

In Figure 71, the recorded force platform readings in each session are shown. In Figure 72- Figure 75 the plotted socket load distributions for each session are collated. The values are shown as the mean of the recordings in each session, and plotted with ± 1 standard deviation bands.

The values from the key locations in each averaged set of socket load data are shown in Table 59 to Table 62 (mean and standard deviation).



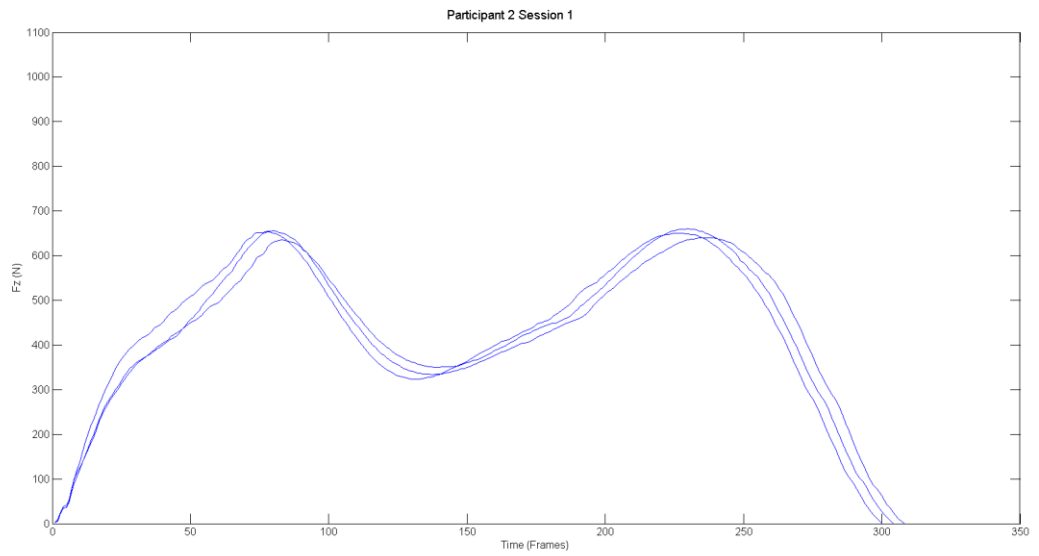
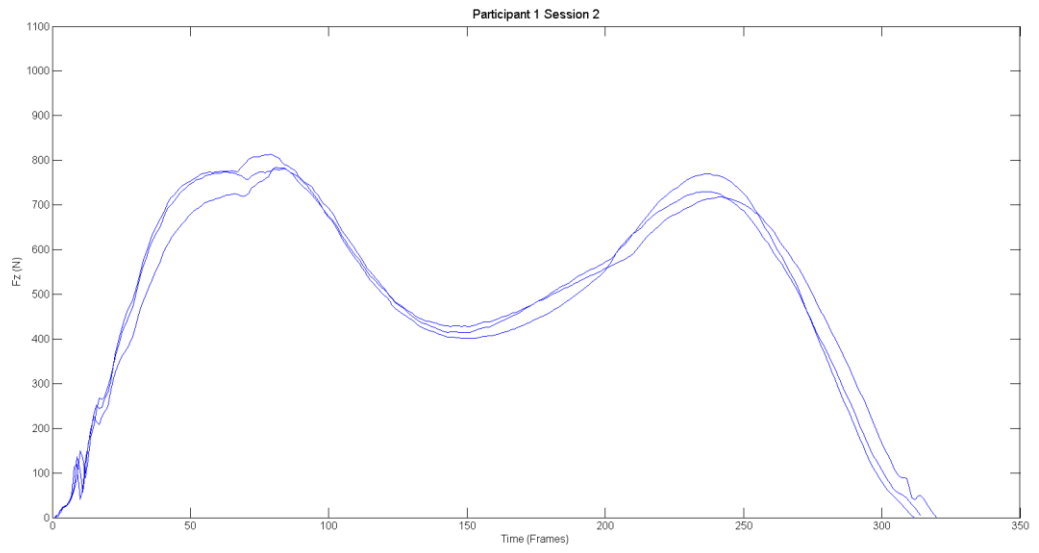


Figure 71 - Vertical force components recorded in each measurement session

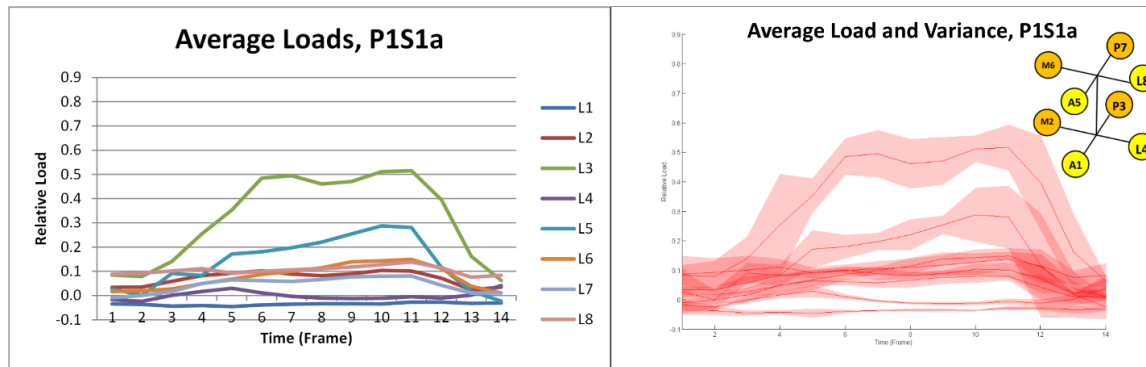


Figure 72 - Mean and variance graphs for Participant 1, Session 1a

Participant 1, Session 1a, Key Event Measurements								
Measure	L1	L2	L3	L4	L5	L6	L7	L8
P1 Mean	-0.04	0.10	0.48	0.01	0.18	0.09	0.06	0.10
T1 Mean	-0.03	0.08	0.46	-0.01	0.22	0.11	0.07	0.11
P2 Mean	-0.03	0.10	0.52	0.00	0.28	0.15	0.08	0.14
P1(SD)	0.01	0.01	0.06	0.01	0.04	0.02	0.01	0.02
T1 (SD)	0.01	0.01	0.08	0.00	0.05	0.03	0.02	0.03
P2 (SD)	0.01	0.02	0.08	0.01	0.11	0.01	0.01	0.04

Table 59 - Relative load values (mean and SD) for each load position in Participant 1, Session 1a for P1=Peak 1, T1=Trough 1, P2=Peak 2

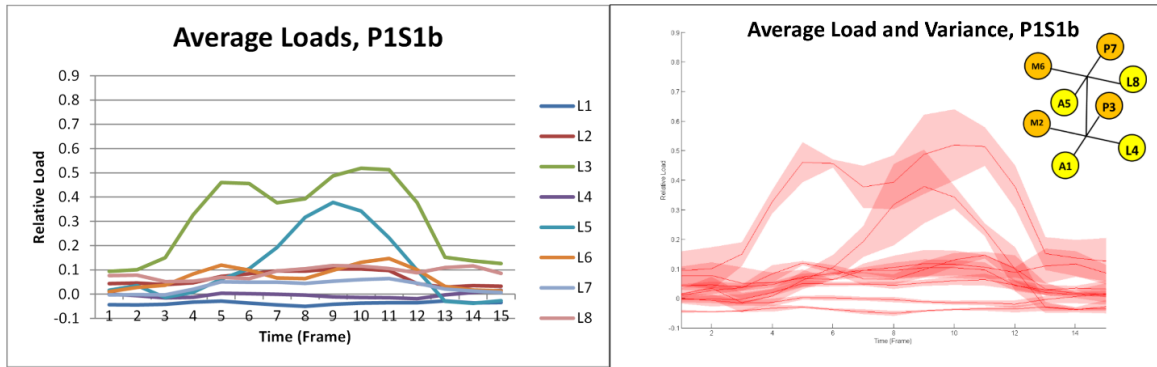


Figure 73 - Mean and variance graphs for Participant 1, Session 1b

Participant 1, Session 1b, Key Event Measurements								
Measure	L1	L2	L3	L4	L5	L6	L7	L8
P1 Mean	-0.03	0.07	0.46	0.00	0.06	0.12	0.05	0.07
T1 Mean	-0.05	0.09	0.39	0.00	0.32	0.06	0.04	0.10
P2 Mean	-0.03	0.10	0.51	-0.01	0.23	0.15	0.06	0.11
P1(SD)	0.00	0.01	0.07	0.01	0.03	0.01	0.01	0.03
T1 (SD)	0.01	0.03	0.09	0.01	0.14	0.02	0.01	0.04
P2 (SD)	0.01	0.03	0.07	0.01	0.02	0.01	0.02	0.04

Table 60 - Relative load values (mean and SD) for each load position in Participant 1, Session 1b for P1=Peak 1, T1=Trough 1, P2=Peak 2

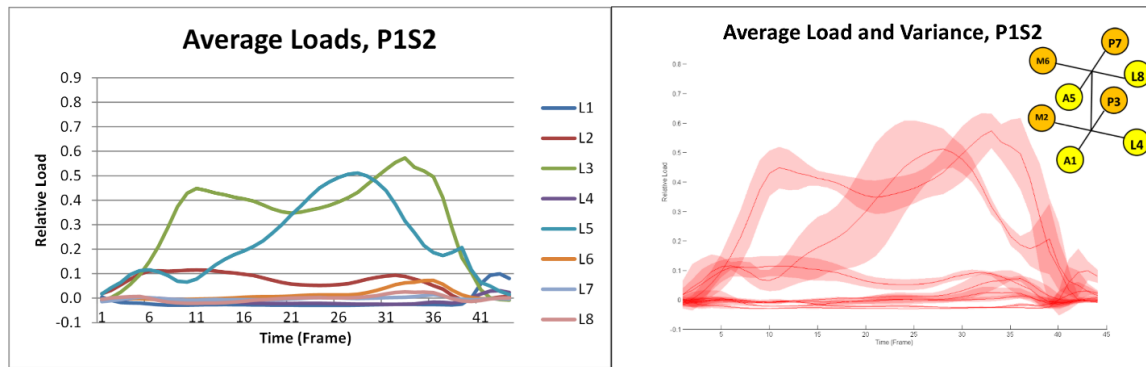


Figure 74 - Mean and variance graphs for Participant 1, Session 2

Participant 1, Session 2, Key Event Measurements								
Measure	L1	L2	L3	L4	L5	L6	L7	L8
P1 Mean	-0.03	0.11	0.45	-0.01	0.08	0.00	-0.01	-0.02
T1 Mean	-0.03	0.05	0.36	-0.02	0.42	0.01	0.00	0.00
P2 Mean	-0.03	0.07	0.52	-0.02	0.21	0.07	0.01	0.02
P1(SD)	0.00	0.03	0.07	0.01	0.05	0.00	0.00	0.00
T1 (SD)	0.00	0.02	0.06	0.00	0.18	0.01	0.01	0.02
P2 (SD)	0.00	0.03	0.09	0.00	0.03	0.01	0.01	0.02

Table 61 - Relative load values (mean and SD) for each load position in Participant 1, Session 2 for P1=Peak 1, T1=Trough 1, P2=Peak 2

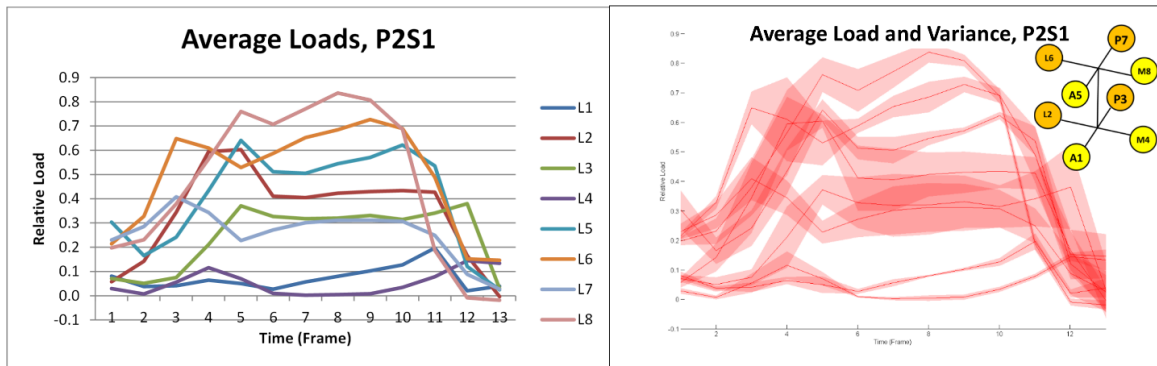


Figure 75 - Mean and variance graphs for Participant 2, Session 1

Participant 2, Session 1, Key Event Measurements								
Measure	L1	L2	L3	L4	L5	L6	L7	L8
P1 Mean	0.05	0.60	0.37	0.07	0.64	0.53	0.23	0.76
T1 Mean	0.06	0.40	0.32	0.00	0.50	0.65	0.30	0.77
P2 Mean	0.10	0.43	0.33	0.01	0.57	0.73	0.31	0.81
P1(SD)	0.03	0.02	0.05	0.02	0.04	0.08	0.04	0.06
T1 (SD)	0.01	0.10	0.11	0.01	0.04	0.04	0.08	0.05
P2 (SD)	0.01	0.07	0.09	0.01	0.01	0.03	0.08	0.02

Table 62 - Relative load values (mean and SD) for each load position in Participant 2, Session 1 for P1=Peak 1, T1=Trough 1, P2=Peak 2

Three sets of statistical comparisons were made to evaluate the differences between and within sessions. The first (Table 63), compares measurements from session P1S1a to P1S1b (i.e. the same participant, the same measurement session but a different set of tests separated by the socket being doffed and donned). Due to the number of tests in this section, the p-value threshold was revised to 0.0006 using a Bonferroni correction.

Comparison of P1S1a and P1S1b								
Measure	L1	L2	L3	L4	L5	L6	L7	L8
P1	0.092	0.005	0.680	0.207	0.003	0.036	0.207	0.147
T1	0.030	0.550	0.289	0.092	0.227	0.032	0.036	0.703
P2	1.000	1.000	0.857	0.207	0.406	1.000	0.124	0.330

Table 63 - Calculated p values from comparisons of socket loads between P1S1a and P1S1b. P1=Peak 1, T1=Trough 1, P2=Peak 2. No values were assessed as reaching significance

The second set of comparisons uses P1S1a and P1S2 (i.e. the same participant in different sessions separated by approximately 8 weeks). The results from t-tests carried out using the mean and standard deviation values for each load position of each of the key points described in Table 64.

Comparison of P1S1a and P1S2								
Measure	L1	L2	L3	L4	L5	L6	L7	L8
P1	0.092	0.550	0.539	0.030	0.020	0.0001	<0.0001	<0.0001
T1	1.000	0.036	0.092	<0.0001	0.076	0.001	0.001	0.001
P2	1.000	0.147	1.000	0.007	0.265	<0.0001	<0.0001	0.002

Table 64 - Calculated p values from comparisons of socket loads between P1S1a and P1S2. P1=Peak 1, T1=Trough 1, P2=Peak 2. Values in red were assessed as reaching significance.

For completeness, the results from participant 1 and participant 2 were compared: in the majority of comparisons significant differences were found (Table 65).

Comparison of P1S1a and P2S1								
Measure	L1	L2	L3	L4	L5	L6	L7	L8
P1	0.001	<0.0001	0.030	0.002	<0.0001	<0.0001	0.0001	<0.0001
T1	<0.0001	0.001	0.085	0.092	<0.0001	<0.0001	0.001	<0.0001
P2	<0.0001	0.0001	0.020	0.207	0.002	<0.0001	0.001	<0.0001

Table 65 - Calculated p values from comparisons of socket loads between P1S1a and P2S1. P1=Peak 1, T1=Trough 1, P2=Peak 2. Values in red were assessed as reaching significance.

8.4.3 Discussion

Observation of the vertical component of ground reaction force indicated that both participants walked consistently – the magnitude and timing of the loading pattern demonstrates that the gait pattern selected was reliable and competent. The patterns revealed the expected ‘M’ shaped curve with both peaks above bodyweight. Results were consistent across and between sessions, both in terms of timing and loading.

Participant one had a loading pattern which emphasised load on two positions over others (Position 3, the posterior distal and position 5, anterior proximal). Of these, the posterior distal featured an ‘M’ shaped curve, whereas position 5 had a notably larger peak in mid-late stance. The remainder of position also exhibited changes in magnitude over stance, but to a lower extent.

Participant 2 had a load distribution that was more equally spread across the measured loading position. A broad ‘M’ curve was present on 6 of 8 channels, although load was higher proximally compared to distally.

Loads were typically variable, with often greater variance on channels with greater magnitude loading. Channels with absent to very low estimated loads generally demonstrated low variance.

In comparing measurement results, P1S1a and P1S1b (the two identical sessions, separated by ~30 minutes and a doffing/donning of the test socket) demonstrated no significant changes in

the measured load on any channel at any of the key times of interest, suggesting that in-session repeatability was good.

When the average of P1S1a was compared to P1S2 (i.e. the same participant, in session separated by approximately 8 weeks), some significant changes in load were observed in channels at all key points in the gait cycle – at peaks 1 and 2 proximally (medial, posterior and lateral) and at the distal posterior point at the central trough. These were all channels reporting low-very low and invariant load. This suggests that the reason for these changes may be from elsewhere: potentially the measurement of the baseline readings to which results were compared. If the participant applied load differently in the ‘rest’ recording, then this would translate into a small baseline offset in dynamic readings.

Participant 1 and participant 2 demonstrated significant differences in the magnitude and position of loading across the socket. Significant differences were identified on 6 of 8 channels, and approached significance in the remainder of events. Inter-participant loads have shown inhomogeneity in previous studies of socket loading: likely due to variance in the residual limb morphology, the differences in socket design and other factors.

A visual inspection of the mean traces suggests that a difference in loading at the anterior-proximal aspect may be present in participant 1. Although differences did not reach significance, the considerable variance, the relatively low number of trials and the large number of significance calculations combined to leave the value beyond the threshold of significance. This limitation is discussed further in the critical evaluation section of this chapter.

8.4.4 Summary

Measurements of socket loads in dynamic conditions were carried out on two transtibial amputees, identifying load-time series in 8 different positions around the sockets. External measurements of walking patterns with a force platform demonstrated a consistent and competent gait pattern in both participants.

The participants exhibited differing patterns of load distribution: the estimate of the load distribution identified two dominant loading positions, and relatively low and invariant load on

the other positions. Participant 2 appeared to load the socket differently, with greater contribution proximally and higher loads in medial and lateral positions.

Both participants loaded the socket in the same 'M' pattern observed in the force platform readings. The load pattern is thought to represent initial weight acceptance, transition over the stance foot and propulsion in late stance, and is consistent with previous work in the literature.

Inter-session testing in participant 1 revealed that within session measurements were repeatable, despite donning and doffing of the socket. The inter-session differences did find some significant changes in the magnitude of relative load at key positions: this was restricted to low magnitude/low variance positions in this participant.

8.5 Variance sources investigation

8.5.1 Methodology

An investigation was carried out to examine the sources of variance in the recordings of participant 1 during flat walking. Biological signals exhibit a natural tendency to vary in pattern – in socket pressure this could be due to factors such as neurological control, ability to maintain a consistent path, slight changes in stump shape and volume and so on. Some researchers (e.g. Chau et al. 2005) suggest that inherent variability fulfils a biomechanical purpose: by varying the structures used to absorb load, then damage or fatigue may be avoided (Goldberger et al. 2002; Hausdorff 2005).

The magnitude of this variability, assessed as the changes between session, between order of trial and between networks used to assess the readings is of interest as it represents an estimate of the reliability of a particular assessor (in this case, each neural network) that takes into account the underlying variance inherent to biomechanical signals.

The value of each network's estimate for every included trial was submitted to a multi-level mixed effects linear regression model. A study of this type is conceptually similar to studies carried out in 3D gait analysis literature to evaluate clinician's repeatability in placing retro-reflective markers onto anatomical landmarks. The position of these markers informs the

construction of a biomechanical model to obtain variables such as joint angles. However, estimating the consistency of this activity is complicated by the natural changes in the selected gait pattern of the study participant. Thus error has several principal sources – the natural variance between trials, between analyst variance from different application of learned techniques and within analyst variance where an individual has to repeat their actions effectively (Baker, 2013, Chapter 13).

In this section, the structure of the variance was modelled according to Figure 76. Each measurement session for participant 1 (separated by ~8 weeks) consisted of 4 measurement trials (given that no significant differences exist between P1S1a and P1S1b, a mixture of trials were selected). Each trial in turn was assessed by each of the 100 networks that made up the ensemble estimate. Each output channel (the 8 load positions) was normalised to 100 samples to account for the difference in sampling frequency between sessions.

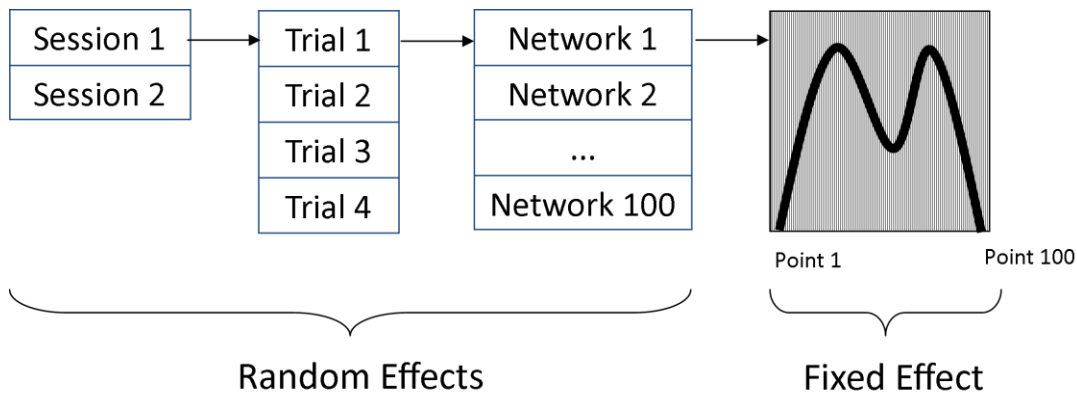


Figure 76 - Multi-Layer linear effects model used in this section

In the model, effects can be modelled as fixed or random. Fixed effects used here are the values from the network output channel, as these have changes in value that follow a particular track. Random effects are specified as the inter-network differences, the differences between trial order and the differences between sessions as these are assumed to vary but not according to a particular pattern. The residual error from the model represents the inherent variability of the measurement.

It is possible to control or reduce the effects of some of these factors. In chapter 6, the effect of reducing variance of the network solutions was examined. By evaluating the contribution of this factor into the overall sum of variability can help determine if this technique is likely to provide a meaningful improvement in system performance when balanced against other sources of variance.

8.5.2 Results

An example of the inter-network variance on a single measurement trial for each output channel is shown in Figure 77.

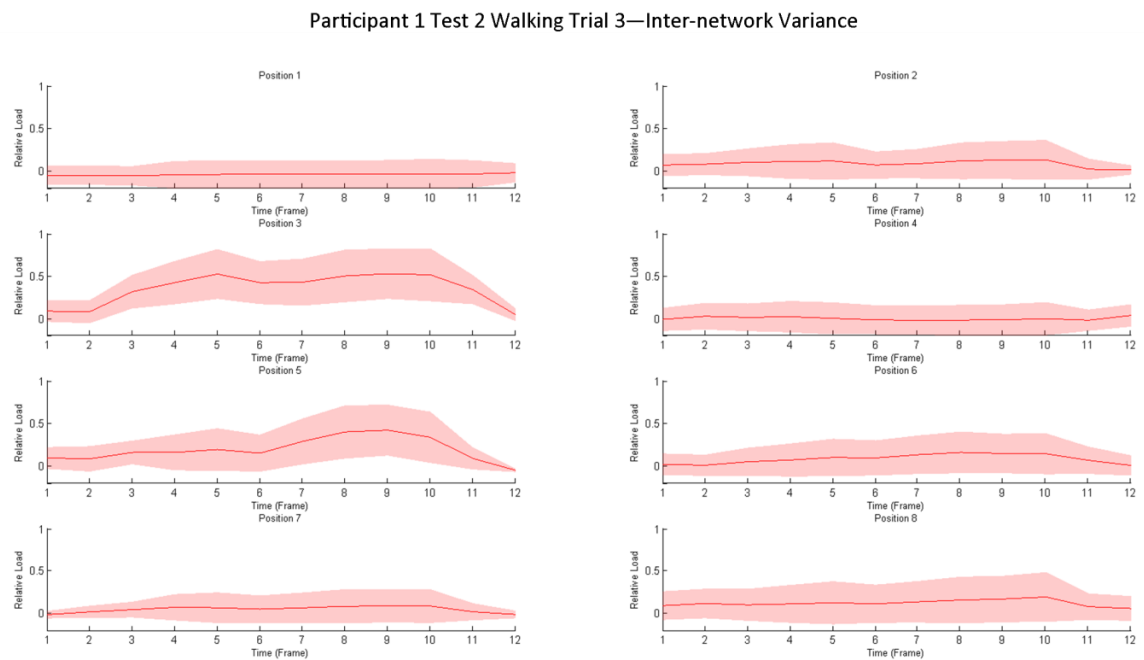


Figure 77 - Inter-network variance for a single trial from participant 1. This figure is taken prior to the time-normalisation procedure

The value of covariance for each output channel, expressed as the sum of residual variance, inter-network variance, trial order variance and session variance is shown in Figure 78, with the results as a percentage in Table 66.

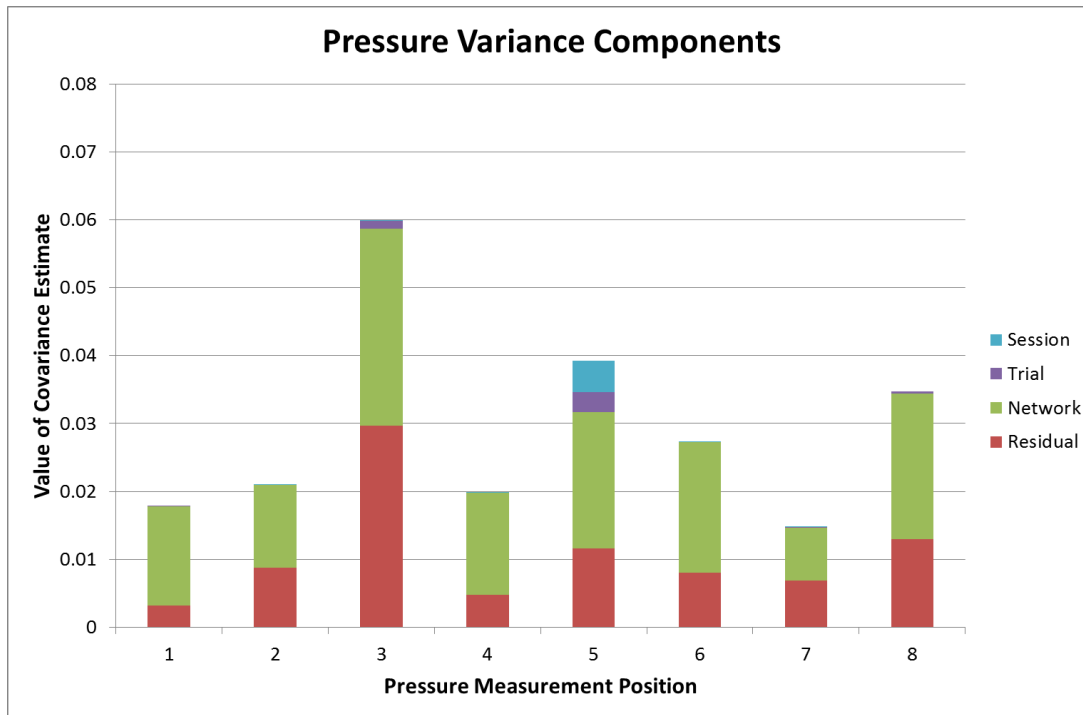


Figure 78 - Results from the output of the multi-layer models of each output channel

Load variance components for each output channel									
Component	P1	P2	P3	P4	P5	P6	P7	P8	Mean (SD)
Residual %	18.0	41.8	49.5	23.9	29.5	29.3	46.7	37.4	34.5 (11.2)
Network %	81.9	58.0	48.4	76.0	51.1	70.6	52.9	61.5	62.5 (12.3)
Trial %	>0.1	0.2	1.8	0.1	7.7	0.1	0.1	1.1	1.4 (2.6)
Session %	>0.1	>0.1	0.3	>0.1	11.7	0.1	0.3	>0.1	1.5 (4.1)

Table 66 - Contributions to covariance estimate from each model, expressed as the percentage of the total

8.5.3 Discussion

In estimating the contributions to the variance, the multi-level model indicated that the majority of explained variance in the model was as a result of the differences in network

estimates – a contribution that was much greater than the combined effects of differences between trials or between sessions. Variance contributions attributed to within-trial effects were highest in regions with the largest relative pressures – positions which also experienced the highest variance between trials and sessions. The greater rate-of-change of pressure in these locations (Figure 78) means that these locations are more susceptible to variance arising from errors from the isolation of the studied gait cycles. The inclusion of a fixed effect for frame number and the time-normalisation procedure employed in the multi-level model is thought to have reduced this effect.

The model exhibited a relatively large residual value meaning that a substantial amount of the variance was not modelled by the network, trial order or session effects. As the model used a random effect to model the inherent variance, it is suggested that the variability of pressure readings is high. However alternative sources of difference cannot be discounted: variance may also result from differences in the selection of the beginning and end of stance as part of the time-normalisation procedure. Given the higher sampling frequency of the force plate relative to the pressure measurement system, this effect should be minimised but not ignored. Such an effect would increase the contribution of the inter-trial variation which was otherwise small in this study (as compared to other studies in kinematic measures (McGinley et al. 2014)).

This study may represent the first use of the multi-level variance analysis technique in pressure distribution time-series: previously published work in gait analysis has examined the variance contributions in 3D kinematic measurements only. The use of this approach to examine the relative magnitude of inter-assessor variance compared to the inherent variance in walking patterns confirms the limitations in using single networks to perform an inverse-problem analysis on biomechanical systems. Effort in reducing the overall variance in estimations between and within- trials can therefore be meaningfully achieved by controlling the variance at the network level.

The use of estimates obtained from groups (ensembles) of networks has been extensively described (Hansen and Salamon 1990). This study has confirmed that using ensembles of estimates of socket pressures using external strain measurements is a technique with

significant advantages, as it will greatly reduce the errors in estimates by networks of equivalent training validity but with variable performance on real data.

8.5.4 Summary

An examination of the contribution to inter-measurement error identified that the largest contributions were the inter-network error and the inherent inter-trial variance in the selected gait pattern. That the typically greatest contributor to variance can be controlled by the construction of ensembles means that the use of this technique is supported by the results from practical measurements in addition to the evidence presented in Chapter 6.

The variance contribution in different sessions and in the order of trials was much smaller than the inter-network variance, indicating that the effect of this is less significant.



Figure 79 - Participant wearing the socket in equal standing

8.6 Critical evaluation

The applicability of the results presented in this chapter is restricted by the low number of participants that took part in the study. This issue is common to many studies in the prosthetic literature, and reflects the commitment required in material, expertise and time required to complete studies of this type. In this study, the construction and instrumentation of a specific

test socket and the attendance of the measurement session for several hours acted to restrict the available recruitment. Significant inter-participant variance that was observed, meaning that the ability to generalise results across participants is reduced even in larger studies.

The low number of tests that were completed as part of each test session also limits applicability. The averages presented in this chapter were obtained from four trials: the effect of this was that estimates of variance were high and that statistical calculations were reduced in power by this. It is possible that if more trials were recorded that greater statistical clarity would be obtained, however the limitation of available recording time meant that many more tests (which required a concurrent force plate measurement) was not feasible, in particular with the number of additional tests described in Chapter 8.

The measurements performed in these chapters did not have a direct validation against another form of in-socket load measurement. This limitation has been recognised in literature reviews which have reported on the neural network technique (Al-Fakih et al. 2016). A second measurement system could not be obtained for dynamic measurements; however it would be difficult to integrate such a system effectively. A through-socket transducer would alter the characteristics of the structure being measured and a finite-element model would require detailed knowledge of the residual limbs of potential participants and of the loading conditions (which was not available). An array-type sensor would be more practical, but locating appropriate positions of load and comparing these is a further feasibility challenge. The additional measurement burden of concurrent measurement with this form of system also threatens that validity of dynamic measurements. Therefore, in this work the conclusions that are drawn are on the consistency of measured values, rather than on absolute accuracy of the load distribution representation. It should be noted that the measurements obtained within this study were broadly consistent with previous measurements from alternative systems.

Although the measurement rig did not noticeably impede movement strategies used by the participants, the additional weight was commented on by both amputees. A review of the literature (Chapter 2.7.5) indicated that mass of this magnitude and with this form of distribution would not create a significant change in amputee movement. Socket suspension remained consistent throughout the study.

Qualitative evaluation of the suitability of the socket was limited to the use of the socket comfort score, which did not reveal any difference between the test socket and the customary prosthesis. Although qualitative tools which deal with socket comfort are not numerous, a more detailed questionnaire (possibly the TAPES tool, (Gallagher and MacLachlan 2000), Chapter 2.4) might reveal more detail on the changes that arise from a revised socket design.

The calculation of significant changes in socket load values was hampered by the relative lack of sophistication of this technique. Use of load values at key positions of the gait cycle makes *a priori* assumptions of the expected loading patterns, and requires accurate isolation and normalisation of the time-series in use. The use of more complex means of summarising biomechanical signal traits has seen more development in the kinematic/kinetic literature than in prosthetics or pressure measurement research.

Finally, the use of large numbers of t-test calculations restricted the identification of significant changes in relative load due to the correction of the p-value threshold to reflect the number of tests (and hence avoid a type I error). Many load outputs (particularly in participant 1) estimated consistently low loads: a potential manner of improving the chance of finding significant changes would be to exclude these cases from the bank of analyses. However, the difficulty of this approach is that the output positions to exclude is not known ahead of time – if data is more often similar to participant 2, then this approach is not workable.

8.7 Conclusions

In this chapter, the lessons in network and ensemble construction obtained in the results from chapters 5-7 were applied to the static and dynamic measurement tasks specified in chapter 4. Participants were able to wear the measurement device, which obtained consistent and meaningful relative load distributions on the prosthetic sockets of two transtibial participants.

The system was able to respond fairly well to variably applied bodyweight, with the values obtained for participant 1 consistent with the changes in total applied load. This was less successful in participant 2, although this may reflect the lower relative change in load applied.

Dynamic studies demonstrated that load distribution varied as anticipated during gait stance, and in participant 1 did not significantly alter on within-session measurements. Some small (but significant) changes were observed between measurements taken 8 weeks apart. Each participant utilised different stump-socket loading patterns: confirming the large inter-participant variance in this population.

A study of sources of variance indicated that the main contributions were from inherent variance in loading pattern and the variance between trained networks rather than trial order or measurement session differences. This supports the conclusion that a valuable technique to improve the quality of results is to construct ensembles of neural networks to produce load estimates.

The work presented in this chapter is used to support the results reported in the subsequent chapter, where the configuration of the prosthesis and the walking situation is perturbed away from an 'optimal' alignment and from flat walking conditions.

Chapter 9 Socket load measurement with perturbation

In the previous chapter the ability of the neural network socket load measurement system to quantify the loading present between tests, sessions and participants was evaluated. The loads present on two transtibial prosthetic sockets were measured during standing with differences in applied bodyweight and during steady-state walking on a flat surface. The participants walked with good consistency in their selected gait pattern: the measurement system provided realistic changes in socket load when varying normal force was applied, and was able to monitor the changes in loading pattern during gait. The load patterns were significantly different between participants: most likely reflecting the differences in stump physiology and socket design. An analysis of the variance contributions identified that the single largest contribution was from the neural networks used to estimate loads. This provided further evidence that using neural network ensembles is important to maintain system reliability.

In Chapter 2, the literature review completed as part of this thesis identified that changing aspects of the walking conditions experienced by amputees would create differences in the patterns of applied load. Examples of configuration changes include altering prosthetic components, changing device alignment and from walking on different terrain. The review of previous work found only limited work had been carried out: a brief study of medial/lateral alignment change in one participant in standing. In those results, the system appeared to provide the capability to distinguish gross changes in socket alignment: however the adduction/abduction induced was extreme, and no study of changes during dynamic loading was made. The capability of a system of this type to detect changes in applied load created from common walking conditions and clinically relevant changes in device configuration is therefore yet to be established.

In Chapter 4, the design of a study protocol that included evaluation of static and dynamic loads during socket adduction/abduction, slope walking and the change to a different socket liner was described, and ethical approval granted. The results in this section report the measurements taken in those tests, and critically evaluate the ability of the system to distinguish these conditions.

9.1 Alignment perturbation

9.1.1 Methodology

The two participants recruited for this study each completed a session where tests were conducted with the socket in a neutral alignment (considered optimal by the study prosthetist and the participant), and where the socket was placed in varus and valgus via an induced alignment change of approximately 5° in the coronal plane away from the neutral alignment. The participant was given time (~10 minutes) to become accustomed to the new configuration, and then asked to complete the same battery of tests as described in chapter 8 (i.e. light, equal and heavy static standing, and flat walking at a comfortable pace). Recordings were referenced to an unloaded state from the same collection trial, and a time-average of 3-4 seconds was made of the static measurements. Walking tests were isolated using concurrent measurements from the force platform. Events within the load-time series were identified with the relevant indices from the force platform values. Loads were estimated from surface measurements using the same ensembles used in Chapter 8.

9.1.2 Results

The changes in estimated socket load during varied bodyweight standing are shown in Figure 80 and Figure 81.

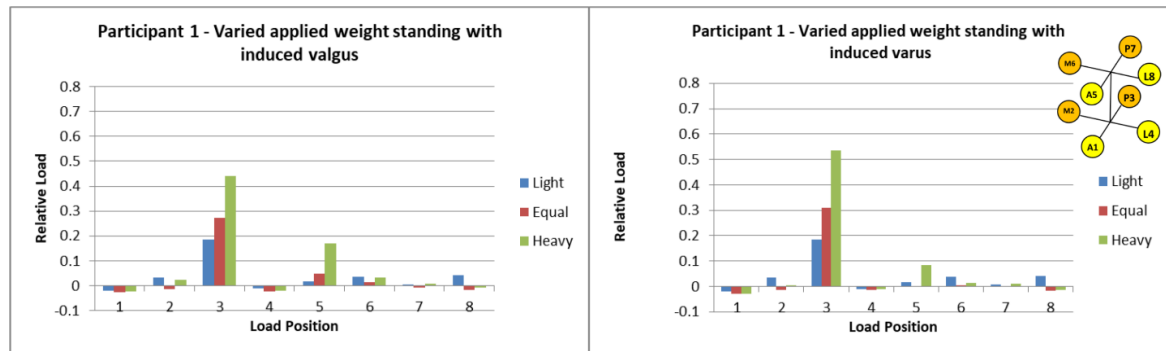


Figure 80 - Static load distribution with change in applied bodyweight. Participant 1, induced varus and valgus

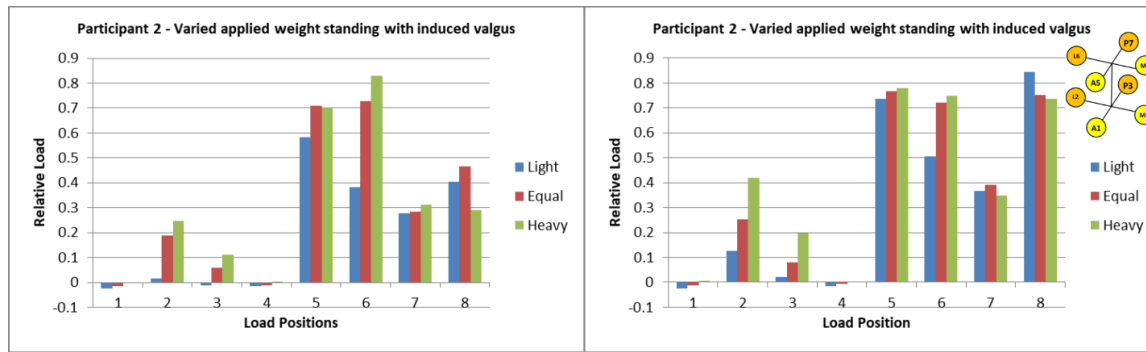


Figure 81- Static load distribution with change in applied bodyweight. Participant 2, induced varus and valgus

Four load distributions of single gait cycles were combined into a group average. The mean load traces are shown in Figure 82 and Figure 83 for participant 1 and Figure 84 and Figure 85 for participant 2.

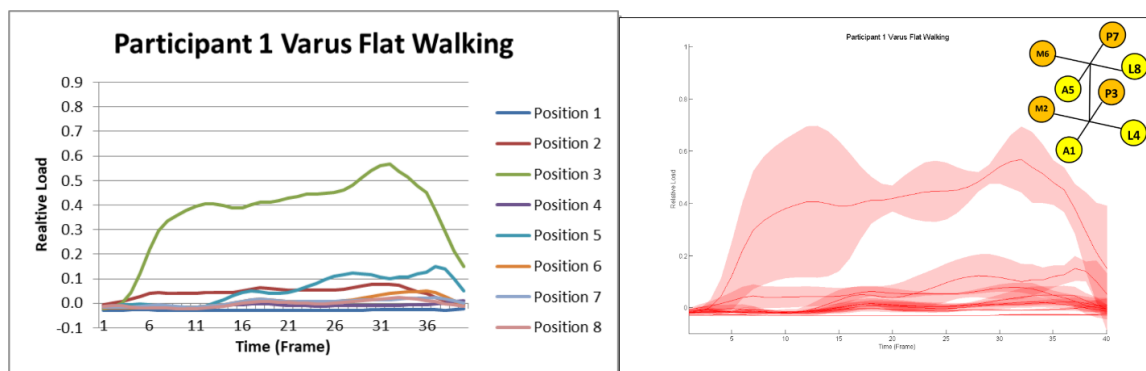


Figure 82 - Participant 1, mean and variance of flat walking with induced varus. Red bands indicate +/- 1 SD

Participant 1, Varus Flat Walking								
Measure	L1	L2	L3	L4	L5	L6	L7	L8
P1 Mean	-0.03	0.04	0.41	-0.02	-0.01	-0.01	-0.01	-0.02
T1 Mean	-0.03	0.05	0.43	-0.01	0.04	0.01	0.01	0.00
P2 Mean	-0.03	0.08	0.57	-0.01	0.10	0.04	0.02	0.02
P1(SD)	0.00	0.04	0.29	0.01	0.02	0.00	0.01	0.01
T1 (SD)	0.00	0.02	0.08	0.01	0.06	0.02	0.02	0.02
P2 (SD)	0.00	0.02	0.13	0.00	0.07	0.03	0.01	0.02

Table 67 - Key values for participant 1 during flat walking with induced varus.

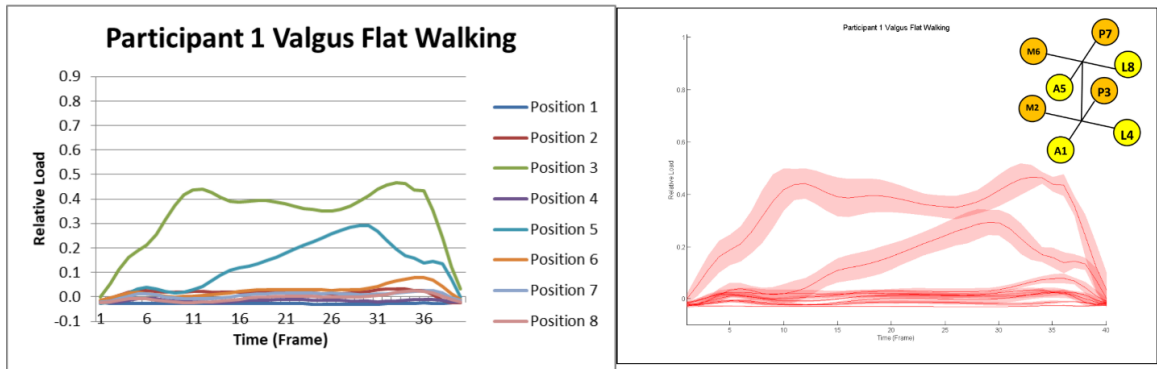


Figure 83 - Participant 1, mean and variance of flat walking with induced valgus. Red bands indicate +/- 1 SD

Participant 1, Valgus Flat Walking								
Measure	L1	L2	L3	L4	L5	L6	L7	L8
P1 Mean	-0.03	0.02	0.44	-0.02	0.03	0.00	-0.01	-0.02
T1 Mean	-0.03	0.01	0.35	-0.01	0.26	0.03	0.01	0.00
P2 Mean	-0.03	0.03	0.44	-0.01	0.16	0.08	0.02	0.03
P1(SD)	0.00	0.01	0.06	0.01	0.04	0.01	0.01	0.00
T1 (SD)	0.00	0.01	0.04	0.01	0.05	0.01	0.01	0.02
P2 (SD)	0.00	0.00	0.03	0.01	0.04	0.02	0.01	0.02

Table 68 - Key values for participant 1 during flat walking with induced valgus.

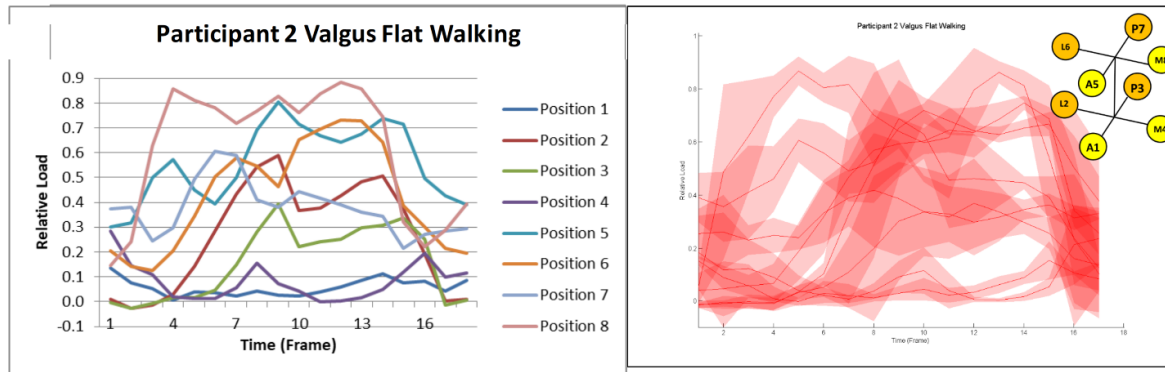


Figure 84 - Participant 2, mean and variance of flat walking with induced varus. Red bands indicate +/- 1 SD

Participant 2, Varus Flat Walking								
Measure	L1	L2	L3	L4	L5	L6	L7	L8
P1 Mean	0.00	0.03	0.02	0.02	0.57	0.20	0.30	0.86
T1 Mean	0.03	0.59	0.39	0.07	0.81	0.46	0.38	0.83
P2 Mean	0.06	0.43	0.25	0.00	0.64	0.73	0.39	0.88
P1(SD)	0.02	0.07	0.03	0.03	0.08	0.13	0.13	0.17
T1 (SD)	0.01	0.10	0.04	0.04	0.08	0.05	0.12	0.02
P2 (SD)	0.02	0.06	0.06	0.01	0.05	0.02	0.03	0.01

Table 69 - Key values for participant 2 during flat walking with induced varus.

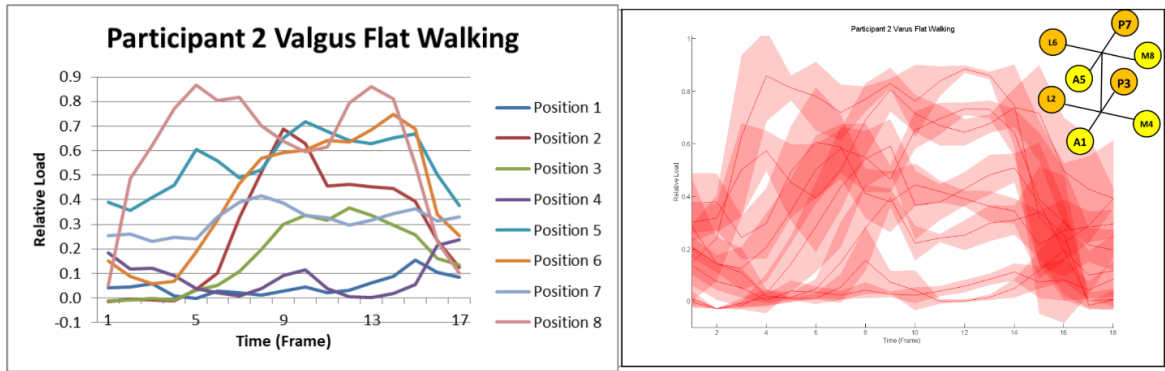


Figure 85 -Participant 2, mean and variance of flat walking with induced valgus. Red bands indicate +/- 1 SD

Participant 2, Valgus Flat Walking								
Measure	L1	L2	L3	L4	L5	L6	L7	L8
P1 Mean	0.00	0.04	0.03	0.04	0.61	0.19	0.24	0.87
T1 Mean	0.04	0.63	0.34	0.12	0.72	0.60	0.34	0.60
P2 Mean	0.06	0.45	0.34	0.00	0.63	0.68	0.32	0.86
P1(SD)	0.01	0.02	0.03	0.06	0.08	0.11	0.04	0.05
T1 (SD)	0.04	0.09	0.17	0.09	0.05	0.05	0.14	0.15
P2 (SD)	0.03	0.10	0.10	0.01	0.03	0.06	0.09	0.04

Table 70 - Key values for participant 2 during flat walking with induced valgus.

The values of load distribution at key points are reported in Table 67 to Table 70, showing the mean and standard deviation of estimates at this times. The values at these times are compared to the neutral recording using t-tests. A Bonferroni correction to the p value threshold was implemented in order to account for the number of tests completed ($p < 0.001$). The results of this analysis are shown in Table 71 and Table 72.

Participant 1, Varus/Valgus Flat Walking p-values								
Comparison	L1	L2	L3	L4	L5	L6	L7	L8
Varus P1	0.849	0.028	0.772	1.000	0.015	0.104	1.000	1.000
Varus T1	0.849	1.000	0.212	0.097	0.007	0.858	0.467	0.839
Varus P2	0.375	0.664	0.564	0.071	0.025	0.148	0.424	0.946
Valgus P1	0.095	0.002	0.786	0.137	0.159	0.518	0.611	1.000
Valgus T1	0.093	0.013	0.777	0.257	0.135	0.072	0.083	1.000
Valgus P2	0.365	0.026	0.128	0.174	0.072	0.504	0.109	0.729

Table 71 - Significance calculations comparing participant 1 flat walking to induced varus/valgus alignment changes.

Participant 2, Varus/Valgus Flat Walking p-values								
Comparison	L1	L2	L3	L4	L5	L6	L7	L8
Varus P1	0.043	<0.001	<0.001	0.023	0.154	0.006	0.421	0.364
Varus T1	0.004	0.036	0.253	0.018	0.001	0.001	0.302	0.070
Varus P2	0.008	0.835	0.176	0.202	0.029	0.915	0.110	0.001
Valgus P1	0.021	<0.001	<0.001	0.234	0.472	0.002	0.772	0.035
Valgus T1	0.487	0.015	0.882	0.034	<0.001	0.141	0.659	0.066
Valgus P2	0.049	0.738	1.000	0.295	0.011	0.219	0.924	0.063

Table 72 - Significance calculations comparing participant 2 flat walking to induced varus/valgus alignment changes. Values in red assessed as significant changes.

9.1.3 Discussion

In participant 1, the introduction of varus and valgus had only limited effect on the static measures of socket load. Load tended to reduce at position 3 (posterior-distal) and position 5 (anterior-proximal). Smaller load was also indicated at positions 6 and 8 (medial-proximal and lateral-proximal). Induced valgus had a more even distribution between positions 3 and 5, whereas when an induced varus was applied, the posterior-distal position was loaded more heavily. This result is somewhat unexpected, as coronal plane alignment changes would be expected to alter the loading on the medial and lateral aspects rather than in the sagittal plane.

This effect was observed to a greater extent in participant 2. Here, the induced valgus produced a greater tendency to load position 8 (the medial-proximal position). A corresponding

reduction in lateral-distal load (position 2 in this case) was also seen in valgus. Position 5 (anterior-proximal) was also increased in both varus and valgus.

During dynamic testing, an observation of the traces produced during varus walking suggested that reduction in load at position 5 persisted in participant 1. The trace for position 3 appeared flatter on the average graph, but this conceals a much greater variance in loading, particularly at the first peak. An induced valgus had a similar effect, but with a reduced magnitude. A statistical evaluation comparing the recordings from induced varus and valgus did not identify significant changes in load in this participant.

Conversely, both varus and valgus alignment changes created significant changes in load distribution in participant 2. However, trends related to the alignment changes were difficult to discern: however the first peak at position 2 (posterior-distal) and position 3 (medial-distal) reduced. Another aspect was that the participant tended to walk slower in these configurations (stance time 0.81s in normal walking to 1.06s in both misaligned cases). As in participant 1, variance within output channels increased in misaligned configurations.

As in the significance calculations described in Chapter 8, the relatively low number of measurement trials and the comparatively high number of statistical tests made confirming statistical changes more difficult: in participant 2 in particular, many other comparisons approached significance.

9.1.4 Summary

Both participants completed static and dynamic tests following induced alignment changes in the coronal plane of approximately 5° in each direction to produce varus and valgus offsets. In comparison to neutrally aligned recordings collected in the same session, limited differences in recordings were observed. These only partially conformed to biomechanical expectations of adjusting alignment in this way.

In common with the results presented in Chapter 8 there were large differences in loading between each participant, precluding combination of recordings across participants. It is

possible that increasing the number of recordings within each group would aid in identifying meaningful changes in load pattern.

9.2 Slope walking

9.2.1 Methodology

Both participants were asked to walk at a comfortable speed up and down a 5° slope while the socket load measurement device recorded the strains on the external surface of the socket. Two gait cycles were isolated from each trial, and two trials recorded for a total of four gait cycles in up-slope walking and down-slope walking. Due to a telemetry failure, the results for participant 2 were not suitable for analysis. Results are compared to the flat ground walking reported in Chapter 8. As the force platform was not available in this configuration, the timings of features of the gait cycle were identified by inspection.

9.2.2 Results

The mean load-time series for each network output channel for up-slope walking are shown in Figure 86, along with a representation of the standard deviation of the results. The corresponding results for down-slope walking are shown in Figure 87. The table of results of key event loads is shown in Table 73 and Table 74.

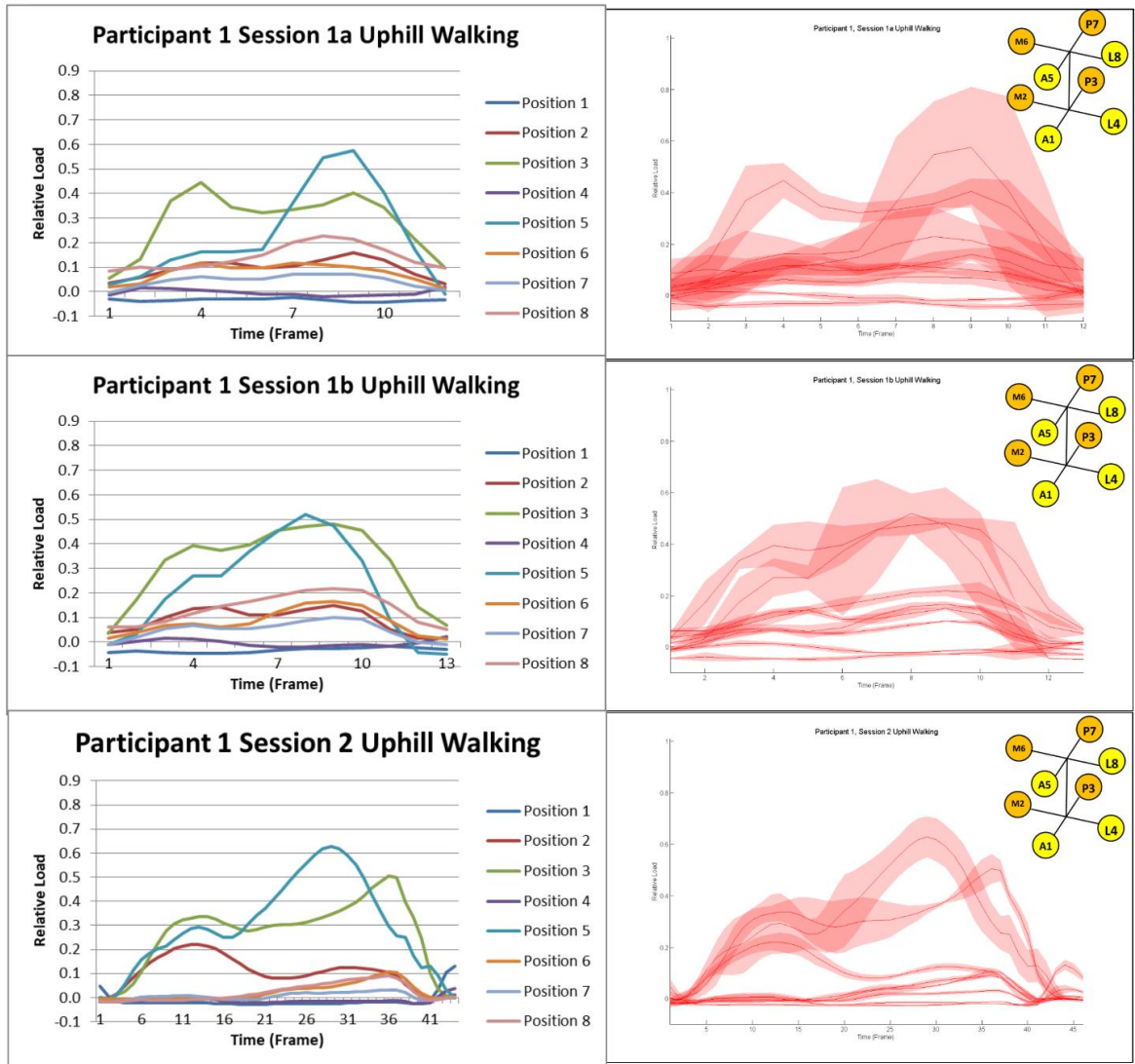


Figure 86 - Mean and variance of participant 1 walking uphill in sessions 1a, 1b and 2. Red bands indicate +/- 1SD

Participant 1 Uphill Walking Key Values								
Comparison	L1	L2	L3	L4	L5	L6	L7	L8
S1a P1	-0.03	0.12	0.45	0.01	0.16	0.12	0.06	0.11
S1a T1	-0.02	0.10	0.33	-0.01	0.36	0.12	0.07	0.20
S1a P2	-0.04	0.16	0.40	-0.02	0.57	0.10	0.07	0.21
S1a P1 (SD)	0.01	0.04	0.07	0.00	0.06	0.03	0.02	0.06
S1a T1 (SD)	0.01	0.02	0.04	0.01	0.26	0.01	0.02	0.13
S1a P2 (SD)	0.01	0.02	0.05	0.01	0.23	0.03	0.03	0.07
S1b P1	-0.04	0.14	0.39	0.01	0.27	0.07	0.07	0.12
S1b T1	-0.03	0.11	0.46	-0.02	0.45	0.12	0.07	0.19
S1b P2	-0.03	0.15	0.48	-0.01	0.47	0.17	0.10	0.22
S1b P1 (SD)	0.00	0.01	0.08	0.01	0.07	0.01	0.01	0.02
S1b T1 (SD)	0.01	0.02	0.03	0.00	0.20	0.02	0.01	0.02
S1b P2 (SD)	0.00	0.00	0.02	0.00	0.15	0.01	0.00	0.02
S2 P1	-0.02	0.22	0.34	0.00	0.29	0.00	0.01	-0.01
S2 T1	-0.03	0.08	0.30	-0.02	0.45	0.03	0.01	0.03
S2 P2	-0.02	0.11	0.48	-0.01	0.36	0.10	0.03	0.09
S2 P1 (SD)	0.00	0.04	0.04	0.01	0.12	0.00	0.02	0.01
S2 T1 (SD)	0.00	0.01	0.09	0.01	0.10	0.02	0.01	0.01
S2 P2 (SD)	0.00	0.01	0.06	0.00	0.10	0.02	0.01	0.01

Table 73 – Mean and standard deviation of load estimates for participant 1 in uphill walking in each test session

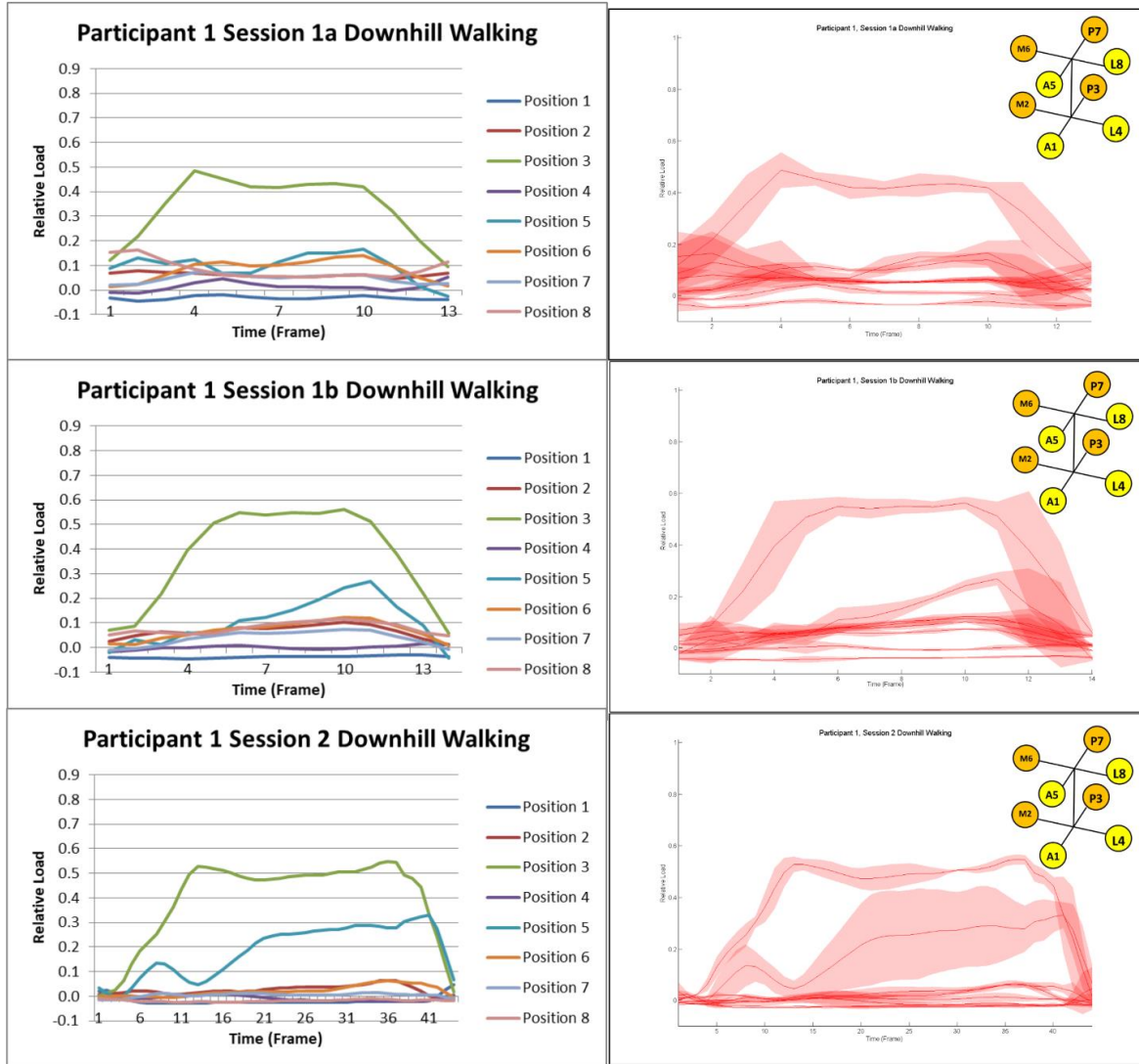


Figure 87 - Mean and variance of participant 1 walking downhill in sessions 1a, 1b and 2. Red bands indicate ± 1 SD

Participant 1 Downhill Walking Key Values								
Comparison	L1	L2	L3	L4	L5	L6	L7	L8
S1a P1	-0.02	0.07	0.49	0.03	0.12	0.11	0.07	0.09
S1a T1	-0.03	0.05	0.42	0.01	0.11	0.10	0.05	0.05
S1a P2	-0.02	0.06	0.42	0.01	0.17	0.14	0.06	0.06
S1a P1 (SD)	0.01	0.01	0.07	0.01	0.09	0.02	0.03	0.03
S1a T1 (SD)	0.00	0.00	0.03	0.01	0.04	0.01	0.00	0.01
S1a P2 (SD)	0.02	0.01	0.02	0.01	0.05	0.03	0.02	0.01
S1b P1	-0.04	0.07	0.51	0.01	0.05	0.07	0.05	0.06
S1b T1	-0.04	0.08	0.55	-0.01	0.15	0.10	0.06	0.10
S1b P2	-0.04	0.10	0.56	-0.01	0.24	0.12	0.07	0.12
S1b P1 (SD)	0.01	0.01	0.07	0.03	0.04	0.02	0.02	0.01
S1b T1 (SD)	0.00	0.01	0.03	0.00	0.03	0.01	0.01	0.01
S1b P2 (SD)	0.00	0.00	0.02	0.00	0.02	0.01	0.00	0.01
S2 P1	-0.03	0.01	0.53	0.00	0.05	0.01	0.00	-0.02
S2 T1	-0.02	0.04	0.49	-0.01	0.25	0.02	0.00	-0.02
S2 P2	-0.02	0.06	0.54	-0.02	0.28	0.06	0.01	-0.02
S2 P1 (SD)	0.00	0.01	0.03	0.01	0.03	0.00	0.01	0.00
S2 T1 (SD)	0.00	0.02	0.04	0.01	0.17	0.02	0.02	0.00
S2 P2 (SD)	0.00	0.01	0.02	0.01	0.09	0.01	0.01	0.00

Table 74 - Mean and standard deviation of load estimates during downhill walking in participant 1

The values of loads were compared to the flat walking condition collected at the same measurement session using t tests. A Bonferroni correction altered the p-value threshold to $p < 0.0006$. The results of this analysis are reported in Table 75 and Table 76.

Participant 1 Uphill walking p-values								
Comparison	L1	L2	L3	L4	L5	L6	L7	L8
P1S1a P1	0.248	0.596	0.489	0.598	0.617	0.226	1.000	0.880
P1S1a T1	0.124	0.085	0.028	0.785	0.311	0.668	1.000	0.243
P1S1a P2	0.248	0.006	0.049	0.169	0.063	0.004	0.513	0.117
P1S1b P1	0.104	<0.001	0.235	0.077	0.002	0.002	0.040	0.053
P1S1b T1	0.017	0.317	0.210	0.008	0.320	2.447	0.030	0.008
P1S1b P2	0.104	0.016	0.466	1.000	0.017	0.064	0.007	0.003
P1S2 P1	0.113	0.002	0.028	0.268	0.015	1.000	0.147	0.003
P1S2 T1	0.104	0.046	0.319	0.625	0.815	0.112	0.189	0.016
P1S2 P2	<0.001	0.048	0.487	0.098	0.029	0.038	0.012	<0.001

Table 75 - Significance calculations for participant 1 uphill walking compared to equivalent flat walking. Values in red represent significant changes

Participant 1 Downhill walking p-values								
Comparison	L1	L2	L3	L4	L5	L6	L7	L8
P1S1a P1	0.014	0.009	1.000	0.081	0.283	0.555	0.486	0.495
P1S1a T1	1.000	0.002	0.329	<0.001	0.009	0.550	0.095	0.008
P1S1a P2	0.369	0.030	0.049	0.250	0.104	0.513	0.093	0.010
P1S1b P1	0.271	0.258	0.415	0.732	0.546	0.007	0.781	0.249
P1S1b T1	0.008	0.723	0.015	0.375	0.058	0.020	0.015	0.888
P1S1b P2	1.000	0.899	0.217	0.365	0.477	0.010	0.188	0.815
P1S2 P1	0.113	0.002	0.028	0.268	0.015	1.000	0.147	0.669
P1S2 T1	0.104	0.046	0.319	0.137	0.815	0.112	0.189	0.016
P1S2 P2	<0.001	0.048	0.487	0.098	0.033	0.025	0.015	<0.001

Table 76 - Significance calculations for participant 1 downhill walking when compared to equivalent flat walking. Red values indicate significant differences

9.2.3 Discussion

Both participants completed the requested actions without issue or requiring additional forms of support. This is in part a demonstration of the high-quality movement that the participants

were capable of: slope walking is reported as one of the most challenging activities for amputee walkers.

The equipment failure experienced in this section is not thought to be a reflection of the task that was specified. As the slope walking tests were completed at the end of the test session, a battery fault on one of the collection nodes meant that some channels were not transmitted to the host PC. Unfortunately, one limitation of the neural network system is that all measurement channels are required for the estimate to remain valid.

During uphill walking, participant 1 demonstrated a walking pattern which increased posterior load and decreased anterior load, a result that was anticipated from a review of the literature (Chapter 2). The opposite pattern was observed in downhill walking: the anterior load was somewhat increased (although with reduced variance across the gait cycle, with the distinction between peaks and troughs greatly reduced), and the posterior load reduced. This is biomechanically consistent with the alteration in load to the socket caused from sagittal walking on slopes.

Limited statistical changes were observed in these tests, which were conducted on a per-session basis. This acted to increase the number of statistical tests carried out, reducing the p-value threshold. An alternative approach that combines the measurements across sessions would have acted to reduce this: however it was not clear that this would be effective in improving the statistical quality as the corresponding variance of the comparison would also increase. Nevertheless, some comparisons reached statistical significance. These were predominantly in the sagittal plane, as would be expected.

One reason suggested for the lack of change in load values during the downhill slope walking was that the participant used an active ankle design. This form of prosthetic ankle is intended to adjust the value of ankle flexion in response to changes in the angle of slope being navigated. If this feature functions as intended, a potential effect is that the overall impact of slope walking on socket loading is substantially mitigated. This may go some way to explain the relative lack of change in measured parameters when compared to other results in the

literature (Chapter 2) as these tend to use older forms of artificial foot/ankle without these features.

As with the evaluation of alignment changes, the very high gait competence of the included participants may have also limited the effects of the induced condition changes.

9.2.4 Summary

Walking on slopes generated reliable changes in the pattern of applied load in the socket of participant 1 that was generally consistent with biomechanical expectation. Statistically significant differences were observed in several measurement positions across the socket, predominantly in the sagittal plane.

Although changes were observed, these were reduced in magnitude when compared to those in previous literature. Several reasons are suggested for this effect: these include the use of a more sophisticated artificial ankle and the overall high quality of the participant's gait pattern.

9.3 Liner change

9.3.1 Methodology

Both participants used a prosthesis featuring a thick silicone liner between the socket and the residuum. The particular characteristics of this component are part of the device prescription, and the optimal solution may not be clear without attempting various models of component. Participant 1 had liners with two different diameters, their customary device used in the assessments presented in Chapter 8 and in sections 9.1 and 9.2 in this chapter, and one that was one size larger (i.e. one with a larger diameter, meaning that the compression applied to the residuum in lower). The participant doffed the test socket, changed to the alternate liner and re-donned the socket. The socket was kept in the neutral alignment that had been used in the previous test configuration. The participant then completed the same group of tests described in the preceding sections (varied weight standing, flat walking and slope walking). Results were then compared to those collected in the same measurement session.

9.3.2 Results

The graphs of socket load mean and variance are shown in Figure 88. This is the combination of four distinct gait cycles. The key values are tabulated in Table 77, with the values at key points in the gait cycle identified via the vertical force component from the force platform as before.

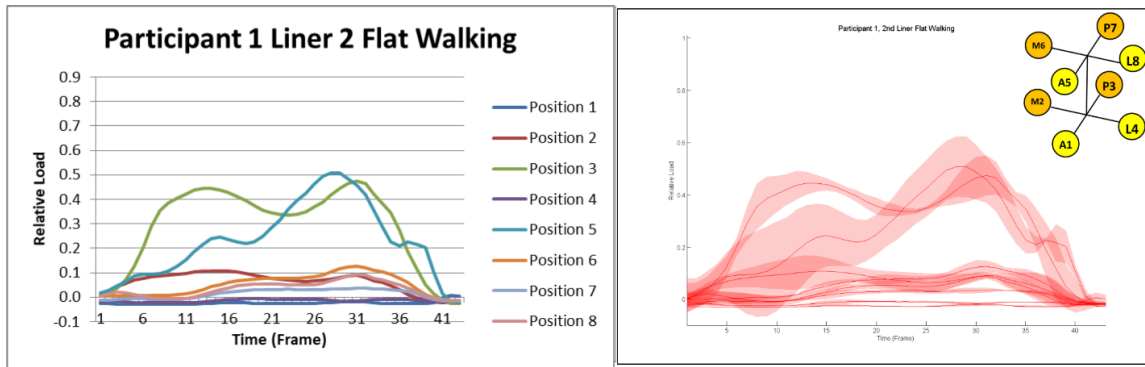


Figure 88 - Mean and variance of participant 1 flat walking using the second liner. Red bands indicate +/- 1SD

Participant 1, Session 2, Liner 2 Flat Walking								
Measure	L1	L2	L3	L4	L5	L6	L7	L8
P1 Mean	-0.02	0.11	0.44	-0.01	0.24	0.04	0.01	0.02
T1 Mean	-0.03	0.07	0.34	-0.01	0.36	0.08	0.03	0.05
P2 Mean	-0.02	0.09	0.47	-0.02	0.49	0.12	0.03	0.09
P1(SD)	0.00	0.06	0.03	0.01	0.13	0.01	0.01	0.01
T1 (SD)	0.00	0.03	0.01	0.00	0.10	0.01	0.01	0.02
P2 (SD)	0.01	0.01	0.08	0.01	0.10	0.03	0.01	0.02

Table 77 - Key values of socket load from participant 1 wearing the second liner in flat walking

The participant completed slope walking testing in the same manner as described in section 9.2. The average of four up-slope gait cycles is shown in Figure 89, and the average of four down-slope gait cycles in Figure 90. The values at key points identified by inspection are shown in Table 78 and Table 79.

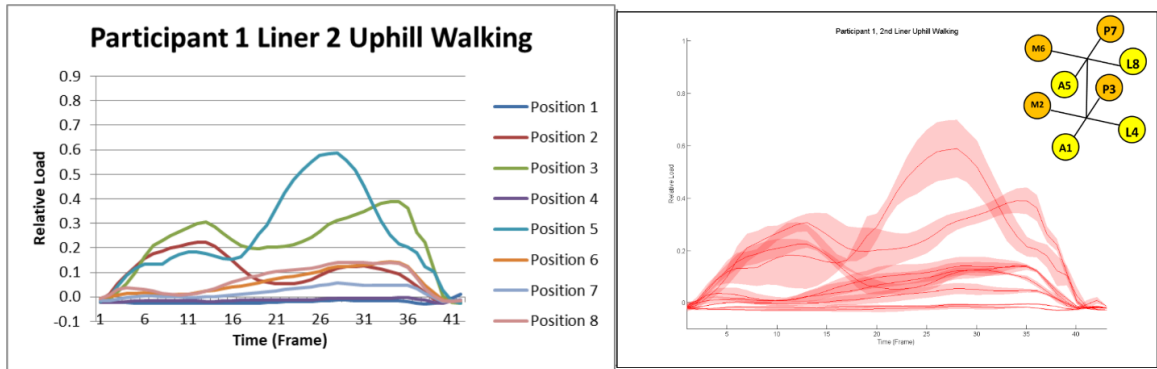


Figure 89 - Mean and variance of participant 1 uphill walking using the second liner. Red bands indicate +/- 1 SD

Participant 1, Session 2, Liner 2 Uphill Walking								
Measure	L1	L2	L3	L4	L5	L6	L7	L8
P1 Mean	-0.03	0.22	0.31	-0.02	0.18	0.03	0.00	0.02
T1 Mean	-0.02	0.05	0.21	-0.01	0.42	0.08	0.03	0.11
P2 Mean	-0.01	0.13	0.33	-0.01	0.52	0.13	0.05	0.14
P1(SD)	0.01	0.01	0.03	0.01	0.12	0.02	0.01	0.02
T1 (SD)	0.01	0.02	0.06	0.00	0.05	0.04	0.02	0.04
P2 (SD)	0.01	0.01	0.03	0.00	0.10	0.03	0.02	0.04

Table 78 - Key values of socket load from participant 1 wearing the second liner in uphill walking

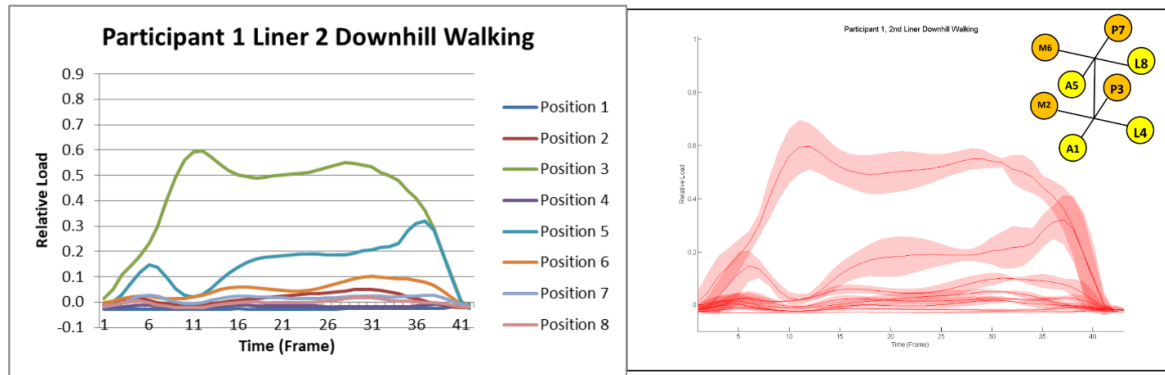


Figure 90 - Mean and variance of participant 1 downhill walking using the second liner. Red bands indicate +/- 1SD.

Participant 1, Session 2, Liner 2 Downhill Walking								
Measure	L1	L2	L3	L4	L5	L6	L7	L8
P1 Mean	-0.03	-0.01	0.60	-0.02	0.03	0.03	0.00	-0.02
T1 Mean	-0.03	0.02	0.50	-0.02	0.18	0.05	0.02	0.00
P2 Mean	-0.02	-0.01	0.02	-0.02	-0.01	0.00	-0.01	-0.01
P1(SD)	0.00	0.01	0.09	0.00	0.02	0.01	0.01	0.00
T1 (SD)	0.00	0.02	0.08	0.00	0.08	0.02	0.01	0.01
P2 (SD)	0.01	0.01	0.04	0.01	0.02	0.01	0.01	0.01

Table 79 - Key values of socket load from participant 1 wearing the second liner in downhill walking.

The results for dynamic studies were compared to the original liner using t-tests. This analysis is reported in Table 80. P-value thresholds were revised in line with other work in this chapter.

Participant 1, Session 2, Liner 2 P Values								
Comparison	L1	L2	L3	L4	L5	L6	L7	L8
Flat P1	0.098	0.954	0.803	0.537	0.062	0.003	0.036	0.001
Flat T1	0.094	0.340	0.366	0.047	0.567	<0.001	0.005	0.011
Flat P2	0.012	0.559	0.394	0.406	0.002	0.003	0.015	0.001
Up P1	1.000	0.960	0.271	0.237	0.218	0.015	0.588	0.254
Up T1	1.000	0.036	0.078	1.000	0.714	0.033	0.147	0.010
Up P2	1.000	0.083	0.005	<0.001	0.059	0.127	0.088	0.039
Down P1	1.000	0.049	0.190	0.023	0.412	0.002	0.703	1.000
Down T1	1.000	0.049	0.190	0.023	0.412	0.002	0.703	1.000
Down P2	0.212	<0.001	<0.001	0.200	0.001	<0.001	0.061	0.456

Table 80 - P Values calculated for new liner test comparisons. Significance threshold was revised to $p < 0.00069$. Values in red assessed as significant.

The participant was questioned as to which liner they preferred – they reported that there was not a great difference between them, but that the second (larger) liner was slightly more comfortable.

9.3.3 Discussion

The results presented in this section suggest that the change to a larger silicone liner had only a limited effect on the load measurements made by the system. The patterns recorded corresponded well with those collected in the same measurement session and with the flat, uphill and downhill walking conditions.

No significant changes were identified in four measurement channels in any condition (L1, L5, L7 and L8). During flat walking, pressure was significantly different in L6 in the central trough reading only, and the overall pattern was very similar to that of the original liner.

Similarly, the load changes in uphill walking were also minimal when compared to uphill walking completed with the original liner in the same session. Again, only one position demonstrated a significant change: the peak 2 measurement of load position 4. In downhill walking, the second peak demonstrated significant changes in three positions: L2, L3 and L6. Once again, a visual observation of the load measurements indicated that the loading pattern applied was consistent with the measurements taken in the original configuration.

The reasons for this are unclear. Potentially, the change to a new liner had only minimal effects, and so there was not a meaningful alteration to the imposed socket loading. This is supported by the relatively low variance between measurements across recording trials, and that the participant reported very little difference. However, it is possible that there were meaningful changes in the load distribution and that the system was insufficiently sensitive to detect these differences.

One potential reason for the minor changes in loading is that the participant necessarily doffed the liner and socket, and then donned the socket again. Although a matching positioning of the residuum within the socket is attempted, this may not be achieved in practice. Thus small changes in the load distribution may result. If this is the case, the magnitude of change would be expected to be similar to the effect of the within-session comparison of loading (described in Chapter 8.4). This in fact was the case – differences were greater than those measured without a liner change, but smaller than inter-session differences.

9.3.4 Summary

The ideal configuration of the prosthetic prescription remains unclear, and it is hoped that through systems that provide a quantitative measurement that some issues regarding the suitable use of devices where varying options exist.

Participant one completed a set of walking tests on flat, uphill and downhill slopes whilst wearing an alternative silicone liner that was one size larger than their customary device. When results were compared to the equivalent recordings obtained using the original liner, only minor changes were observed (and which failed to reach significance in the majority of cases). This potentially confirms the qualitative experience of the participant that the liner change had only a very minor effect on the quality of the prosthesis.

9.4 Combined perturbation

9.4.1 Methodology

The socket loading effects of combined changes in device alignment and walking condition have only a limited representation in the prosthetic literature. Of the studies included in a

systematic review of alignment changes with pressure measurement in transtibial amputees (Chapter 3), none performed an assessment of alignment in conditions other than flat walking.

In this work, to see if effects of alignment change and slope walking effects were additive, participant 1 completed the up- and down-slope walking described in section 9.2 using the prosthesis alignment changes described in section 9.1. The participant completed two walks up the slope and two down, with two gait cycles from steady state walking isolated in each case for four cycles in each condition. This was carried out twice with the induced varus and valgus alignment changes.

9.4.2 Results

The results from up-slope walking are shown in Figure 91 and Figure 92. The loads at key timings of the signals are reported in Table 81.

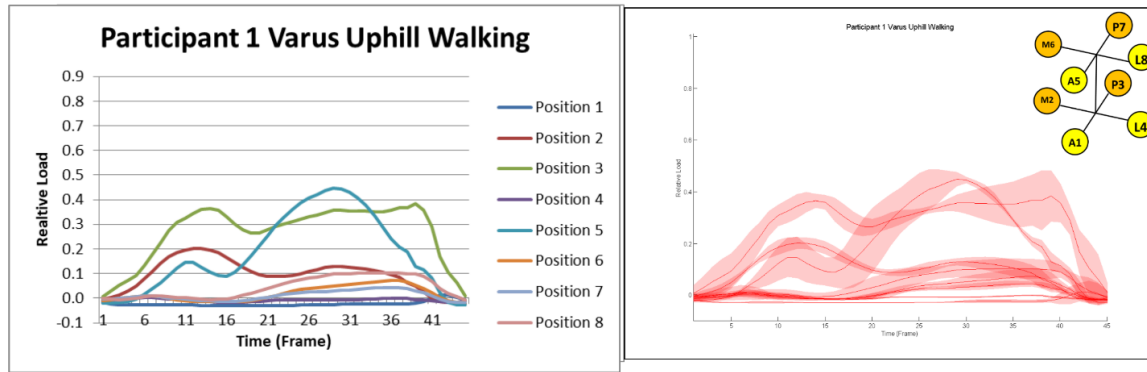


Figure 91 – Mean and variance of socket loads of participant 1 walking uphill with induced varus. Red bands indicate +/- 1SD

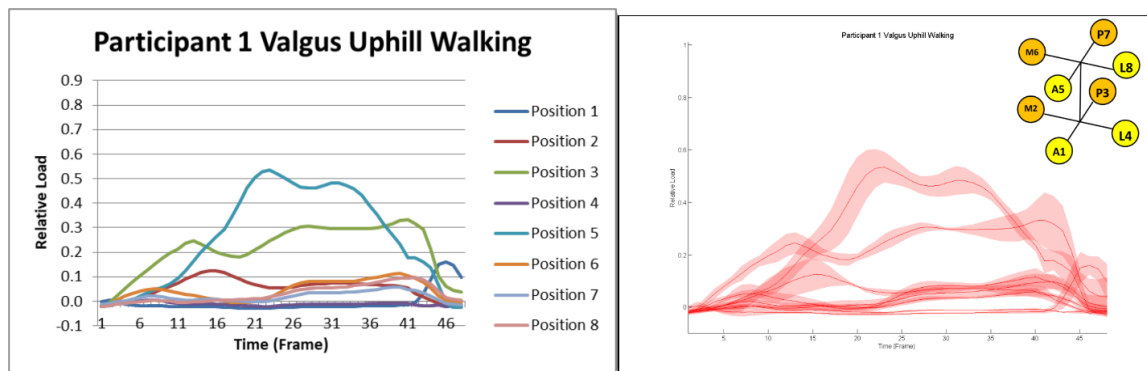


Figure 92 - Mean and variance of socket loads of participant 1 walking uphill with induced valgus. Red bands indicate +/- 1SD

Participant 1, Session 2, Uphill Walking								
Varus								
Measure	L1	L2	L3	L4	L5	L6	L7	L8
P1 Mean	-0.03	0.20	0.34	-0.01	0.15	-0.01	-0.01	0.00
T1 Mean	-0.03	0.12	0.35	-0.01	0.44	0.05	0.03	0.09
P2 Mean	0.00	0.01	-0.01	-0.01	-0.01	0.00	0.00	-0.01
P1(SD)	0.00	0.02	0.05	0.01	0.08	0.00	0.01	0.02
T1 (SD)	0.00	0.01	0.02	0.00	0.05	0.01	0.01	0.02
P2 (SD)	0.01	0.03	0.01	0.01	0.01	0.01	0.01	0.02
Valgus								
Measure	L1	L2	L3	L4	L5	L6	L7	L8
P1 Mean	-0.02	0.07	0.21	-0.01	0.09	0.03	0.01	0.00
T1 Mean	-0.02	0.07	0.31	-0.01	0.46	0.08	0.03	0.05
P2 Mean	-0.02	0.07	0.30	-0.01	0.43	0.09	0.04	0.07
P1(SD)	0.00	0.06	0.04	0.01	0.04	0.02	0.01	0.01
T1 (SD)	0.00	0.01	0.01	0.00	0.04	0.02	0.01	0.02
P2 (SD)	0.00	0.01	0.04	0.00	0.03	0.01	0.01	0.02

Table 81 - Key socket loads for participant 1 walking uphill with induced varus/valgus

The results (mean and variance) from down-slope walking are presented in Figure 93 and Figure 94, again as the average of the four collected trials. The results from this section are shown in Table 82.

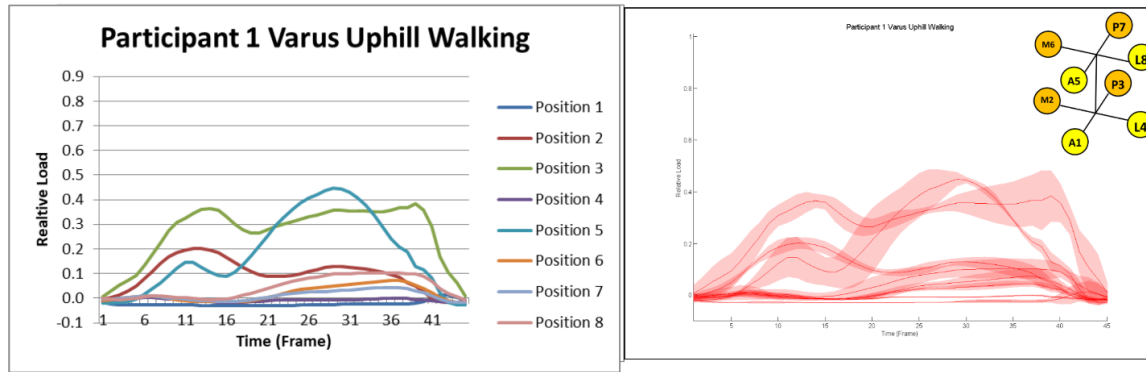


Figure 93 - Mean and variance of socket loads of participant 1 walking downhill with induced varus. Red bands indicate +/- 1SD

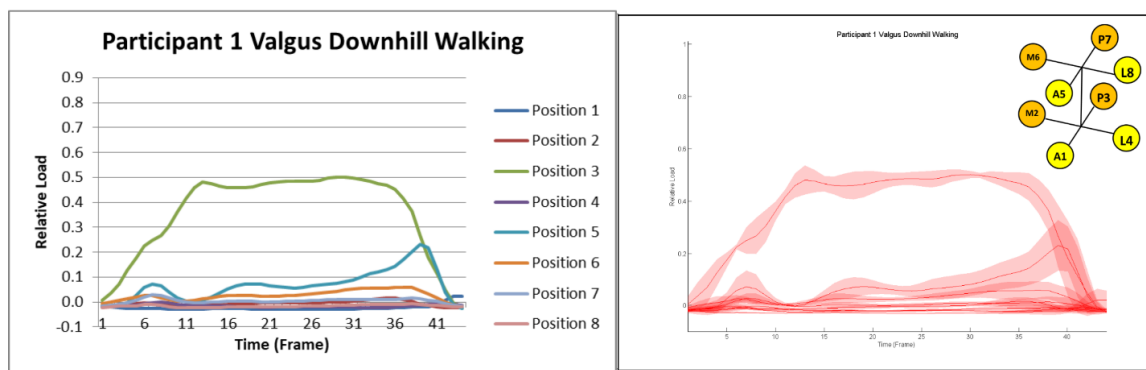


Figure 94 - Mean and variance of socket loads of participant 1 walking downhill with induced valgus. Red bands indicate +/- 1SD

Participant 1, Session 2, Downhill Walking								
Varus								
Measure	L1	L2	L3	L4	L5	L6	L7	L8
P1 Mean	-0.03	0.00	0.62	0.00	0.01	-0.01	-0.01	-0.02
T1 Mean	-0.03	0.02	0.56	-0.01	0.13	0.02	0.01	-0.01
P2 Mean	-0.01	0.00	-0.01	-0.01	-0.01	-0.01	-0.01	-0.01
P1(SD)	0.00	0.00	0.07	0.01	0.01	0.00	0.00	0.00
T1 (SD)	0.00	0.01	0.07	0.00	0.09	0.01	0.01	0.01
P2 (SD)	0.01	0.01	0.01	0.02	0.01	0.01	0.01	0.02
Valgus								
Measure	L1	L2	L3	L4	L5	L6	L7	L8
P1 Mean	-0.03	-0.01	0.36	-0.01	0.02	0.00	0.01	-0.02
T1 Mean	-0.03	0.00	0.48	-0.02	0.06	0.03	0.00	-0.02
P2 Mean	-0.03	0.01	0.49	-0.02	0.10	0.06	0.01	-0.01
P1(SD)	0.00	0.01	0.04	0.01	0.01	0.00	0.01	0.00
T1 (SD)	0.00	0.01	0.02	0.00	0.02	0.01	0.01	0.00
P2 (SD)	0.00	0.01	0.02	0.00	0.05	0.03	0.01	0.01

Table 82 - Key socket loads for participant 1 walking downhill with induced varus/valgus

The results were compared to slope walking in neutral alignment using a set of t-tests. The p-value threshold was revised to account for test repetitions. The results from this are shown in Table 83 and Table 84.

Participant 1, Combined Alignment/Slope Walking - Uphill								
Comparison	L1	L2	L3	L4	L5	L6	L7	L8
Varus P1	0.012	0.416	0.672	0.432	0.082	<0.001	0.296	0.425
Varus T1	0.008	0.002	0.293	0.362	0.858	0.212	0.057	0.003
Varus P2	0.120	0.001	<0.001	0.686	<0.001	<0.001	0.004	<0.001
Valgus P1	1.000	0.004	0.005	0.476	0.014	0.026	0.915	0.059
Valgus T1	1.000	0.178	0.906	1.000	0.769	0.011	0.021	0.138
Valgus P2	0.001	0.002	0.002	1.000	0.182	0.175	0.016	0.128

Table 83 - Significance calculations of difference between uphill walking and induced alignment uphill walking. Values in red represent significant differences to unaltered uphill walking (after adjustment of the p value threshold)

Participant 1, Combined Alignment/Slope Walking - Downhill								
Comparison	L1	L2	L3	L4	L5	L6	L7	L8
Varus P1	<0.001	0.021	0.046	0.852	0.064	<0.001	0.830	1.000
Varus T1	0.008	0.365	0.088	0.877	0.694	0.920	0.573	0.091
Varus P2	0.107	<0.001	<0.001	0.272	0.001	<0.001	0.043	0.832
Valgus P1	<0.001	0.002	0.001	0.268	0.120	0.098	0.211	1.000
Valgus T1	0.005	0.011	0.868	0.248	0.224	0.284	0.160	<0.001
Valgus P2	0.016	<0.001	0.007	1.000	0.015	0.732	0.890	0.261

Table 84 - Significance calculations of difference between downhill walking and induced alignment downhill walking. Values in red represent significant differences to unaltered downhill walking (after adjustment of the p value threshold)

9.4.3 Discussion

In uphill walking, the pattern established in section 9.2 was maintained: anterior loading was depressed and posterior loading increased. Walking was somewhat slower than in corresponding unaltered uphill walking: 0.73s compared to 0.67s. This is potentially the cause of the reduction in peak load as the maximum applied force will reduce with walking speed. Differences were also observed with between varus and valgus readings: with induced varus loading increased on position 2 in particular (distal-medial).

When results were compared to unaltered uphill walking, numerous statistically significant changes were identified. These were predominantly located at the second peak (i.e. propulsive) phase of gait. These values were lower than the corresponding value: this suggests that this function was impaired with the impact of additional misalignment of the prosthesis.

Downhill walking did not produce a change in walking speed; this remained consistent at a stance time of 0.67s. Significant changes were also identified within the varus and valgus induced alignment changes. Loads were increased at the posterior distal position relative to other positions. A visual inspection appeared to show a reduction at the anterior proximal position: however this did not reach significance (this was likely due to the large variance that was observed in this channel in the unaltered case, this variance was not present in other downhill sessions). Nevertheless, numerous changes were identified in both conditions and walking states.

The introduction of multiple perturbation sources in these walking tests appears to have been successful in inducing greater change in the recorded socket loads. Although it is thought that amputees of good walking ability can adapt to changes in walking conditions effectively, it is also thought that there are regions of acceptable device configurations. It may be the case that the additional effect on socket load caused by the slope walking is sufficient to force the configuration into a less acceptable position and making the amputee unable to compensate effectively. Thus although the tests described could only identify limited changes due to alignment or slope walking alone: in combination these were large enough to alter loading significantly.

One major limitation of this analysis is that results are restricted to one participant. Furthermore, this particular participant placed the majority of the recorded load through the anterior and posterior surfaces of the socket, in contrast to participant 2 who loaded the socket more evenly. As slope walking would be expected to alter sagittal plane moment most strongly, it is consistent that these changes were most obvious on the measured traces. The alignment changes were completed in the coronal plane: given that load was very low, it is unsurprising that the effects were minimal. However when this change was combined with additional alteration of the gait pattern, the changes became apparent.

9.4.4 Summary

The effect of changes in socket load in prosthesis alignment in conditions other than flat walking at comfortable speed has been substantially neglected in the amputee literature. This is surprising given the clinical interest in socket load, the commonality of alignment as a set-up requirement and the frequency with which amputees experience situations other than flat walking. The results produced in this sub-section are limited and are not comprehensive in terms of understanding this issue, but represent one of the few studies of this effect.

The results from this participant appear to suggest that combinations of perturbation produced a greater number of significant changes in load than either slope or alignment changes alone. Results were generally consistent with biomechanical expectation, but are restricted in applicability due to the relatively low number of tests and the characteristics of this particular participant.

9.5 Critical appraisal of approach

The results from this chapter are novel in terms of performing perturbed walking measurements using a neural network load measurement system. However, the applicability of the results are subject to some limitations as a result of the approach taken.

Most significant is the relatively low number of test sessions included within each average. The variance of some measurement channels (particularly those exhibiting more substantial loads) were often subject to large variance in the magnitude and timing of load. The effect of this is that significant changes are harder to establish within the comparisons made.

Although both participants in the study were capable of and did complete the required tests, equipment failure meant that only one set of slope walking data was available. The impact of this is mitigated by the substantial inter-participant differences observed, which restrict the meaningful combination of results.

The tests completed are not exhaustive: from the table presented in Chapter 1 alignment changes in particular can also be made in the sagittal and transverse planes, and by extension of the pylon. This was not carried out in this study (although slope walking is conceptually similar to sagittal alignment change). Similarly, the change in magnitude of alignment change was not investigated, providing a further avenue for future study.

9.6 Summary

Measurements of varus and valgus misalignment were investigated in two amputee participants during flat walking. The neural network system was capable of detecting limited changes in socket loading caused by this misalignment.

Values of socket load in one participant were evaluated in one participant walking on uphill and downhill slopes. Visual examination of mean socket loads suggested that the loading patterns altered in a manner consistent with biomechanical expectation. Significance calculations revealed limited change – this was likely due to high variance in key load parameters which meant statistical calculations were restricted in use.

One participant also completed walking tests with a different silicone liner. This recorded similar load distribution to the original liner, with patterns on slopes remaining consistent with earlier measurements. The measurements were consistent with the qualitative opinion of the amputee in that changes in socket fit were minimal.

The final set of measurements examined the combined effect of alignment changes and slope walking. This identified substantially more significant changes within the load distribution recorded in both varus and valgus configurations.

10. Critical Appraisal and Future Work

10.1 Introduction

In the previous chapters developments to an artificial neural network method of estimating prosthetic socket loads were described. In particular, techniques to configure the input data, network design, post-processing, and ensemble construction were investigated. The developed system was then tested in a range of clinically relevant situations – a pair of transtibial amputees wearing instrumented sockets during a set of standing and walking tasks, with induced perturbation of the prosthesis and environment.

This work concluded that there are meaningful improvements in accuracy and reliability that can be achieved via control of the specification of network ensembles. This acts to eliminate one of the major components of socket load variance, making the system able to provide a more consistent measure of a parameter of clinical importance. The developed system proved capable of distinguishing commonly encountered device and situation configurations.

In this section, the approach taken within each chapter is evaluated, and critically discussed. Each section will provide a suggestion for future work in this application.

10.2 Chapter 4 – Testing specification

One clear limitation of the presented work was the relatively low number of trials used to construct the averages. This was in some ways a practical limit, given the amount of time required for testing, construction of a socket, instrumentation and analysis. The commitment required for experimental studies was not too great, but the processing and analysis time was substantial. With work, the analysis of the produced data can be streamlined, and this would be required before the system is suitable for clinical use.

An alternative means of measurement that would provide many more gait cycles of information to analyse would be to utilise a treadmill for the collection of walking data. This has the advantage of providing a large number of consistent gait patterns, although at the cost of potentially forcing the participant into a particular walking style. Such an analysis makes

possible the supply of the data into pattern recognition software: similar to neural networks, these require a large number of cases to converge onto a solution. This could in turn provide the foundation for a system for identifying system configurations from the load distribution.

The developed system continued the use of foil strain gauges to provide the input to the neural network – these were a cost-effective and functional solution. Recent work completed in Malaysia has investigated the use of Fibre-Bragg sensors which are integrated into the socket wall to measure loading directly (Al-Fakih et al. 2013). These sensors are attractive for a number of reasons (see Chapter 2), and can form the basis for a Smart socket in which sensing is permanently integrated.

The participants recruited for this thesis were exclusively traumatic transtibial amputees. These were chosen to provide a comparison to existing work using this technique, and because these form the largest segment of the amputee population that require a weight-bearing prosthesis. The forms of adjustment in this group are more restricted than in other forms of prosthesis. The application of the neural network measurement system is not limited to transtibial amputees – in fact the system may be better suited to some newer forms of socket, such as the Hi-Fi socket. This form of socket features bands of closely fitting and open sections: other solutions of socket load measurement would struggle to accurately monitor these values. Future work may wish to examine additional socket types.

The system of socket loading described in Chapter 4 and used in previous work described in Chapter 2 may not form the most effective means of training the socket. The adequate representation of the loading is a critical aspect of the training process, and an isolated application of load in one position might not be most effective technique.

One method that has been proposed is to fill the socket with a surrogate stump (potentially using a gel or sand that would ‘flow’ in a manner reminiscent of tissue) and then loading in particular locations using an inflatable bladder. Then, as the pressure in the bladder increases, the forces are applied to the socket wall at that position, and the flow of the ‘stump’ loads the remainder of the socket in a more realistic manner. Such a technique has been examined in principle as part of a final year engineering project: although the training system was shown to

converge on a loading solution, this was not investigated in further detail. Future work may wish to examine alternative loading techniques.

One published work using the neural network method performed a sensitivity analysis of the instrumentation gauges in order to optimise the efficiency of the system and eliminate gauges that provided little distinguishing power (Amali et al. 2008). This task was not performed in the current study due to the much lower number of gauges used (single gauges as opposed to rosettes). Gauges are required to provide meaningful differentiation between loading states, but further advice on placement is not available. A potential avenue of research would be to model the socket and identify locations on the surface that respond to load effectively and target these.

10.3 Chapter 5 – Network design

In this chapter, the parameters varied were restricted to the method and magnitude of the noise injection performed onto the training data and on the number of hidden neurons within the neural networks. These features were chosen as these were readily controllable, and would cover both modelling of the input space and also the performance of the neural networks being considered. These are not the only possible ways of altering the design and training of neural networks.

One potential avenue is to vary the training algorithm in use. This project exclusively used the Levenberg-Marquardt training algorithm. This provided a good balance of training speed and reliability of convergence, and appeared to provide equivalent performance to previous work. Other training algorithms exist, but were not reviewed in detail (Hagan et al. 1996).

The noise injection models used within this thesis are also not exhaustive, but were instead chosen to represent two differing potential representations of the kinds of error seen within the system.

A detailed examination of the means of halting training was not considered, although it is possible that training was set to finish too early or too late. The measures included in the implementation appeared to be sufficient to produce a reasonable solution in each trained

network, but the potential to improve this via the training end procedure may yet yield improvements in generalisation performance.

10.4 Chapter 6 – Ensemble networks

The size of constructed ensembles was kept constant at 100. This was sufficient to provide meaningful variance in the solutions generated, and was able to demonstrate a normal distribution of each load estimate which is required for the ensemble combination to use a simple average. A time and storage efficiency may be made by reducing the size of ensembles: however this has the risk of increasing the weighting effect of outlier estimates.

Although constituent networks were varied in specification, aspects of the design and training of this process were not investigated. In particular, all networks used the same training algorithm (Levenberg-Marquardt). Although this choice is thought to represent a good balance between training performance and speed, it is possible that alternatives are available that provide a better solution to the identification of the transfer function of the system.

Some work has suggested that a selection of particular ensemble constituent networks may provide a better solution than including every value supplied in the final estimate (Zhou et al. 2002). For example, at positions where the load estimate is low or high, a bias in the selection of estimate constituents may be able to selectively improve the overall performance measure. This is a different method than the polynomial function described in Chapter 5 as it functions at the ensemble summation level rather than at the level of individual estimates or at the level of the sum of values. This may represent a practical means of developing the performance of the system further.

10.5 Chapter 7 – Polynomial functions

As described above, other options for providing a correction factor are possible. Polynomial functions were examined in this thesis and proved to adequately model the relationship between the error and applied load at function orders above 3 (and order did not meaningfully affect the quality of results at higher orders). Other functions may provide a better solution, but were not identified in this work.

More sophisticated means of correcting for network error may also exist. One in particular is the use of ‘stacked’ neural networks – ones that combine the results from constituent networks into a second model which is used to provide a more appropriate solution. Such a method that has been used in other situations is known as Wolpert stacking (Wolpert 1992). One future step for this project would be to apply such a technique to the data obtained within this work and evaluate this.

10.6 Chapter 8 – Static and dynamic recording

The recordings of dynamic walking used a relatively low sampling rate when compared to other work in the literature (Chapter 2). This choice was a functional restriction: the original design specification supplied devices thought to be capable of this, but in practical testing a battery limitation on one measurement node meant that wireless testing required a reduction in sampling rate. This will have missed certain high frequency events within the recordings. An increased sample rate would be required for pattern recognition using certain data summation techniques (e.g. frequency analysis of wavelet analysis).

Additional data sources may be usefully integrated into the neural network system. An example could be the segment angle (Yang and Hsu 2010), measured via accelerometers or measurements of stump volume through skin conductivity (Sanders et al. 2007). This could provide additional contextual information about the activity being assessed (the portion of the gait cycle for example, or the activity being performed) that can configure the output of the neural network more effectively. This plays to one of the advantages of neural networks in that the incorporation of disparate data sources is simple to carry out. In turn, this can become the basis for a smart prosthetic that can understand and react to changes in the prosthesis situation.

10.7 Chapter 9 – Perturbed walking

Perturbed walking is gaining in popularity as a means of providing distinguishing power in evaluating the competence of walking (in amputees, e.g. Sheehan et al. 2015 and other groups e.g. (Bruijn et al. 2013). Providing greater challenge to participants may be more effective at defining the limits of ability. Other methods of providing this perturbation have been evaluated in other research – for example terrain, other forms of alignment change, unstable/uneven

ground. A fuller quantification of the system performance may wish to examine these scenarios in more detail.

Interpretation of results is somewhat restricted by the difficulties in visualising the distribution of loads. This is common to all representations of socket loading – in contrast to other forms of biomechanical interface measurement (e.g. seated loads (Swain and Bader 2002) or in-shoe loading (Giacomozzi 2010) the interface has a 3D distribution. Attempting to understand the importance of measurements when these have a more complex positional and contextual presents a substantial issue in clinical use. Preliminary work to create a 3D representation of load distribution is shown in Figure 95.

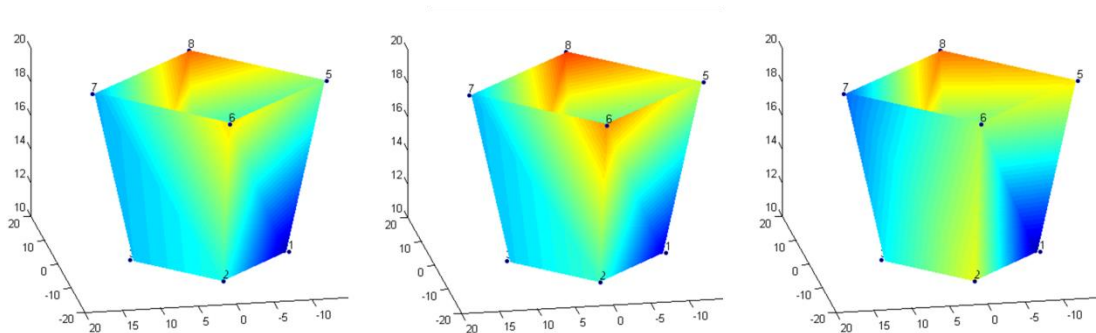


Figure 95 - Socket load distributions, participant 2 flat walking. Each vertex is scaled to the relative load, and colours linearly interpolated across the surface

Another approach may be to use techniques such as augmented reality. This has the potential to locate loading patterns on a socket model of the correct size and shape and to overlay these on the actual socket. An early example of this is shown in Figure 96.



Figure 96 - Augmented reality application prototyped in this project. Orientation and load values can be visualised on a realistic socket model

High quality presentation of the results is critical for clinical acceptance of measurement tools (Hafner and Sanders 2014). Future work should develop the application of these techniques.

10.8 Summary

Although the work presented in this thesis represents a significant improvement in the accuracy and reliability of the neural network solution to prosthetic socket load, and the extension of measurement to controlled static, dynamic and perturbed walking conditions, several aspects are subject to critical appraisal about the study design and future work.

In particular, these consist of additional features worthy of subsequent analysis and for alternative avenues of investigation. Key to this is the combination of additional sources of information into the neural network system: these have the potential to provide significant additional context to the information provided by the system. Future work should also extend the application into other areas of prosthetics and medical engineering more generally.

11. Conclusions

11.1 Background, Aims and Objectives

The understanding of socket load in ambulatory amputees is a clinical problem without a straightforward solution. Load distribution is recognised as a valuable measurement to aid in the design of prosthetic sockets, and yet engineering systems to provide this information are not in routine clinical use (Al-Fakih et al. 2016). Existing systems of socket load distribution measurement suffer from substantial issues which restrict practical use (Sewell et al. 2000).

In this work, a relatively recent approach to socket load measurement was investigated and evaluated. A system that utilises neural networks to estimate structural loads using measures of structural deformation had been developed, and the principle applied to prosthetic sockets in a limited set of experimental studies. With the essential function of the method demonstrated, this project examined the accuracy and reliability of the neural network system, the effectiveness of various techniques to quantitatively improve the quality of the load estimates and the capability for measurement in a range of static and dynamic situations.

A review of literature, presented in Chapter 2, reiterated the clinical importance of socket load measurement. Lower-limb amputation remains a relatively widespread issue in the UK and worldwide, with many individuals who require rehabilitation and life-long assistive technology to support ambulation and independence. Despite technological advancement in many areas of prosthetic care, socket technology was found to still be a largely artisanal process, limited to qualitative assessment and positive outcomes dependent on skill and experience of individual clinicians. The biomechanical importance of socket load as a determinant of high quality function was confirmed, as was the range of conceptual approaches taken to produce suitable devices.

A wider review of measurement techniques identified significant limitations in previously developed measurement techniques. Direct measurement of socket load is made difficult by the challenging environment within the socket, and the restrictions imposed by measurement equipment on the evaluation of clinically relevant situations limit the uptake of quantitative assessment.

A systematic review presented in Chapter 3 confirmed the difficulties in assessment: the relatively insubstantial literature in the field of transtibial socket load measurement in response to changes in device alignment was evaluated. Existing research was typically subject to numerous challenges to the confidence that could be placed in the measured outcomes, largely due to measurement and methodological limitations.

A detailed review of previous work on neural network load assessment was also undertaken. This identified that the technique held several advantages over contemporary methods: in the limited impact on the socket environment and the flexibility of the measurement output in particular. However, several areas relating to the technique remained unexplored – these included inter-network reliability and the impact of techniques designed to improve estimate quality. Further to this, the sensitivity of the system to the changes in load experienced during typical static and dynamic situations had not been established.

11.2 Contributions to knowledge

A summary of the conclusions of the previous chapters is presented here. These conclusions represent new understanding of the qualities and limitations of the neural network system as applied to the socket load problem.

- Varying hidden node architecture in an artificial neural network method of load measurement has a limited effect on prosthetic load estimation
- A linear noise injection model can significantly improve neural network accuracy on a prosthetic socket load problem when compared to constant magnitude noise injection
- Combining networks into ensembles provides a significant improvement in socket load estimates, and customising ensemble constituents improves this further
- Higher order polynomial functions are not effective in improving socket load estimates, but functions of at least 3rd order can provide a meaningful improvement in system accuracy
- Transtibial amputee static loading can be adequately monitored with a neural network load measurement system, although response is not completely representative of the changes in load magnitude

- Dynamic measurements of flat walking can be reliably obtained within and between sessions using a neural network load measurement system
- The system is sensitive to changes in load induced by walking on slopes, but it is unclear if coronal plane alignment can be detected

11.3 Limitations of Approach

There are several criticisms that can be made of the approach taken in this research.

Concerning the evaluation of training data processing techniques, the options evaluated were only a small subset of the possible techniques available. The choice to examine the noise injection methods was taken as this is a controllable parameter with a clear link to the possible models of error in the estimated transfer function. Similarly, the hidden neuron number is an adjustable value that can only be optimised by experiment, and so is a natural choice for examination of the network solution.

The relatively low number of participants and measurement sessions acts to somewhat restrict the applicability of the results. The nature of the recruited participants may also limit the strength of conclusions that may be drawn. By restricting recruitment to experienced and capable volunteers, emerging issues with using the technique more common clinical populations may not have been detected. However the nature of this technique as a research tool rather than one that has clearly demonstrated clinical suitability means that this approach can be justified as an extension to the proof-of-concept.

The neural network load estimate has also yet to be directly validated against a concurrent measurement system. The issue is complicated by the lack of a clear 'gold standard' in this field, along with several practical concerns that make producing a suitable comparison difficult. However, the results produced here and in previous work generally conform to biomechanical expectations about loading and the likely changes induced. Future work (Section 11.5) may wish to investigate this approach further.

11.4 Difficulties in Approach

Several aspects of the work presented had practical or procedural difficulties. The decision to use of-the-shelf hardware (Chapter 4) undoubtedly simplified some parts of the process of creating a viable measurement device, but also meant that time was spent attempting to suitably interface the measurement software with the neural network code. A bespoke solution may have resulted in a more convenient final system.

Experimental issues were also experienced. The nature of adjusting prosthetic limbs means that access to the pylon-socket connection is required, and when this is surrounded by instrumentation this was somewhat awkward, and tolerated only with the cooperation of the participants. In the less able or those with lower endurance/tolerance, the measurement interventions may have been less successful.

An issue that was only appreciated at the conclusion of the project was the importance of robust management of training data, calculated networks and the estimates of load. As already noted in this work, the volume of data generated in analyses of this type is extensive, and clarity in information management is valuable for coherent evaluation of results.

11.5 Implications

The results presented here broadly confirm the suitability of the neural network load measurement technique in applications of this type. What was unclear before the start of this work was the reliability of individual network's solutions to load problems. It is clear that 'acceptable' solutions may still contain significant variance, and countermeasures to account for this (e.g. the ensembles generated throughout this work) should be considered in future applications.

The system created demonstrated suitability for evaluating a range of clinically relevant changes in prosthesis set-up. This supports the continued development of this technique and the extension of the system to additional situations or measurement problems.

11.6 Recommendations for future work

There are several directions for future work that are suggested by the results of this work. One major possibility is to extend the methods to a larger cohort of participants. The majority of interventional studies in prosthetic research suffer from low numbers of participants, and so the consistency and applicability of results is unclear. On a similar note, all studies of neural network estimate of socket load have examined transtibial sockets. Whilst this has advantages in comparability of measurements, other amputation levels are yet to be examined.

Understanding the applicability of the approach to smaller sockets (e.g. paediatric sockets) or to larger sockets (e.g. transfemoral sockets) will be a useful extension of the work. Other structural measurement problems – both in medical engineering and elsewhere – may also benefit from the approach described.

The work presented here (and in previous iterations of systems of this type) used foil strain gauges mounted on the external surface. Although this approach has several practical advantages in a research setting, it is less likely to be acceptable in clinical settings. Research into embedded sensors in so-called ‘Smart’ sockets may be a suitable area for using neural network techniques to provide long-term device monitoring.

Another possibility is to examine further some of the methods discussed in this research. In chapter 7, the effect of post-estimate processing was examined. One option arising from the conclusions of that chapter is that improvements in accuracy and reliability of the ensemble solution may be possible if a more sophisticated means of aggregating the results of individual networks.

Although this study investigated several aspects of prosthesis configuration and walking perturbation, there remain several unexplored directions. The work presented here represents (to the author’s knowledge) one of the only examinations of combinations of alignment and perturbation change in prosthetic socket loading. Other adjustments or component changes are yet to be examined (as described in Chapter 3), and are eminently achievable with a system of the type described in this work.

The potential for more refined presentation of the results of load distribution analysis is another avenue for future research. As discussed in Chapter 10, the large volume of data generated by measurements of this kind makes unassisted analysis difficult. This is a particular problem in socket evaluation, as there is a clear three dimensional aspect to the relationship of loads, in combination with changes in the prosthesis components or configuration that have to be understood by clinicians. The brief investigation into augmented reality or other data presentation options reported in that chapter may serve as a basis for future development.

11.7 Final Considerations

The completion of the work presented here has reinforced the impression that this technique is a potentially powerful approach to the problem of non-invasive estimation of load distribution. The results generated in the experimental work confirm that the method is capable of high quality estimates, and, with suitable data conditioning and processing, can be a reliable and accurate means of assessment of prosthetic socket load. The review of the field of socket design and amputee management concluded that there remain significant gaps in theoretical and practical understanding. The development, testing and refinement of novel techniques to aid in solving the continuing issues of amputee comfort and function has to continue to provide the best in evidence-based care.

References

- Agilent, 1999 *Practical Strain Gauge Measurements* UK: Agilent Technologies
- Al-Fakih, A. E., Abu Osman, N. A. and Mahamad Adikan, R. F., 2016a. Techniques for Interface Stress Measurements within Prosthetic Sockets of Transtibial Amputees: A Review of the Past 50 Years of Research. *Sensors*, 16 (7), 1–30.
- Al-Fakih, A. E., Abu Osman, N. A., Rafiq, F., Adikan, M., Eshraghi, A. and Jahanshahi, P., 2016b. Development and Validation of Fiber Bragg Grating Sensing Pad for Interface Pressure Measurements. *IEEE Sensors Journal*, 16 (4), 965–974.
- Al-Fakih, A. E., Abu Osman, N. A., Eshraghi, A. and Mahamad Adikan, F. R., 2013. The capability of fiber Bragg grating sensors to measure amputees' trans-tibial stump/socket interface pressures. *Sensors*, 13 (8), 10348–57.
- Al-Fakih, A. E., Abu Osman, N. A. and Mahamad Adikan, F. R., 2012. The use of fiber Bragg grating sensors in biomechanics and rehabilitation applications: the state-of-the-art and ongoing research topics. *Sensors*, 12 (10), 12890–926.
- Amali, R., Cooper, S. and Noroozi, S., 2014. Application of Artificial Neural Network to Predict Static Loads on an Aircraft Rib. In: *International Conference on Artificial Intelligence Applications and Innovations* 576–584.
- Amali, R., Noroozi, S. and Vinney, J., 2000. The application of combined artificial neural network and finite element method in domain problems. In: *Proceedings of the International Conference on Engineering Applications of Neural Networks*. Kingston on Thames, UK
- Amali, R., Noroozi, S., Vinney, J., Sewell, P. and Andrews, S., 2001. A novel approach for assessing interfacial pressure between the prosthetic socket and the residual limb for below knee amputees using artificial neural networks. In: *Proceedings of the International Joint Conference on Neural Networks*. Washington DC, USA 2689–2693.
- Amali, R., Noroozi, S., Vinney, J., Sewell, P. and Andrews, S., 2006. Predicting Interfacial Loads between the Prosthetic Socket and the Residual Limb for Below-Knee Amputees - A Case Study. *Strain*, 42 (1), 3–10.
- Amali, R., Noroozi, S., Vinney, J., Sewell, P. and Andrews, S., 2008. An artificial intelligence approach for measurement and monitoring of pressure at the residual limb/socket interface – a clinical study. *Insight - Non-Destructive Testing and Condition Monitoring*, 50 (7), 374–383.
- Andrews, S., Noroozi, S., Vinney, J., Amali, R. and Sewell, P., 2001. A novel approach to assess

- prosthetic socket fit based on combining experimental and empirical techniques. *In: 10th World Congress of the International Society of Prosthetics and Orthotics*. Glasgow, UK
- Appoldt, F. A., Bennett, L. and Contini, R., 1968. Stump-socket pressure in lower extremity prostheses. *Journal of Biomechanics*, 1 (4), 247–257.
- Baker, R., 2013. *Measuring Walking: A Handbook of Clinical Gait Analysis*. London, UK: MacKeith Press.
- Barton, B. and Peat, J., 2014 *Medical Statistics: A Guide to SPSS, Data Analysis and Critical Appraisal*. Somerset, GB: BMJ Books.
- Barton, J. G., Lees, A., Lisboa, P. and Attfield, S., 2006. Visualisation of gait data with Kohonen self-organising neural maps. *Gait and Posture*, 24 (1), 46–53
- Bascou, J., Villa, C., Jacquot, D., Tonnelier, A., Mangenot, D., El Fettahi, N., Drevelle, X. and Fode, P., 2015. External Measurement of 3D Interactions Between the Residual Limb of an Amputee Person and the Socket. *Prosthetics and Orthotics International*, 39 (Supplement 1), 509.
- Baxt, W. G., 1992. Improving the accuracy of an artificial neural network using multiple differently trained networks. *Neural Computing*, 4 (5), 772–780.
- Beil, T. L. and Street, G. M., 2004. Comparison of interface pressures with pin and suction suspension systems. *Journal of Rehabilitation Research and Development*, 41 (6), 821–828.
- Beil, T. L., Street, G. M. and Covey, S. J., 2002. Interface pressures during ambulation using suction and vacuum-assisted prosthetic sockets. *Journal of Rehabilitation Research and Development*, 39 (6), 693–700.
- Beltran, E. J., Dingwell, J. B. and Wilken, J. M., 2014. Margins of stability in young adults with traumatic transtibial amputation walking in destabilizing environments. *Journal of Biomechanics*, 47 (5), 1138–43.
- Bennett, L., Kavner, D., Lee, B. K. and Trainor, F. A., 1979. Shear vs pressure as causative factors in skin blood flow occlusion. *Archives of Physical Medicine and Rehabilitation*, 60 (7), 309–14.
- Berne, N., Lawes, P., Solomonidis, S. E. and Paul, J. P., 1975. A shorter pylon transducer for measurement of prosthetic forces and moments during amputee gait. *Engineering in Medicine*, 4 (4), 6–8.
- Boone, D. A., 2005. *Investigation of socket reactions from transtibial prosthesis misalignment*.

Thesis (PhD) Hong Kong Polytechnic University

- Boone, D. A., Kobayashi, T., Chou, T. G., Arabian, A. K., Coleman, K. L., Orendurff, M. S. and Zhang, M., 2012. Perception of socket alignment perturbations in amputees with transtibial prostheses. *Journal of Rehabilitation Research and Development*, 49 (6), 843–53.
- Brand, P. W., 2006. Pressure Sores - the Problem. *Journal of Tissue Viability*, 16 (2), 9–11.
- Brånemark, R., Brånemark, P. I., Rydevik, B. and Myers, R. R., 2001. Osseointegration in skeletal reconstruction and rehabilitation: a review. *Journal of Rehabilitation Research and Development*, 38 (2), 175–181.
- Breakey, J. W., 1973. Criteria for the use of supracondylar and supracondylar-suprapatellar suspension for below-knee prostheses. *Prosthetics and Orthotics International*, 27 , 14–18.
- Breiman, L., 1996. Bagging Predictors. *Machine Learning*, 24 (421), 123–140.
- Bruijn, S. M., Meijer, O. G., Beek, P. J. and van Dieën, J. H., 2013. Assessing the stability of human locomotion: a review of current measures. *Journal of the Royal Society, Interface*, 10 (83), 20120999.
- Bui, K. M., Raugi, G. J., Nguyen, V. Q. and Reiber, G. E., 2009. Skin problems in individuals with lower-limb loss: Literature review and proposed classification system. *Journal of Rehabilitation Research and Development*, 46 (9), 1085–1090.
- Buis, A. and Convery, P., 1997. Calibration problems encountered while monitoring stump/socket interface pressures with force sensing resistors: techniques adopted to minimise inaccuracies. *Prosthetics and Orthotics International*, 21 (3), 179–82.
- Butler, K., Bowen, C., Hughes, A. M., Torah, R., Ayala, I., Tudor, J. and Metcalf, C. D., 2014. A systematic review of the key factors affecting tissue viability and rehabilitation outcomes of the residual limb in lower extremity traumatic amputees. *Journal of Tissue Viability*, 23 (3), 81–93.
- Chau, T., Young, S. and Redekop, S., 2005. Managing variability in the summary and comparison of gait data. *Journal of Neuroengineering and Rehabilitation*, 2 (1), 22.
- Childress, D. S. and Schnur, D. S., 1987. Computer Aided Analysis of Below-Knee Socket Pressure. *Journal of Rehabilitation Research and Development*, 25 (1), 18–19.
- Cluitmans, J. and Geboers, M., 1994. Experiences with respect to the ICEROSS system for transtibial prostheses. *Prosthetics and Orthotics International*, 18 , 78–83.

- Coleman, S., Nixon, J., Keen, J., Wilson, L., McGinnis, E., Dealey, C., Stubbs, N., Farrin, A., Dowding, D., Schols, J. M. G. A., Cuddigan, J., Berlowitz, D., Jude, E., Vowden, P., Schoonhoven, L., Bader, D. L., Gefen, A., Oomens, C. W. J. and Nelson, E. A., 2014. A new pressure ulcer conceptual framework. *Journal of Advanced Nursing*, 70 (10), 2222–34.
- Convery, P. and Buis, A., 1998. Conventional patellar-tendon-bearing (PTB) socket/stump interface dynamic pressure distributions recorded during the prosthetic stance phase of gait of a trans-tibial amputee. *Prosthetics and Orthotics International*, 22 (3), 193–8.
- Courtney, A., Orendurff, M. S. and Buis, A., 2016. Effect of alignment perturbations in a trans-tibial prosthesis user: A pilot study. *Journal of Rehabilitation Medicine*, 48 (4), 369–401.
- Curtze, C., Hof, A. L., Postema, K. and Otten, B., 2011. Over rough and smooth: amputee gait on an irregular surface. *Gait and Posture*, 33 (2), 292–6.
- Dickinson, A. S., Steer, J. W. and Worsley, P. R., 2017. Finite element analysis of the amputated lower limb: A systematic review and recommendations. *Medical Engineering & Physics*, 43, 1–18.
- Dillingham, T. R., Pezzin, L. E. and MacKenzie, E. J., 2002. Limb amputation and limb deficiency: epidemiology and recent trends in the United States. *Southern Medical Journal*, 95 (8), 875–883.
- Dillingham, T. R., Pezzin, L. E., MacKenzie, E. J. and Burgess, A. R., 2001. Use and satisfaction with prosthetic devices among persons with trauma-related amputations: a long-term outcome study. *American Journal of Physical Medicine and Rehabilitation*, 80 (8), 563–71.
- Dou, P., Jia, X., Suo, S., Wang, R. and Zhang, M., 2006. Pressure distribution at the stump/socket interface in transtibial amputees during walking on stairs, slope and non-flat road. *Clinical Biomechanics (Bristol, Avon)*, 21 (10), 1067–73.
- Dudek, N. L., Marks, M. B., Marshall, S. C. and Chardon, J. P., 2005. Dermatologic conditions associated with use of a lower-extremity prosthesis. *Archives of Physical Medicine and Rehabilitation*, 86 (4), 659–63.
- Dumas, R., Cheze, L. and Frossard, L., 2009. Loading applied on prosthetic knee of transfemoral amputee: comparison of inverse dynamics and direct measurements. *Gait and Posture*, 30 (4), 560–2.
- Eshraghi, A., Abu Osman, N. A., Gholizadeh, H., Ali, S. and Wan Abas, W. A. B., 2015. Interface Stress in Socket/Residual limb With Transtibial Prosthetic Suspension Systems During Locomotion on Slopes and Stairs. *American Journal of Physical Medicine and*

- Rehabilitation*, 94 (1), 1–10.
- Fernie, G. R. and Holliday, P. J., 1982. Volume Fluctuations in the Residual Limbs of Lower Limb Amputees. *Archives of Physical Medicine and Rehabilitation*, 63 (4), 162–165.
- Foort, J., 1965. The Patellar-Tendon-Bearing Prosthesis for Below-Knee Amputees: A Review of Technique and Criteria. *Artificial Limbs*, 1, 4–13.
- Frossard, L., Beck, J., Dillon, M. and Evans, J., 2003. Development and Preliminary Testing of a Device for the Direct Measurement of Forces and Moments in the Prosthetic Limb of Transfemoral Amputees during Activities of Daily Living. *Journal of Prosthetics and Orthotics*, 15 (4), 135–143.
- Frossard, L. and Stevenson, N., 2011. Categorization of activities of daily living of lower limb amputees during short-term use of a portable kinetic recording system: A preliminary study. *Journal of Prosthetics and Orthotics*, 23 (1), 2–11.
- Gabriel, R. A., 2013. *Between Flesh and Steel : A History of Military Medicine From the Middle Ages to the War in Afghanistan*. Dulles USA: Potomac Books Inc.
- Gailey, R. S., Nash, M. S., Atchley, T. A., Zilmer, R. M., Moline-Little, G. R., Morris-Cresswell, N. and Siebert, L. I., 1997. The effects of prosthesis mass on metabolic cost of ambulation in non-vascular trans-tibial amputees. *Prosthetics and Orthotics International*, 21 (1), 9–16.
- Gailey, R. S., Wenger, M. A., Raya, M., Kirk, N., Erbs, K., Spyropoulos, P. and Nash, M. S., 1994. Energy expenditure of trans-tibial amputees during ambulation at self-selected pace. *Prosthetics and Orthotics International*, 18 (2), 84–91.
- Gallagher, P., Franchignoni, F., Giordano, A. and MacLachlan, M., 2010. Trinity Amputation and Prosthesis Scales - A Psychometric Assessment Using Classical Test Theory and Rasch Analysis. *American Journal of Physical Medicine and Rehabilitation*, 89 (6), 487–496.
- Gallagher, P. and MacLachlan, M., 2000. Development and psychometric evaluation of the Trinity Amputation and Prosthesis Experience Scales (TAPES). *Rehabilitation Psychology*, 45 (2), 130–154.
- Galton, F., 1907. Vox Populi. *Nature*, 75 (7), 450–451.
- Galvão, J. R., Zamarreño, C. R., Martelli, C., Carlos, J., Arregui, F. J. and Matías, I. R., 2017. Strain Mapping in Carbon-Fiber Prosthesis Using Optical Fiber Sensors. *IEEE Sensors Journal*, 17 (1), 3–6.
- Gard, S., 2006. Use of Quantitative Gait Analysis for the Evaluation of Prosthetic Walking Performance. *Journal of Prosthetics and Orthotics*, 18 (6), 93–104.

- Garhwal, R., 2013. Artificial neural networks. *International Journal of Science Technology and Management*, 1 (4), 74–80.
- Gates, D. H., Dingwell, J. B., Scott, S. J., Sinitiski, E. H. and Wilken, J. M., 2012. Gait characteristics of individuals with transtibial amputations walking on a destabilizing rock surface. *Gait and Posture*, 36 (1), 33–9.
- Gates, D. H., Scott, S. J., Wilken, J. M. and Dingwell, J. B., 2013. Frontal plane dynamic margins of stability in individuals with and without transtibial amputation walking on a loose rock surface. *Gait and Posture*, 38 (4), 570–5.
- Gholipour, A. and Arjmand, N., 2016. Artificial neural networks to predict 3D spinal posture in reaching and lifting activities; Applications in biomechanical models. *Journal of Biomechanics*, 49 (13), 2946–2952.
- Gholizadeh, H., Abu Osman, N. A., Eshraghi, A., Arifin, N. and Chung, T. Y., 2016. A comparison of pressure distributions between two types of sockets in a bulbous stump. *Prosthetics and Orthotics International*, 40 (4), 509–516.
- Ghoseiri, K. and Safari, M. R., 2014. Prevalence of heat and perspiration discomfort inside prostheses: Literature review. *Journal of Rehabilitation Research and Development*, 51 (6), 855–68.
- Giacomozzi, C., 2010. Potentialities and Criticalities of Plantar Pressure Measurements in the Study of Foot Biomechanics: Devices, Methodologies and Applications. *Annali dell'Istituto Superiore Di Sanita*, 46 , 158–167.
- Goh, J. C. H., Lee, P. V. S. and Chong, S. Y., 2004. Comparative study between patellar-tendon-bearing and pressure cast prosthetic sockets. *Journal of Rehabilitation Research and Development*, 41 (3B), 491–501.
- Goldberger, A. L., Amaral, L. A. N., Hausdorff, J. M., Ivanov, P. C., Peng, C. K. and Stanley, H. E., 2002. Fractal dynamics in physiology: alterations with disease and aging. *Proceedings of the National Academy of Sciences of the United States of America*, 99 (s1), 2466–72.
- Hachisuka, K., Dozono, K., Ogata, H., Ohmine, S., Shitama, H. and Shinkoda, K., 1998. Total surface bearing below-knee prosthesis: advantages, disadvantages, and clinical implications. *Archives of Physical Medicine and Rehabilitation*, 79 (7), 783–9.
- Hachisuka, K., Nakamura, T., Ohmine, S., Shitama, H. and Shinkoda, K., 2001. Hygiene problems of residual limb and silicone liners in transtibial amputees wearing the total surface bearing socket. *Archives of Physical Medicine and Rehabilitation*, 82 (9), 1286–90.

- Hachisuka, K., Takahashi, M., Ogata, H., Ohmine, S., Shitama, H. and Shinkoda, K., 1998. Properties of the flexible pressure sensor under laboratory conditions simulating the internal environment of the total surface bearing socket. *Prosthetics and Orthotics International*, 22, 186–192.
- Hafner, B. J., 2008. *American Academy of Orthotists and Prosthetists State of the Science Evidence Report Guidelines*. Washington DC, USA
- Hafner, B. J. and Sanders, J. E., 2014. Considerations for development of sensing and monitoring tools to facilitate treatment and care of persons with lower-limb loss: A review. *Journal of Rehabilitation Research and Development*, 51 (1), 1–14.
- Hagan, M. T., Demuth, H. B. and Beale, M. H., 1996. *Neural network design*. London, UK: PWS Publishing.
- Hagan, M. T. and Menhaj, M. B., 1994. Training Feedforward Networks with the Marquardt Algorithm. *IEEE Transactions on Neural Networks*, 5 (6), 989–993.
- Hagberg, K. and Brånemark, R., 2001. Consequences of non-vascular trans-femoral amputation: A survey of quality of life, prosthetic use and problems. *Prosthetics and Orthotics International*, 25 (3), 186–194.
- Hagberg, K. and Brånemark, R., 2009. One hundred patients treated with osseointegrated transfemoral amputation prostheses—Rehabilitation perspective. *Journal of Rehabilitation Research and Development*, 46 (3), 331–344.
- Hansen, L. K. and Salamon, P., 1990. Neural network ensembles. *IEEE Transactions on Pattern Analysis and Machine Intelligence*, 12 (10), 993–1001.
- Hanspal, R. S., Fisher, K. and Nieveen, R., 2003. Prosthetic socket fit comfort score. *Disability and Rehabilitation*, 25 (22), 1278–1280.
- Hausdorff, J. M., 2005. Gait variability: methods, modeling and meaning. *Journal of Neuroengineering and Rehabilitation*, 2 (19)
- Hebert, J. S., Wolfe, D. L., Miller, W. C., Deathe, A. B., Devlin, M. and Pallaveshi, L., 2009. Outcome measures in amputation rehabilitation: ICF body functions. *Disability and Rehabilitation*, 31 (19), 1541–1554.
- Heinemann, A. W., Connelly, L., Ehrlich-Jones, L. and Fatone, S., 2014. Outcome Instruments for Prosthetics: Clinical Applications. *Physical Medicine and Rehabilitation Clinics of North America*, 25 (1), 179–198.
- Highsmith, M. J., Kahle, J. T., Miro, R. M., Orendurff, M. S., Lewandowski, A. L., Orriola, J. J.,

- Sutton, B. and Ertl, J. P., 2016. Prosthetic interventions for people with transtibial amputation: Systematic review and metaanalysis of high-quality prospective literature and systematic reviews. *Journal of Rehabilitation Research and Development*, 53 (2), 157–184.
- Hillery, S. C., Wallace, E. S., McIlhagger, R. and Watson, P., 1997. The effect of changing the inertia of a trans-tibial dynamic elastic response prosthesis on the kinematics and ground reaction force patterns. *Prosthetics and Orthotics International*, 21 (2), 114–123.
- Hof, A. L., van Bockel, R. M., Schoppen, T. and Postema, K., 2007. Control of lateral balance in walking. Experimental findings in normal subjects and above-knee amputees. *Gait and Posture*, 25 (2), 250–8.
- Hoffmann, K., 1986. *Applying the Wheatstone Bridge Circuit*. 3rd Edition. Hottinger Baldwin Messtechnik Darmstadt, Germany.
- Hsu, L. H., Huang, G. F., Lu, C., Hong, D. Y. and Liu, S. H., 2010. The development of a rapid prototyping prosthetic socket coated with a resin layer for transtibial amputees. *Prosthetics and Orthotics International*, 34 (1), 37–45.
- Huang, Z. J. and Luo, L., 2015. It takes the world to understand the brain. *Science*, 350 (6256), 42–44.
- Jia, X., Suo, S., Meng, F. and Wang, R., 2008. Effects of alignment on interface pressure for transtibial amputee during walking. *Disability and Rehabilitation: Assistive Technology*, 3 (6), 339–43.
- Jia, X., Wang, R., Zhang, M. and Li, X., 2008. Influence of prosthetic sagittal alignment on trans-tibial amputee gait and compensating pattern: A case study. *Tsinghua Science and Technology*, 13 (5), 581–586.
- Jia, X., Zhang, M. and Lee, W. C., 2004. Load transfer mechanics between trans-tibial prosthetic socket and residual limb--dynamic effects. *Journal of Biomechanics*, 37 (9), 1371–7.
- Jimenez, D., 1998. Dynamically Weighted Ensemble Neural Networks for Classification. In: *IEEE World Congress on Computational Intelligence*. Anchorage, Alaska, USA 753–756.
- Jimenez, D., Darm, T., Rogers, B. and Walsh, N., 1997. Locating Anatomical Landmarks for Prosthetics Design using Ensemble Neural Networks. In: *International Conference on Neural Networks*. Houston, Texas, USA 81–85.
- Jordan, R. W., Marks, A. and Higman, D., 2012. The cost of major lower limb amputation: a 12-year experience. *Prosthetics and Orthotics International*, 36 (4), 430–434.

- Kamruzzaman, J. and Begg, R. K., 2006. Support Vector Machines and Other Pattern Recognition Approaches to the Diagnosis of Cerebral Palsy Gait. *IEEE Transactions on Biomedical Engineering*, 53 (12), 2479–2490
- Kanade, R., van Deursen, R., Burton, J., Davies, V., Harding, K. and Price, P., 2007. Re-amputation occurrence in the diabetic population in South Wales, UK. *International Wound Journal*, 4 (4), 344–353.
- Kang, P., Kim, J. H. and Roh, J. S., 2006. Pressure Distribution in Stump/Socket Interface in Response to Socket Flexion Angle Changes in Trans-Tibial Prostheses with Silicone Liner. *Physical Therapy Korea*, 13 (4), 71–78.
- Kent, J. A. and Franklyn-Miller, A., 2011. Biomechanical models in the study of lower limb amputee kinematics: a review. *Prosthetics and Orthotics International*, 35 (2), 124–39.
- Klute, G. K., Berge, J. S., Biggs, W., Pongnumkul, S., Popovic, Z. and Curless, B., 2011. Vacuum-assisted socket suspension compared with pin suspension for lower extremity amputees: effect on fit, activity, and limb volume. *Archives of Physical Medicine and Rehabilitation*, 92 (10), 1570–5.
- Klute, G. K., Kantor, C., Darrouzet, C., Wild, H., Wilkinson, S., Iveljic, S. and Creasey, G., 2009. Lower-limb amputee needs assessment using multistakeholder focus-group approach. *Journal of Rehabilitation Research and Development*, 46 (3), 293–304.
- Kobayashi, T., Arabian, A. K., Orendurff, M. S., Rosenbaum-Chou, T. G. and Boone, D. A., 2014a. Effect of alignment changes on socket reaction moments while walking in transtibial prostheses with energy storage and return feet. *Clinical Biomechanics (Bristol, Avon)*, 29 (1), 47–56.
- Kobayashi, T., Orendurff, M. S., Arabian, A. K., Rosenbaum-Chou, T. G. and Boone, D. A., 2014b. Effect of prosthetic alignment changes on socket reaction moment impulse during walking in transtibial amputees. *Journal of Biomechanics*, 47 (6), 1315–1323.
- Kobayashi, T., Orendurff, M. S. and Boone, D. A., 2015. Dynamic alignment of transtibial prostheses through visualization of socket reaction moments. *Prosthetics and Orthotics International*, 39 (6), 512–516.
- Kobayashi, T., Orendurff, M. S., Zhang, M. and Boone, D. A., 2014c. Individual responses to alignment perturbations in socket reaction moments while walking in transtibial prostheses. *Clinical Biomechanics*, 29 (5), 590–594.
- Koc, E., Tunca, M., Akar, A., Erbil, A. H., Demiralp, B. and Arca, E., 2008. Skin problems in

- amputees: a descriptive study. *International Journal of Dermatology*, 47 (5), 463–6.
- Koehler, S. R., Dhaher, Y. Y. and Hansen, A. H., 2014. Cross-validation of a portable, six-degree-of-freedom load cell for use in lower-limb prosthetics research. *Journal of Biomechanics*, 47 (6), 1542–7.
- Kristinsson, O., 1993. The ICEROSS concept: a discussion of a philosophy. *Prosthetics and Orthotics International*, 17 (1), 49–55.
- Krogh, A. and Vedelsby, J., 1994. Neural Network Ensembles, Cross Validation, and Active Learning. *In: Advances in Neural Information Processing Systems* 231–238.
- Laing, S., Lee, P. V. S. and Goh, J. C. H., 2011. Engineering a trans-tibial prosthetic socket for the lower limb amputee. *Annals of the Academy of Medicine, Singapore*, 40 (5), 252–9.
- Laszczak, P., Jiang, L., Bader, D. L., Moser, D. and Zahedi, S., 2015. Development and validation of a 3D-printed interfacial stress sensor for prosthetic applications. *Medical Engineering and Physics*, 37 (1), 132–137.
- Lee, W. C., Zhang, M. and Mak, A. F., 2005. Regional differences in pain threshold and tolerance of the transtibial residual limb: including the effects of age and interface material. *Archives of Physical Medicine and Rehabilitation*, 86 (4), 641–9.
- Legro, M. W., Reiber, G. E., del Aguila, M., Ajax, M. J., Boone, D. A., Larsen, J. A., Smith, D. G. and Sangeorzan, B., 1999. Issues of importance reported by persons with lower limb amputations and prostheses. *Journal of Rehabilitation Research and Development*, 36 (3), 155–63.
- Lehmann, J. F., Price, R., Okumura, R., Questad, K., De Lateur, B. J. and Négretot, A., 1998. Mass and mass distribution of below-knee prostheses: Effect on gait efficacy and self-selected walking speed. *Archives of Physical Medicine and Rehabilitation*, 79 (2), 162–168.
- Levy, S. W., 1980. Skin problems of the leg amputee. *Prosthetics and Orthotics International*, 4 (1), 37–44.
- Lin, C. C., Chang, C. H., Wu, C. L., Chung, K. C. and Liao, I. C., 2004. Effects of liner stiffness for trans-tibial prosthesis: a finite element contact model. *Medical Engineering and Physics*, 26 (1), 1–9.
- Linder-Ganz, E. and Gefen, A., 2008. Stress Analyses Coupled With Damage Laws to Determine Biomechanical Risk Factors for Deep Tissue Injury During Sitting. *Journal of Biomechanical Engineering*, 131 (1), 11003.
- Loerakker, S., Manders, E., Strijkers, G. J., Nicolay, K., Baaijens, F. P. T., Bader, D. L. and

- Oomens, C. W. J., 2011. The effects of deformation, ischemia, and reperfusion on the development of muscle damage during prolonged loading. *Journal of Applied Physiology*, 111 (4), 1168–1177.
- Loeser, J. D. and Treede, R. D., 2008. The Kyoto Protocol of IASP Basic Pain Terminology. *Pain*, 137 (3), 473–477.
- Lyon, C. C., Kulkarni, J., Zimerson, E., van Ross, E. and Beck, M. H., 2000. Skin disorders in amputees. *Journal of the American Academy of Dermatology*, 42 (3), 501–7.
- Mak, A. F., Zhang, M. and Boone, D. A., 2001. State-of-the-art research in lower-limb prosthetic biomechanics-socket interface: a review. *Journal of Rehabilitation Research and Development*, 38 (2), 161–74.
- Mak, A. F., Zhang, M. and Tam, E. W. C., 2010. Biomechanics of Pressure Ulcer in Body Tissues Interacting with External Forces during Locomotion. *Annual Review of Biomedical Engineering*, 12, 29–53.
- McCulloch, W. S. and Pitts, W., 1943. A logical calculus of the ideas immanent in nervous activity. *The Bulletin of Mathematical Biophysics*, 5 (4), 115–133.
- McGinley, J., Wolfe, R., Morris, M., Pandy, M. and Baker, R., 2014. Variability of walking in able-bodied adults across different time intervals. *Journal of Physical Medicine and Rehabilitation Sciences*, 17, 6–10.
- Meier, R. H., Meeks, E. D. and Herman, R. M., 1973. Stump-socket fit of below-knee prostheses: comparison of three methods of measurement. *Archives of Physical Medicine and Rehabilitation*, 54 (12), 553–8.
- Meulenbelt, H. E., Geertzen, J. H. B., Jonkman, M. F. and Dijkstra, P. U., 2009. Determinants of skin problems of the stump in lower-limb amputees. *Archives of Physical Medicine and Rehabilitation*, 90 (1), 74–81.
- Mueller, M. J. and Maluf, K. S., 2002. Tissue adaptation to physical stress: a proposed “Physical Stress Theory” to guide physical therapist practice, education, and research. *Physical Therapy*, 82 (4), 383–403.
- NASDAB, 1999. *National Amputee Statistical Database 1997-1998*. Edinburgh, UK
- Neumann, E. S., 2009. State-of-the-science review of transtibial prosthesis alignment perturbation. *Journal of Prosthetics and Orthotics*, 21 (4), 175–187.
- Neumann, E. S., Brink, J., Yalamanchili, K. and Lee, J. S., 2013a Regression Estimates of Pressure on Transtibial Residual Limbs Using Load Cell Measurements of the Forces and Moments

- Occurring at the Base of the Socket. *Journal of Prosthetics and Orthotics*, 25 (1), 1–12.
- Neumann, E. S., Brink, J., Yalamanchili, K. and Lee, J. S., 2013b Use of a load cell and force-moment curves to compare transverse plane moment loads on transtibial residual limbs: a preliminary investigation. *Prosthetics and Orthotics International*, 38 (3), 253–262.
- Neumann, E. S., Yalamanchili, K., Brink, J. and Lee, J. S., 2012. Transducer-based comparisons of the prosthetic feet used by transtibial amputees for different walking activities: a pilot study. *Prosthetics and Orthotics International*, 36 (2), 203–16.
- Nielsen, C. C., 1991. A Survey of Amputees: Functional Level and Life Satisfaction, Information Needs, and the Prosthetist's Role. *Journal of Prosthetics and Orthotics*, 3 (1), 125–129.
- Nielsen, C. C., Psonak, R. A. and Kalter, T. L., 1989. Factors Affecting the Use of Prosthetic Services. *Journal of Prosthetics and Orthotics*, 1 (4), 242–249.
- Noroozi, S., Amali, R. and Vinney, J., 2004. Inverse Problem Approach using Photoelastic Analysis and Artificial Neural Networks in Tandem Introduction to Photoelasticity. *Strain*, 40 (2), 73–77.
- Noroozi, S., Amali, R., Vinney, J. and Sewell, P., 2005. Use of Artificial Neural Networks for Real Time Determination of Loads on In-Service Components. *International Journal of Engineering Simulation*, 6 (1), 3–8.
- Noroozi, S., Rahman, A., Dupac, M., Ong, Z., Al-Attas, M. and Davenport, P., 2016. Condition monitoring and diagnostics of an extruder motor and its gearbox vibration problem. *Insight - Non-Destructive Testing and Condition Monitoring*, 58 (2), 101–107.
- Noroozi, S., Sewell, P. and Vinney, J., 2006. The application of a hybrid inverse boundary element problem engine for the solution of potential problems. *CMC Tech Science Press*, 4 (3), 171.
- Pandey, B. and Mishra, R. B., 2009. Knowledge and intelligent computing system in medicine. *Computers in Biology and Medicine*, 39 (3), 215–30.
- Papaoiannou, G., Mitrogiannis, C., Nianios, G. and Fiedler, G., 2010. Assessment of Internal and External Prosthesis Kinematics during Strenuous Activities Using Dynamic Roentgen Stereophotogrammetric Analysis. *Journal of Prosthetics and Orthotics*, 22 (2), 91–105.
- Pearson, J. R., Holmgren, G., March, L. and Oberg, K., 1973. Pressures in critical regions of the below-knee patellar-tendon-bearing prosthesis. *Bulletin of Prosthetics Research*, 10 (19), 52–76.
- Peery, J. T., Klute, G. K., Blevins, J. J. and Ledoux, W. R., 2006. A three-dimensional finite element model of the transibial residual limb and prosthetic socket to predict skin

- temperatures. *IEEE Transactions on Neural Systems and Rehabilitation Engineering*, 14 (3), 336–343.
- Pezzin, L. E., Dillingham, T. R. and MacKenzie, E. J., 2000. Rehabilitation and the long-term outcomes of persons with trauma-related amputations. *Archives of Physical Medicine and Rehabilitation*, 81 (3), 292–300.
- Pezzin, L. E., Dillingham, T. R., MacKenzie, E. J., Ephraim, P. L. and Rossbach, P., 2004. Use and satisfaction with prosthetic limb devices and related services. *Archives of Physical Medicine and Rehabilitation*, 85 (5), 723–729.
- Pirouzi, G., Abu Osman, N. A., Eshraghi, A., Ali, S., Gholizadeh, H. and Wan Abas, W. A. B., 2014. Review of the Socket Design and Interface Pressure Measurement for Transtibial Prosthesis. *Scientific World Journal*, 2014
- Polliack, A. A. and Landsberger, S., MacNeal, D.R., Craig, D., Sieh, R., 1998. Scientific Characterization of the Rincoe Socket and Tekscan F-Socket Interface Pressure Measurement Systems: Implications for Clinical Utility. *Rehabilitation Engineering Program*. California, USA
- Polliack, A. A., Sieh, R. C., Craig, D. D., Landsberger, S., McNeil, D. R. and Ayyappa, E., 2000. Scientific validation of two commercial pressure sensor systems for prosthetic socket fit. *Prosthetics and Orthotics International*, 24 (1), 63–73.
- Portnoy, S., Siev-Ner, I., Yizhar, Z., Kristal, A., Shabshin, N. and Gefen, A., 2009. Surgical and morphological factors that affect internal mechanical loads in soft tissues of the transtibial residuum. *Annals of Biomedical Engineering*, 37 (12), 2583–2605.
- Portnoy, S., van Haare, J., Geers, R. P. J., Kristal, A., Siev-Ner, I., Seelen, H. A. M., Oomens, C. W. J. and Gefen, A., 2010. Real-time subject-specific analyses of dynamic internal tissue loads in the residual limb of transtibial amputees. *Medical Engineering and Physics*, 32 (4), 312–23.
- Portnoy, S., Yarnitzky, G., Yizhar, Z., Kristal, A., Oppenheim, U., Siev-Ner, I. and Gefen, A., 2007. Real-time patient-specific finite element analysis of internal stresses in the soft tissues of a residual limb: a new tool for prosthetic fitting. *Annals of Biomedical Engineering*, 35 (1), 120–35.
- Portnoy, S., Yizhar, Z., Shabshin, N., Itzchak, Y., Kristal, A., Dotan-Marom, Y., Siev-Ner, I. and Gefen, A., 2008. Internal mechanical conditions in the soft tissues of a residual limb of a trans-tibial amputee. *Journal of Biomechanics*, 41 (9), 1897–909.

- Quesada, P. and Skinner, H. B., 1991. Analysis of a below-knee patellar tendon-bearing prosthesis: A finite element study. *Journal of Rehabilitation Research and Development*, 28 (3), 1–12.
- Radcliffe, C. W. and Foort, J., 1961. *The Patellar-Tendon Bearing Below-Knee Prosthesis*. Biomechanics Laboratory, Berkeley USA
- Rae, J. W. and Cockrell, J. L., 1971. Interface pressure and stress distribution in prosthetic fitting. *Bulletin of Prosthetics Research*, 10 (15), 64–111.
- Rajtukova, V., Michalikova, M., Bednarcikova, L., Balogova, A. and Zivcak, J., 2014. Biomechanics of lower limb prostheses. *Procedia Engineering*, 96, 382–391.
- Ramazani, M. R., Noroozi, S., Sewell, P., Khandan, R. and Cripps, B., 2013. Using artificial neural networks and strain gauges for the determination of static loads on a thin square fully-constrained composite marine panel subjected to a large central displacement. *Insight - Non-Destructive Testing and Condition Monitoring*, 55 (8), 442–448.
- Resnik, L. and Borgia, M., 2015. Predicting prosthetic prescription after major lower-limb amputation. *Journal of Rehabilitation Research and Development*, 52 (6), 641–652.
- Rogers, B., Bosker, G., Faustini, M. C., Walden, G., Neptune, R. R. and Crawford, R. H., 2008. Case Report: Variably Compliant Transtibial Prosthetic Socket Fabricated Using Solid Freeform Fabrication. *Journal of Prosthetics and Orthotics*, 20 (1), 1–7.
- Rogers, J. and Wilson, L. F., 1975. Preventing recurrent tissue breakdowns after “pressure sore” closures. *Plastic and Reconstructive Surgery*, 56 (4), 419–22.
- Rosen, B., 1996. Ensemble Learning Using Decorrelated Neural Networks. *Connection Science*, 8 (3), 373–384.
- Ryall, N. H., Eyres, S. B., Neumann, V. C., Bhakta, B. B. and Tennant, A., 2003. The SIGAM mobility grades: a new population-specific measure for lower limb amputees. *Disability and Rehabilitation*, 25 (15), 833–844.
- Safari, M. R. and Meier, M. R., 2015. Systematic review of effects of current transtibial prosthetic socket designs—Part 1: Qualitative outcomes. *Journal of Rehabilitation Research and Development*, 52 (5), 491–508.
- Sanders, J. E., Bell, D. M., Okumura, R. M. and Dralle, A. J., 1998. Effects of alignment changes on stance phase pressures and shear stresses on transtibial amputees: measurements from 13 transducer sites. *IEEE Transactions on Rehabilitation Engineering*, 6 (1), 21–31.
- Sanders, J. E., Cagle, J. C., Harrison, D. S., Myers, T. R. and Kathryn, J., 2013. How does adding

- and removing liquid from socket bladders affect residual-limb fluid volume? *Journal of Rehabilitation Research and Development*, 50 (6), 845–860.
- Sanders, J. E. and Daly, C. H., 1993.a Measurement of stresses in three orthogonal directions at the residual limb-prosthetic socket interface. *IEEE Transactions on Rehabilitation Engineering*, 1 (2), 79–85.
- Sanders, J. E. and Daly, C. H., 1993.b Normal and shear stresses on a residual limb in a prosthetic socket during ambulation: comparison of finite element results with experimental measurements. *Journal of Rehabilitation Research and Development*, 30 (2), 191–204.
- Sanders, J. E. and Daly, C. H., 1999. Interface pressures and shear stresses: sagittal plane angular alignment effects in three trans-tibial amputee case studies. *Prosthetics and Orthotics International*, 23 (1), 21–9.
- Sanders, J. E., Daly, C. H. and Burgess, E. M., 1993. Clinical measurement of normal and shear stresses on a trans-tibial stump: Characteristics of wave-form shapes during walking. *Prosthetics and Orthotics International*, 17 (1), 38–48.
- Sanders, J. E. and Fatone, S., 2011. Residual limb volume change: Systematic review of measurement and management. *Journal of Rehabilitation Research and Development*, 48 (8), 949–986.
- Sanders, J. E., Goldstein, B. S. and Leotta, D. F., 1995. Skin response to mechanical stress : Adaptation rather than breakdown — A review of the literature. *Journal of Rehabilitation Research and Development*, 32 (3), 214–226.
- Sanders, J. E., Greve, J. M., Clinton, C. and Hafner, B. J., 2000. Clinical study: Changes in interface pressure and stump shape over time: Preliminary results from a transtibial amputee subject. *Prosthetics and Orthotics International*, 24 (2), 163–168.
- Sanders, J. E., Lam, D., Dralle, A. J. and Okumura, R., 1997. Interface pressures and shear stresses at thirteen socket sites on two persons with transtibial amputation. *Journal of Rehabilitation Research and Development*, 34 (1), 19–43.
- Sanders, J. E., Miller, R. A., Berglund, D. N. and Zachariah, S. G., 1997. A modular six-directional force sensor for prosthetic assessment: a technical note. *Journal of Rehabilitation Research and Development*, 34 (2), 195–202.
- Sanders, J. E., Murthy, R., Cagle, J. C., Allyn, K. J., Phillips, R. H. and Otis, B. P., 2012. Device to monitor sock use in people using prosthetic limbs: Technical Report. *Journal of*

- Rehabilitation Research and Development*, 49 (8), 1229–1238.
- Sanders, J. E., Rogers, E. L. and Abrahamson, D. C., 2007. Assessment of residual-limb volume change using bioimpedence. *Journal of Rehabilitation Research and Development*, 44 (4), 525.
- Sanders, J. E., Zachariah, S. G., Jacobsen, A. K. and Ferguson, J. R., 2005. Changes in interface pressures and shear stresses over time on trans-tibial amputee subjects ambulating with prosthetic limbs: comparison of diurnal and six-month differences. *Journal of Biomechanics*, 38 (8), 1566–73.
- Saunders, C. G., Bannon, M., Sabiston, R., Jenks, S. L., Wood, I. R. and Raschke, S., 1989. The CANFIT System: Shape Management Technology for Prosthetic and Orthotic Applications An Overview of Below-Knee Socket Design. *Journal of Prosthetics and Orthotics*, 1 (3), 122–130.
- Saunders, C. G., Foort, J., Bannon, M., Lean, D. and Panych, L., 1985. Computer Aided Design of Prosthetic Sockets for Below-Knee Amputees. *Prosthetics and Orthotics International*, 9 (1), 17–22.
- Schöllhorn, W. I., 2004. Applications of artificial neural nets in clinical biomechanics. *Clinical Biomechanics (Bristol, Avon)*, 19 (9), 876–98.
- Schwenk, H. and Bengio, Y., 2000. Boosting Neural Networks. *Neural Computation*, 12 (8), 1869–1887.
- Seelen, H. A. M., Anemaat, S., Janssen, H. M. H. and Deckers, J. H. . M., 2003. Effects of prosthesis alignment on pressure distribution at the stump/socket interface in transtibial amputees during unsupported stance and gait. *Clinical Rehabilitation*, 17 (7), 787–796.
- Selles, R. W., Bussmann, J. B., Klip, L. M., Speet, B., Van Soest, A. J. and Stam, H. J., 2004. Adaptations to mass perturbations in transtibial amputees: Kinetic or kinematic invariance? *Archives of Physical Medicine and Rehabilitation*, 85 (12), 2046–2052.
- Selles, R. W., Bussmann, J. B., Wagenaar, R. C. and Stam, H. J., 1999. Effects of prosthetic mass and mass distribution on kinematics and energetics of prosthetic gait: a systematic review. *Archives of Physical Medicine and Rehabilitation*, 80 (12), 1593–9.
- Sengeh, D. M., Moerman, K. M., Petron, A. and Herr, H., 2016. Multi-material 3-D viscoelastic model of a transtibial residuum from in-vivo indentation and MRI data. *Journal of the Mechanical Behavior of Biomedical Materials*, 59, 379–392.
- Sewell, P., Noroozi, S., Davenport, P., Bascou, J., Villa, C. and Zahedi, S., 2016. Technological

- Innovations in prosthetic socket fitting – an external method to assess the residual limb/socket interaction. *In: ISPO-France*. Lille, France
- Sewell, P., Noroozi, S. and Vinney, J., 2000. A Tool for Monitoring the Real-Time Interface Stress Distribution on Transtibial Prosthetic Socket: A Preliminary Study. *The International Journal of COMADEM*, 3 (4), 16–21.
- Sewell, P., Noroozi, S., Vinney, J., Amali, R. and Andrews, S., 2010. Improvements in the accuracy of an Inverse Problem Engine's output for the prediction of below-knee prosthetic socket interfacial loads. *Engineering Applications of Artificial Intelligence*, 23 (6), 1000–1011.
- Sewell, P., Noroozi, S., Vinney, J., Amali, R. and Andrews, S., 2012. Static and dynamic pressure prediction for prosthetic socket fitting assessment utilising an inverse problem approach. *Artificial Intelligence in Medicine*, 54 (1), 29–41.
- Sewell, P., Noroozi, S., Vinney, J. and Andrews, S., 2000. Developments in the trans-tibial prosthetic socket fitting process: a review of past and present research. *Prosthetics and Orthotics International*, 24 (2), 97–107.
- Sewell, P., Vinney, J., Noroozi, S. and Andrews, S., 2005. *New Methods to Improve the Assessment, Analysis and Quality of Prosthetic Socket Fit - Final Technical Report*. Bristol, UK
- Sheehan, R. C., Beltran, E. J., Dingwell, J. B. and Wilken, J. M., 2015. Mediolateral angular momentum changes in persons with amputation during perturbed walking. *Gait and Posture*, 41 (3), 795–800.
- Shoham, N. and Gefen, A., 2012. Deformations, mechanical strains and stresses across the different hierarchical scales in weight-bearing soft tissues. *Journal of Tissue Viability*, 21 (2), 39–46.
- Silver-Thorn, M. B., Steege, J. W. and Childress, D. S., 1992. Measurements of Below-Knee Residual Limb/Prosthetic Socket Interface Pressures. *In: Proceedings of the 7th World Congress of the ISPO* 280.
- Silver-Thorn, M. B., Steege, J. W. and Childress, D. S., 1996. A review of prosthetic interface stress investigations. *Journal of Rehabilitation Research and Development*, 33 (3), 253–66.
- Smith, J. D. and Martin, P. E., 2013. Effects of prosthetic mass distribution on metabolic costs and walking symmetry. *Journal of Applied Biomechanics*, 29 (3), 317–328.
- Sonck, W. A., Cockrell, J. L. and Koepke, G. H., 1970. Effect of linear material on interface

- pressures in below-knee prostheses. *Archives of Physical Medicine and Rehabilitation*, 51 (11), 666–9.
- Staats, T. B. and Lundt, J., 1987. The UCLA Total Surface Bearing Suction Below-Knee Prosthesis. *Clinical Prosthetics and Orthotics*, 11 (3) , 118–130.
- Steege, J. W., Schnur, D. S. and Childress, D. S., 1987a. Prediction of pressure in the below-knee socket interface by finite element analysis. In: *ASME Symposium on the Biomechanics of Normal and Pathological Gait* 39–44.
- Steege, J. W., Schnur, D. S., van Vorhis, R. L. and Rovick, J. S., 1987b. Finite element analysis as a method of pressure prediction at the below-knee socket interface. In: *Proceedings of RESNA 10th Annual Conference*. California, USA 814–16.
- Steege, J. W., Silver-Thorn, M. B. and Childress, D. S., 1992. Design of prosthetic sockets using finite element analysis. In: *Proceedings of the 7th World Congress of the ISPO*. Chicago, Illinois, USA.
- Surowiecki, J., 2004. The Wisdom of Crowds: Why the many are smarter than the few and how collective wisdom shapes business. *Economies, Societies and Nations*, 296
- Swain, I. D. and Bader, D. L., 2002. The measurement of interface pressure and its role in soft tissue breakdown. *Journal of Tissue Viability*, 12 (4), 132–146.
- Tang, J., Jiang, L., Bader, D., Laszczak, P., Gao, J., McGrath, M., Moser, D., Zahedi, S., McCarthy, J. and Bradbury, R., 2015. Use of Gait Lab 3D Motion Capture for Dynamic Assessment of Amputee Socket Interface Biomechanics with Validation using TRIPS Sensor Systems - a Case Study. In: *43rd ISPO UK MS Annual Scientific Meeting*. Oxford, UK.
- Tang, P. C. Y., Ravji, K., Key, J. J., Mahler, D. B., Blume, P. A. and Sumpio, B., 2008. Let them walk! Current prosthesis options for leg and foot amputees. *Journal of the American College of Surgeons*, 206 (3), 548–60.
- T Walley Williams, M. A. and Altobelli, D. E., 2011. Prosthetic sockets stabilized by alternating areas of tissue compression and release. *Journal of Rehabilitation Research and Development*, 48 (6), 679.
- UNIPOD, 2012, *Limbless Statistics Annual Report 2010-2011*. University of Salford
- UNIPOD, 2013. *Limbless Statistics Annual Report 2011-2012*. University of Salford
- Vamos, E. P., Bottle, A., Edmonds, M. E., Valabhji, J., Majeed, A. and Millett, C., 2010. Changes in the incidence of lower extremity amputations in individuals with and without diabetes in England between 2004 and 2008. *Diabetes Care*, 33 (12), 2592–2597.

- Vinney, J., Noroozi, S., Sewell, P. and Blount, G., 2000. Case-Based Prosthetic Socket Design. *The Design Journal*, 3 (2), 36–45.
- Waters, R. L. and Mulroy, S., 1999. The energy expenditure of normal and pathologic gait. *Gait and Posture*, 9 (3), 207–31.
- Williams, R. B., Porter, D., Roberts, V. C. and Regan, J. F., 1992. Triaxial force transducer for investigating stresses at the stump/socket interface. *Medical and Biological Engineering and Computing*, 30 (1), 89–96.
- Winarski, D. J. and Pearson, J. R., 1987. Least-Squares Matrix Correlations Between Stump Stresses and Prosthesis Loads for Below-Knee Amputees. *Journal of Biomechanical Engineering*, 109 (3), 238–246.
- Wolpert, D. H., 1992. Stacked Generalization. *Neural Networks*, 5 (2), 241–259.
- Yang, C. C. and Hsu, Y. L., 2010. A review of accelerometry-based wearable motion detectors for physical activity monitoring. *Sensors (Basel, Switzerland)*, 10 (8), 7772–88.
- Yeung, L. F., Leung, A. K. L., Zhang, M. and Lee, W. C., 2013. Effects of long-distance walking on socket-limb interface pressure, tactile sensitivity and subjective perceptions of trans-tibial amputees. *Disability and Rehabilitation: Assistive Technology*, 35 (11), 888–93.
- Yu, H. and Wilamowski, B. M., 2011. Levenberg-Marquardt training. In: *Industrial Electronics Handbook*, 5 (12), 1–16.
- Zachariah, S. G. and Sanders, J. E., 2000. Finite element estimates of interface stress in the trans-tibial prosthesis using gap elements are different from those using automated contact. *Journal of Biomechanics*, 33 (7), 895–899.
- Zhang, M., Lord, M., Turner-Smith, A. R. and Roberts, V. C., 1995. Development of a non-linear finite element modelling of the below-knee prosthetic socket interface. *Medical Engineering and Physics*, 17 (8), 559–566.
- Zhang, M., Mak, A. F. and Roberts, V. C., 1998. Finite element modelling of a residual lower-limb in a prosthetic socket: a survey of the development in the first decade. *Medical Engineering and Physics*, 20 (5), 360–73.
- Zhang, M. and Roberts, C., 2000. Comparison of computational analysis with clinical measurement of stresses on below-knee residual limb in a prosthetic socket. *Medical Engineering and Physics*, 22 (9), 607–12.
- Zhang, M., Turner-Smith, A. R., Tanner, A. and Roberts, V. C., 1998. Clinical investigation of the pressure and shear stress on the trans-tibial stump with a prosthesis. *Medical Engineering*

and Physics, 20 (3), 188–98.

Zhou, Z. H., Wu, J. and Tang, W., 2002. Ensembling Neural Networks: Many Could Be Better Than All. *Artificial Intelligence*, 137 (1–2), 239–263.

Ziegler-Graham, K., MacKenzie, E. J., Ephraim, P. L., Trivison, T. G. and Brookmeyer, R., 2008. Estimating the prevalence of limb loss in the United States: 2005 to 2050. *Archives of Physical Medicine and Rehabilitation*, 89 (3), 422–9.

Appendix

A1 – ISPO World Congress, Lyon France (2015)	313
A2 Medical Physics and Engineering Conference, Manchester UK (2016).....	314
A3 Multidisciplinary Engineering Optimisation Conference, Belgrade Serbia (2016)	315
A4 Systematic Literature Review, Journal of Medical and Biological Engineering (2017)...	316
A5 ISPO Annual Scientific Meeting, Lille France (2016)	317
A6 ISPO World Congress, Cape Town South Africa (2017)	319
A7 ISPO World Congress, Cape Town South Africa (2017)	320
A8 World Congress on Condition Monitoring, London UK (2017).....	321
A9 Study Risk Assessment.....	322
A10 Full Study Protocol.....	323
A11 Full Study Participant Information Sheet	334
A12 Full Study Participant Consent Form	338
A13 Participant Data Collection Form Template	339
A14 VLink-LXRS Data Sheet (Lord Microstrain).....	341
A15 Mounting Rig Plate 1	343
A16 Mounting Rig Plate 2-4	344
A17 LabView ANN MATLAB Code	345
A18 Polynomial Fitter MATLAB Code.....	346
A19 Polynomial Correction MATLAB Code	348
A20 Ensemble Generation MATLAB Code	349
A21 Ensemble Analysis MATLAB Code.....	350
A22 Ensemble Summation MATLAB Code	352
A23 Ensemble Evaluation MATLAB Code.....	353
A24 MATLAB Distribution Generation Code.....	355

A25 LabView LXRS Collection Code 356

A26 LabView VLink Average Code 359

A27 LabView VLink Conditioning Code 360

A28 LabView File Path Code 363

A29 LabView DAQ Conditioning Code 364

A30 LabView DAQ Average Code 368

A31 LabView Ensemble Specification Code 369

A32 Abbreviations 371

Title:

A proposed system for automatic categorisation of lower-limb prosthesis alignment using Learning Vector Quantisation and an inverse problem pressure measurement approach.

Abstract:

Background:

Current methods for evaluating the set-up of lower-limb prostheses are limited by their inability to provide information on optimal socket fit and device alignment to the prosthetist and user as they rely substantially on clinical experience [1]. A non-invasive method for evaluating pressure distribution based on artificial neural networks has been reported [2]. An extension of this system to enable alignment classification is described.

Aim:

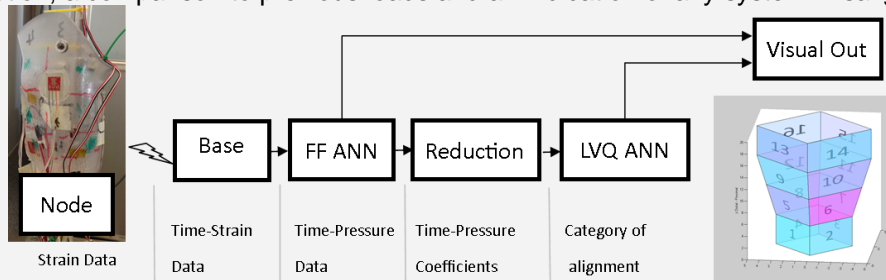
To develop a system capable of mapping socket pressure distribution using external sensors and characterising these results in terms of changes in socket/pylon alignment.

Method:

Strain gauges on the external surface of the socket are used as inputs to a neural network. After training with known loads, an estimate of the unknown distribution in the clinical case is made. It is hypothesised that changes in pressure distribution with different alignments will be separable. Literature on automatic classification of gait data was reviewed for techniques suitable for this application. In particular, time series data must be reduced to represent the gait cycles concisely. As data can be collected at different known alignments, supervised learning techniques may be used. Improvements to hardware are described.

Results:

The physical elements are a network of strain sensors sampled at 128Hz through nodes transmitting wirelessly to a hub. These voltages are used as inputs to a feed forward back propagation network - this is trained to estimate internal socket loads as in [2] to produce a set of pressure-time series. This data is then reduced using fast Fourier transforms and using these coefficients as the inputs to a Learning Vector Quantisation network (as in e.g. [3]) - with results categorised using collected data in altered alignment conditions. When new data is introduced to the system, it can produce an estimate of the internal load distribution, a comparison to previous loads and an indication of any system misalignment.



Discussion & Conclusion :

Several challenges must be overcome before such a system could be used outside the laboratory. Tests to describe reliability and accuracy are on-going, and generalisability of results is yet to be quantified. However this method may represent an improvement on current techniques in measurement of prosthesis fit and alignment, and provide a valuable interpretation tool for clinicians.

References :

- [1] Pirouzi et al. (2014) *Scientific World Journal*
- [2] Amali et al. (2008) *Insight – Non Destructive Testing and Condition Monitoring*
- [3] Köhle et al. (1998) *Proc. 8th Int. Conf. on Artificial Neural Networks*

Title:

Impact of varying training components for an ensemble neural network system of estimating prosthetic socket pressure distribution

Abstract: (Your abstract must use Normal style and must fit into the box. Do not enter author details)

Existing methods of measuring the pressure distribution within prosthetic sockets suffer from interference with the interface under examination [1]. An inverse-problem solution – relating the external strains on the socket with the internal pressures using a neural network – has shown promise in mitigating these issues [2]. However the optimisation of the neural network training procedure has not been examined in detail for this application.

Ensemble averaging has long been proposed as a mechanism for improving network performance [3]. Individual networks' estimates of load distribution are expected to vary between over- and under-estimation of particular values depending on factors such as the initial network weights and the order of training cases. Therefore, by evaluating the response of multiple networks and finding the average of their estimates, a better overall model of the pressure-strain relationship can be made.

Neural network literature suggests that performance is improved by including varying network designs within the ensemble [4]. In this work, this was achieved by several methods – by varying the architecture of the networks in terms of hidden neurons and through altering the method of noise injection.

The impact of these changes was evaluated systematically using a separate measurement file and calculating the sum of errors between the known loads and each ensemble. Preliminary results confirm the expected improvement in performance from the use of ensembles, and given the low computational cost their use within this application is recommended.

[1] Pirouzi et al. (2014) Scientific World ID849073

[2] Sewell et al. (2012), 54 (1), Artificial Intelligence in Medicine p29

[3] Hansen and Salomon (1990), 12(10), IEEE Trans Pattern Analysis p993

[4] Krogh and Vedelsby (1995), 7, Adv. In Neural Information Processing p231

Applying Ensemble Neural Networks to an Inverse Problem Solution to Prosthetic Socket Pressure Measurement

P Davenport, S Noroozi, P Sewell
Faculty of Science and Technology
Bournemouth University
Poole, UK
PDavenport@bournemouth.ac.uk

S Zahedi
Chas A Blatchford and Sons Ltd.
Basingstoke, UK

Abstract— Ensemble neural networks are a commonly used as a method to boost performance of artificial intelligence applications. By collating the response of multiple networks with differences in composition or training and hence a range of estimation error, an overall improvement in the appraisal of new problem data can be made. In this work, artificial neural networks are used as an inverse-problem solver to calculate the internal distribution of pressures on a lower limb prosthetic socket using information on the deformation of the external surface of the device. Investigation into the impact of noise injection was studied by changing the maximum noise alteration parameter and the differences in network composition by altering the variance around this maximum noise value. Results indicate that use of ensembles of networks provides a meaningful improvement in overall performance. RMS error expressed as a percentage of the total applied load was 3.86% for the best performing ensemble, compared to 5.32% for the mean performance of the networks making up that ensemble. Although noise injection resulted in an improvement in typical network estimates of load distribution, ensembles performed better with low noise and low variance between network training patterns. These results mean that ensembles have been implemented in the research tool under development

Keywords—artificial intelligence; amputees; normal stress

I. INTRODUCTION

The lower-limb prosthetic socket is a crucial component in an artificial limb to ensure that an active amputee can mobilize efficiently and in comfort [1]. A wide range of techniques have been employed to evaluate the pressure distribution caused by standing and walking: however all suffer from significant limitations [2]. No systems are in routine use in rehabilitation. For this reason, an inverse problem solution has been developed. This relates strain measurements from the external surface of the socket wall to internal pressures using a neural network. Doing so maintains the integrity of the stump/socket interface, without requiring detailed knowledge of the socket geometry or tissue properties. The principle of this approach has been demonstrated previously [3], as have several techniques to improve the accuracy and reliability of the networks in use, including noise injection and via a correction

factor from mapping polynomial functions to the network response [4].

A natural extension of these measures is to incorporate ensembles of neural networks into the solution: this being a well-established technique for boosting overall performance by averaging estimates across multiple separate networks [5]. Such ensembles benefit from diversity in the constituent networks; however this property is likely problem specific. In this work, the changes in ensemble variance were systematically altered by changing the magnitude and spread of the noise injection values. The impact of this on overall performance was evaluated using a separate set of measurement cases.

II. METHODS

Prosthetic sockets are structures that are challenging to analyze using traditional analytical techniques. These devices are created to fit the contours of the residual limb in a manner which enables secure and consistent application of forces to the appropriate regions of the stump. This means that every socket differs in shape and size according to the specific requirements of the user and the intentions and skills of the prosthetist [6]. Individual sockets may have inhomogeneous material thickness from the manufacturing processes used. The advantage of an inverse problem approach utilizing artificial neural networks over traditional numerical analysis is that knowledge of the size, shape and thickness of the socket is not required, nor specific details of the residual limb beyond identification of regions where pressure information is valuable.

This work is sponsored by Chas A Blatchford and Sons Ltd. and an EPSRC CASE Industrial Studentship



Systematic Review of Studies Examining Transtibial Prosthetic Socket Pressures with Changes in Device Alignment

Philip Davenport¹ · Siamak Noroozi² · Philip Sewell² · Saeed Zahedi³

Received: 25 July 2016 / Accepted: 30 November 2016
© The Author(s) 2017. This article is published with open access at Springerlink.com

Abstract Suitable lower-limb prosthetic sockets must provide an adequate distribution of the pressures created from standing and ambulation. A systematic search for articles reporting socket pressure changes in response to device alignment perturbation was carried out, identifying 11 studies. These were then evaluated using the American Academy of Orthotists and Prosthetists guidelines for a state-of-the-science review. Each study used a design where participants acted as their own controls. Results were available for 52 individuals and five forms of alignment perturbation. Four studies were rated as having moderate internal and external validity, the remainder were considered to have low validity. Significant limitations in study design, reporting quality and in representation of results and the suitability of calculations of statistical significance were evident across articles. Despite the high inhomogeneity of study designs, moderate evidence supports repeatable changes in pressure distribution for specific induced changes in component alignment. However, there also appears to be a significant individual component to alignment responses. Future studies should aim to include greater detail in the presentation of results to better support later meta-analyses.

Keywords Below-knee · Protheses · Misalignment · Normal stress · Pressure distribution

✉ Philip Davenport
PDavenport@bournemouth.ac.uk

¹ Department of Design and Engineering, Bournemouth University, Poole, UK

² Bournemouth University, Poole, UK

³ Chas A Blatchford and Sons Ltd., Basingstoke, UK

1 Introduction

Suitable pressure distribution within the lower-limb prosthetic socket is important for the comfort and function of the amputee [1–3], and an adequately fitting socket is required for extensive use of a functional prosthesis [4]. Inappropriate sockets have been implicated in cases of dermatological issues [5, 6] and pressure injury [7, 8]. Furthermore, socket comfort and socket fit are widely cited by users as the most important factor in their satisfaction with a prosthetic lower limb [9].

Different design philosophies exist in the production of transtibial prosthetic sockets. From the early 1960s, patellar tendon bearing (PTB) sockets became commonplace—in these designs, the socket is crafted to selectively load areas that are load-tolerant while at the same time offloading regions where applied pressure can be painful. Later, total surface bearing (TSB) designs were introduced, where the load is more evenly distributed around the entire residual limb. This was developed further into hydrostatic designs, where an equally applied hydraulic or pneumatic pressure is used to the form a socket shape where the residual limb tissues are forced to ‘flow’ into a configuration with equal pressure distribution. Clearly the aims of establishing a pressure distribution vary in each case, however in all cases a well-fitting socket is considered crucial for the successful use of a prosthetic limb [10].

A related aspect of device set-up is in the alignment of the device with the residual limb. Prosthetic limbs are adjustable in both rotation and translation in each plane, and poor alignment has been shown to affect multiple aspects of the gait of transtibial amputees [11–14]. Alignment has long been theorised to produce systematic changes in the pressure distribution at the socket interface [15]. Although amputees are able to tolerate a range of

Innovations technologiques dans la réalisation d'emboîtures pour prothèses de membre inférieur - une méthode externe d'estimation des interactions entre membre résiduel et prothèse

Orateurs :

Docteur Philip SEWELL, Professeur Siamak NOROOZI

Auteurs :

Monsieur Philip DAVENPORT - Bournemouth University, Royaume Uni, Docteur Joseph BASCOU - INI Paris (75), Docteur Coralie VILLA - INI Paris (75), Professeur Saeed ZAHEDI, Blatchford and Sons Ltd, Royaume-Uni

Introduction :

L'objectif d'une emboîture de prothèse du membre inférieur est de distribuer de manière adéquate les efforts issus de la position debout et de la déambulation de la personne amputée, exercés sur le membre résiduel. En ce qui concerne les personnes amputées transbiales, deux philosophies de répartition prédominent : les emboîtures portant l'appui sur le tendon patellaire (dites « PTB », pour « Patellar Tendon Bearing ») et les emboîtures hydrostatiques. La première cherche à appliquer la charge de manière sélective sur les régions considérées comme capables de tolérer une pression importante. La seconde méthode cherche à répartir équitablement la charge sur toute la surface de contact du membre résiduel. Aucune approche n'a pu prouver de manière parfaite son efficacité : de nombreuses études (voir Goh et al.¹) ont montré que les emboîtures PTB entraînent des efforts différents de ceux qui étaient voulu lors de leur conception. De la même manière, des études similaires ont montré que les emboîtures hydrostatiques entraînaient de fortes discontinuités de pression dans des activités de la vie courante^{2,3}. La maîtrise totale de la biomécanique des efforts dans l'emboîture n'est donc pas encore atteinte⁴.

La distribution de pression dans l'emboîture est importante pour le confort et le bon fonctionnement de la prothèse⁵⁻⁷. Une emboîture ajustée de manière adéquate est nécessaire pour une utilisation convenable de la prothèse⁸. Des emboîtures inadéquates participent à la formation de problèmes dermatologiques^{9,10} et au développement de blessures^{11,12}.

Mots clés :

interactions, moignon, emboîture, mesure externe, amputé de membre inférieur

Corps du résumé / Matériels et méthodes :

Une nouvelle méthode permettant de quantifier les interactions entre le membre résiduel et l'emboîture a été développée, en cherchant à fournir au prothésiste un outil clinique, l'aidant à l'ajustement de l'emboîture et à la compréhension de la biomécanique de l'emboîture¹³⁻¹⁷. Cette méthode adopte une approche où les interactions peuvent être estimées en utilisant des capteurs situés sur la surface externe de l'emboîture, afin de surmonter les limites d'autres méthodes de mesure existantes, qui peuvent interférer avec l'interaction membre résiduel/emboîture.

Discussion :

N/C

Résultats :

L'état actuel des technologies seront présentées en même temps qu'une étude actuellement en cours, menée en parallèle par l'INI/CERAH pour valider cette nouvelle méthodologie.

Bibliographie / Références :

1. Goh JCH, Lee PVS, Chong SY. Static and dynamic pressure profiles of a patellar-tendon-bearing (PTB) socket. *Proc Inst Mech Eng H [Internet]*. 2003;217(2):121–6.
2. Kahle JT. Conventional and Hydrostatic Transtibial Interface Comparison. *J Prosthetics Orthot*. 1999;11(4):85–91.
3. Goh JCH, Lee PVS, Chong SY. Comparative study between patellar-tendon-bearing and pressure cast prosthetic sockets. *J Rehabil Res Dev*. 2004 May;41(3B):491–501.
4. Laing S, Lee PVS, Goh JCH. Engineering a trans-tibial prosthetic socket for the lower limb amputee. *Ann Acad Med Singapore*. 2011 May;40(5):252–9.
5. Webster JB, Hakimi K, Williams RM, Turner AP, Norvell DC, Czerniecki JM. Prosthetic fitting, use, and satisfaction following lower-limb amputation: a prospective study. *J Rehabil Res Dev*. 2012 Jan;49(10):1493–504.
6. Hannah RE, Morrison JB, Chapman AE. Prostheses alignment: effect on gait of persons with below-knee amputations. *Arch Phys Med Rehabil [Internet]*. 1984;65(4):159–62.
7. Klute GK, Kantor C, Darrouzet C, Wild H, Wilkinson S, Iveljic S, et al. Lower-limb amputee needs assessment using multistakeholder focus-group approach. *J Rehabil Res Dev*. 2009;46(3):293–304.
8. Fergason J, Smith DG. Socket considerations for the patient with a transtibial amputation. *Clin Orthop Relat Res [Internet]*. 1999;(361):76–84.
9. Levy SW. Skin problems of the leg amputee. *Prosthet Orthot Int*. 1980;4(1):37–44.
10. Meulenbelt HE, Dijkstra PU, Jonkman MF, Geertzen JHB. Skin problems in lower limb amputees: a systematic review. *Disabil Rehabil [Internet]*. 2006;28(10):603–8.
11. Mak AF, Zhang M, Tam EWC. Biomechanics of Pressure Ulcer in Body Tissues Interacting with External Forces during Locomotion. *Annu Rev Biomed Eng*. 2010;12:29–53.
12. Butler K, Bowen C, Hughes AM, Torah R, Ayala I, Tudor J, et al. A systematic review of the key factors affecting tissue viability and rehabilitation outcomes of the residual limb in lower extremity traumatic amputees. *J Tissue Viability [Internet]*. 2014;23(3):81–93.
13. Amali R, Noroozi S, Vinney J, Sewell P, & Andrews S. Predicting interfacial loads between the prosthetic socket and the residual limb for below-knee amputees - a case study. *Strain*. 2006;42:3–10.
14. Sewell P, Noroozi S, Vinney J, Amali R, & Andrews S. Improvements in the Accuracy of an Inverse Problem Engine's Output for the Prediction of Below-Knee Prosthetic Socket Interfacial Loads. *Engineering Applications of Artificial Intelligence*. 2010;23(6):1000–1011.
15. Sewell P, Noroozi S, Vinney J, Amali R, & Andrews S. (). Static and dynamic load prediction for prosthetic socket fitting assessment utilising an inverse problem approach. *Artificial Intelligence in Medicine*. 2012;54(1):29–41.
16. Davenport P, Noroozi S, Sewell P & Zahedi S. A proposed system for automatic categorisation of lower-limb prosthesis alignment using Learning Vector Quantisation and an inverse problem pressure measurement approach. In: *International Society for Prosthetics & Orthotics (ISPO) World Congress 2015 22-25 June 2015 Lyon, France*.
17. Bascou J, Villa C, Jacquot D, Tonnelier A, Mangenot D, El Fettahi N, Drevelle X, Fode P. External measurement of 3D interactions between the residual limb of an amputee person and the socket. In: *International Society for Prosthetics & Orthotics (ISPO) World Congress 2015 22-25 June 2015 Lyon, France*.

SENSITIVITY OF AN INVERSE-PROBLEM SOCKET PRESSURE MEASUREMENT SYSTEM TO CHANGES IN APPLIED FORCES FROM STANDING

Philip Davenport¹, Siamak Noroozi¹, Philip Sewell¹, Saeed Zahedi², Joseph McCarthy², Mike McGrath²

¹Bournemouth University, Poole, UK, ²Chas A Blatchford and Sons Ltd, Basingstoke, UK

BACKGROUND

Measurement of relative pressure distribution in prosthetic sockets using an inverse problem solution has seen promising results in preliminary testing [1, 2]. Such a system has the potential for significant advantages over existing methods, including avoiding interference at the interface, providing complete coverage of the socket and not requiring detailed knowledge of the limb/socket properties [3]. However, a system that is intended for clinical use must be sensitive to measured changes in applied force, and this is the subject of this report.

AIM

The aim of this study was to assess the ability of an inverse-problem solver in measuring the magnitude of differences in total applied pressure through a transtibial amputee’s socket during the application of different proportions of body weight.

METHOD

The TSB socket of a traumatic transtibial amputee (M, age 53, amputee for 24 years) was instrumented with 11 strain gauges on the external surface. These strains were recorded using 3 LXRS devices (Lord Microstrain) and transmitted wirelessly to the host PC. The relationship between these the changes in these strain values and the sum of internal pressures in 8 positions was estimated using an ensemble of 100 neural networks. Data collection was performed using custom LabView (National Instruments) software, and neural networks of a feedforward-backpropagation design were implemented with the MATLAB (Mathworks) neural network toolbox.

The participant was asked to stand with their prosthesis side on a force platform, and to stand while applying ~25%/50%/75% of bodyweight through the prosthesis side. The proportional change in applied load was compared to that recorded by the force platform, taken as an average over two seconds of stable standing.

Ethical approval study was granted by the University Ethics Committee.

RESULTS

The participant’s comfortable standing placed 49% of total bodyweight through the prosthetic side. Heavy standing increased this to 81%, and light standing reduced this to 20%. Estimates from the artificial neural network mirrored this pattern: the sum of estimates from the 8 sites measured increased for heavy weight bearing and reduced for light

Condition	Force Plate	Pressure Measurement
Heavy Standing	167%	138%
Balanced Standing	100%	100%
Light Standing	42%	60%

Table 1 - Changes in measured and estimated total applied force in response to different measurement conditions, expressed as a percentage of the ‘balanced’ standing condition.

DISCUSSION & CONCLUSION

The system correctly evaluated the change in overall applied pressure magnitude. The exact changes in pressure magnitude did not reflect the changes in total applied force – this may be because the measurements did not completely cover the socket interface, that there was a significant component of force applied as shear rather than as normal stress or it may reflect a residual systemic inaccuracy in the neural network estimation.

The fact that light standing was overestimated and heavy load underestimated may point to a previously reported bias in the ANN method which can be substantially corrected using a polynomial correction factor [4]. Through developing and refining the parameters used in the construction and validation of the neural networks, the reliability may be improved further, as will increased understanding of the changes in pressure measurement in different circumstances.

REFERENCES

- [1] Davenport et al, (2015) *ISPO World Congress, Lyon*
- [2] Amali et al, (2008), *Insight*
- [3] Al Fakh et al (2016), *Sensors*
- [4] Sewell et al (2012), *Artif. Intel. Med.*

AN AUGMENTED REALITY METHOD OF VISUALISING TRANSTIBIAL SOCKET PRESSURES AND LIMB ORIENTATION

Philip Davenport¹, Siamak Noroozi¹, Philip Sewell¹, Saeed Zahedi², Joseph McCarthy², Mike McGrath²

¹Bournemouth University, Poole, UK, ²Chas A Blatchford and Sons Ltd, Basingstoke, UK

BACKGROUND

The measurement of in-socket pressure distribution has been a research concern for decades. Inappropriate application of pressure to the residuum has been implicated in discomfort, pressure injury, development of skin conditions and subsequent reduction in function [1]. Despite this interest, measurement systems have not moved from research tools into routine practice. One reason suggested for this is difficulty in interpretation: they lack the context of position relative to the measured socket and in associating the results with the orientation of the socket during movement [2]. These aspects may be improved by using an augmented reality system to visualise results by providing a scaled model, displaying measured pressure values and oriented to provide positional context.

AIM

To investigate the potential for using an augmented reality system on a recording of transtibial socket pressure distribution obtained using an inverse-problem measurement system.

METHOD

A representative 3D model of a transtibial socket was created in Solidworks and imported to an augmented reality application (eDrawings iOS) in order to be associated with a positioning barcode. A set of dynamic measurements of in-socket pressures in eight locations during walking was obtained using a neural network-based system (reported in detail elsewhere [3]). The changes in pressure distribution were represented on the socket model by altering the colour of patches on the socket surface, and socket orientation modified to represent different phases of the gait cycle. The finished model was viewed using a smartphone.

RESULTS

Researchers were able to successfully observe changes in 3D position and relative load of different measurement locations on a scaled model of the participant's socket. An example of this is shown in figure 1.

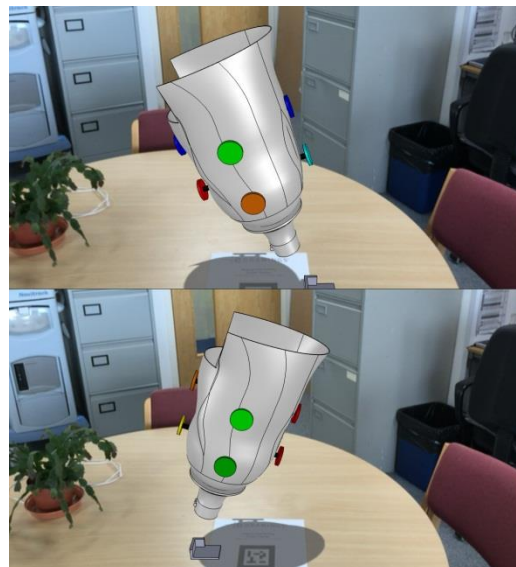


Figure 1. Virtual socket with coloured patches to indicate relative load distribution, and orientated to display early and late stance

DISCUSSION & CONCLUSION

Although it proved possible to visualise relative pressure distribution using this commercial system, it was time-consuming and complex to achieve using this implementation with commercially available software. Validation of the utility of such a presentation system in a clinical setting is also required as part of the development process. A future implementation using a custom program may be a more effective and flexible solution in this particular application.

REFERENCES

- [1] Butler et al (2014), *J. Tissue Viability*
- [2] Pirouzi et al (2014), *Sci. World*
- [3] Sewell et al (2012), *Artif. Intell. Med.*

Monitoring the suitability of the fit of a lower-limb prosthetic socket using an artificial neural network in commonly encountered walking conditions

Philip Davenport, Siamak Noroozi, Philip Sewell
Bournemouth University
Poole, Dorset, BH12 5BB, United Kingdom
Phone 01202 261994
Fax 01202 965314
pdavenport@bournemouth.ac.uk

Saeed Zahedi
Chas A Blatchford and Sons Ltd.
Basingstoke, Hampshire, RG24 8PZ, United Kingdom

Abstract

Prosthetic sockets are still routinely designed without the aid of quantitative measurement, relying instead on the experience and skill of clinicians. Sockets remain the most common cause for complaint regarding the suitability of a prosthesis, and poor pressure distribution is implicated in many forms of unacceptable care outcomes.

Monitoring pressure distribution has been effectively restricted to laboratory settings, and only limited work has examined conditions other than flat walking. In this work, a transtibial amputee completed static and dynamic tasks on flat ground, on slopes and with changes to prosthetic materials and alignment. This was achieved using a set of wireless measurement nodes and custom LabView and MATLAB code, using external strain measurements and a neural network to understand the internal pressure distribution.

Future work will focus on modifying the software to be more user-friendly for a clinical operator, and in simplifying the required hardware. Although the system in its current form facilitated the desired measurements effectively, it required engineering support to function accurately. Improving the reliability and stability of the system will be necessary before routine use is possible.

1. Introduction

Lower-limb amputees represent a significant population requiring long term provision of assistive technology for cosmetic, postural and functional purposes⁽¹⁾. In such devices, the prosthetic socket is a key component – the interface between the residual limb and the device, it is responsible for the successful application of the forces generated from standing and walking onto the tissues of the stump. Sockets are designed and constructed on an individual basis in order to account for the particular qualities of the residuum, the requirements of the limb suspension method, the preferences of the

A9 Study Risk Assessment

Measuring prosthetic socket pressures with changes in device alignment and walking conditions – Pilot Study – Risk Assessment

Activities with risk:
f) Equipment – use of custom devices
o) Lifting, moving and handling – fitting of devices
aa) sport/exercise activities – walking, stair climbing
gg) Other – working with people with restricted mobility

Potential Hazards:
5. Electrical Hazards
9. Friction/Abrasion
10. Trapping
15. Slips/Trips

Risks prior to action				
Description	Probability	Harm	Risk	Ref
Use of electrical measurement device	Highly Unlikely	Slight	Trivial	A
Friction on residual limbs from new socket can cause tissue damage	Unlikely	Moderate	Moderate	B
Trapping of fingers in device mounting rig	Unlikely	Slight	Tolerable	C
Participant tripping/falling whilst conducting requested tests	Unlikely	Moderate	Moderate	D

Ref	Mitigation and Control Measures
A	Measurement devices (i.e. LXRS nodes) are CE marked for electrical safety and are being used within manufacturers guidelines
	Electrical contacts are either contained within resin or within a connection block.
	Sockets being used are made of an insulating material
	All devices are low voltage/low current, and always isolated from mains current when in use with participants
B	Sockets are designed, constructed and applied by experienced clinicians
	All tests use a recently fitted socket that will closely match the residual limb
	Time spent using the study socket will be limited to a couple of hours
	Breaks may be taken if requested
C	The mounting rig is lightweight
	The device can be fitted incrementally, and is locked in position
D	Tests are designed to be well within the capabilities of the recruited participants
	Tests are carried out at a pace comfortable to the participant
	Tests are completed in a facility designed for testing people of limited mobility
	Tests are carried out under the supervision of experienced clinicians
	Participants are free to decline to complete a task they are uncomfortable with
	The revised device and mounting rig is wireless and lightweight, with sensor wiring at a minimum length, reducing tripping hazards

Risks after mitigation				
Description	Probability	Harm	Risk	Ref
Use of electrical measurement device	Highly Unlikely	Slight	Trivial	A
Friction on residual limbs from new socket can cause tissue damage	Unlikely	Slight	Tolerable	B
Trapping of fingers in device mounting rig	Highly Unlikely	Slight	Trivial	C
Participant tripping/falling whilst conducting requested tests	Highly Unlikely	Moderate	Tolerable	D



Protocol Document

Contents

Measuring prosthetic socket pressures with changes in device alignment and walking conditions – Developed testing	2
Background	2
Design.....	2
Population	2
Recruitment	2
Inclusion Criteria	3
Exclusion Criteria.....	3
Protocol Review	3
Data Collection.....	3
Collection Overview	3
Prior to collection.....	3
Session 1.....	3
Intersession Activity	4
Session 2.....	4
Test Facilities.....	6
Researchers Details.....	6
Measurement Devices	6
Data Storage.....	8
Data Analysis	9
Risk Assessment	9
Study Limitations.....	9
Reporting.....	10
Proposed Timeline	10
References.....	10
Measuring prosthetic socket pressures with changes in device alignment and walking conditions	12
Risk Assessment	14

Measuring prosthetic socket pressures with changes in device alignment and walking conditions – Developed testing

Background

The project is designed to provide detailed data on the pressure distribution characteristics at the residual limb/socket interface in multiple lower-limb amputee participants. Previous work in earlier iterations of the project has been carried out over the last decade at this university and elsewhere¹⁻³. As part of this PhD project, previous studies that have been granted ethical clearance include literature search on socket pressures (Reference ID 10094) and for bench testing of updated measurement devices (Reference ID 8894). A pilot study testing the equipment and substantial aspects of the experimental protocol was approved in summer 2016 (Reference ID 12229).

Prosthetic socket pressure measurement has been of significant clinical and engineering interest for over 60 years. Despite this, no quantitative measurement devices are in routine use in amputee treatment and rehabilitation⁴. This work uses an alternative method of estimating the loads experienced in the residual limb in standing and walking – an inverse problem solution. External strains on the socket body are related to the internal pressure distribution using an artificial neural network.

The purpose of this study is to examine the magnitude of inter-participant differences in socket pressures in response to changes in prosthesis configuration. Information on this will determine if the analysis of pressure distribution should progress with personalised techniques for identifying fault cases in device set-up, or if generic approach to pattern recognition can be successful.

Design

This study is in the form of a case series in which participants act as their own controls, comparing an original or ‘neutral’ prosthesis configuration with minor adjustments to the alignment of the device and the underfoot walking conditions, similar to those experienced in everyday life and the routine prescription of prostheses. In common with comparable literature, such a study is rated O5 by the American Academy of Orthotists and Prosthetists⁵.

Population

The population to be studied consists of active, unilateral transtibial amputees. Activity will be evaluated using the Special Interest Group in Amputee Medicine (SIGAM) grading, as assessed by a prosthetist – SIGAM grades D, E or F represent walking on level ground outdoors for greater than 50m with a walking aid up to near normal gait ability⁶.

Recruitment

Previous studies within the research group have recruited participants who fit the criteria for this study. Recruitment for this pilot will come from lower-limb amputees who have previously expressed an interest in taking part in future research. The commercial partner maintains a directory of individuals who have previously expressed an interest in taking part in research and development activities. Six participants matching the inclusion criteria will be recruited from this list.

Protocol Document

Participants are free to withdraw from the study at any point up to the completion of data collection and the anonymisation of data. This is made clear in the participant information sheet.

Inclusion Criteria

- Unilateral, transtibial amputee
- Amputee is established: i.e. an amputation more than 6 months old
- Walking ability equivalent to SIGAM grade D/E/F
- Cognitive ability provide informed consent and to understand instructions in tests
- Amputation as a result of trauma

Exclusion Criteria

- Skin damage or pressure injury on the residual limb
- Significant co-morbidity such as peripheral vascular disease, neurological or other conditions

Protocol Review

The protocol is developed as part of a PhD project, and as is written and reviewed by the lead researcher and by the project supervisors. The research is conducted in collaboration with Chas A. Blatchford and Sons Ltd., a prosthetics manufacturer with extensive experience in device development and amputee research. The proposal is reviewed by the Bournemouth University ethics procedure, and the tasks described are substantially similar to a previous cleared pilot study.

Data Collection

The principal means of data collection is of strain measurements on a prosthetic socket, supplemented by measurement of ancillary measures of gait conditions and by video recording of movement. The quantitative measurements are supported by limited qualitative analysis of the comfort of socket fit.

Collection Overview

Data collection is planned in two separate sessions, both of which will take place at Blatchford's facility in Basingstoke. The first is intended to enable construction of a test socket and to confirm details about the participant that are relevant to the results. The second is for the evaluation of pressure distribution during walking.

Prior to collection

Before any collection sessions take place, the participants will be approached for participation, and sent a copy of the information sheet and consent form. The participant will have the chance to consider these for around a week before the participation is confirmed and the initial data collection appointment booked.

Session 1

The session will begin with reviewing the information sheet and protocol, and completing the consent form.

Protocol Document

Following this, a history of the participant and their amputation will be taken. The data for collection follows recent recommendations for participant data collection in prosthetics studies⁷. In particular, this will collect:

- Age, height and weight
- Time since amputation
- Amputation reason
- Dimensions of residuum, and particulars of the stump condition
- Technical details of the prescribed prosthesis – artificial foot, socket type and suspension

The participant's subjective opinion of the quality of their socket fit will be evaluated using the Socket Comfort Score (SCS), a validated assessment tool⁸. This takes the form of a single verbal question: "On a 0 to 10 scale, if zero represents the most comfortable socket fit, how would you score the comfort of your socket fit of your artificial limb at the moment?"

In this session, a cast of the participant's residual limb will be taken in order to produce a new prosthetic socket. The process is identical to the clinical procedure for creating a socket, and is experienced by amputees regularly and is part of the skill set of certified prosthetists. This task will be carried out by the prosthetist staff of Blatchford's Ltd. The process is described below:

1. The participant is seated, with the knee held in 45° of flexion
2. The residual limb is wrapped in plaster coated bandages, wetted and moulded to shape
3. Aspects of the residual limb are marked using a pen, e.g. bony protrusions so that in the final socket these regions can be modified.
4. The cast is removed from the participant.

Following this, the session is complete for the participant. The time for the second session is confirmed at this point.

Intersession Activity

Several activities are scheduled between the participant measurement sessions. In particular, the negative cast of the residual limb is used to create a clear plastic socket for use in the second session. This is a routine task that can be completed by the Blatchford's prosthetic team.

This clear socket will be instrumented with 12 foil strain gauges, glued to the external surface. These are connected to four VLink measurement nodes mounted on a rig that can be affixed to the prosthesis pylon. This system then communicates wirelessly to a host PC. The rig weighs approximately 1 kg.

The response of the socket to internal loading is measured using a custom loading device. The values of strain for 10 internal positions, plus an unloaded state are used to generate multiple training patterns of load which together are used to create a neural network. This network is stored prior to the second collection session.

Session 2

This session is intended to be the venue for the collection of meaningful socket pressure measurements. The session begins with the fitting of the new socket to the participant. The process will be carried out by the prosthetists at Blatchford's, and consists of the participant wearing the socket and suspension, and performing simple standing and walking while the alignment of the device components are confirmed or modified as necessary. If required, the socket shape can be modified to some extent using a heat gun (however this will require a second socket training procedure).

Protocol Document

Some acclimatisation time is required for the wearing of the test socket. The participant will be allowed to walk and sit wearing the socket and measurement rig until they declare that they are comfortable with the new device. It is anticipated that this process will take 10-30 minutes. This will also allow the strain gauges to stabilise in temperature.

The participant will further be fitted with a set of markers in order to capture information regarding the position and motion of the prosthetic and intact limbs. 16 markers are attached to the limbs and pelvis in positions corresponding to skeletal features. The markers emit light in a specific pattern which is recorded by two specialised cameras and used to plot the 3D position of each part of the participant's limbs.

Markers are attached using double-sided tape and are easily applied and removed from skin and clothing. To support the use of this system, several measurements are required in order to complete the necessary calculations: these are the inter-ASIS distance across the front of the pelvis, limb lengths and knee and ankle widths. These measurements will be completed using a simple tape measure, and conducted by the supporting prosthetist. Further details on the equipment in use are included in the section "Measurement Devices".

At this point the VLink nodes will be turned on, and telemetry with the host PC confirmed. After a final check that the participant is happy to continue with measurements, the standing and walking tests will be completed.

Initial tests will examine flat standing. The participant will be asked to stand with bodyweight comfortably and roughly equally borne between the prosthetic and intact sides. This will be assessed by the use of a force platform, and the test recorded using video cameras.

If the participant is comfortable, they will be asked to vary the amount of bodyweight passed through the prosthetic side at: 0%, ~25%, ~50% and ~75%. To facilitate this, a support will be placed in front of them so that they can use their arms for balance if necessary. Recordings will be made for approximately 5 seconds.

Next, the participant will be asked to walk along a short walkway (~10 metres long) such that their prosthetic limb comes into contact with the force platform naturally. This will be repeated until at least five successful force plate recordings have been made. Judging from previous studies, this may require up to 10 attempts, for a total walking distance of ~100m.

Following this set of tests, the participant will be asked if they require to take a break.. It is expected that a break of 0-10 minutes would be sufficient. At this point, the comfort of the socket will also be rated, using the SCS score described earlier.

The next battery of tests requires the modification of the device alignment in order to examine the sensitivity of the system to these changes. Prosthetists regularly use a device to modify the height of the heel and toe of the shoe in order to correct alignment to the optimum. This device resembles a sandal with adjustable heel and toe inserts, and which straps around the existing shoe. Four additional alignment configurations will be tested (in randomised order): heel +5 and +10mm and toe +5 and +10mm. The procedure for measurement will follow the same protocol as for flat testing, and with the same provision for breaks.

Finally, walking on slopes will be evaluated. The Blatchford's facility contains a slope with a known gradient of 5°. This corresponds to the limit for ramp gradients in UK building regulations (2004 Part

Protocol Document

M). The participant will be able to negotiate this at their own pace, and using a handrail for support if required. Both up and down slopes will be evaluated. As force platform data is not available in this condition, only 6 measurements are required. Slopes are recognised as more challenging for amputees than flat walking, but these tests mimic in a controlled manner conditions that are frequently encountered in daily living. As before, if breaks are requested, they can be taken.

Following the conclusion of all measurements, the test prosthesis and measurement rig are removed, and the original device restored. The participant is then free to leave the session.

Test Facilities

The test sessions will take place at the Blatchford's centre in Basingstoke. The centre is used extensively for the manufacture and testing of prosthetic and orthotic devices. The facilities used will be as follows:

Session 1 – Clinic room. This will provide a quiet, private space for the discussion of the participant's amputation history, and for the creation of the socket cast.

Intersession – The manufacturing equipment will be used in the production of the participants test socket, then passed to the researchers at Bournemouth University for fitting instrumentation and network training.

Session 2 – The clinic room will again be used for the fitting of the prosthesis, the initial alignment defined by the prosthetist staff, and the fitting of the measurement rig to the prosthesis. The testing will then move to the gait testing facility. This is a larger area set aside for more extensive movements and which contains the force plate and camera equipment.

Post-Session – Processing of data will take place in the PhD student offices at Bournemouth University.

Researchers Details

The lead researcher for this project is Philip Davenport, a PhD student at Bournemouth University. In addition to engineering qualifications, he is also a state-registered Clinical Scientist (Registration number CS19093), and competent to carry out movement measurement sessions on those with movement pathologies.

The first project supervisor is Professor Siamak Noroozi, an engineer with extensive experience in prosthetics studies and with supervising PhD level projects. The second supervisor is Dr Philip Sewell, a researcher with over a decade's experience in measurements in amputees using a similar device.

The support supplied at Blatchford's Ltd is managed by Professor Saeed Zahedi, 3rd supervisor to the PhD project and technical director of the company and a prosthetist with a great deal of experience of amputee studies.

Direct prosthetist support will come from Joseph McCarthy, a registered prosthetist/orthotist (Registration number PO00463), who will carry out the stump casting and socket manufacturing processes. He will assist in supervising the actual measurement sessions with the participant.

Measurement Devices

Protocol Document

Measurements will be collected using a Bournemouth university laptop, using the password protection and encryption installed as standard by IT services.

The primary source of measurement is from the strain data, collected wirelessly via VLink nodes. The sensors in use are WFLA-2-350-11-1L strain gauges, manufactured by the Tokyo Sokki Kenkyujo Company Ltd. These are affixed to the wall of the socket using cyanoacrylate (superglue). The socket itself is made from Northplex plastic, a material supplied by North Sea Plastics, specifically intended for use in creating check sockets in prosthetics.

Each strain gauge is connected, in groups of 4, to a VLink wireless collection node (supplied by Lord Microstrain). Each channel contains quarter-bridge completion circuitry. Each node communicates with the WSDA Basestation using WiFi communication protocols. A further channel of data from a footswitch (Odstock Medical Ltd.) is also collected, with the switch itself taped to the heel of the shoe to register ground contact. All data are collected at 128 Hz.

The nodes are connected to the prosthesis pylon using a custom-made rig. This consists of a Manfrotto camera mount (rated to 2.5 Kg) and 4 aluminium plates, hinged together. The mount is intended to fix around the prosthesis pylon, between the socket and the artificial foot. The plates are bolted directly to this, and sit around the socket. The shape of the plates is maintained using caps which keep the plates at 90° angles to each other. The VLink nodes are bolted securely to the aluminium plates. The entire rig is shown in Figure 1.

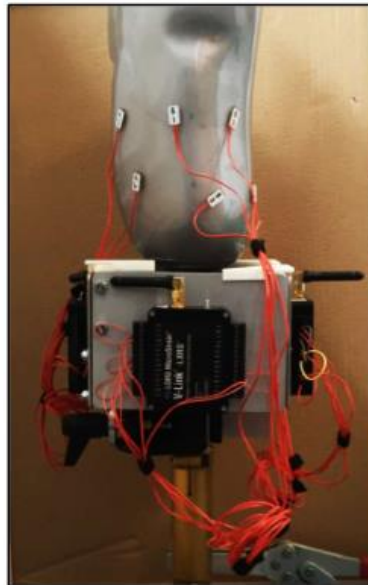


Figure 1 - Socket with test rig mounted. The rig fits below and around the socket, and does not interfere with walking. The wires shown are longer than in the measurement case.

The socket training rig has been used in previous research³. In brief, it consists of a spring loaded arm used to apply a point load to particular locations on the interior socket wall. The arm is instrumented using 350Ω strain gauges, and data collected from these using the same VLink collection hardware as the socket strains. This connection is removed once training is complete.

Protocol Document

Collection of this data relies on the use of custom software, in particular LXRS_v5.1.vi and ANN_code_v4.vi. These programs enable the collection and processing of strain data and the generation of neural networks. These programs include as dependencies the proprietary LORD Microstrain software and the Mathworks MATLAB Neural Network Toolbox.

Gait data are collected two CX1 cameras and CodaMotion Odin software. Outputs from this software consist of .c3d format files containing data on the position of each marker within the laboratory space, processed data that converts the position data into relative orientation of each body segment and, where force plate data are available, information of the moments and joint power is also included here. Further analysis of this data will be carried out using custom LabView and Matlab software.

Image post-processing will be carried out using the Adobe Master Collection CS6 group of software.

Force platform data (obtained through a Kistler force plate operating at 1000Hz) are also collected using CodaMotion Odin software, and exported into .CSV format for later analysis. The force plate data is monitored 'live' during static tests to evaluate percentage bodyweight being borne through the prosthesis.

Data Storage

Three sources of information exist, and the requirements for storage and collection are described here.

The participants information (as collected in session 1) is collected on a written form (included in the appendix to this document). The hardcopy of this form is stored with a signed copy of the participant consent form, and stored with the project documentation in a restricted access office at Bournemouth University. The information will also be digitised in an anonymous format, and stored with the remainder of the digital information.

The second source of data is the strain measurements from the prosthesis testing rig (along with limited ancillary measures, such as foot contact timing switches). These are stored as comma-separated-variable text files on the host PC, and contain time-series data, without any personal information present. Information on collection session is stored within the file header. This data is stored in an anonymised format on the encrypted BU laptop.

The final source of data is the gait analysis system. This consists of time-series data (force platform measurements) and linked video collection of walking. This is identified using the alphanumeric code assigned to the participant. If this video data contains personal identifiable images (i.e. of faces), these will be edited to preserve anonymity. Interim storage is on the secure equipment of Blatchford's Ltd, this will be transferred the BU laptop at the conclusion of the session.

Long-term data storage is on the secure servers at Bournemouth University, and will be kept for five years after the conclusion of the data collection sessions. This is made clear in the participant information sheet.

Data Analysis

The calibration files will be used to create multiple artificial neural networks with which the time-series strain data will be analysed. Individual footsteps will be separated using the footswitch information.

The pressure distribution will be compared to existing published information and correlated with the expected biomechanical performance as indicated by the force platform data and confirmed by the video information.

Patterns of distribution and their variance between footsteps will be compared to estimate the reliability of collection. Comparisons between alignment states will indicate the sensitivity of the measurements to alterations in the device configuration.

Additional analysis techniques will identify if the patterns produced are separable automatically. This will use techniques such as the movement deviation profile, learning vector quantisation and self-organising maps. This will require additional processing of the raw data using key feature analysis, discrete Fourier transform and wavelet analysis.

Risk Assessment

A detailed assessment of the risks has been completed, based on the experiences from the pilot study. Activities with risks were identified in the use of equipment and in the requested walking testing. Particular hazards in electrical safety, friction/abrasion, trapping and slips/trips were recorded. No risks were rated above moderate.

Nevertheless, several mitigation and control measures were implemented prior to design of this protocol. Specifically, elements with the highest risk are allayed by restricting time and activities within the test socket, and by sourcing socket design from the manufacturing partner.

The risk assessment is included in the appendix to this document, and is available online at: <https://risk.bournemouth.ac.uk/assessment/print/372d805d-ae83-4d2f-8a34-a6a4d6110a45>

Study Limitations

Effective blinding of the participant to system alignment changes is considered unlikely. Nevertheless, explicit reference to the alignment state will not be described to the participant.

Acclimatisation time is restricted within the study. Some prosthetic studies allow much longer acclimatisation to new componentry – on the order of days or weeks – for equipment such as joints or suspension types. This is not possible in this study due to the use of temporary socket materials and the requirement for semi-permanent instrumentation of the socket walls. As a result, extensive use of alternatives to the participant's regular equipment is not practical. The decision to restrict acclimatisation time in this way is thought to be less crucial in a socket modification study as a newer

socket is likely to be more suitable for the user given it will account for more recent changes in residual limb volume.

A formal power calculation has been based on data from Seelen et al⁹. This study represents the most suitable source for this calculation – it is the largest study of pressure changes with prosthesis alignment, and one of the few to present complete mean and variance values. As an example, that study found the mean difference in patellar tendon pressure, expressed as percentage of bodyweight was 7% (pooled SD 0.165). For a two-tailed comparison of means test, a desired power of 0.8 and a significance boundary of 0.05, the minimum sample size is calculated at 88.

This is impractical for this project, both in terms of time required, expense of materials and availability of lab support. For these reasons, a smaller sample of six has been specified. Although this presents a significant limitation to the study, a published article based on a sample of six would still be the 4th largest study of transtibial pressure and alignment ever presented, and the largest in the last 13 years.

Reporting

The primary means of publishing the results of this study will be as part of the lead researcher’s PhD thesis. Other forms of distribution include as part of conference proceedings and in journal articles. Methods for preserving participant anonymity have been described previously.

The consent form has the option for requesting a copy of any published material featuring their data. To do so will require the participant to supply an email address. This information is kept in the same secure manner as the remainder of the written data, and used for this purpose only.

Proposed Timeline

Week	Activity
1	Confirmation of ethical approval, approach to potential participants.
2	Participants receive information sheet and review. Researchers confirm materials required for study.
3	Confirmation of interest for participants.
4	P1+P2 Session 1.
5	P1+P2 Socket construction. P3+P4 Session 1.
6	P1+P2 Socket instrumentation. P3+P4 Socket construction. P5+P6 Session 1.
7	P1+P2 Session 2. P3+P4 Socket Instrumentation. P5+P6 Socket Construction.
8	P1+P2 Analysis. P3+P4 Session 2. P5+P6 Socket Instrumentation.
9	P3+P4 Analysis. P5+P6 Session 2.
10	P5+P6 Analysis.
11+	Processing, Analysis and Reporting

References

- Noroozi S, Amali R, Vinney J. Inverse Problem Approach using Photoelastic Analysis and Artificial Neural Networks in Tandem Introduction to Photoelasticity. *Strain*. 2004;40:73–77.
- Amali R, Noroozi S, Vinney J, Sewell P, Andrews S. An artificial intelligence approach for measurement and monitoring of pressure at the residual limb/socket interface – a clinical study. *Insight - Non-Destructive Test Cond Monit [Internet]*. 2008 Jul;50(7):374–383.
- Sewell P, Noroozi S, Vinney J, Amali R, Andrews S. Static and dynamic pressure prediction for

Protocol Document

- prosthetic socket fitting assessment utilising an inverse problem approach. *Artif Intell Med*. 2012 Jan;54(1):29–41.
4. Pirouzi G, Abu Osman NA, Eshraghi A, Ali S, Gholizadeh H, Wan Abas WAB. Review of the Socket Design and Interface Pressure Measurement for Transtibial Prosthesis. *Sci World J*. 2014;2014:1–9.
 5. Hafner BJ. State of the Science Evidence Report Guidelines. 2008.
 6. Ryall NH, Eyres SB, Neumann VC, Bhakta BB, Tennant A. The SIGAM mobility grades: a new population-specific measure for lower limb amputees. *Disabil Rehabil*. 2003;25(15):833–844.
 7. Neumann ES. State-of-the-science review of transtibial prosthesis alignment perturbation. *J Prosthetics Orthot*. 2009;21(4):175–187.
 8. Hanspal RS, Fisher K, Nieveen R. Prosthetic socket fit comfort score. *Disabil Rehabil [Internet]*. 2003;25(22):1278–1280.
 9. Seelen HAM, Anemaat S, Janssen HMH, Deckers JH. M. Effects of prosthesis alignment on pressure distribution at the stump/socket interface in transtibial amputees during unsupported stance and gait. *Clin Rehabil*. 2003 Oct 1;17(7):787–796.



Participant Information Sheet

Measuring prosthetic socket pressures with changes in device alignment and walking conditions – Developed testing

You are being invited to take part in a research project that aims to test a new method of measuring the pressures inside your prosthetic socket that are caused by standing and walking. Before you decide if you would like to participate, it is important that you understand why the research is being done and what you would be asked to do. Please read the following information carefully – you may discuss it with other people if you wish. If you would like any more information about the study, or if anything you read is unclear, please contact us using the details at the end of this document. Take the time to decide whether or not you wish to take part.

The lead researcher for this project is Philip Davenport, a PhD student at Bournemouth University. His research is supervised at the university by Professor Siamak Noroozi and Dr Philip Sewell. Technical support at Chas A Blatchford and Sons Ltd. is provided by Dr Saeed Zahedi.

What is the purpose of this research?

Engineers based at Bournemouth University have developed a new method of measuring the pressures inside amputee's prosthetic sockets. Users, prosthetists and other clinicians consider understanding pressure distribution to be very important for designing and building comfortable and functional prosthetic sockets. At the moment there are very few practical methods of monitoring this pressure distribution – the new method we have created addresses some of the issues these other methods face. We are interested to see how well this system can measure more challenging movements, and seeing what differences are there between different amputees.

Why have I been chosen?

In this study, we are interested in measuring the socket pressures of six below knee amputees who have an active lifestyle. You have been asked as you have previously expressed an interest in participating in research of this type.

Do I have to take part?

Participating in this research is entirely voluntary. If you decide to take part, you will receive a copy of this information sheet to keep, and you will be asked to sign a participant agreement form covering your participation and the use of your data. You can withdraw from the study up to the point of the completion of the data collection and the anonymisation of your data. You do not have to give a reason for withdrawing from the study. Taking part will not affect your prosthetic care.

What do I have to do?

If you want to take part in this research, you will be asked to attend two sessions at Blatchford's Ltd. in Basingstoke. At the first session, you will be asked for details on your residual limb and your current prosthesis, and measurements such as height, weight and stump shape taken. An experienced prosthetist will also take a cast of your residual limb – this will be used to create a prosthetic socket for use in the remainder of the study. This appointment will take 1-2 hours.

At the second session, you will be asked to wear this new socket, and carry out some walking tests using the new pressure measurement system. The new system uses sensors that measure changes in the shape of the socket – these are all attached to the outside surface of the socket, and are connected to set of wireless transmitters that will be attached to your socket pylon. This is shown in Figure 1.

Participant Information Sheet

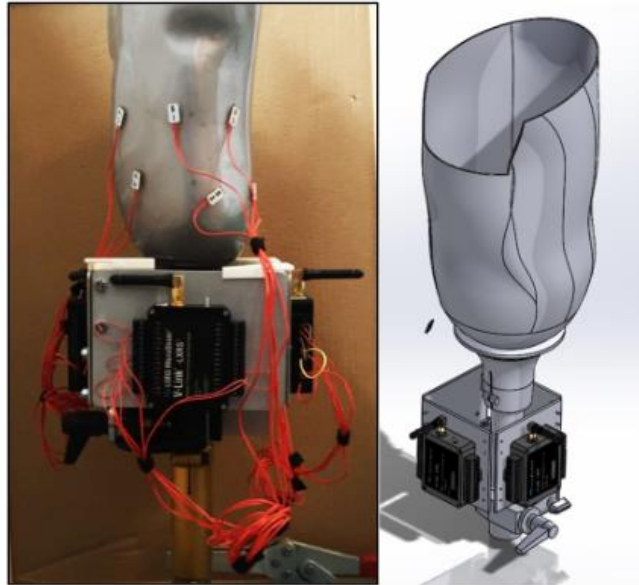


Figure 1: The measurement system you would wear for tests. The additional weight is around one kilogram (two lb).

At the same time we will use a 3D motion capture system to collect information on your walking. This involves attaching reflective markers to the skin on your legs. You will be asked to walk at a comfortable pace indoors on a level surface. We will then modify the alignment of the prosthesis by altering the height of the heel and toe of the footwear on your prosthetic side. You will be free to take a break at any time, and the test will be monitored by an experienced prosthetist for safety. We would also like you to rate the comfort of each alignment condition, using a simple 1-10 scale.

Finally we would like to measure your walking on gentle uphill and downhill slopes. These tests can all be completed inside Blatchford's test facility. Once again, you can go at whatever pace is comfortable and can take breaks if you would like to.

The total time for the second session is expected to be 2-3 hours. Your personal prosthesis or footwear will not be altered during the study. As part of the study we will make video recordings of your walking –these will focus on your legs and torso, and will be edited to remove faces if published. We may also wish to take photographs of your residual limb for later reference: these will also be anonymised.

The researcher for this project is a postgraduate student at Bournemouth University. He is also a state-registered clinician scientist. Prosthetist assistance is supplied by Blatchford's Ltd.

What are the possible disadvantages and risks of taking part?

As you will know from your own prosthetic prescription, new sockets may cause slight discomfort when worn – the socket can be modified to improve comfort before the measurement tests take place. The time spent wearing the socket is quite short, and breaks may be taken if needed.

Participant Information Sheet

Similarly, altering the device alignment can cause mild discomfort due to the changes in how the forces from walking are applied to your residual limb. To limit this discomfort, all tests will be completed using small alignment changes, and with the guidance of the prosthetic team.

If you feel a particular configuration or task is too uncomfortable or unsafe, you do not have to complete that measurement. You will be allowed time to get used to each alignment state before completing the tests. We expect the process to be similar to the way your regular prosthesis is adjusted during the initial set-up of the device.

What are the possible benefits of taking part?

Although there are no direct benefits to yourself or your prosthetic care as a result of your participation in this study, the knowledge gained will help in the development of new clinical assessment tools to be used by clinicians and engineers in the future. You will be compensated for travel expenses for trips to the test location in Basingstoke.

How will the results of this study be used?

If you decide to take part, you will be assigned a participant number that will be used to label your data. Access to this reference is limited to those researchers directly involved in this study, and will be securely stored electronically at Bournemouth University. Any physical documents that include identifiable information (e.g. participant agreement forms) will be kept securely at Bournemouth University.

All data relating to the study will be kept by Bournemouth University for 5 years on a password protected secure network and drive.

This research will be included in a doctoral thesis being completed by the lead researcher. Data may be included as part of publications in academic journals or conferences. If you would like a copy of these publications, you can indicate your interest on the participant agreement form and receive a copy once it is available. If you choose to supply your email address, it will be used for this purpose only. The information will be kept for the same length of time as the rest of the supplied information.

All information that is collected as part of the study is therefore strictly confidential. You will not be personally identified in any report or publication produced as part of this research. Any photographs or videos collected will also be edited to ensure anonymity.

What information will be sought from me and why is this relevant to project?

We will ask you for details regarding your residual limb and usual prosthesis. This will include questions such as the reason for and time since your amputation, your experience with your prosthesis and for an estimate of your activity levels. Past research has shown that pressure distribution can vary depending on these differences, and so having this information will help us interpret the results.

During testing, we will also ask you to rate the comfort of your socket. This will help us understand how changes in alignment are experienced by amputees, as well as the sensitivity of the new measurement method.

Participant Information Sheet

Who is organising and funding the research?

The work is being completed by researchers at Bournemouth University with financial and technical support from Chas A Blatchford and Sons Ltd. The project is part of an EPSRC CASE industrial studentship, ID 4114.

Contact details for further information

The principal researcher for this project is:

Philip Davenport BEng, MSc, CSci MIPEM
Clinical Scientist and Postgraduate Researcher
Bournemouth University
Poole House Room 517
Fern Barrow
Poole
BH12 5BB
PDavenport@bournemouth.ac.uk
01202 961994

The lead academic supervisor for this project is:

Professor Siamak Noroozi BSc, MEng, PhD, MIET, CEng
Bournemouth University
Poole House Room 121
Fern Barrow
Poole
BH12 5BB
snoroozi@bournemouth.ac.uk
01202 965554

If you have any queries about this study or the research in general, please contact the principal researcher. If you have a complaint about the conduct of the study, please contact the deputy dean for research and professional practice Matt Bentley for details of the university complaints procedure. Professor Bentley is otherwise independent of the research project.

Professor Matt Bentley BSc PhD
Deputy Dean – Research and Professional Practice
Bournemouth University
Christchurch House Room C227
Fern Barrow
Poole
BH12 5BB
mbentley@bournemouth.ac.uk
01202 962203

Thank you for taking the time to read this information sheet. If you have any questions about the project or your participation, please contact the research team. If you agree to take part in the study, you will be given a copy of this document to keep along with a copy of your participant agreement form.

A12 Full Study Participant Consent Form



Participant Agreement Form

25/08/2016

Measuring prosthetic socket pressures with changes in device alignment and walking conditions – Developed testing

Project Researcher:
Philip Davenport
 Clinical Scientist and Postgraduate Researcher
 Bournemouth University
 Poole House Room 517
 Fern Barrow
 Poole
 BH12 5BB
 PDavenport@bournemouth.ac.uk
 01202 261994

Lead Project Supervisor:
Professor Siamak Noroozi
 Bournemouth University
 Poole House Room 121
 Fern Barrow
 Poole
 BH12 5BB
 SNoroozi@bournemouth.ac.uk
 01202 965554

Please Initial Here

I confirm that I have read and understood the participant information sheet (Dated 25/08/2016, Version 1) for this research project.	
I have had the opportunity to ask questions about the project, and have these answered to my satisfaction.	
I understand that my participation is entirely voluntary and that I am free to withdraw from the study up to the point of anonymisation without giving a reason and without any negative consequences.	
I understand that I am free to decline to answer any question or complete any test.	
I give permission for members of the research team to have access to my anonymised data and responses.	
I understand that my name will not be linked with the research materials, and I will not be identified or identifiable in any published material from the project.	
I give permission for the research team to collect video and photographic material where this is essential for the research project, as described in the participant information sheet, and that any video or photographic material will be anonymised prior to publication.	
I agree to take part in this research project	

 Name of Participant Date Signature

If you would like to receive copies of published research,
 please leave your email address here: _____

 Name of Researcher Date Signature


The signed consent form should be kept by the participant for future reference, along with the participant information sheet. A copy will be stored securely with the project documentation.

A13 Participant Data Collection Form Template



Participant Data Collection Form

Measuring prosthetic socket pressures with changes in device alignment and walking conditions – Pilot Study

Name	
Participant ID	P01
Date of Assessment	
Date of Birth	
Height (m)	
Weight (kg)	
Amputation Side	
Amputation Level	
Amputation Date	
Amputation Reason	
Stump Description	
Stump Dimensions	
Prescribed Socket Comfort Score	
Prescribed Socket Qualitative Description	
Test Socket Comfort Score	
Test Socket Qualitative Description	

Participant Data Collection Form

T01		T17	
T02		T18	
T03		T19	
T04		T20	
T05		T21	
T06		T22	
T07		T23	
T08		T24	
T09		T25	
T10		T26	
T11		T27	
T12		T28	
T13		T29	
T14		T30	
T15		T31	
T16		T32	

LORD PRODUCT DATASHEET

V-Link® -LXRS®

Wireless 7 Channel Analog Input Sensor Node

The V-Link® -LXRS® Wireless 7 Channel Analog Input Sensor Node features 4 differential input channels with optional bridge completion, 3 single ended input channel with 0-3 volt excitation, and an internal temperature sensor channel. This array supports a wide range of user-supplied Wheatstone bridge and analog sensors including strain, load cells, torque, pressure, acceleration, vibration, magnetic fields, displacement, geophones and more. V-Link data is 16-bit resolution. The node can log data to internal memory, transmit real-time data, or support event driven triggers with both pre- and post- event buffers. **Node Commander®** software supports configuration of the wireless node including discovery, initialization, radio frequency, sample rate, reading/writing to node EEPROM, calibrating node sensors, managing node batteries, and upgrading node firmware. The V-Link is compatible with any **WSDA®** -Base, WSDA® -1000 or **SensorCloud™**.



Features & Benefits

Wireless Simplicity, Hardwired Reliability

- LXRS® reliable and synchronized wireless data
- Event driven triggers for efficient monitoring
- Long term deployment with low-power systems
- SensorCloud web-base data, report, & alerts

Ease of Evaluation & Integration

- No wires - scalably installed wireless form factor
- Rapid development via comprehensive SDK

Cost Effective

- Low-cost per channel with 7 input channels per node
- Aggressive volume discount schedule

Applications

- Rotating Component Health
- Condition-Based Monitoring of Machines
- Health Monitoring of Aircraft, Structures and Vehicles
- Experimental Test and Measurement
- Robotics and Machine Automation

System Overview

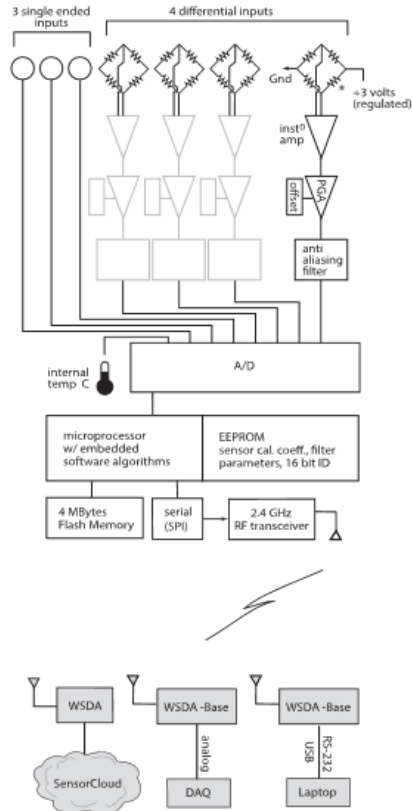
Lord **MicroStrain®** Sensing Systems offer wireless sensors for remote sensor data acquisition, storage, analysis, and response systems. A system comprises wireless sensor nodes, **WSDA®** gateways, and software. Using the MicroStrain® LXRS (Lossless Extended Range Synchronized) protocol, one gateway can coordinate thousands of unique nodes for synchronized and lossless data delivery. Bidirectional wireless communication allows gateways to collect data and configure nodes up to 2 km away (line of sight). Gateways can be connected locally by PC or DAQ, and remotely to the web, by Ethernet, cellular, or satellite. The selection of available nodes allows monitoring with most standard sensor types. Nodes are IEEE 802.15.4 compliant (license free worldwide) and can sample in a large range of rates and configurations to suit the widest possible variety of end user needs. Node Commander® and SensorCloud™ software platforms allow both local and remote network management from almost anywhere on the planet.



V-Link® -LXRS® Wireless 7 Channel Analog Input Sensor Node

Specifications

Input channels	up to 7 input channels: 4 full differential, 350 Ω resistance or higher (with optional bridge completion), and 3 single ended inputs (0-3 volts maximum), plus an internal temperature sensor
Temperature sensor	-40 °C to 70 °C range, typical accuracy ±2 °C (at 25 °C)
Anti-aliasing filter bandwidth	-3 dB cutoff at 250 Hz (factory adjustable)
Resolution	16 bit
DC bridge excitation	+3 volts DC at 50 mA maximum (pulsed to sensors for sample rates of 16 Hz and below to conserve power)
Programmable gain	software programmable for differential input channels from 21 to 13074 (can be reduced with hardware resistor change)
Programmable offset	software programmable
Data storage capacity	4 megabytes (approximately 2,000,000 data points)
Sampling modes	synchronized, armed datalogging, streaming, low duty cycle
Synchronized sampling rates	1 sample/hour - 512 Hz continuous
Synchronized sampling mode network capacity	Transmit real time data from node to PC - rate depends on number of active channels and transmitting nodes. e.g., 3 nodes, 1 channel, 512 Hz 15 nodes, 1 channel, 256 Hz 31 nodes, 1 channel, 128 Hz 63 nodes, 1 channel, 64 Hz 127 nodes, 1 channel, 32 Hz sample rates and # of channels are easily configured within Node Commander® Network Configuration Wizard
Synchronization between nodes	± 32 μsec with 10 second beacon interval
Synchronization rate stability	± 3 ppm
Armed datalogging sampling rates	1 channel enabled: 32 Hz to 4096 Hz; 2 or more channels enabled: 32 Hz to 2048 Hz
Streaming sampling rates (approximate)	1 channel enabled: 736 Hz; 3 channels enabled: 617 Hz per channel; 8 channels enabled: 424 Hz per channel
Low duty cycle sampling rates	1 sample/hour - 512 Hz
Event driven monitoring	user-definable event threshold trigger; 200,000 bytes pre- event datalogging and/or transmitting
Shunt calibration	channels 1 to 4, internal shunt calibration resistor 499 KΩ
Radio frequency (RF) transceiver carrier	2.4 GHz direct sequence spread spectrum, license free worldwide (2.405 to 2.480 GHz) – 14 channels, radiated power programmable from 0 dBm (1 mW) to 16 dBm (39 mW); limited to 10 dBm (10 mW) outside of US
RF data packet standard	IEEE 802.15.4, open communication architecture
RF data downloading	8 minutes to download full memory
Range for bi-directional RF link	programmable communication range from 70 meters to 2 kilometers los (line of sight); 70 m to 1 km los range outside of US
Status LEDs	battery charging, battery charged, node activity
Power	internal: 3.7 volt 650 mAh lithium ion rechargeable battery; external: +3.2 to +9.0 VDC
Power consumption	see power profiles at www.microstrain.com/wireless/v-link
Operating temperature	-20 °C to +60 °C with standard internal battery and enclosure, extended temperature range optional with custom battery and enclosure, -40 °C to +85 °C for electronics only
Maximum acceleration limit	500 g standard (high g option available)
Dimensions	74 mm x 79 mm x 20 mm without antenna
Weight	141 grams
Enclosure material	anodized aluminum
ROHS	compliant
Compatible base stations	all WSDA®-Base and WSDA®-1000
Software	Node Commander® Windows XP/Vista/7 compatible
Software development kit (SDK)	includes data communications protocol, EEPROM maps and sample code (OS and computing platform independent)
FCC ID	XJQMSLINK0003
IC ID	8505A-MSLINK0003

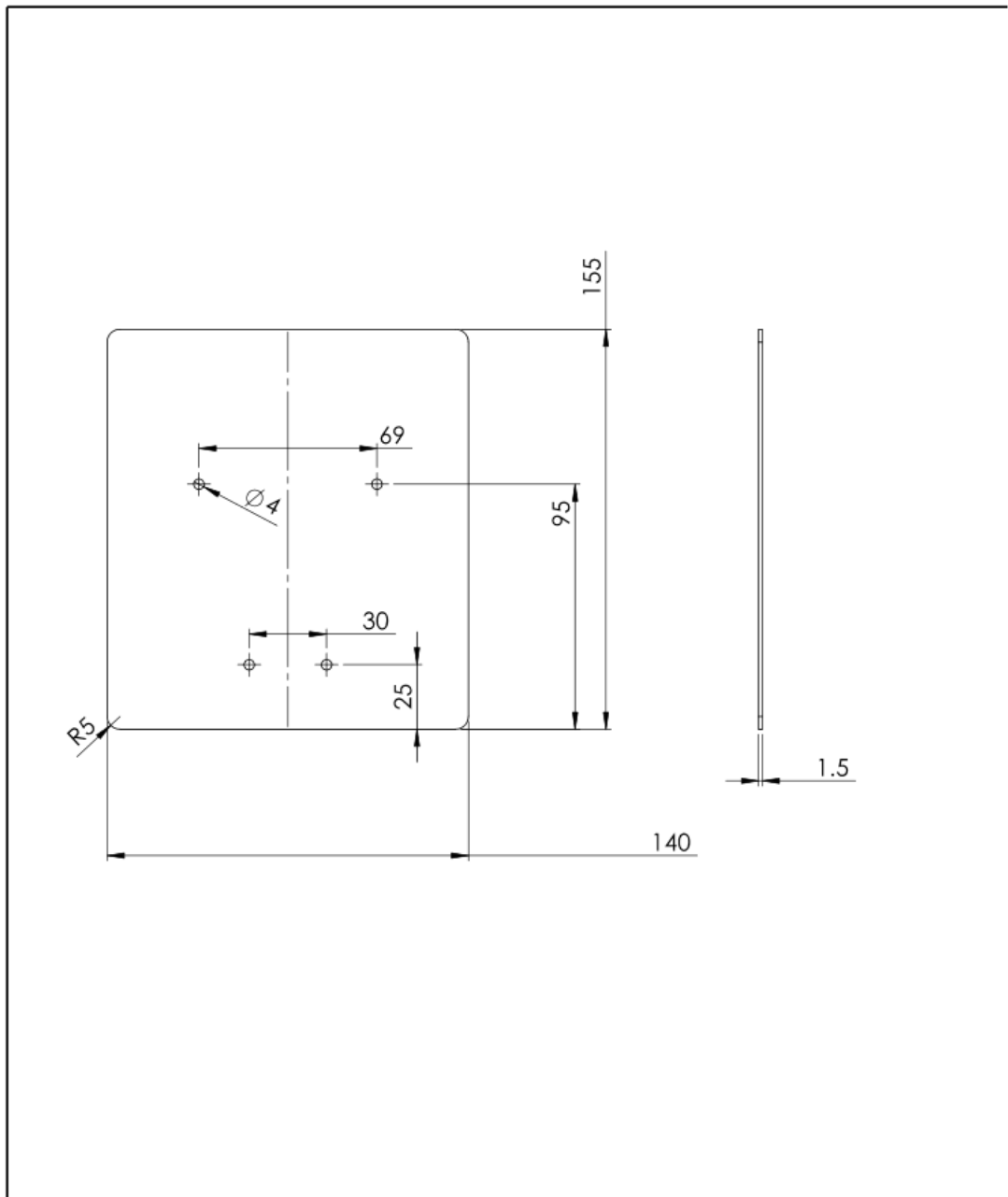


* Optional on-board bridge completion

Copyright © 2014 LORD Corporation
 IEPE-Link™, Torque-Link™, 3DM-RQ1™, Strain Wizard®, DEMOD-DC®, DVRT®, DVRT-Link™, WSDA®, HS-Link®, TC-Link®, G-Link®, V-Link®, SG-Link®, ENV-Link™, Watt-Link™, Shock-Link™, SHM-Link™, LXRS®, Node Commander®, SensorCloud™, Live Connect™, MathEngine®, EH-Link®, 3DM®, FAS-A®, 3DM-GX1®, 3DM-GX3®, 3DM-GX4™, 3DM-DH®, 3DM-DH3™, EmbedSense®, MicroStrain®, and Little Sensors, Big Ideas® are trademarks of LORD Corporation.
 8400-0012 rev 001
 Specifications are subject to change without notice. 1.00c

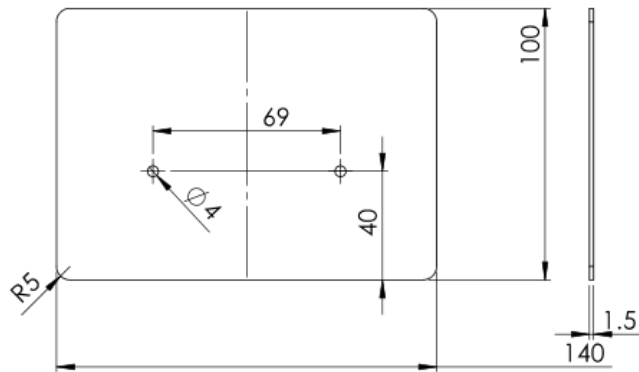
LORD Corporation
MicroStrain® Sensing Systems
 459 Hurricane Lane,
 Suite 102
 Williston, VT 05495 USA
www.microstrain.com
 ph: 800-449-3878
 fax: 802-863-4093
sensing_sales@LORD.com
sensing_support@LORD.com

A15 Mounting Rig Plate 1



UNLESS OTHERWISE SPECIFIED: DIMENSIONS ARE IN MILLIMETERS		FINISH:		DEBUR AND BREAK SHARP EDGES		DO NOT SCALE DRAWING		REVISION	
SURFACE FINISH:									
TOLERANCES:									
LINEAR:									
ANGULAR:									
NAME		SIGNATURE		DATE		TITLE:			
DRAWN									
CHK'D									
APPV'D									
MFG									
Q.A						MATERIAL:		DWG NO.	
						Aluminium		Extended Plate	
						WEIGHT:		SCALE:1:2	
								SHEET 1 OF 1	
								A4	

A16 Mounting Rig Plate 2-4



UNLESS OTHERWISE SPECIFIED: DIMENSIONS ARE IN MILLIMETERS				FINISH:		DEBUR AND BREAK SHARP EDGES		DO NOT SCALE DRAWING		REVISION	
SURFACE FINISH:											
TOLERANCES:											
LINEAR:											
ANGULAR:											
NAME		SIGNATURE		DATE				TITLE:			
DRAWN											
CHK'D											
APP'VD											
MFG											
Q.A						MATERIAL:		DWG NO.		Plate	
						Aluminium				A4	
						WEIGHT:		SCALE:1:2		SHEET 1 OF 1	

A17 LabView ANN MATLAB Code

28/03/17 12:13 \\bournemouth.ac.uk\da...\labviewANN v4.m 1 of 1

```
function [Lnet] = labviewANN_v4(layers,epochs,goal,input,output,control,name)

if control==1
    Lnet=feedforwardnet(layers);
    Lnet.trainParam.epochs=(epochs);
    Lnet.trainParam.goal=(goal);
    Lnet.layers{2}.transferFcn='tansig';
    Lnet.layers{1}.transferFcn='poslin';
    Input=input';
    Output=output';

    Lnet=train(Lnet,Input,Output);
    save('Lnet.mat','Lnet');
    newname=['C:\LnetIterations\' ,name, '.mat'];
    save(newname,'Lnet');
    Lnet;

else

end
```

A18 Polynomial Fitter MATLAB Code

28/03/17 12:20 \\bournemouth.ac.uk\data\...\polyfitter.m 1 of 2

```
function [fits,bestfits] = polyfitter(evaluation,TOV0p)

% The differences between the 'perfect' data and the 'calculated' data
differences=TOV0p-evaluation;

% Get the sizes of the comparison arrays
ndifferences=size(differences);
n1=ndifferences(1);
n2=ndifferences(2);

% Set up container cell-arrays to hold data
fits=cell(n2,7);
bestfits=cell(n2,1);

% Prep for graphs, using the maximum in the data
maximum=max(TOV0p);
xt=(1:1:maximum);
%figure

for i=1:n2
    % Pull out each row of the input arrays
    difference=differences(:,i);
    answer=TOV0p(:,i);

    % Calculate different order polynomial coefficients
    p3=polyfit(answer,difference,3);
    p4=polyfit(answer,difference,4);
    p5=polyfit(answer,difference,5);
    p6=polyfit(answer,difference,6);
    p7=polyfit(answer,difference,7);
    p8=polyfit(answer,difference,8);
    p9=polyfit(answer,difference,9);

    fits(i,1:7)=(p3,p4,p5,p6,p7,p8,p9);

%Evaluate each fit
f3=polyval(p3,answer);
f4=polyval(p4,answer);
f5=polyval(p5,answer);
f6=polyval(p6,answer);
f7=polyval(p7,answer);
f8=polyval(p8,answer);
f9=polyval(p9,answer);

fArray=[f3 f4 f5 f6 f7 f8 f9];

% Calculate the error between the fit and the actual values
e3=difference-f3;
e4=difference-f4;
e5=difference-f5;
e6=difference-f6;
e7=difference-f7;
e8=difference-f8;
e9=difference-f9;
```

```
eArray=[e3 e4 e5 e6 e7 e8 e9];

% Calculate the total RMS error across the range of measurements
rms3=rms(e3);
rms4=rms(e4);
rms5=rms(e5);
rms6=rms(e6);
rms7=rms(e7);
rms8=rms(e8);
rms9=rms(e9);

RMSArray=[rms3 rms4 rms5 rms6 rms7 rms8 rms9];

% Find the minimum error out of each fit
[M,Iraw]=min(RMSArray);
bestfits(i)={Iraw};

% Log each best fit and the coefficients into an exportable cell array
bestindex=bestfits(i);
bestcoeff=fits(i,bestindex);

% Plot each best fit on a subplot
%yl=polyval(bestcoeff,xt);
%subplot(n2,1,i);
%plot(xt,y1);

end

% Make overall values available for export
fits;
bestfits;
```

A19 Polynomial Correction MATLAB Code

28/03/17 12:20 \\bournemouth.ac.uk...\polycorrectionv2.m 1 of 1

```
function [correctedvalues,isofits] = polycorrectionv2(values,fits,bestfits)

% Find the number of output channels from the list of best polynomial fits
nchannel=size(values);
nchannels=nchannel(2);

%Set up cell container with the best poly coefficients
nfit=size(bestfits);
nfits=nfit(1);
isofits=cell(nfits,1);

for j=1:nfits
    selection=bestfits(j);
    isofits(j)=fits(j,selection);
end

%Initialise container array for the corrected values
correctedvalues=zeros(size(values));

for i=1:nchannels

    %For each channel, find the right set of answers and the best
    %polynomial coefficients
    value=values(:,i);

    correctionpoly=isofits(i);

    %Evaluate polynomial across the output values
    correctionfactor=polyval(correctionpoly,value);

    %Make the appropriate correction to the output values
    correctedgraph=value+correctionfactor;

    %Add the corrected values to the new output array
    correctedvalues(:,i)=correctedgraph;

end
isofits;
correctedvalues;
```

A20 Ensemble Generation MATLAB Code

28/03/17 12:45 \\bournemou...\labviewANN_ensemblenodes.m 1 of 1

```
function [] = labviewANN_ensemblenodes(input,output,control,iteration,run,nodes)

if control==1
    Lnet=feedforwardnet(nodes);
    Lnet.trainParam.epochs=(100);
    Lnet.trainParam.goal=(0.001);
    Lnet.layers(1).transferFcn='poslin';
    Lnet.layers(2).transferFcn='tansig';

    Input=input';
    Output=output';

    Lnet=train(Lnet,Input,Output);

    run=num2str(run);
    foldername=['C:\LnetIterations','\',run,'\']

    mkdir(foldername)
    it=num2str(iteration);

    name=['C:\LnetIterations\','\',run,'\','Lnet',it, '.mat'];
    save(name, 'Lnet');

else

end
```

A21 Ensemble Analysis MATLAB Code

28/03/17 12:20 \\bournemout...\EnsembleAnalysisVlpolym.m 1 of 2

```
function [Structure] = EnsembleAnalysisVlpolym(Structure,Test,Answers,trainin,↵
trainout)

Test=Test';
Answers=Answers';
sizes=size(Structure);
n=sizes(2);

for i=1:n

    Lnet=Structure(i).Lnet;

    trainr=Lnet(trainin');
    Structure(i).TrainingResults=trainr;
    trainr=trainr';

    %[fits,bestfits] = polyfitter(trainr,trainout);
    %Modify to polyfitterma to control the polynomial order directly
    [fits,bestfits] = polyfitterma(trainr,trainout);

    Structure(i).Fits=fits;
    Structure(i).Bestfits=bestfits;

    iteration1=polycorrectionv2(trainr,fits,bestfits);
    [fitsb,bestfitsb]=polyfitter(iteration1,trainout);
    %Modify to polyfittermb to control the polynomial order directly
    %[fits,bestfits] = polyfittermb(trainr,trainout);

    Structure(i).Fitsb=fitsb;
    Structure(i).Bestfitsb=bestfitsb;

    results=Lnet(Test);
    Structure(i).Results=results;
    difference=results-Answers;
    Structure(i).Difference=difference;

    rmsvalues=rms(difference);
    Structure(i).RMSValues=rmsvalues;
    rmstotal=sum(rmsvalues);
    Structure(i).RMSTotal=rmstotal;

    suman=sum(Answers);
    sumanswers=sum(suman);

    rmstotalp=sum((rmstotal/sumanswers)*100);
    Structure(i).RMStotalP=rmstotalp;

    %mod this section to alter the implementation of the polycorrection
    [resultscorra,isofta]=polycorrectionv2(results',fits,bestfits);
    %[resultscorb,isoftb]=polycorrectionv2limited(resultscorra,fitsb,bestfitsb);
    [resultscorb,isoftb]=polycorrectionv2(resultscorra,fitsb,bestfitsb);
```



```
Structure(i).ResultsCorrecteda=resultscorra;
Structure(i).ResultsCorrectedb=resultscorrb;

Structure(i).Isfitsa=isofita;
Structure(i).Isfitsb=isofitb;

diffcorra=resultscorra'-Answers;
diffcorrb=resultscorrb'-Answers;
Structure(i).DifferenceCorrecteda=diffcorra;
Structure(i).DifferenceCorrectedb=diffcorrb;

rmsvaluescorra=rms(diffcorra);
rmsvaluescorrb=rms(diffcorrb);
Structure(i).RMSValuesCorrecteda=rmsvaluescorra;
Structure(i).RMSValuesCorrectedb=rmsvaluescorrb;

rmstotalcorra=sum(rmsvaluescorra);
rmstotalcorrb=sum(rmsvaluescorrb);
Structure(i).RMSTotalCorrecteda=rmstotalcorra;
Structure(i).RMSTotalCorrectedb=rmstotalcorrb;

rmstotalpcorra=sum((rmstotalcorra/sumanswers)*100);
rmstotalpcorrb=sum((rmstotalcorrb/sumanswers)*100);
Structure(i).RMStotalPCorrecteda=rmstotalpcorra;
Structure(i).RMStotalPCorrectedb=rmstotalpcorrb;

Structure(i).Improvementa=rmstotalp-rmstotalpcorra;
Structure(i).Improvementb=rmstotalp-rmstotalpcorrb;

end

Structure;
```

A22 Ensemble Summation MATLAB Code

28/03/17 12:20 \\bournemouth.ac.uk\d...\EnsembleFullv2.m 1 of 1

```
function [Structure,Ensemble,Report]=EnsembleFullv2(Struct,testin,testout,trainin,trainout)

[Structure] = EnsembleAnalysisV1polym(Struct,testin,testout,trainin,trainout);

[Ensemble,Report]=Multiple_evaluationv3(Structure,testin,testout);

Report(1).RMSTotalPCons=[Structure.RMStotalP];
Report(1).RMSTotalPConsCorrecteda=[Structure.RMStotalPCorrecteda];
Report(1).RMSTotalPConsCorrectedb=[Structure.RMStotalPCorrectedb];

Ensemble;
Structure;
Report;
```

A23 Ensemble Evaluation MATLAB Code

28/03/17 12:20 \\bournemouth...\Multiple_evaluationv3.m 1 of 2

```
function [Ensemble,Report]=Multiple_evaluationv3(Struct,Input,Output)
%Version for Lnet structures
%v3 intended for checking polynomial corrections
n=[Struct.('Lnet')];
n=length(n);
Input=Input';

for i=1:n;

    results=Struct(i).Lnet(Input);
    Ensemble(i).Results=results;

    Ensemble(i).Fits=Struct(i).Fits;
    Ensemble(i).Bestfits=Struct(i).Bestfits;

    fits=Struct(i).Fits;
    bestfits=Struct(i).Bestfits;

    [resultscorr,isofit]=polycorrectionv2(results',fits,bestfits);
    Ensemble(i).ResultsCorrected=resultscorr';
    Ensemble(i).Isofits=isofit;

end

[m,o]=size(Ensemble(1).Results);

summary=zeros(m,o,n);
summarycorr=summary;

for j=1:n
    for k=1:o
        for l=1:m
            summary(l,k,j)=Ensemble(j).Results(l,k);
        end
    end
end

for j=1:n
    for k=1:o
        for l=1:m
            summarycorr(l,k,j)=Ensemble(j).ResultsCorrected(l,k);
        end
    end
end

Summary=summary;
Summarycorr=summarycorr;

Averages=zeros(m,o);
Averagescorr=Averages;

Averages=mean(Summary,3);
Averagescorr=mean(Summarycorr,3);
```

```
Output=Output';
difference=Averages-Output;
differencecorr=Averagescorr-Output;

rmsvalues=rms(difference);
rmsvaluescorr=rms(differencecorr);
rmstotal=sum(rmsvalues);
rmstotalcorr=sum(rmsvaluescorr);

suman=sum(Output);
sumanswers=sum(suman);

rmstotalp=sum((rmstotal/sumanswers)*100);
rmstotalpcorr=sum((rmstotalcorr/sumanswers)*100);

Report(1).Answers=Output;
Report(1).Averages=Averages;
Report(1).AveragesCorrected=Averagescorr;
Report(1).Difference=difference;
Report(1).DifferenceCorrected=differencecorr;
Report(1).RMSValues=rmsvalues;
Report(1).RMSCorrected=rmsvaluescorr;
Report(1).RMSTotal=rmstotal;
Report(1).RMSTotalCorrected=rmstotalcorr;
Report(1).RMSTotalP=rmstotalp;
Report(1).RMSTotalPCorrected=rmstotalpcorr;
```

A24 MATLAB Distribution Generation Code

28/03/17 12:42 \\bournemouth.ac.uk\data\Stu...\distgen.m 1 of 1

```
function [dist]=distgen(number,average,deviation)

dist=deviation.*randn(number,1)+average;
```

LXRS_v5.2.vi
 H:\LabVIEW Data\Test VIs\Thesis Versions\LXRS_v5.2.vi
 Last modified on 28/03/2017 at 12:25
 Printed on 29/03/2017 at 16:09

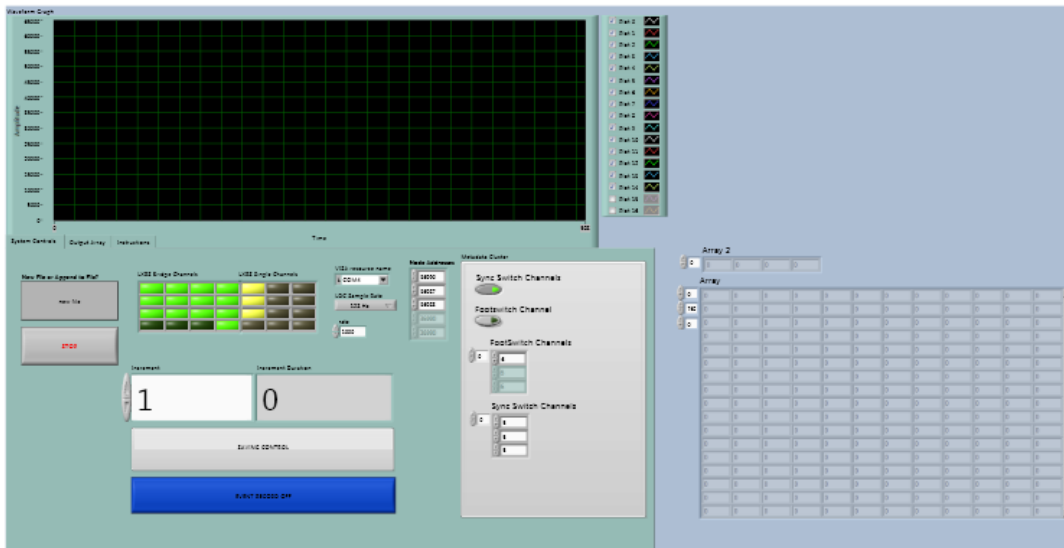
Connector Pane

LXRS_v5.2.vi

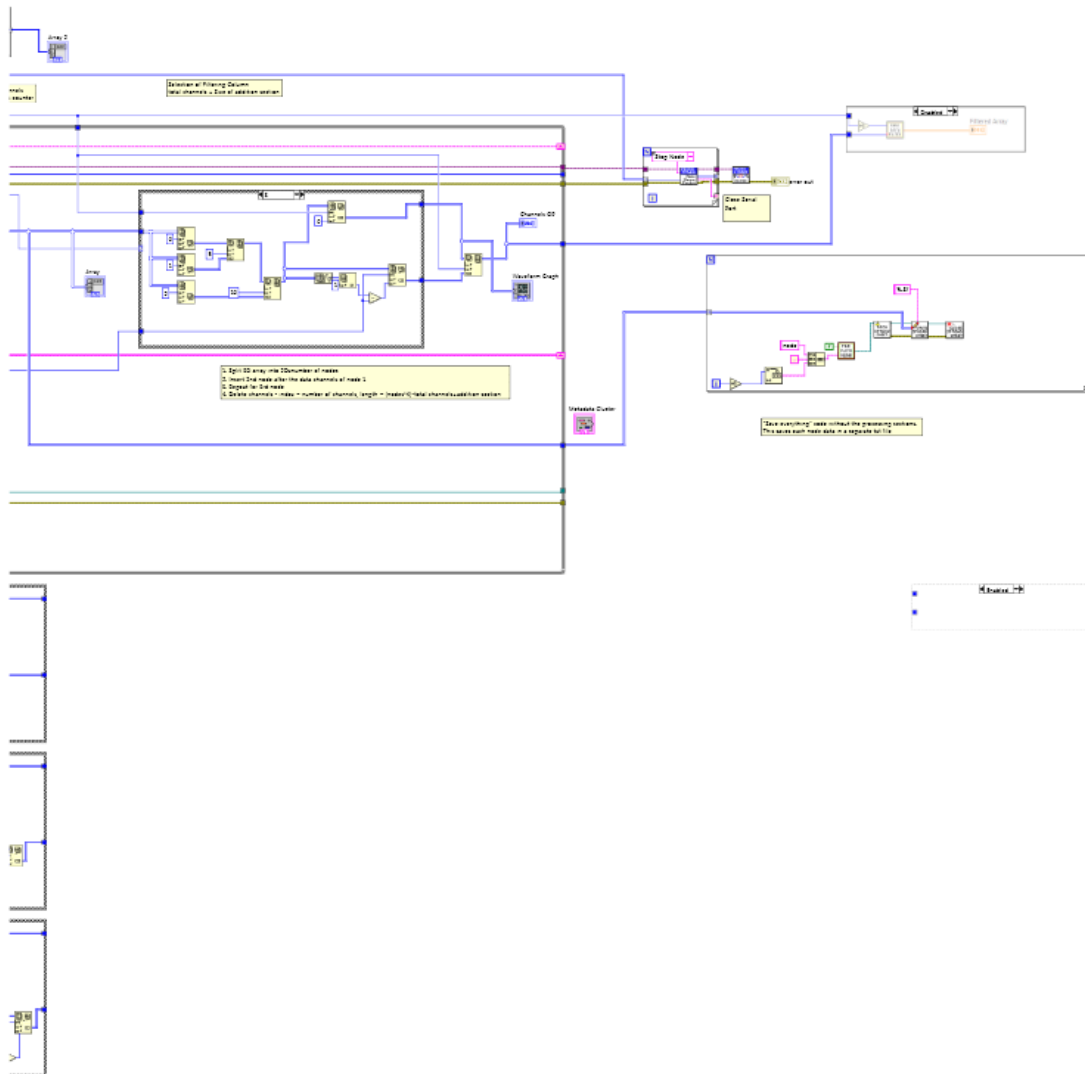


Places node(s) into LDC mode at a given sampling rate and for a specific number of sweeps. Incoming packets are then recieved and parsed. When stop is pressed, the node(s) are woken up and the program ended.

Front Panel



LXRS_v5.2.vi
H:\LabVIEW Data\Test VIs\Thesis Versions\LXRS_v5.2.vi
Last modified on 28/03/2017 at 12:25
Printed on 29/03/2017 at 16:09

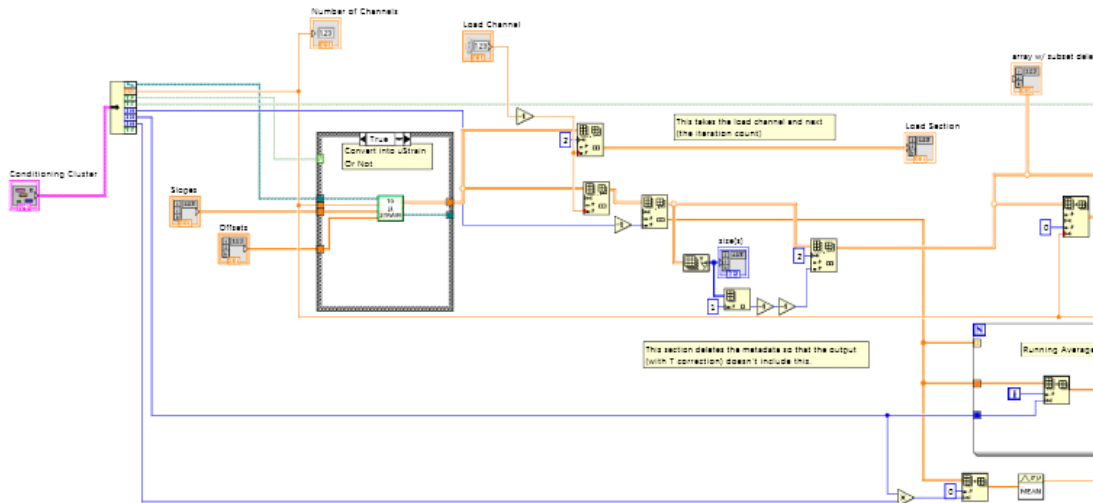
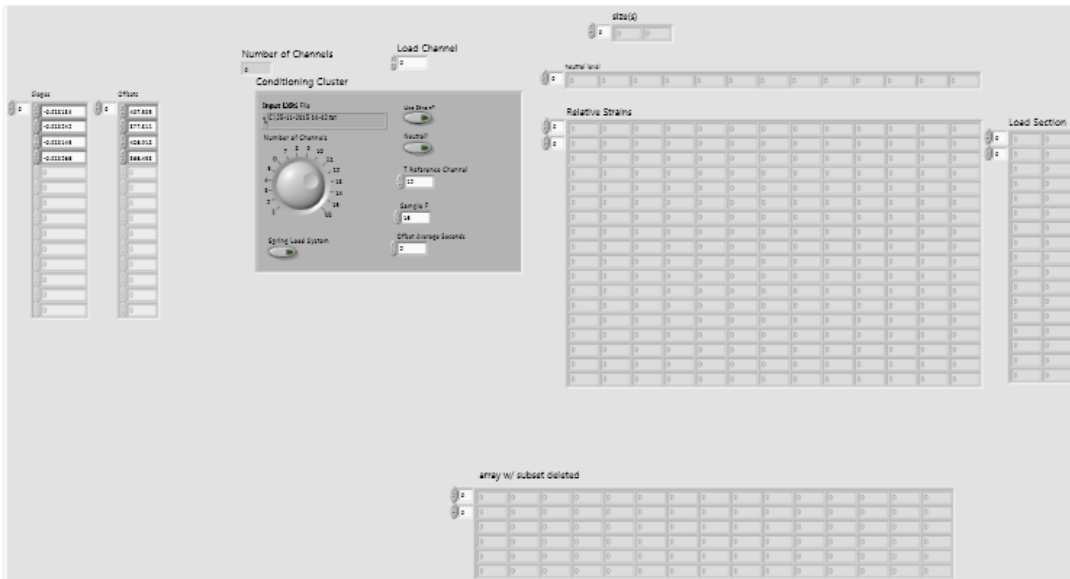
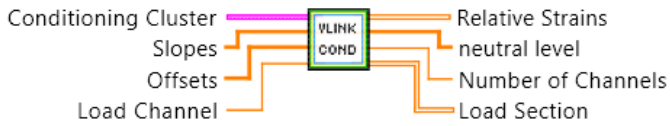


A27 LabView VLink Conditioning Code

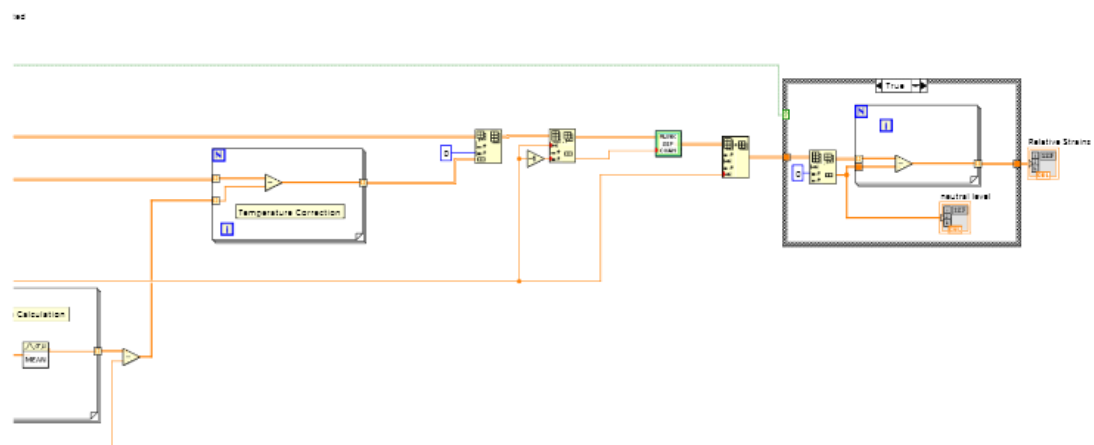


VLink_conditioning_v2.vi
 H:\LabVIEW Data\Test VIs\Thesis Versions\VLink_conditioning_v2.vi
 Last modified on 28/03/2017 at 12:27
 Printed on 29/03/2017 at 16:13

VLink_conditioning_v2.vi



VLink_conditioning_v2.vi
H:\LabVIEW Data\Test VIs\Thesis Versions\VLink_conditioning_v2.vi
Last modified on 28/03/2017 at 12:27
Printed on 29/03/2017 at 16:13

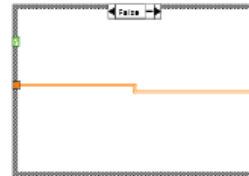




VLink_conditioning_v2.vi
H:\LabVIEW Data\Test VIs\Thesis Versions\VLink_conditioning_v2.vi
Last modified on 28/03/2017 at 12:27
Printed on 29/03/2017 at 16:13



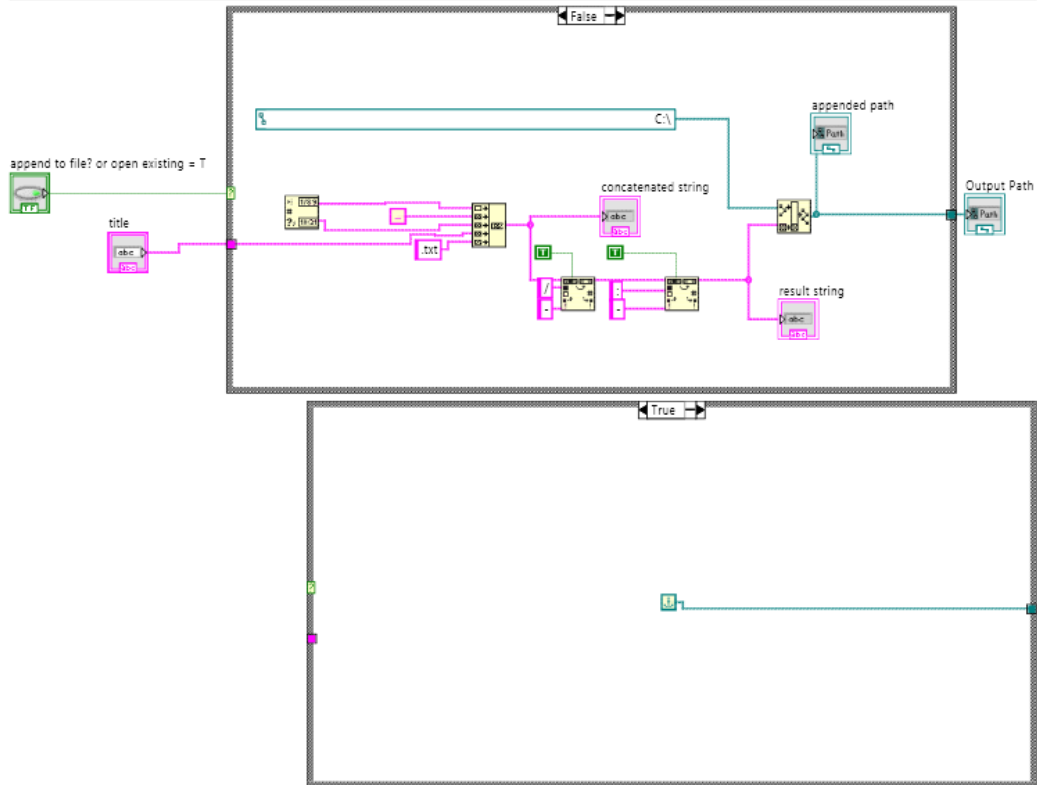
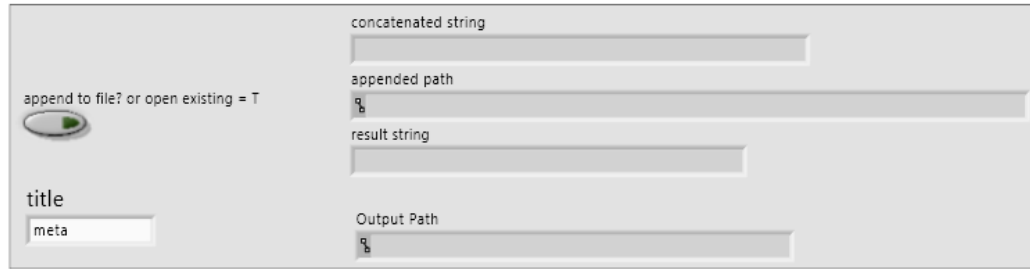
VLink_conditioning_v2.vi
H:\LabVIEW Data\Test VIs\Thesis Versions\VLink_conditioning_v2.vi
Last modified on 28/03/2017 at 12:27
Printed on 29/03/2017 at 16:13



A28 LabView File Path Code

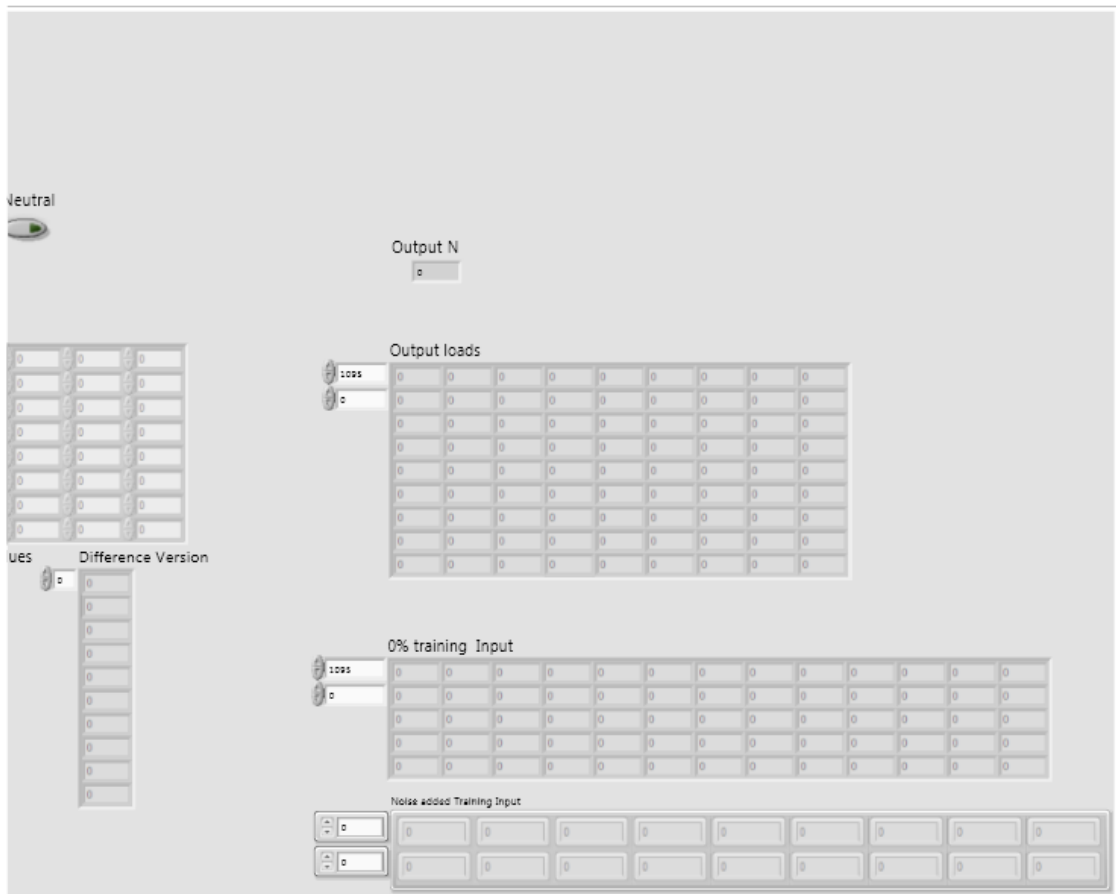
file_path_v3.vi
H:\LabVIEW Data\Test VIs\Thesis Versions\file_path_v3.vi
Last modified on 28/03/2017 at 12:25
Printed on 29/03/2017 at 16:15

file_path_v3.vi



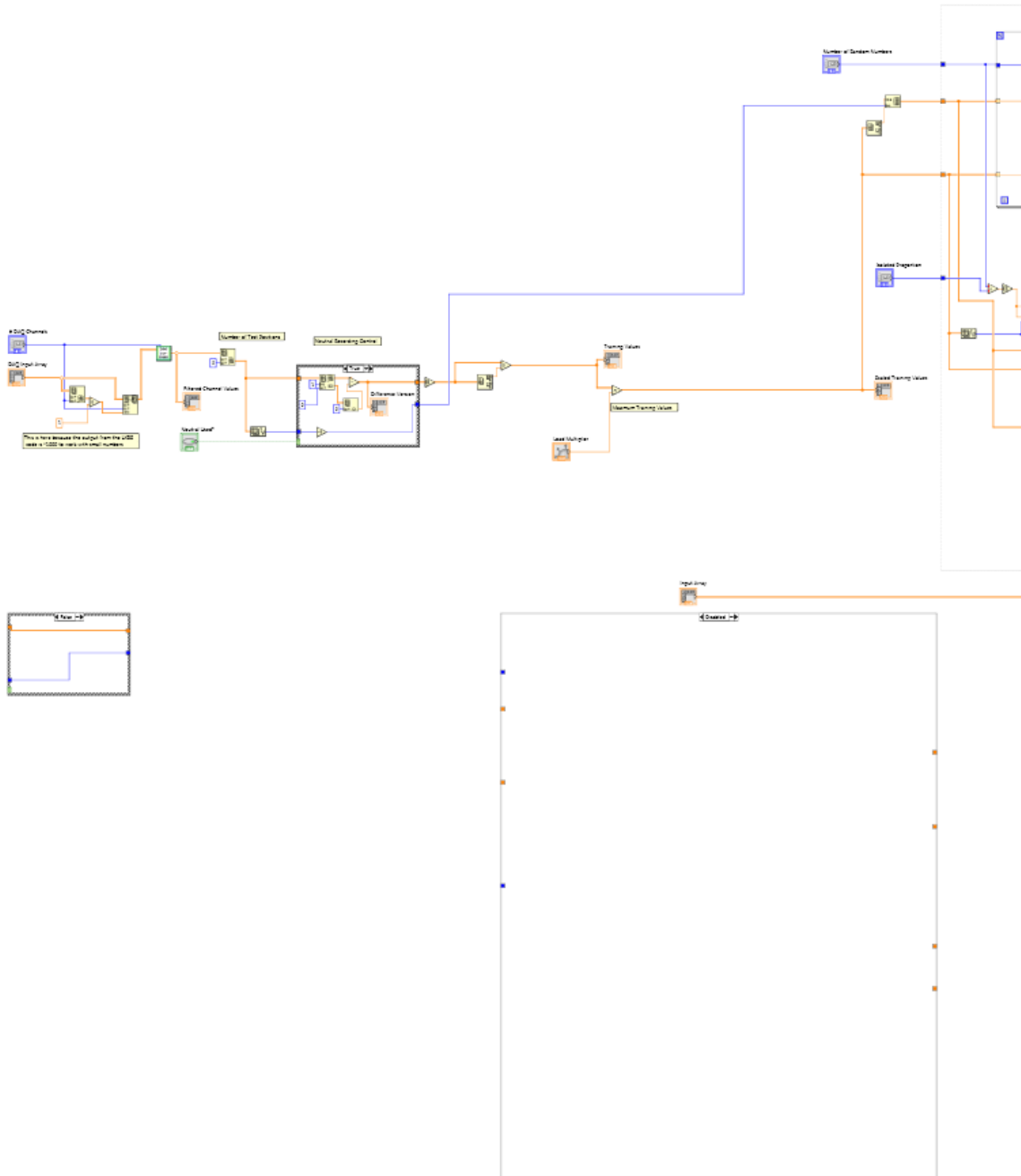


daq_conditioner_v2.vi
H:\LabVIEW Data\Test VIs\Thesis Versions\daq_conditioner_v2.vi
Last modified on 28/03/2017 at 12:31
Printed on 29/03/2017 at 16:16





daq_conditioner_v2.vi
H:\LabVIEW Data\Test VIs\Thesis Versions\daq_conditioner_v2.vi
Last modified on 28/03/2017 at 12:31
Printed on 29/03/2017 at 16:16



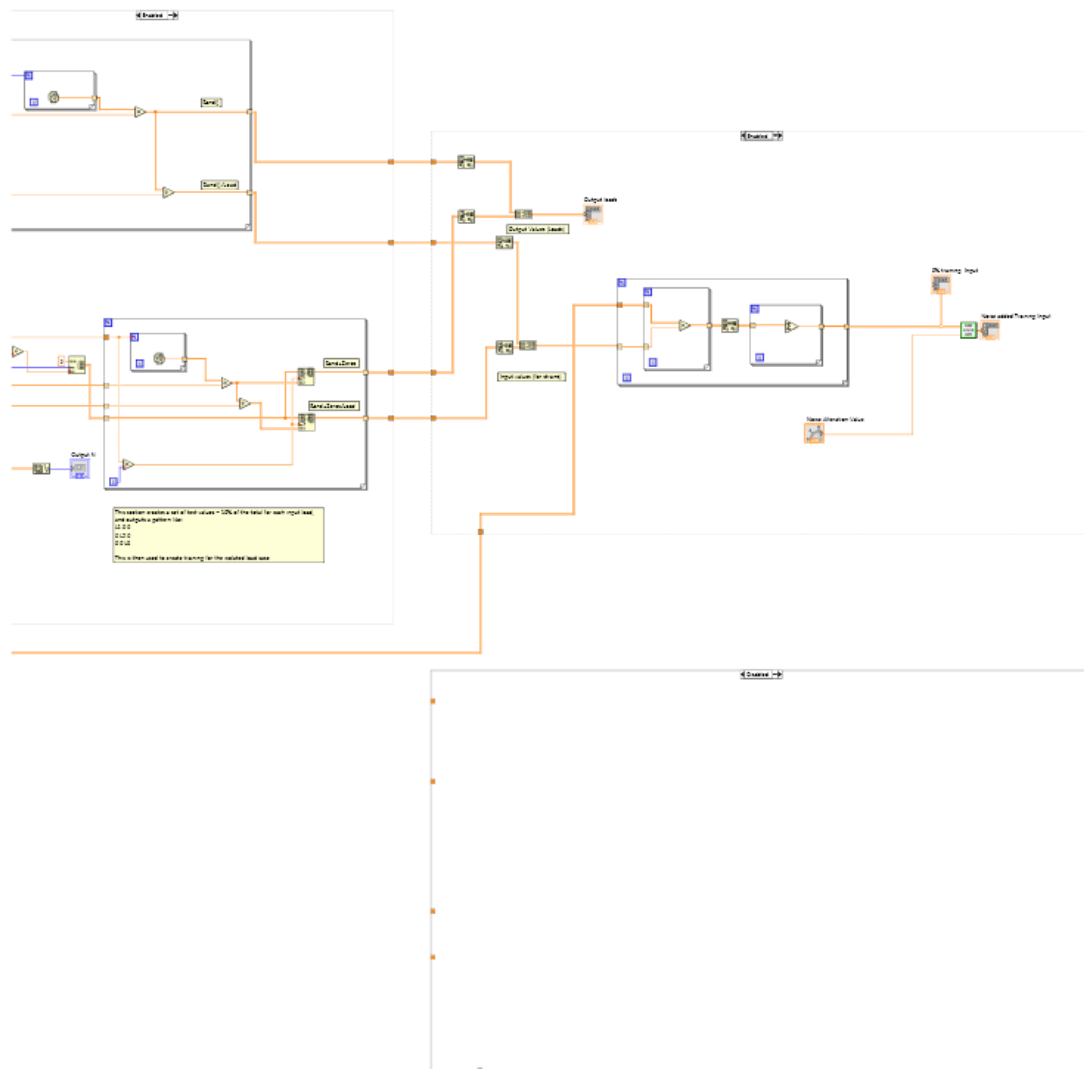


daq_conditioner_v2.vi

H:\LabVIEW Data\Test VIs\Thesis Versions\daq_conditioner_v2.vi

Last modified on 28/03/2017 at 12:31

Printed on 29/03/2017 at 16:16



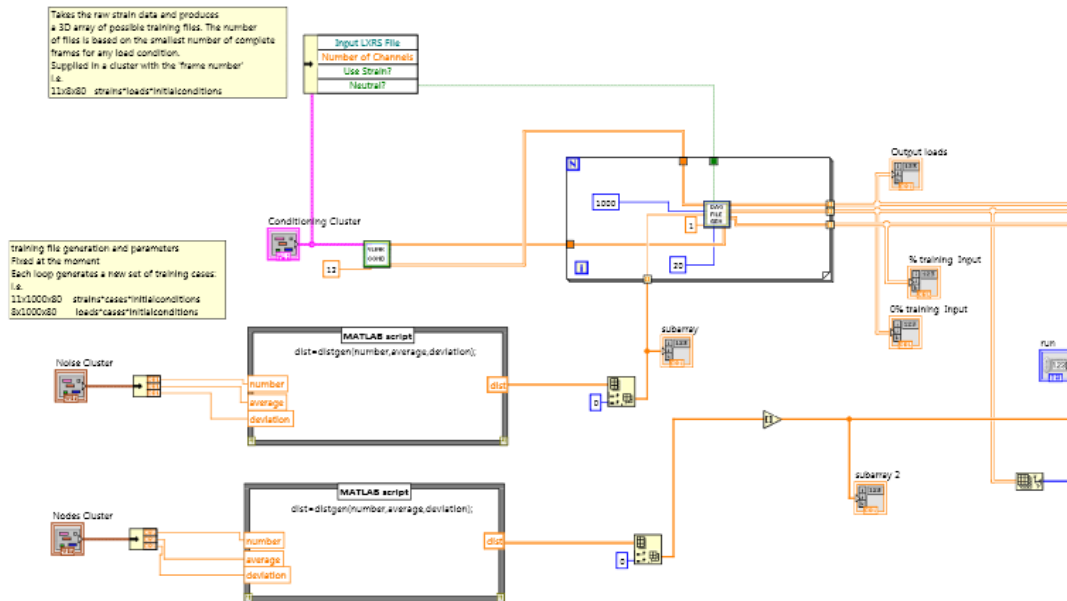


ANN_code_ensemble_v3.vi
 H:\LabVIEW Data\Test VIs\Thesis Versions\ANN_code_ensemble_v3.vi
 Last modified on 28/03/2017 at 12:27
 Printed on 29/03/2017 at 16:19

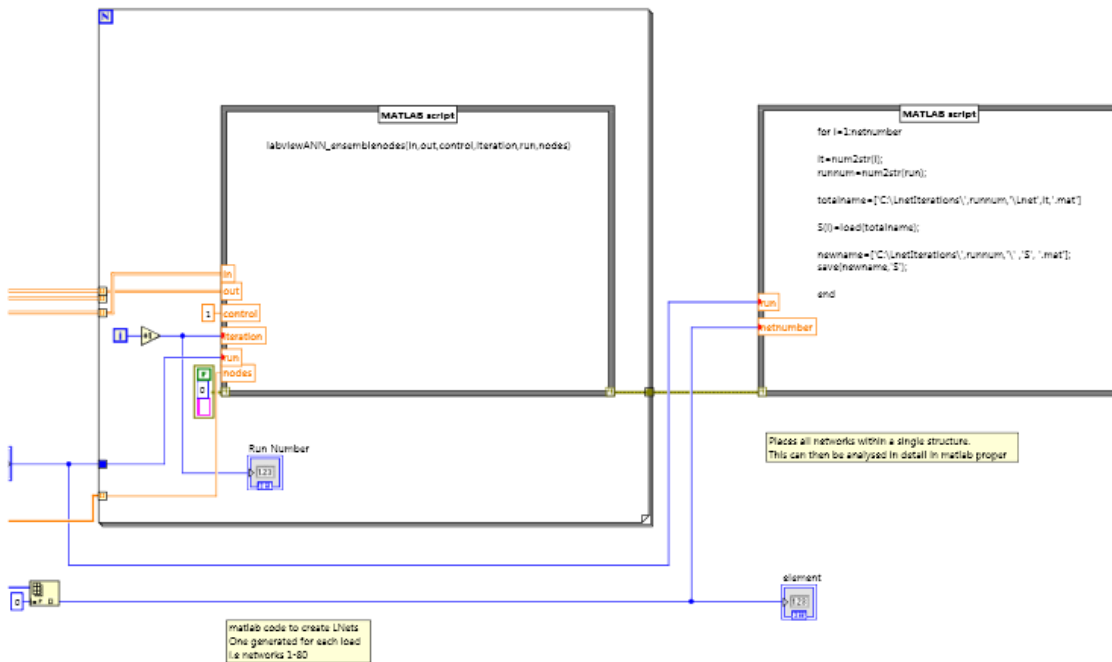
ANN_code_ensemble_v3.vi



Locates the corresponding load file



ANN_code_ensemble_v3.vi
 H:\LabVIEW Data\Test VIs\Thesis Versions\ANN_code_ensemble_v3.vi
 Last modified on 28/03/2017 at 12:27
 Printed on 29/03/2017 at 16:19



A32 Abbreviations

Ab/Ad	Abduction/Addition
ANN	Artificial Neural Network
ANOVA	Analysis of Variance
AP	Anterior/Posterior
AR	Augmented Reality
CAD	Computer Aided Design
CAM	Computed Aided Manufacturing
CSV	Comma Separated Variable (File)
FBG	Fibre-Bragg Grating
FE	Flexion/Extension
FEA	Finite Element Analysis
FFBP	Feedforward Backpropagation
FSR	Force Sensitive Resistor
LM	Levenberg-Marquardt
ML	Medial/Lateral
MSE	Mean Square Error
NR	Not Reported
PP	Probability Plot
PTB	Patellar Tendon Bearing
RMS	Root Mean Square
SCS	Socket Comfort Score
TAPES	Trinity Amputee Prosthetic Scale
TSB	Total Surface Bearing
TSP	Temporal Spatial Parameters
VI	(LabView) Virtual Instrument